MAX-PLANCK-INSTITUT FÜR KOHLENFORSCHUNG

technische universität dortmund

# Total syntheses of (-)-Scabrolide B and related marine natural products

**Dissertation**

zur Erlangung des akademischen Grades eines

Doktors der Naturwissenschaften

(Dr. rer. nat.)

der Fakultät für Chemie und Chemische Biologie

der Technischen Universität Dortmund

vorgelegt von

Davy Sébastien Lin

Mülheim an der Ruhr, Dezember 2025

# Eidesstattliche Versicherung (Affidavit)

_____ _____

Name, Vorname
(Surname, first name)

Matrikel-Nr.
(Enrolment number)

Belehrung:
Wer vorsätzlich gegen eine die Täuschung über Prü fungsleistungen betreffende Regelung einer Hochschul prüfungsordnung verstößt, handelt ordnungswidrig. Die Ordnungswidrigkeit kann mit einer Geldbuße von bis zu 50.000,00 € geahndet werden. Zuständige Verwaltungs behörde für die Verfolgung und Ahndung von Ordnungswidrigkeiten ist der Kanzler/die Kanzlerin der Techni-

schen Universität Dortmund. Im Falle eines mehrfachen oder sonstigen schwerwiegenden Täuschungsversu ches kann der Prüfling zudem exmatrikuliert werden, § 63 Abs. 5 Hochschulgesetz NRW.

Die Abgabe einer falschen Versicherung an Eides statt ist strafbar.

Wer vorsätzlich eine falsche Versicherung an Eides statt abgibt, kann mit einer Freiheitsstrafe bis zu drei Jahren oder mit Geldstrafe bestraft werden, § 156 StGB. Die fahrlässige Abgabe einer falschen Versicherung an Eides statt kann mit einer Freiheitsstrafe bis zu einem Jahr oder Geldstrafe bestraft werden, § 161 StGB.

Die oben stehende Belehrung habe ich zur Kenntnis genommen:

Official notification:

Any person who intentionally breaches any regulation of university examination regulations relating to deception in examination performance is acting improperly. This offence can be punished with a fine of up to EUR 50,000.00. The competent administrative authority for the pursuit and prosecution of offences of this type is the chancellor of the TU Dortmund University. In the case of multiple or other serious attempts at deception, the candidate can also be unenrolled, Section 63, paragraph 5 of the Universities Act of North Rhine-Westphalia.

The submission of a false affidavit is punishable.

Any person who intentionally submits a false affidavit can be punished with a prison sentence of up to three years or a fine, Section 156 of the Criminal Code. The negligent submission of a false affidavit can be punished with a prison sentence of up to one year or a fine, Section 161 of the Criminal Code.

I have taken note of the above official notification.

_____ _____

Ort, Datum
(Place, date)

Unterschrift
(Signature)

Titel der Dissertation:
(Title of the thesis):

_____

_____

_____

Ich versichere hiermit an Eides statt, dass ich die vorliegende Dissertation mit dem Titel selbstständig und ohne unzulässige fremde Hilfe angefertigt habe. Ich habe keine anderen als die angegebenen Quellen und Hilfs mittel benutzt sowie wörtliche und sinngemäße Zitate kenntlich gemacht.
Die Arbeit hat in gegenwärtiger oder in einer anderen Fassung weder der TU Dortmund noch einer anderen Hochschule im Zusammenhang mit einer staatlichen oder akademischen Prüfung vorgelegen.

I hereby swear that I have completed the present dissertation independently and without inadmissible external support. I have not used any sources or tools other than those indicated and have identified literal and analogous quotations.

The thesis in its current version or another version has not been presented to the TU Dortmund University or another university in connection with a state or academic examination.*

*Please be aware that solely the German version of the affidavit ("Eidesstattliche Versicherung") for the PhD thesis is the official and legally binding version.

_____ _____

Ort, Datum
(Place, date)

Unterschrift
(Signature)

technische universität
dortmund

Fakultät für Chemie und Chemische Biologie

Datum:

An die/den Vorsitzende/n des Promotionsausschusses
der Fakultät für Chemie und Chemische Biologie der TU Dortmund

## Eigenständigkeitserklärung für Dissertationen

nach der Ergänzung zur Promotionsordnung vom 29.10.2010
(Promotionsstudiengang) am 20.11.2023

Ich versichere hiermit an Eides statt, dass ich die vorliegende Dissertation mit dem folgenden Titel

_____

_____

_____

selbstständig und ohne unzulässige fremde Hilfe verfasst habe. Ich habe keine anderen als die angegebenen Quellen und Hilfsmittel benutzt sowie wörtliche und sinngemäße Zitate kenntlich gemacht. Ich erkläre zudem, dass ich beim Einsatz von Schreib- und Bildwerkzeugen, die durch Künstliche Intelligenz (KI) unterstützt werden, diese in der Übersicht verwendeter Hilfsmittel mit ihrem Produktnamen, meiner Bezugsquelle sowie der spezifischen Methodik vollständig aufgeführt habe und, bei Übernahme von durch generative Schreibwerkzeuge erstellten Texten, die betreffenden Textstellen in der Arbeit als mit KI-generierter Unterstützung verfasst gekennzeichnet habe. Die Arbeit hat in gleicher oder ähnlicher Form noch keiner Prüfungsbehörde vorgelegen. Ich habe sichergestellt, dass durch die Verwendung generativer Modelle kein fremdes geistiges Eigentum verletzt wurde und ich kein wissenschaftliches Fehlverhalten etwa in Form von Plagiaten begangen habe.

Name: _____, Vorname _____

Matrikelnummer: _____

Datum, Unterschrift _____

Stand 29.01.2024

1. Berichterstatter: Prof. Dr. Alois Fürstner
2. Berichterstatter: Prof. Dr. Martin Hiersemann

Die vorliegende Arbeit entstand unter Anleitung von Prof. Dr. Alois Fürstner in der Zeit von Januar 2022 bis September 2025 am Max-Planck-Institut für Kohlenforschung in Mülheim an der Ruhr. Teile dieser Arbeit wurden bereits in folgenden Beiträgen veröffentlicht:

Lin, D.S., Späth, G., Meng, Z., Wieske, L.H., Farès, C., Fürstner, A., Total Synthesis of the Norcembranoid Scabrolide B and Its Transformation into Sinuscalide C, Ineleganolide, and Horiolide. *J. Am. Chem. Soc.* **2024**, 146, 24250 – 24256.

Die praktischen Arbeiten erfolgten zum Teil in Zusammenarbeit mit Dr. Georg Späth, Dr. Zhanchao Meng, Dr. Lianne H. Wieske und Dr. Christophe Farès. Die beschriebenen Ergebnisse bilden eine vollständige Darstellung dieser gemeinsamen Arbeiten. Die von diesen Mitarbeitern alleinverantwortlich erzielten Ergebnisse wurden als solche an entsprechender Stelle gekennzeichnet.
Diese Arbeit wurde vom Autor eigenständig verfasst. Die Sprachtools DeepL und ChatGPT wurden ausschließlich zur Unterstützung bei der Korrektur von Grammatik und Sprache verwendet, was zu geringfügigen Änderungen führte.
Die deutschen Teile dieses Dokuments wurden mit dem Sprachtool DeepL übersetzt und von deutschsprachigen Kollegen überprüft.

## Acknowledgements

My first thanks go to my doctoral supervisor Prof. Dr. Alois Fürstner for allowing me to pursue my PhD in his group at the MPI on such an interesting and challenging project. I also gratefully acknowledge Prof. Dr. Martin Hiersemann for taking on the role of second examiner.

My great thanks go to my project co-workers Dr. Zhanchao Meng and Dr. Georg Späth, for their significant contributions to the project, their encouragement, and the many fruitful and constructive discussions we had. Working together helped me grow greatly as a scientist, and I will be forever grateful to you for that. I am also grateful to Dr. Lianne H. Wieske and Dr. Christophe Farès for their amazing work in accurately computing the structure of Scabrolide B, kickstarting this project.

My deepest gratitude goes to Sandra Tobegen from the NMR department, for all the structure elucidations she performed for me and the interesting discussions we had. A big thank goes to all the analytical departments at our institute, and I especially want to thank Sandra Klimmek for the purification of numerous natural products.

I am deeply grateful to the technicians of our institute for their essential support and maintenance work, which enables efficient research. In particular, I would like to thank the technicians of our group: Andrea Bosserhoff, Christian Wille, Christopher Rustemeier, Saskia Schulthoff, and Yannick Sell, as well as their apprentices. A special thank goes to Yannick Sell for his help on the project.

I want to thank the members of the Fürstner group for creating a very pleasant and stimulating working atmosphere. In particular, I thank Dr. Kenzo Yahata and Dr. Marco Mijangos Linares for the many engaging late-evening discussions and brainstorming sessions on the project, and Dr. Jack Sutro for insightful one-to-one discussions. In our group, a particular thank goes to all Box 5 members, especially Dr. Georg Späth, Dr. Juan Carlos Babon Molina, Dr. Mira Holzheimer and Albert Hermann, and to my co-starter Dr. Thomas Varlet.

A special thank goes to Albert Hermann, Jagon Ngan, Dr. Lucas Marchal, Dr. William Parisot and Dr. Nikolai Rossouw for proofreading this manuscript.

I thank both StuCons 23 and 25 teams for organizing the events together, particularly Dr. Emanuele Antico and Dr. Beatrice Lansbergen. Thank you, Bea, also for the very smooth transition as PhD Representative. I am also grateful to Dr. Daniel SantaLucia for the support and encouragement during my second year, when I needed it most.

I thank the recent spirits tasting group, especially Dr. Alexios Stamoulis, Dr. Lucas Mele, Dr. Ricardo Molina, and Quentin Riedl, for the enjoyable moments we shared together.

I want to thank my former university and placement supervisors for entrusting, teaching, and encouraging me while we were working together.

I had the delight to be involved within the Max Planck PhDnet through my PhD, where I could meet highly intelligent, remarkable, and admirable people who decided to

stand for others. I had the honour to coordinate the Survey Group for two years. For this, my great thanks go to Julia Teufel, who co-coordinated the group with me for one year, for the highly enjoyable collaboration and the amazing work we did together; to my predecessors Dr. Beatriz Vieira Mourato and Dr. Adriana Vucetic; and to those I worked in close proximity: Dr. Ellen Rumley, Janniek Wester, Jessica Donzowa, Manuel Herschel, and Prithwitosh Dey as well as the past, present, and future members of the Survey Group for maintaining and continuing the amazing work done. I am also grateful to all the PhD representatives in the MPG, especially those who encouraged us in our work, in particular Zsofi Igo, Annabelle Kaiser and Dr. Isabela de Oliveira. I want to thank the past, present and future Steering Groups for advocating for us. In particular, I want to thank Dr. Elisabeth Bobkova for her constant advocacy and guidance regarding the Survey. Beth, thank you so much also for our weekly writing meetings and all the associated encouragements, which brought that extra motivation to write some additional lines or pages every day.

With the Survey Group, I also had the chance to work on a joint survey with $N^2$, and for this, I want to thank all our collaborators, in particular Dr. Agnieszka Seretny and Julius Petrausch from the other research organizations. I also want to thank the editorial team of Offspring magazine, for their support and involvement in the writing activities.

In general, I want to thank anybody who selflessly decides to speak out for other people's rights. Kindness is a quality that is becoming increasingly rare, and it is heart-warming to see that some people still care about others and about the world.

A special thanks goes to Deutsche Bahn and to the Deutschlandticket, for allowing me to visit so many areas in NRW, Rheinland-Pfalz and beyond, making me discover this geographically amazing country and for never making me feel I was missing a car.

Des remerciements spéciaux vont aux deux Antoine pour le soutien à distance. Drôle de coïncidence que mes meilleurs amis aient également décidé de faire des doctorats en sciences naturelles. Une pensée va également pour le groupe de francophones à Düsseldorf, en particulier Lucile et Nathalie, pour ces formidables afterworks.

Outside of work, I had the chance to contribute to the local hiking and board game communities, which helped me maintain balance and meet admirable and kind people. I am grateful to the hiking community, especially Andrea, Elene, Ivanna, Jason and Pamela, and to the board game community, particularly Alex, Antonio, Daniel, Gregor, Jagoda, Jana and Stefan for the enjoyable shared experiences.

I want to give a deep acknowledgement to my therapist, for encouraging me, helping me regain confidence, and supporting me in moving forward during challenging periods.

Enfin, un remerciement va à mes parents et à mon frère Willy, pour leur soutien pendant toutes ces années, qui m'a permis d'en arriver là où j'en suis, malgré des origines socio-professionnelles peu favorables pour des études doctorales.

# Zusammenfassung

Die von Furanobutenolid abgeleiteten Norcembranoidditerpene sind eine seltene Familie von Naturstoffen, die hauptsächlich in Weichkorallen vom Typ *Sinularia* isoliert wurden. Diese Moleküle zeichnen sich durch ein dicht funktionalisiertes polycyclisches Gerüst von hoher topologischer Komplexität aus.

So wurde erst 2022 entdeckt, dass Scabrolid B ein deutlich anderes carbocyclisches Gerüst als sein Schwesterprodukt Scabrolid A aufweist, nämlich ein 6/7/5/5-Ringsystem anstelle des ursprünglich angenommenen 7/6/5/5-Skeletts. Diese unerwartete strukturelle Neubewertung, zusammen mit dem Fehlen jeglicher synthetischer Vorarbeit zu diesem Gerüst, motivierte die in dieser Arbeit vorgestellten Untersuchungen. Zu Beginn dieser Arbeit war kein Naturstoff mit diesem Skelett synthetisiert worden.

Es wurden zwei unterschiedliche konvergente Ansätze für Scabrolid B untersucht, die jeweils auf einem Ringschluss des zentralen siebengliedrigen Rings beruhen: einer durch Ringschlussmetathese (RCM), der andere durch intramolekulare Enolat-Alkenylierung.

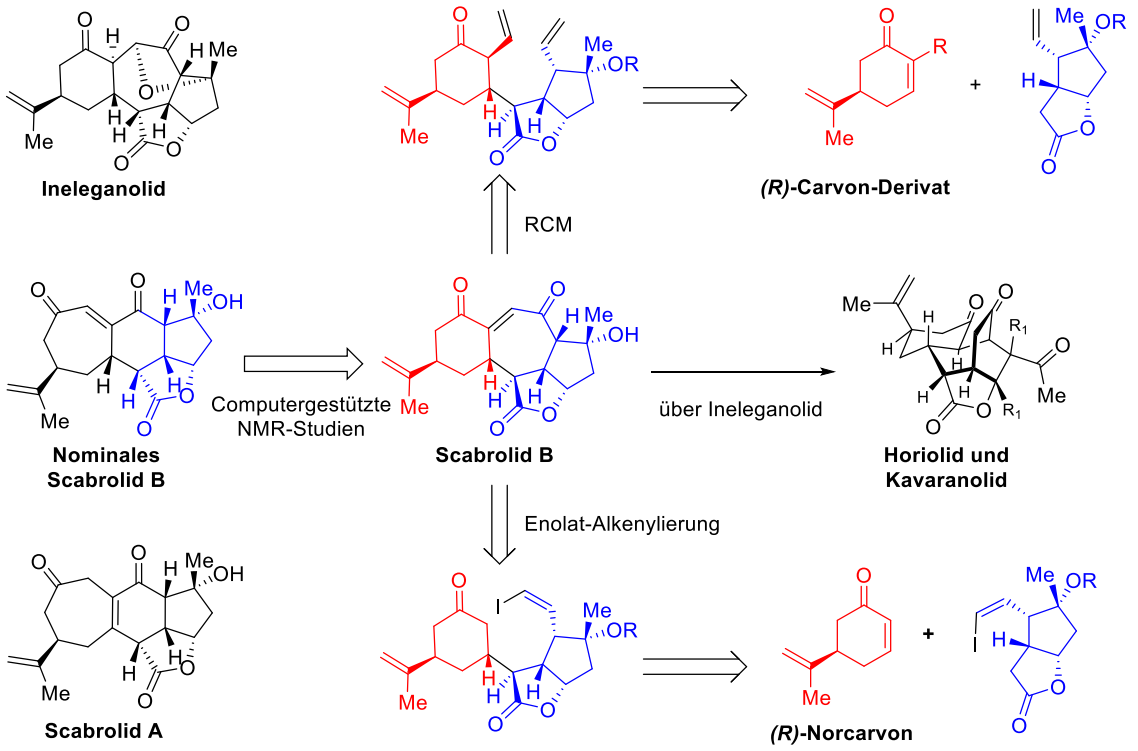

Die für den Ringschluss erforderlichen Vorläufer durch eine 1,4-Addition eines geschützten bicyclischen Lactona und eines (*R*)-Carvon-Derivats wurden synthetisiert. Beim RCM-Ansatz erwies sich die räumliche Orientierung der Alkene als entscheidend für eine produktive Ringbildung, während der Alkenylierungsansatz leichter die für die Cyclisierung erforderliche stereochemische Anordnung lieferte. Obwohl beide Ansätze auf dem Weg zur Totalsynthese von Scabrolid B zu einem gemeinsamen Zwischenprodukt konvergieren, lieferte nur der Alkenylierungsweg einen skalierbaren zugang zum Naturprodukt, wobei in einem einzigen Durchgang über 19 Schritte (längste lineare Sequenz) 110 mg und eine Gesamtausbeute von 1.2 % erzielt wurden.

Scabrolid B wurde anschließend in die Schwester-Norcembranoids Fragilolid A, Sinuscalid C und Ineleganolid umgewandelt, wobei die letztere Umwandlung möglicherweise einen bisher unbekannten biosynthetischen Zusammenhang zwischen beiden Naturstoffen aufdeckte. Weiters konnte Ineleganolid in Horiolid und Kavaranolid umgewandelt werden, was die in der Literatur vorgeschlagene biosynthetische Sequenz stützt.

Insgesamt wurde eine Reihe von polycyclischen Norcembranoiden und deren Derivaten synthetisiert, die wertvolles Material und Erkenntnisse für zukünftige Studien zur biologischen Aktivität dieser seltenen Molekülfamilie liefern.

## Abstract

The furanobutenolide-derived norcembranoid diterpenes are a rare family of natural products isolated mainly in *Sinularia*-type soft coral. These molecules feature a densely functionalized polycyclic skeleton of high topological complexity.

It was discovered only in 2022 that scabrolide B possesses a notably different carbocyclic skeleton from its sibling scabrolide A, featuring a 6/7/5/5 core instead of the initially postulated 7/6/5/5 core. This unexpected structural revision, together with the lack of any synthetic precedent for this framework, motivated the research presented here. The objective of this thesis was to accomplish a total synthesis of scabrolide B. At the initiation of this thesis, no natural product featuring that skeleton has ever been synthesized.

Two distinct convergent approaches to scabrolide B were investigated, each relying on a ring-closure of the central seven-membered ring: one by ring-closing metathesis (RCM), the other *via* intramolecular enolate alkenylation.

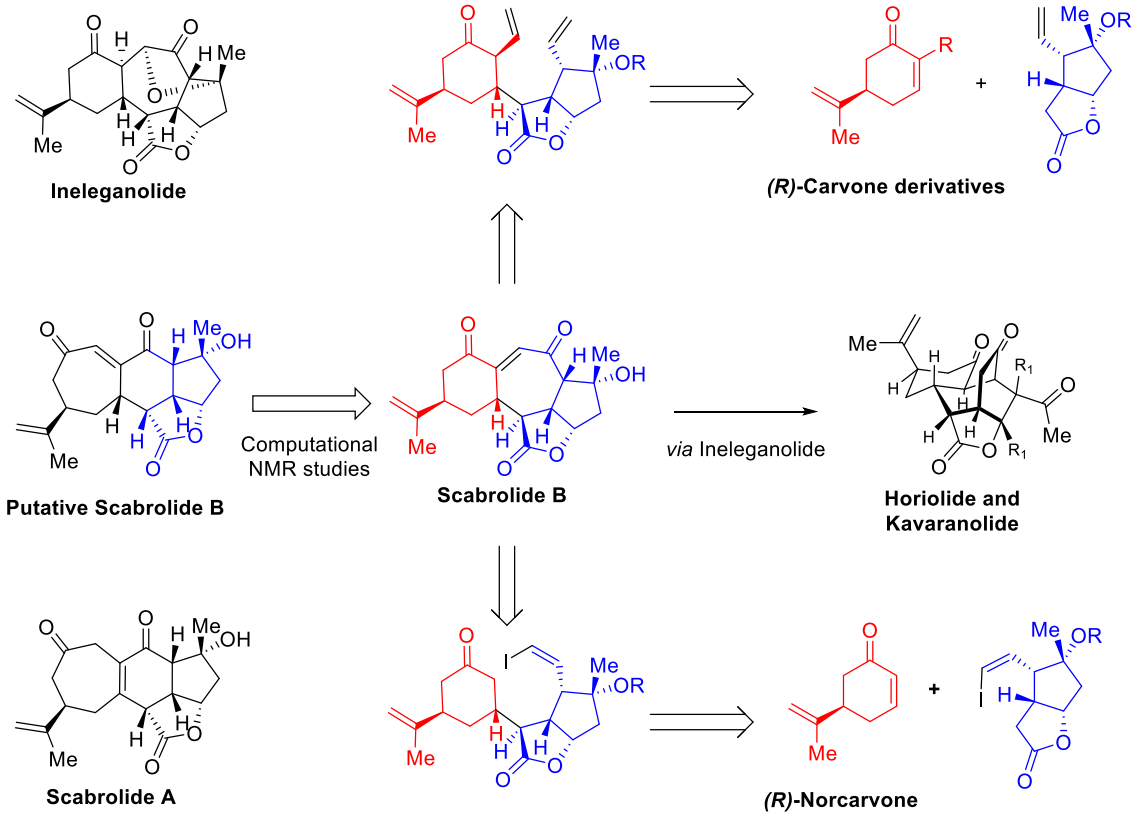


In the forward sense, the precursors required for ring-closure were synthesized by a 1,4-addition between a protected bicyclic lactone and a *(R)*-carvone derivative. In the

RCM approach, the spatial orientation of the alkenes proved crucial for productive ring formation, whereas the alkenylation approach more readily provided the stereochemical arrangement needed for cyclization. Although both approaches converge on a common intermediate *en route* to the total synthesis of scabrolide B, only the alkenylation route afforded a reliable supply of the natural product, providing 110 mg in a single run over 19 steps (longest linear sequence) and 1.2% overall yield.

Scabrolide B was subsequently transformed into the sister norcembranoids fragilolide A, sinuscalide C and ineleganolide, with the latter transformation potentially revealing a previously unrecognized biosynthetic link between both natural products. Ineleganolide could further be converted into horiolide and kavaranolide, supporting the biosynthetic sequence proposed in the literature.

Overall, a series of polycyclic norcembranoids and their derivatives were synthesized, providing valuable material and insight for future studies on the biological activity of this rare family of molecules.

# Table of Contents

# 1. Introduction

## 1.1 Total synthesis and its role in chemistry

It was long believed that organic compounds could only be synthesized by "living organisms". This view was shattered by the syntheses of urea in 1828 from cyanic acid and ammonia,[1] and the synthesis of acetic acid in 1845,[2] both representing the very first examples of natural organic compounds made entirely by artificial means, giving birth to the discipline of organic synthesis. The field then underwent profound changes, in close intercorrelation with advances in other areas of science in general and their applications in chemistry. Early on, synthesis was used to confirm the structure of natural products, achieving remarkable successes with compounds such as quinine,[3] haemin[4] or strychnine (Figure 1.1).[5] These efforts also advanced the understanding of chemical reactivity and led to the development of the first methodologies in that field, further aided also by advances in quantum theory. Structure elucidation through synthesis, however, required the synthesis of substantial amount of the target compound, and was also somewhat error-prone as exemplified by the initially proposed structures of steroids.

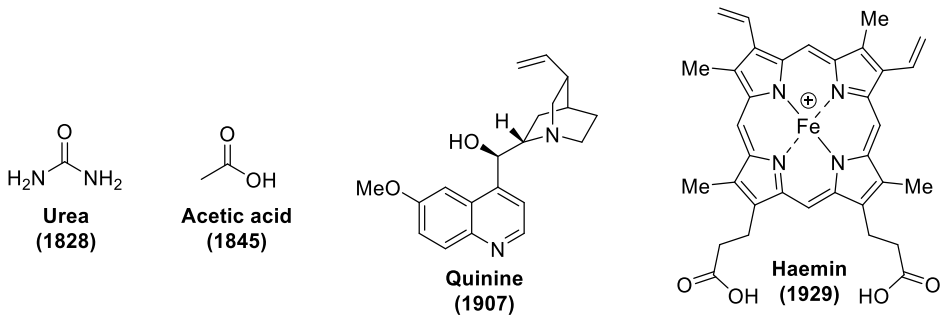


**Figure 1.1.** Structures of the first successes in natural products synthesis.

The development of highly precise and specific analytical methods – such as NMR (Nuclear Magnetic Resonance) spectroscopy, X-ray diffraction and mass spectrometry – allowed the characterization of organic compounds in a much more reliable and efficient manner, requiring much less material, and totally

switched the roles, with these analytical methods then confirming or refuting that a desired organic compound, natural or not, was rightfully synthesized. These techniques and their consequences in organic synthesis also substantially transformed medicinal chemistry, a field that was also strongly tied to the isolation of natural products. These evolutions allowed a much more accurate understanding of the relationship between structure and biological activity, and interaction with the biological target. FDA-approved drugs such as Docetaxel and Eribulin, derived from paclitaxel and halichondrin B, respectively, serve as prominent examples of successful therapies inspired by natural products (Figure 1.2).

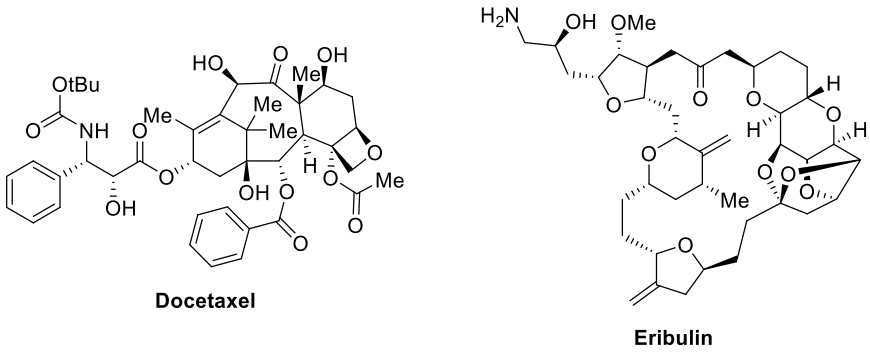


**Figure 1.2.** Docetaxel and Eribulin

However, despite these highly accurate analytical methods, errors in the structural assignment of natural products still happen.[6] If these misassignments usually concern the position of a functional group or the configuration of a stereocenter or two, there are cases where the proposed structure of the natural products has little to do with the actual structure of the natural product.[7] Even X-ray diffraction, often called the platinum standard for characterization, can lead to misassignment (Figure 1.3).[8] In many of these cases, the mistakes were uncovered during synthetic studies towards the targeted natural products, the original structural confirmation (or refutation) function of natural product synthesis therefore still remains in our current days, with its potential consequences in drug design.

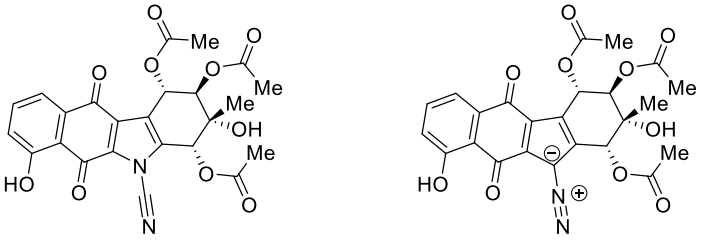


**Figure 1.3.** An example of a natural product misassigned by X-ray crystallography.

Today, natural product synthesis and medicinal chemistry are no longer so interrelated, with the development of robust chemical transformations and technologies which allows the synthesis and screening of complete libraries of compound in a highly time-efficient way. Still, natural products continue to serve as an important inspiration for drug design as they are keepers of a certain biological activity acquired by evolution, with medicinal chemists further directing that evolution.[9]

## 1.2 The polycyclic furanobutenolide-derived norcembranoid diterpenes

### 1.2.1 Structure and biological activity

The furanobutenolide-derived norcembranoids are a family of natural products mainly isolated from *Sinularia*-type soft corals. The first member was discovered in 1995 with the first isolation of dissectolide **1** from *Sinularia dissecta*,[10] followed in 1999 by the isolation of ineleganolide **2** from *Sinularia inelegans*.[11] Structurally, these natural products are characterized by a highly oxygenated polycyclic C19 skeleton with a rigid [5,5]-bicyclic lactone (a [5,6]-bicyclic lactone for horiolide **3**), a cyclohexa- or cycloheptane central ring, and an additional attached cycle on the periphery. Some of these norcembranoids are further decorated with an overarching tetrahydrofuran ring (ineleganolide **2** and sinulochmodin C **4**), bringing an additional level of complexity (Figure 1.4). Given the intricate structure and potential utility of the scaffold for biological investigations, this family of natural products has drawn lots of attention from the synthetic community.

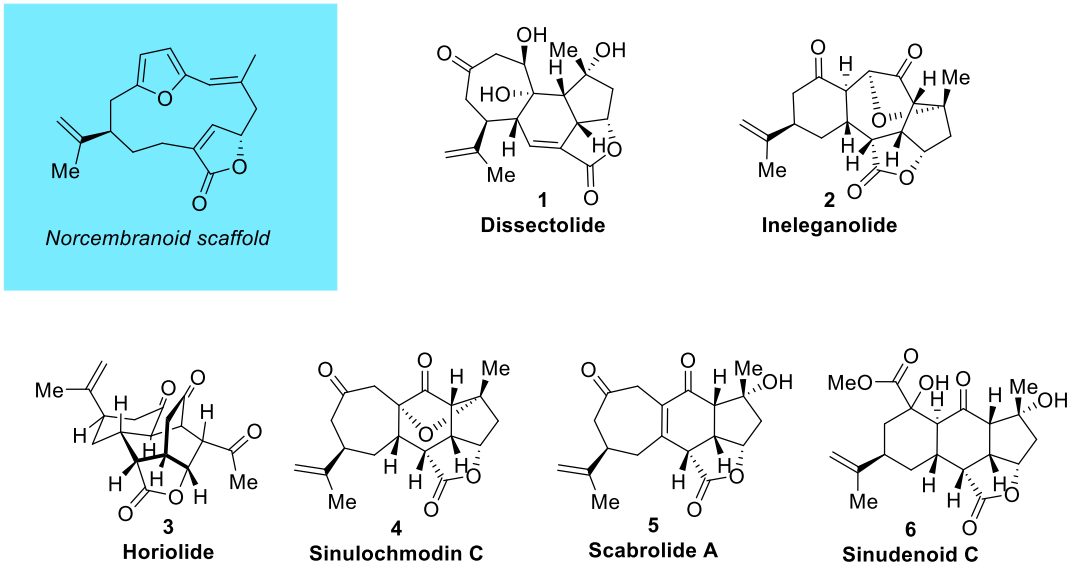


**Figure 1.4.** Furanobutenolide-derived norcembranoid natural products.

It is worthwhile to mention that at the moment of initiation of this project, despite several synthetic campaigns towards other members of the family,[12] only

a single furanobutenolide-derived norcembranoid had been synthesized *de novo*, namely scabrolide A **5** by the groups of Stoltz[13] and Fürstner,[14] even though the original isolation and structural characterization of **5** occurred nearly two decades ago.[12] During the course of the investigations presented in this thesis, ineleganolide **2** was synthesized by the groups of Wood[15] and Stoltz,[16] sinulochmodin C **4** by the group of Wood[15] and havellockate **7** by the group of Stoltz.[17] Among the similar furanobutenolide-derived cembranoids (with a C20 skeleton), rameswaralide **8** was successfully synthesized by the group of Romo (Figure 1.5).[18]

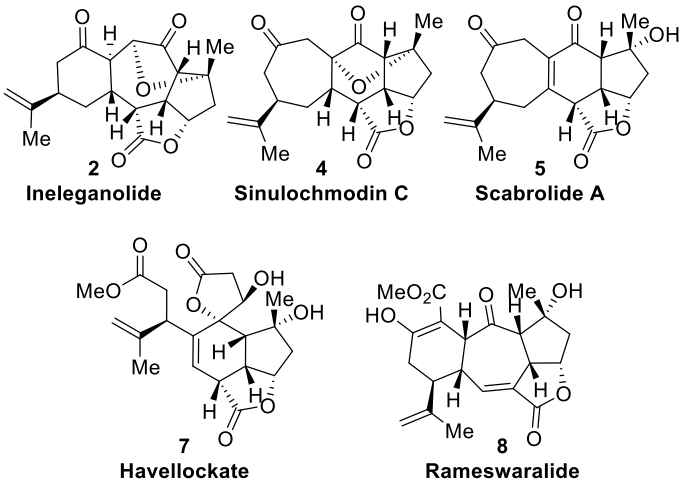


**Figure 1.5.** Successfully synthesized furanobutenolide-derived norcembranoids at the time of completion of this thesis.

The biology of these natural products remains largely unexplored, due to their low isolation yields, their rare occurrence – mainly in *Sinularia* soft corals, and their challenging synthetic accessibility. Despite frequent claims regarding their bioactivity, most of these compounds were inactive in the assays in which they were tested, and no clear trend could be established. For example, ineleganolide **2**—the most frequently targeted member of this family for synthesis—was initially reported as cytotoxic against P-388 cells in the isolation publication and showed some anti-parasitic activity in another assay.[11, 19] However, later studies found it inactive against P-388,[20] as well as in antibacterial, anti-cancer, anti-inflammatory, and other assays.[21] Given their wide occurrence in

*Sinularia* soft corals, it is possible that a suitable biological target has not yet been identified. Supporting this, the Romo group tested stereochemically defined fragments of rameswaralide **8**—comprising the 7/5/5 or 6/5/5 skeletons—against several cancer cell lines, and observed that these fragments do possess anti-cancer activity.[22] Similarly, the Stoltz group tested fragments formed during their synthetic studies toward ineleganolide **2**, most of which exhibited anti-inflammatory activity.[23]

### 1.2.2 Biosynthesis

All the polycyclic furanobutenolide-derived norcembranoid are postulated to come from a common intermediate, 5-episinuleptolide **9**.[24] This compound is thought to originate from geranylgeranyl diphosphate **10**, which cyclizes to give macrocycle **11**, and then undergoes a series of oxidations to form Z-deoxypukalide **12**, the putative common precursor to all norcembranoids and the closely related cembranoids (C20 skeleton). Z-Deoxypukalide **12** might then undergo oxidative furan opening, hydration, and intramolecular oxa-Michael addition to afford compound **14**. Subsequent decarboxylation and C11 hydroxylation provide 5-episinuleptolide **9** (Scheme 1.1).

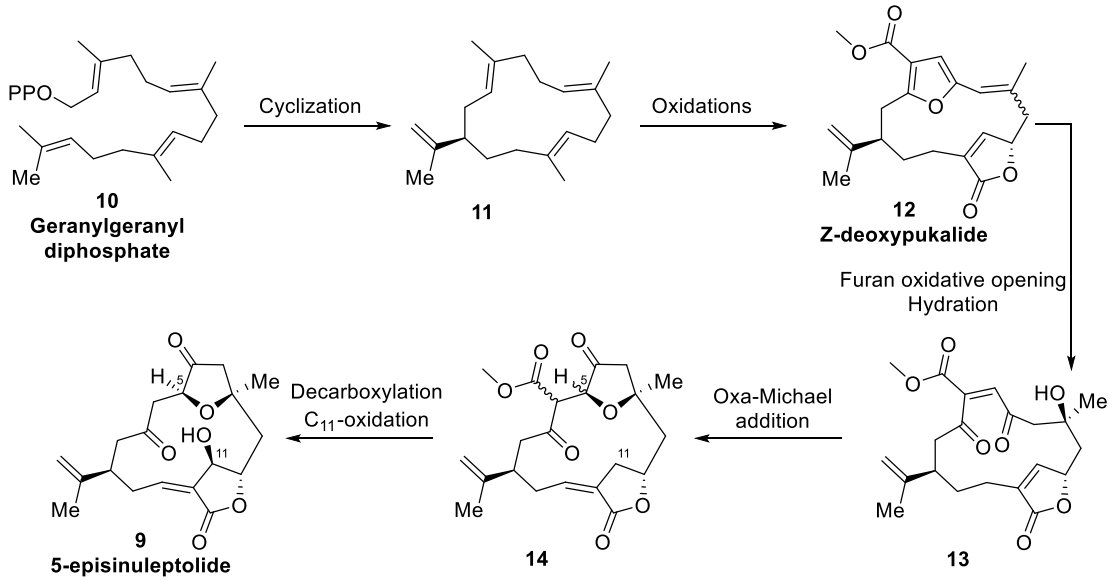


**Scheme 1.1.** Postulated biosynthesis of norcembranoid 5-episinuleptolide **9**.

From this intermediate, a transannular Michael addition to C13 is proposed, either from C4 or C5. A pathway involving attack from C4 generates a 6/10/5/5 ring system which undergoes a second transannular Michael addition, from C7 to C11 to give ineleganolide **2** (Scheme 1.2). Ineleganolide **2** may then undergo a retro-oxa-Michael ring opening of its tetrahydrofuran unit, followed by a retro-aldol/Michael addition cascade to give horiolide **3.** A further retro-oxa-Michael reaction would then furnish kavaranolide **18**. This pathway will be further supported by the results presented in this thesis (Chapter 3.4).

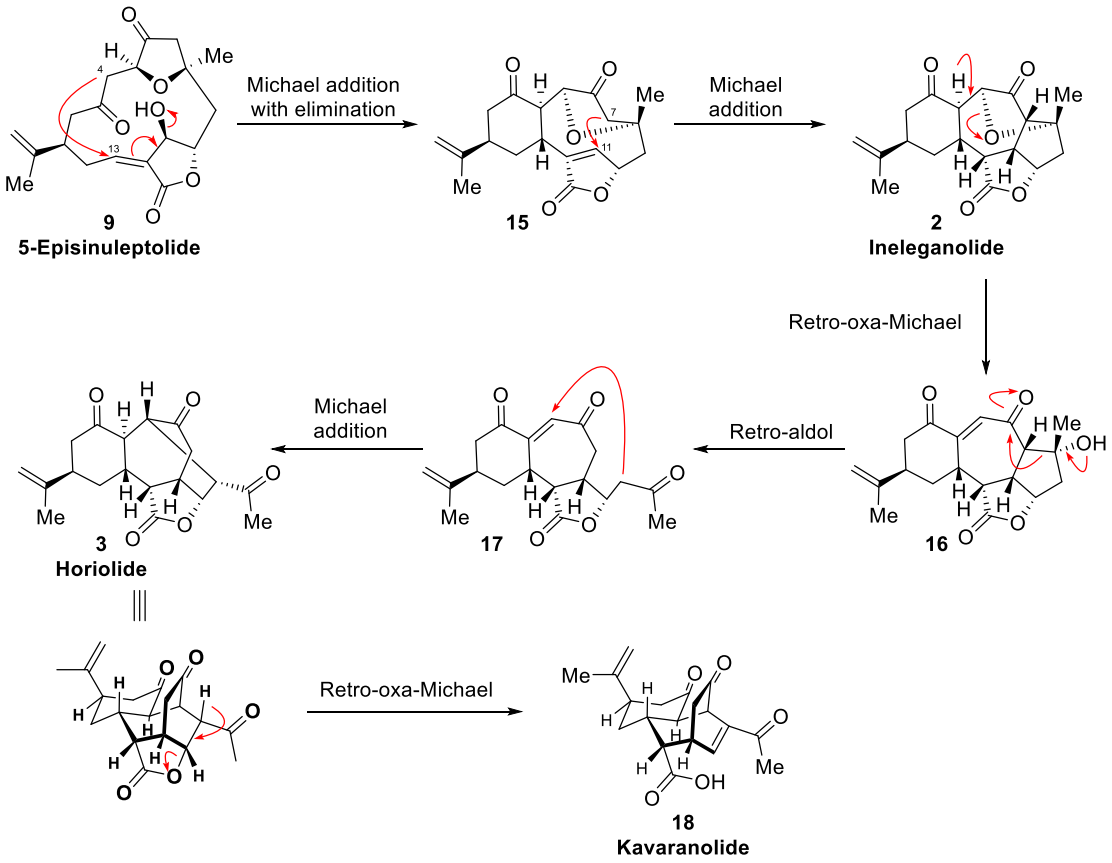


**Scheme 1.2.** Postulated biosynthesis of norcembranoids ineleganolide **2**, horiolide **3** and kavaranolide **18** from 5-episinuleptolide **9**.

In an analogous way, transannular Michael addition from C5 forms a 7/9/5/5 ring system which can also undergo transannular Michael addition from C7 to C11 to give sinulochmodin C **4**. A retro-oxa-Michael reaction followed by alkene isomerization could furnish scabrolide A **5** and, after an additional dehydration, yonarolide **21** (Scheme 1.3). It should be noted that at the time of these biosynthetic

proposals, scabrolide B was thought to have the structure of **20**, appearing as a plausible intermediate *en route* to scabrolide A **5** and included accordingly in the proposed pathway. Subsequent studies, however, showed that this structure was incorrect and that scabrolide B is not a biosynthetic precursor of scabrolide A **5**. The correct structure is described in the following section. (Chapter 1.3).

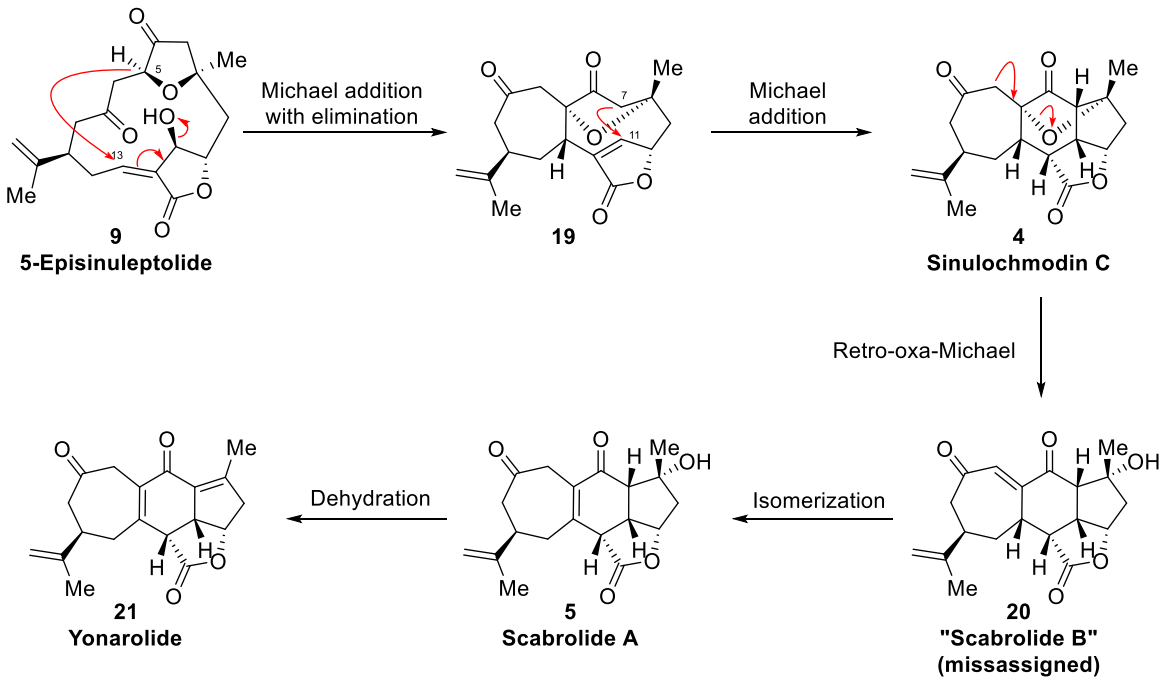


**Scheme 1.3.** Proposed biosynthesis of norcembranoids sinulochmodin C **4**, scabrolide A **5** and yonarolide **19** from 5-episinuleptolide **9**.

To support their propositions, the Pattenden group, who proposed these biosynthetic pathways, accomplished the transformation of 5-episinuleptolide **9** into **2** and **3**, *via* a double transannular Michael addition (Scheme 1.4).[25]

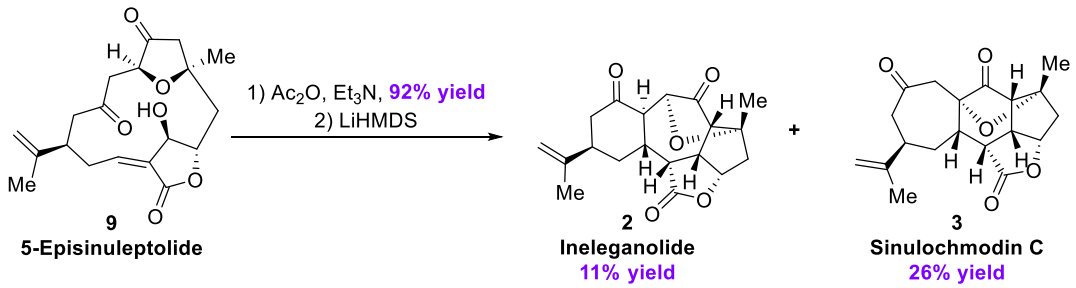


**Scheme 1.4.** Semi-synthesis of ineleganolide **2** and sinulochmodin C **4** by the Pattenden group.

## 1.3 Structure of Scabrolide B and similar syntheses

### 1.3.1 The total syntheses of Scabrolide A and putative Scabrolide B

Our group successfully synthesized scabrolide A in 2022 *via* the proposed structure of scabrolide B.[14]

Coupling between fragments **22** and **23** – derived respectively from *(R)*-carvone and *(R)*-linalool – occurred by S-alkylation to give intermediate **24**. Upon deprotonation, the resulting sulfonium ylide **25** underwent a [2,3]-sigmatropic rearrangement establishing the C12-C13 bond of the natural product and, after deprotection, providing a separable mixture of diastereoisomers **27** and **28**. Diastereoisomer **28**, which bears the same C13 stereochemistry as "scabrolide B" **20**, was exposed to $Bu_3SnH$/AIBN, affording a diastereomeric mixture that was equilibrated with DBU to give triene **29**. The central six-membered ring was then closed by ring closing metathesis (RCM), affording **30** in 77% yield. Notably, RCM was unsuccessful on the C13 epimer of diene **29** (**13-*epi*-29** – not shown) derived from diastereoisomer **27**.

Subsequent acetal deprotection and hydroxy-directed epoxidation of the newly formed bridgehead double bond under $VO(acac)_2$ catalysis furnished epoxide **31**. Treatment of **31** with $NEt_3$ in methanol induced deprotonation $\alpha$ to the ketone, subsequent epoxide opening, and epimerization of the C12 center into the desired configuration, producing alcohol **32**. Finally, an oxidation afforded the compound corresponding to the reported structure of scabrolide B **20**. This compound could be isomerized into scabrolide A **5** (Scheme 1.5).

While the spectral data of scabrolide A **5** was in full accordance with the reported data,[13, 26] a significant mismatch was observed between the spectral data of the synthesized nominal structure of scabrolide B **20** and the reported data of the natural product. To confirm the stereochemistry of the synthesized material, an X-ray crystallographic analysis was performed on precursor **32** which verified

its structure. A similar mismatch was observed for the C12-epimer of putative scabrolide B **12-*epi*-20**, prepared from epoxide **31**. Taken together, these elements highlight the misassignment, based on NMR, of the structure of scabrolide B that went beyond a simple C12 epimer.

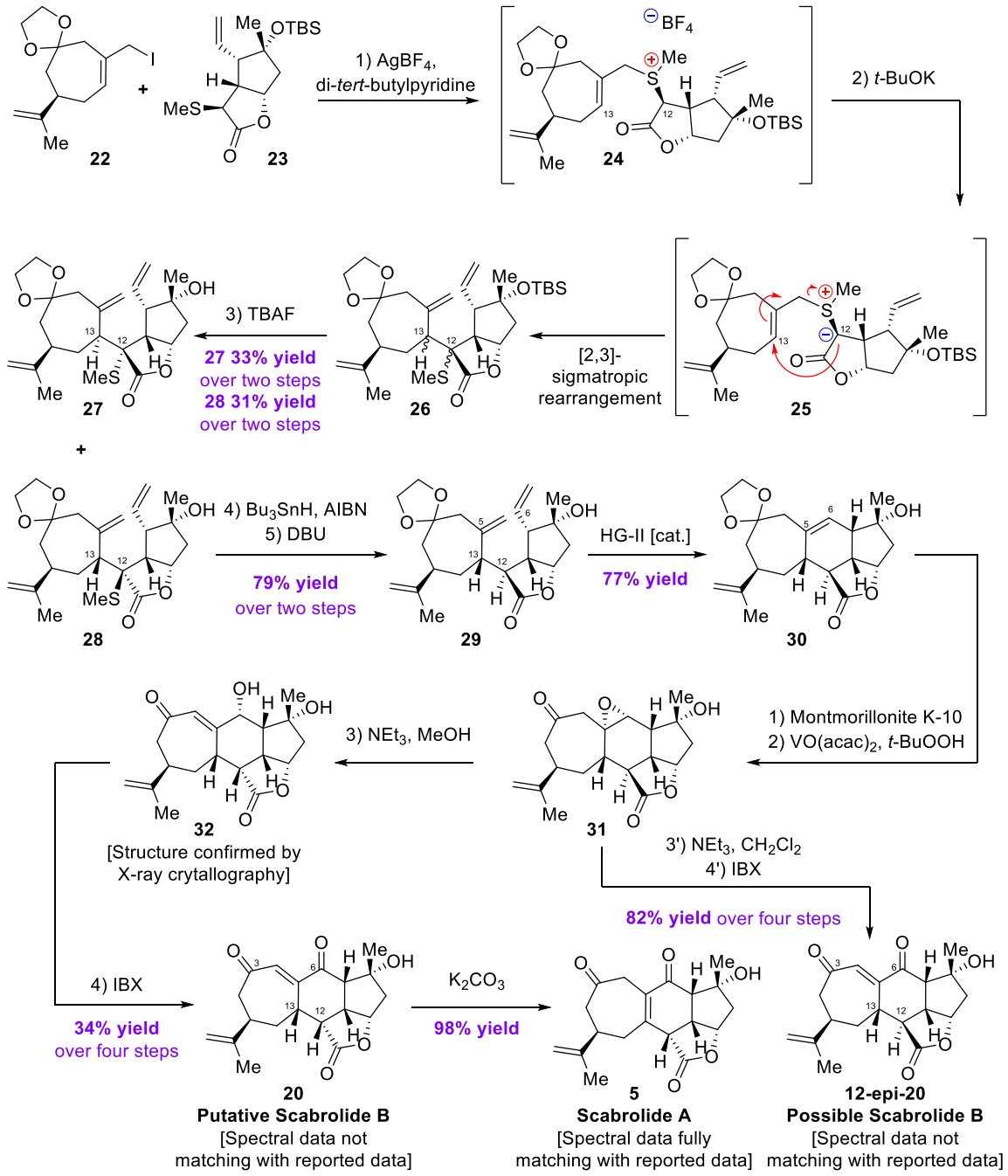


**Scheme 1.5.** Total syntheses of scabrolide A **5** and putative scabrolide B **20**.

### 1.3.2 Revision of the structure of Scabrolide B

Note: the revision of the structure of scabrolide B was done by Dr. Lianne H. Wieske and Dr. Christophe Farès. The revision presented in this chapter constitute a summary of their considerations, the details can be found in the experimental section.

As the available data did not allow a firm structure revision, an in-silico screening was carried out (see the details in the Experimental section). That screening evaluated systematically all the $^{1}H$ and $^{13}C$ chemical shifts of all possible diastereoisomers of scabrolide B. Furthermore, a close look at the original assignment revealed nearly overlapping $^{13}C$ shifts for the two ketones at positions C3 and C6 (202.6 vs 202.3 ppm). This situation led to the misinterpretation of a decisive long-range C-H correlation; indeed, the correlation between the H13 proton to one of the ketones is crucial to identifying the olefinic end (C4 or C5) at which the ring-closing bond from the C13 carbon is formed. It was therefore rationalized that the statistical evaluation should also consider the constitutional isomer (and its diastereoisomers) for which a bond exists between the carbons atoms C13 and C4 (rather than C5) leading to a 6/7/5 fused ring system rather than the proposed 7/6/5 fused ring system (Figure 1.6).

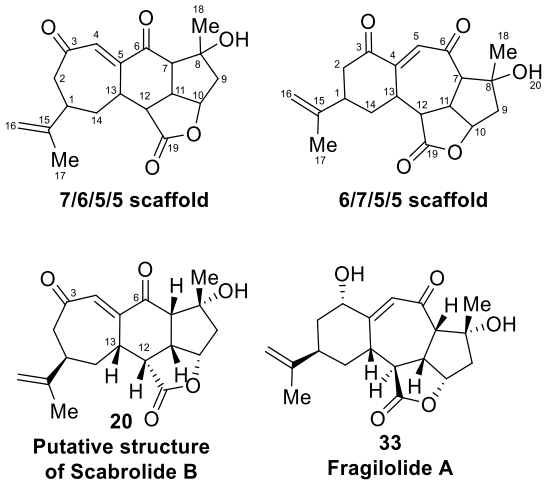


**Figure 1.6.** Basic ring scaffolds 7/6/5 and 6/7/5 with carbon numbering used in the probabilistic analysis, shown alongside the putative structure of scabrolide B **20** and fragilolide A **33**, on which the probabilistic model was benchmarked on.

The plausible scabrolide B constitutional isomers (7/6/5 and 6/7/5) comprise seven stereocenters, each resulting in 128 alternative stereoisomers, which are grouped into 64 pairs of enantiomers. Therefore, the DFT calculations aiming to determine Boltzmann-averaged $^{1}H$ and $^{13}C$ chemical shieldings and coupling constants over an ensemble of interchanging conformers were applied to a total of 128 configurations (64 for each of the two constitutional isomers). The results were compared to the values of natural scabrolide B reported by Sheu *et al.*[26] and evaluated with a Bayesian analysis using the J-DP4+ tool developed by the group of Sarotti.[27] Initially benchmarked on known terpenoid fragilolide A **33**,[28] the results pointed to a single compound **34** with very high confidence (Figure 1.7).

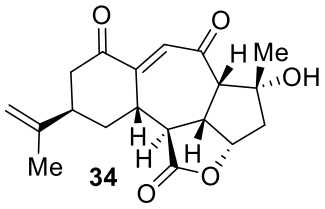


**Figure 1.7.** Suggested structure of scabrolide B **34** from computational NMR studies.

The initial objective of this thesis became the total synthesis of the suggested revised structure of scabrolide B **34**, with structure reassignment. That latter goal became obsolete soon after the computational work described above, as the natural product was reisolated and revised by NMR spectroscopy and X-ray diffraction analysis.[29] That work suggested the same structure shown in Figure 1.7 by the computational studies, confirming that the correct target was predicted. Actually, the compound was independently obtained a second time but published under the name "sinuscalide D", the data of which perfectly match those of scabrolide B, thus further confirming the revision.[30] The objective of this thesis then evolved into accomplishing the first total synthesis of scabrolide B **34**.

The structure of scabrolide B **34** features a 6/7/5/5 skeleton with seven stereocenters, of which six are contiguous. Although relatively few norcembranoids (C19) with this skeleton are known (Figure 1.8), one of these

compounds, ineleganolide **2**,[11] was the target of several synthetic campaigns. Only two of these efforts were successful, and both were published after the start of the work described here.[15-16] Outside of the norcembranoid family, the pambanolides $B_1$ and $B_2$ **36**[31] – isolated as a diastereoisomeric mixture – also share the same polycyclic skeleton (Figure 1.9).

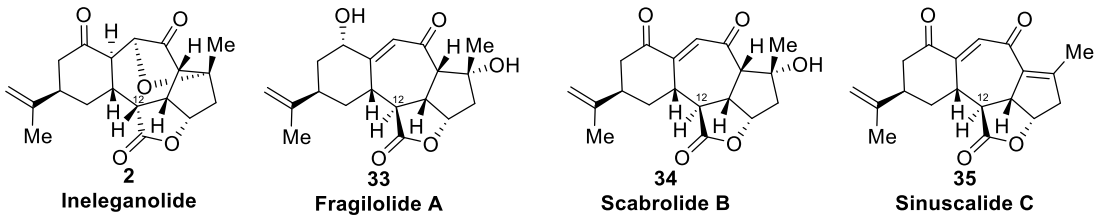


**Figure 1.8.** Norcembranoids featuring the 6/7/5/5 skeleton.

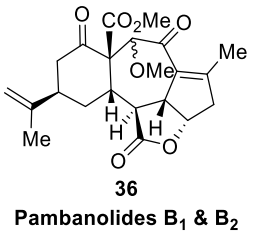


**Figure 1.9.** Other terpenoids featuring the same polycyclic skeleton as **34**.

It is noteworthy that until the isolation of fragilolide A **33**, all the norcembranoids were isolated solely from *Sinularia* soft corals (*Alcyoniidae* family), and were therefore believed to be solely present in this genus. In contrast, fragilolide A **33** was obtained from *Junceella fragilis*, a gorgonian soft coral of the *Ellisellidae* family, along with 5-episinuleptolide **9** and other furanobutenolide-derived norcembranoids. This discovery suggests that this family of molecules may be more widespread than thought, which increases their potential biological relevance.

Although structurally very similar to its congeners with several stereocenters in the same configuration – six out of the seven of scabrolide B **34**, the configuration of the C12 carbon of ineleganolide **2** is inverted compared to all the other compounds shown in Figure 1.7, 1.8 and 1.9, which sets it aside from them. That inverted configuration was a source of several ambiguous or incorrect drawings in

the literature, of either scabrolide B **34**, or ineleganolide **2**, including in the publication where the structure of scabrolide B was reassigned.[15, 29]

When the structural analysis is expanded from the 6/7/5/5 scaffold to the 6/7/5 framework present in ineleganolide **2**, horiolide **3**[32] and kavaranolide **18**[33] emerge as closely related norcembranoids that share a similar carbocyclic skeleton, possess the same C12 configuration, and are suspected to originate biosynthetically from ineleganolide **2** (Scheme 1.2). Neither of these molecules had been synthesized prior to this work (Figure 1.10).

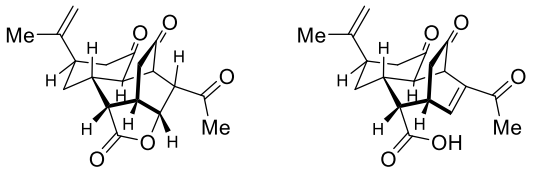


**Figure 1.10.** Structures of norcembranoids horiolide **3** and kavaranolide **18**.

### 1.3.3 Published approaches towards Ineleganolide

The objective of this thesis is the total synthesis of scabrolide B **34**. An examination of previous attempts toward its scaffold can provide valuable information to guide the design of a synthetic approach.

Ineleganolide **2** has been the focus of several synthetic efforts and, until the work presented here, was the only norcembranoid featuring a 6/7/5/5 skeleton targeted by total synthesis. Despite its isolation as early as 1999, a *de novo* synthesis was only achieved at the time of the present thesis, and before that, only a semi-synthesis was known (Scheme 1.4).[25] Two main types of approaches were adopted: *via* synthesis of a macrocyclic intermediate then transannular cyclization to construct the ring system, or *via* direct closure of the central seven-membered ring with a convergently formed polycyclic ring system.

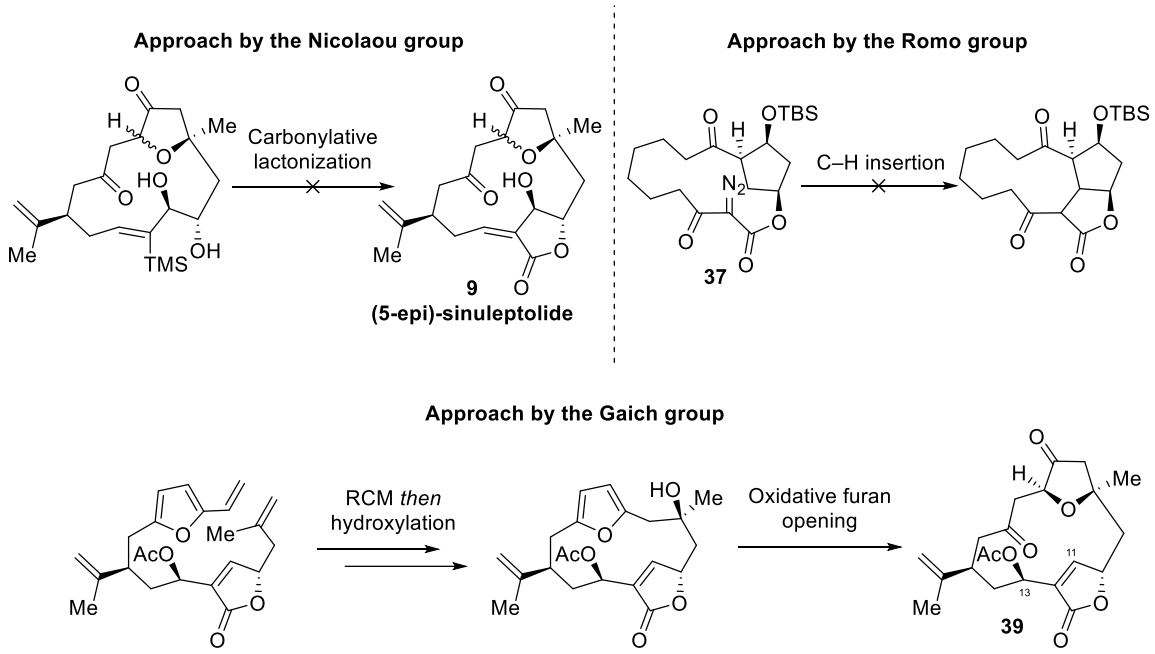


**Scheme 1.6.** Unsuccessful attempts to the synthesis of ineleganolide **2** *via* a macrocyclic intermediate.

Most of the reported approaches relied on macrocyclization. The attempts by the Nicolaou group were thwarted by a failed carbonylative lactonization to compound **9**.[34] The Romo group encountered failure due to an unsuccessful C–H insertion on a model substrate **37**.[35] The Gaich group halted their effort due to side

reactivity observed on macrocycle **39**, isomer of 11-acetyl-5-episinuleptolide (synthesized in the semisynthesis of ineleganolide **2** by the Pattenden group), and due to low material throughput (Scheme 1.6).[36]

Following these unsuccessful forays, the largely bioinspired successful total synthesis of ineleganolide **2** and sinuchmodin C **4** by the Wood group was a major breakthrough in that area (Scheme 1.7).[15] The macrocycle was closed by Nozaki-Hiyama-Kishi cyclization of aldehyde **40** in a similar set up as the total synthesis of intracarene.[37] Next, the tetrahydrofuran ring was installed by singlet-oxygen-mediated-furan oxidation to afford intermediate **41**. Treating that product with LiHMDS, following the same conditions as used in the semi-synthesis by the Pattenden group (Scheme 1.4)[25] triggered a transannular Michael addition which afforded the first synthetic samples of ineleganolide **2** and sinulochmodin C **4**.

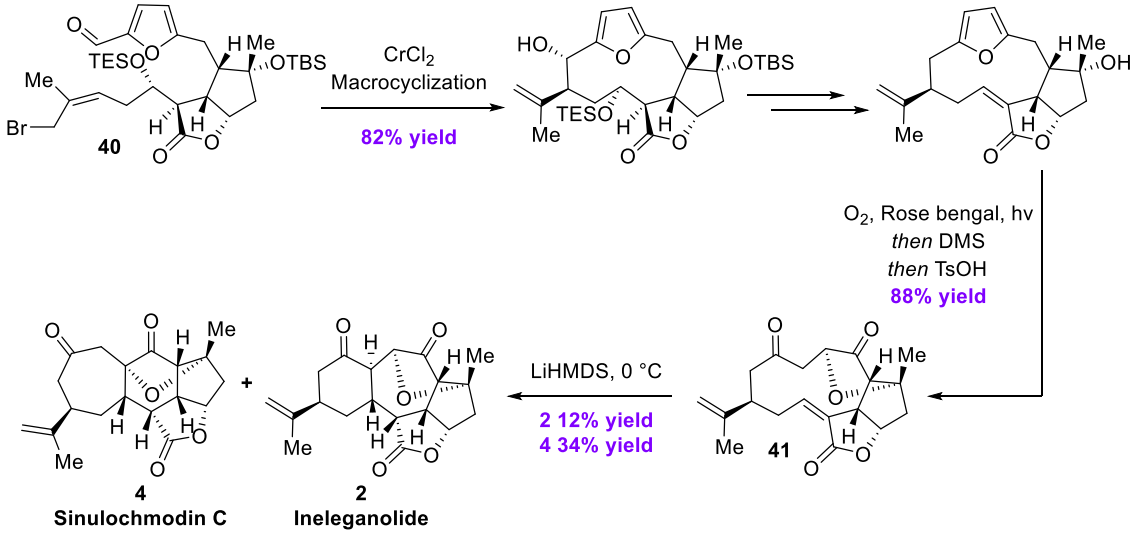


**Scheme 1.7.** The total syntheses of ineleganolide **2** and sinulochmodin C **4** by the Wood group.

The other approaches centered on the formation of the central seven-membered ring. An electrochemical approach to form the central ring of ineleganolide **2** was unsuccessful on a model substrate due to the spatial separation between the coupling sites of the chosen substrate **42** (Scheme 1.8).[38]

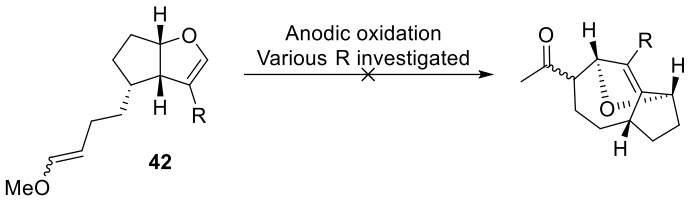


**Scheme 1.8.** Attempted synthesis of the central ring of ineleganolide **2** by an electrochemical method.

The Vanderwal group's attempt to synthesize ent-ineleganolide **ent-2** was thwarted by the impossibility to epimerize the C12 stereocenter after a La-catalyzed diastereoselective Mukaiyama-Michael coupling – these conditions will pave the way to the synthesis described in this thesis. A triflate fragmentation following that epimerization had been envisioned to directly give *ent*-ineleganolide ***ent-2*** (Scheme 1.9).[39]

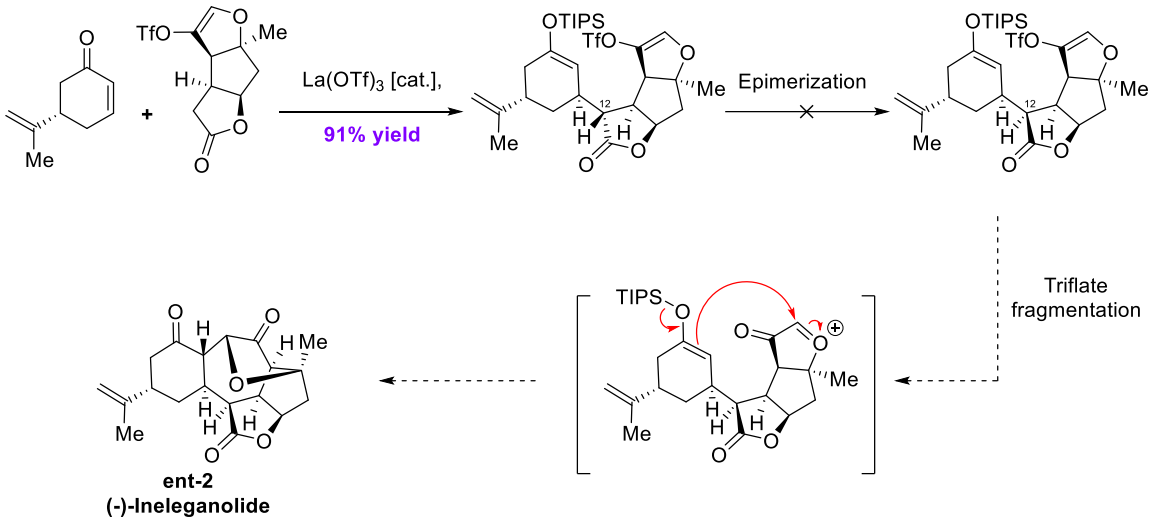


**Scheme 1.9.** Synthetic attempts to ent-ineleganolide **ent-2** by the Vanderwal group.

Extensive studies were made by the Stoltz group towards ineleganolide **2**.[40] They succeeded in forming the central seven-membered ring by intramolecular cyclopropanation of diazo compound **43** which also formed the lactone moiety present in ineleganolide **2**, followed by a Cope-rearrangement on the resulting intermediate **44** to give ketone **45** that bears the polycyclic skeleton of ineleganolide **2** (and scabrolide B **34**). Epoxidation of **45** afforded enone **46**, a formal configurational isomer of ineleganolide **2** (Scheme 1.10).

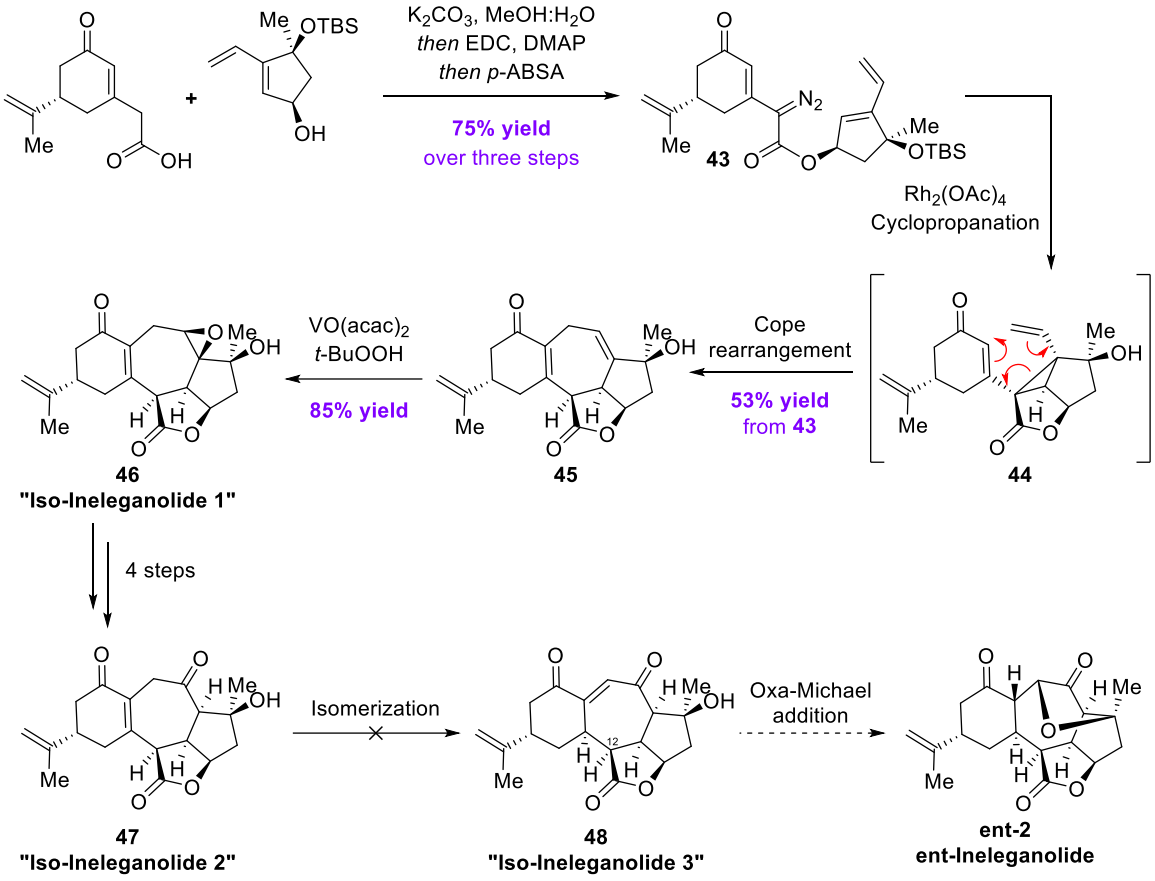


**Scheme 1.10.** Initial synthetic attempts to *ent*-ineleganolide **ent-2** by the Stoltz group.

Attempts to convert enone **46** into the natural product were hampered by competing and unproductive reaction pathways, both during efforts to isomerize **46** and during attempts to construct the tetrahydrofuran ring. After extensive studies, these studies instead led to the formation of intermediate **47**, another configurational isomer of ineleganolide **2**. However, isomerization of **47** into **48** – which is also the 12-epimer of the enantiomer of natural scabrolide B **34** (the structure of which was not known at the time of these attempts) could not be achieved. Had this transformation been possible, only a final oxa-Michael addition would have been required to reach ent-ineleganolide **ent-2**. Consequently, this route was abandoned.

During the course of the work in the present thesis, the Stoltz group disclosed a successful total synthesis of ineleganolide **2** (Scheme 1.11).[16] Fragment coupling was achieved by esterification between acid **49** and enone **50** under specially

developed conditions involving activation of the acid **49** as a triphenylphosphonium salt, furnishing ester **51**. An intramolecular Michael addition then provided lactone **52**, followed by an intramolecular aldol reaction – proposed to proceed via intermediate **53** – that formed the central six-membered ring. This key transformation is believed to involve two successive deprotonations at the C12 stereocenter — a challenge that had previously impeded the Vanderwal group's approach to **ent-2**. Double-bond isomerization of alcohol **54** subsequently installed the correct stereochemistry on C12, yielding compound **55**.

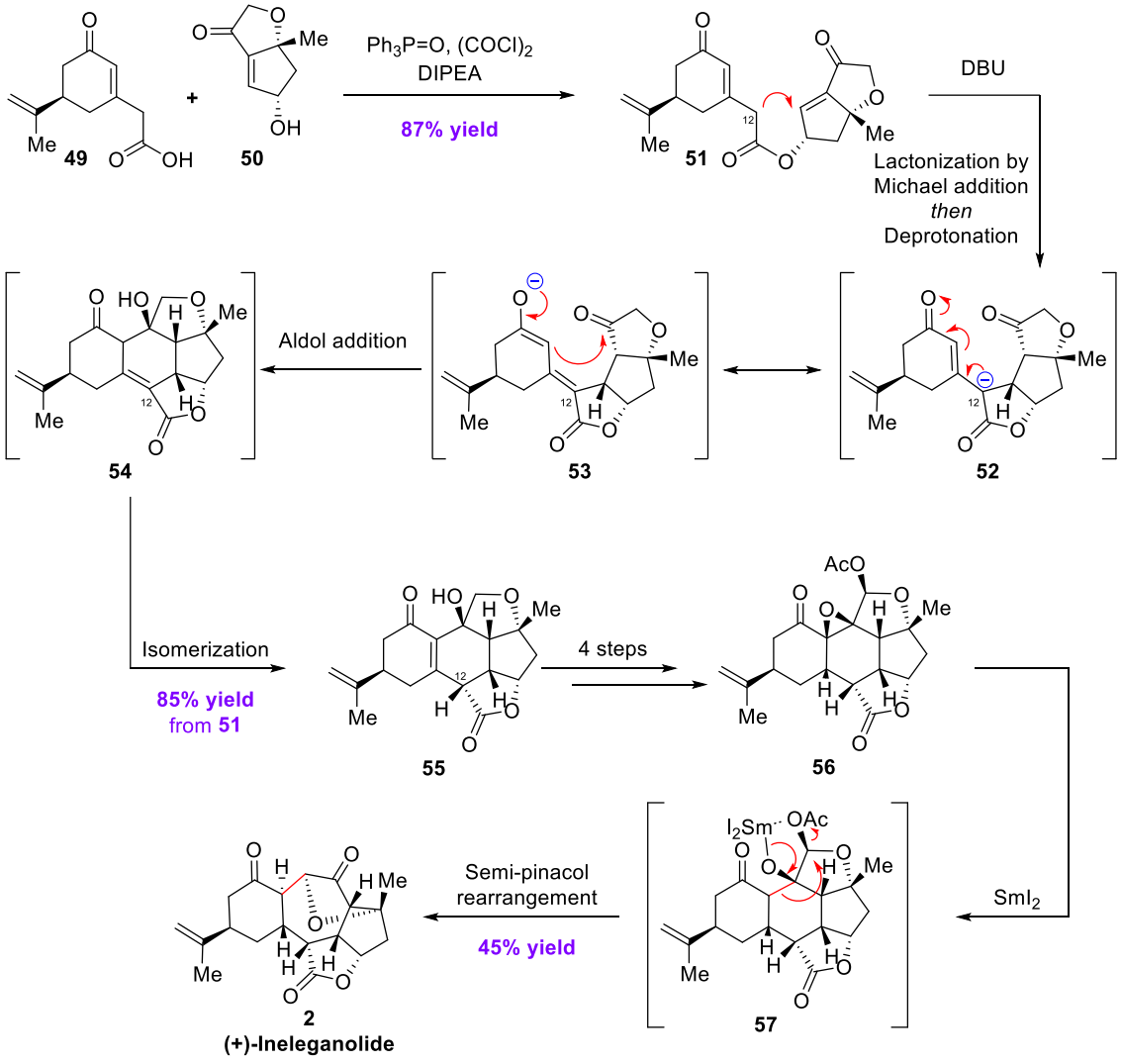


**Scheme 1.11.** The total synthesis of ineleganolide **2** by the Stoltz group.

Oxidative manipulations of **55** afforded lactone **56**, which upon reductive epoxide opening underwent a semi-pinacol rearrangement that expanded the

central ring, furnishing ineleganolide **2**. The rearrangement is proposed to proceed via intermediate **57**.

Following the publication associated with the present thesis, the Sarlah group disclosed their approach to scabrolide B **34** and its transformation into ineleganolide **2** (Scheme 1.12).[41] Although the key intermediates in their synthesis are extremely similar to those of the present work — the main difference lying in a Mukaiyama–aldol reaction used to close the central seven-membered ring — the failed attempts nevertheless provide valuable insight.[42]

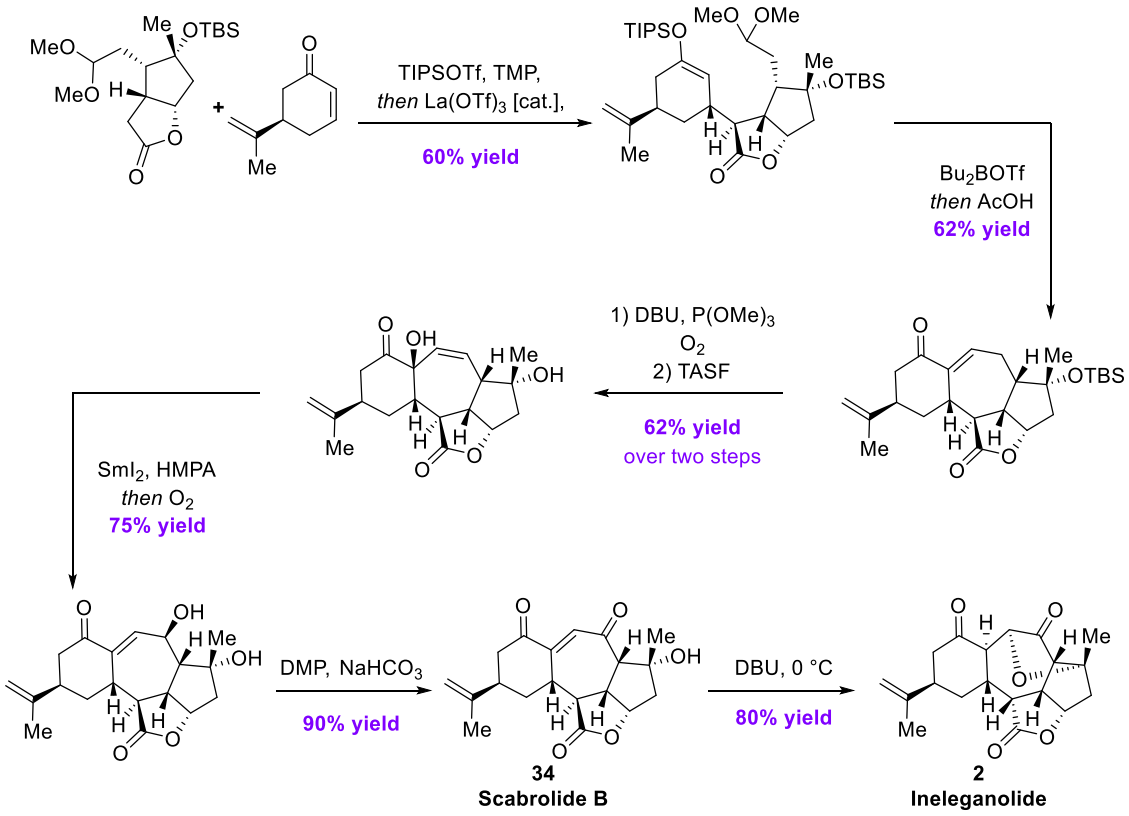


**Scheme 1.12.** The total syntheses of scabrolide B **34** and ineleganolide **2** by the Sarlah group.

Notably, attempts to form the central six- or seven- membered ring through C12-C13 bond formation, largely inspired by that group's earlier total synthesis of scabrolide A,[43] led primarily to the wrong stereochemistry at C13. Correction of this stereochemical outcome proved difficult at later stages, owing to the presence of several more acidic protons in the intermediates. Consequently, the route was

revised to establish the C12-C13 bond prior to construction of the central ring (Scheme 1.13).

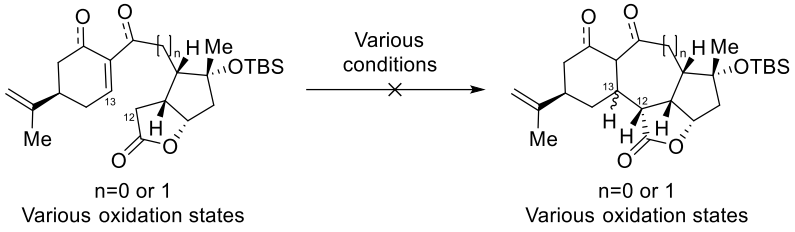


**Scheme 1.13.** Attempts by the Sarlah group to close the central ring *via* formation of the C12-C13 bond.

Finally, as the present thesis was being completed, the Maimone group reported their total synthesis of ineleganolide **2** (Scheme 1.14).[44] Fragment coupling was achieved via a De Mayo cascade. UV-irradiation of **58** and **59** produced cyclobutane **60** as a single diastereomer. The observed *trans*-relationship between the C4 and C13 hydrogen atoms is inconsistent with a concerted photochemical [2+2] cycloaddition, suggesting a stepwise mechanism.

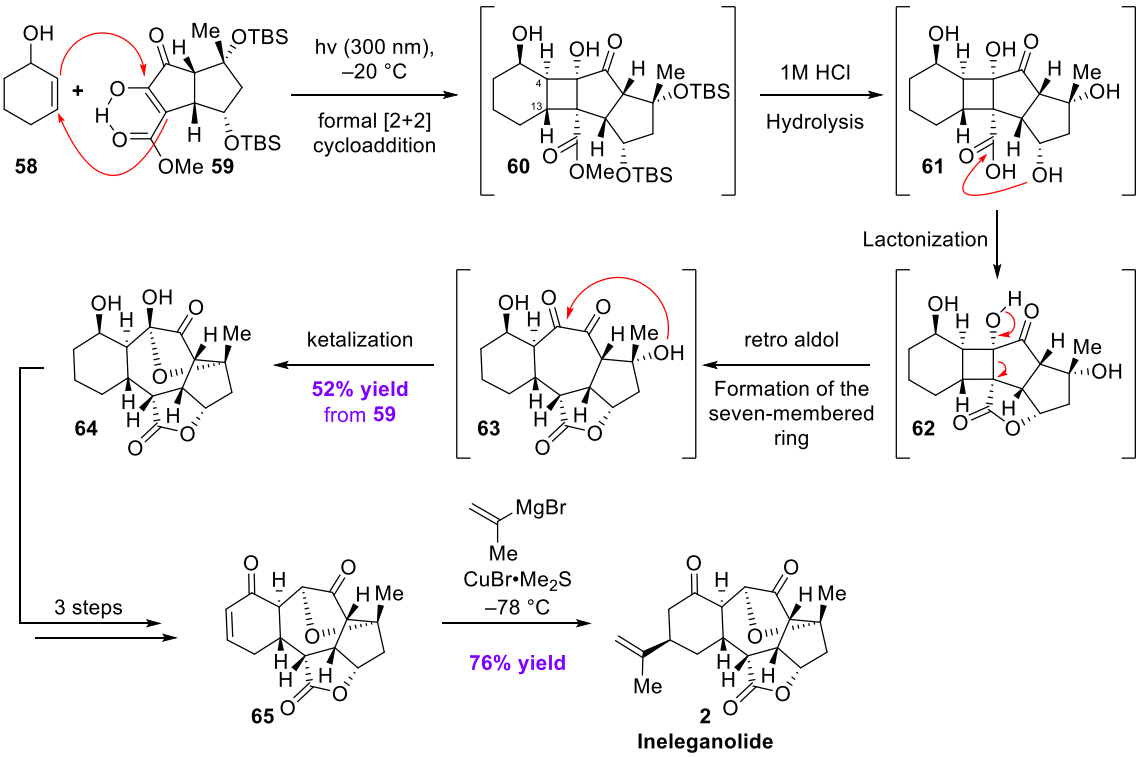


**Scheme 1.14.** The total synthesis of ineleganolide **2** by the Maimone group.

Subsequent treatment of **60** with HCl hydrolyzed both TBS ethers, giving acid **61**, which lactonized to give intermediate **62**. A retro-aldol reaction followed by opening of the cyclobutane effected a formal four- to seven- membered ring expansion, affording product **63**. Ketalization then delivered intermediate **64**, forming the characteristic tetrahydrofuran ring of ineleganolide **2** and establishing four of its stereocenters in 52% yield over this cascade. Installation of the isoprene side chain via cuprate 1,4-addition to enone **65** completed the synthesis.

# 2. First approach: by RCM to form the C5-C6 bond of Scabrolide B

## 2.1 Preliminary studies

The preliminary studies were performed by Dr. Zhanchao Meng and Dr. Georg Späth. This chapter represents a summary of their results.

### 2.1.1 Initial retrosynthesis

With regard to the existing prior art at the start of this project (no total syntheses of ineleganolide **2** were published and the structure of scabrolide B **34** was not yet formally reassigned by X-ray crystallography), a convergent approach was envisioned (Scheme 2.1).

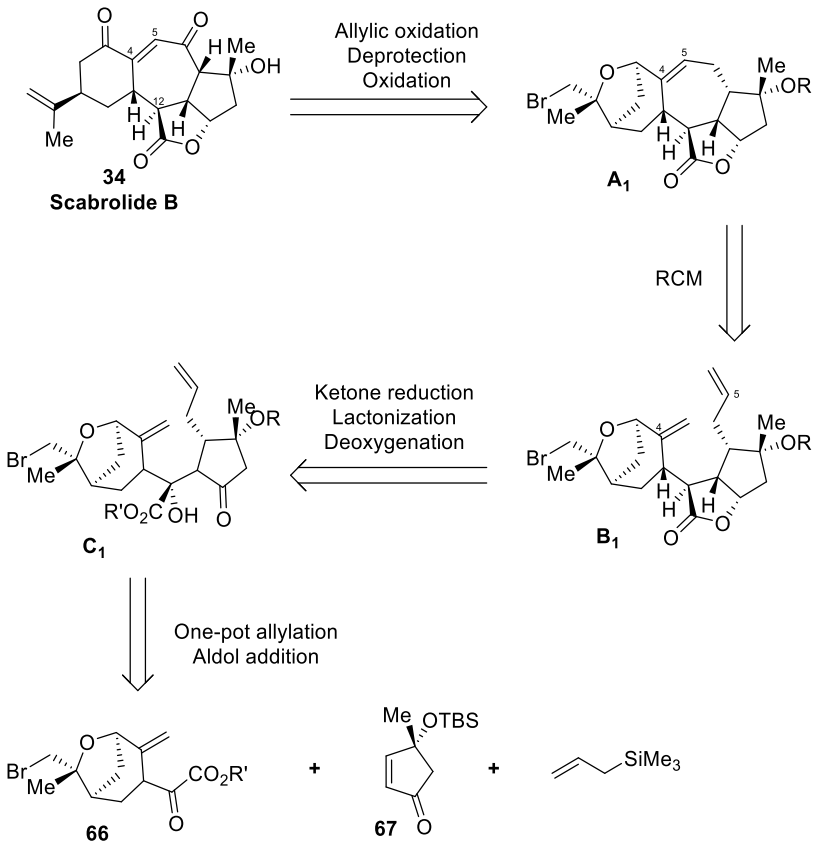


**Scheme 2.1.** Initial retrosynthetic analysis of scabrolide B **34**.

It was decided to take an approach *via* closure of the central seven-membered ring by RCM reaction, in close analogy to our own published total synthesis of putative scabrolide B **20**.[14] As the 1,1-substituted alkene of scabrolide B **34** could

interfere with the RCM step, the western part of the natural products could be protected in form of a bromohydrin. Scabrolide B **34** was therefore envisioned to be synthesized from bromohydrin $\mathbf{A_1}$ *via* allylic oxidation, followed by deprotection of the bromohydrin and oxidation. $\mathbf{A_1}$ could be obtained by RCM of diene $\mathbf{B_1}$, forming the C4-C5 bond of the natural product. $\mathbf{B_1}$ could be synthesized from ketone $\mathbf{C_1}$, which in turn could be produced by a one-pot allylation/aldol addition from ester **66**, enone **67** and trimethyl allyl silane (Scheme 2.1).

### 2.1.2 Initial attempt

The first attempt involved a one-pot allylation/aldol coupling of cyclopentenone **67**[14] and bromohydrin ester **66** (synthesized from bromohydrin **68**).[45] The resulting product **69** could then undergo dehydration to **70**, which would lead to the natural product *via* redox adjustments, lactonization and RCM to form the central seven-membered ring. The bromohydrin there acts as a protecting group of the 1,1-disubstituted alkene, which may react during the envisaged ring-closing alkene metathesis.

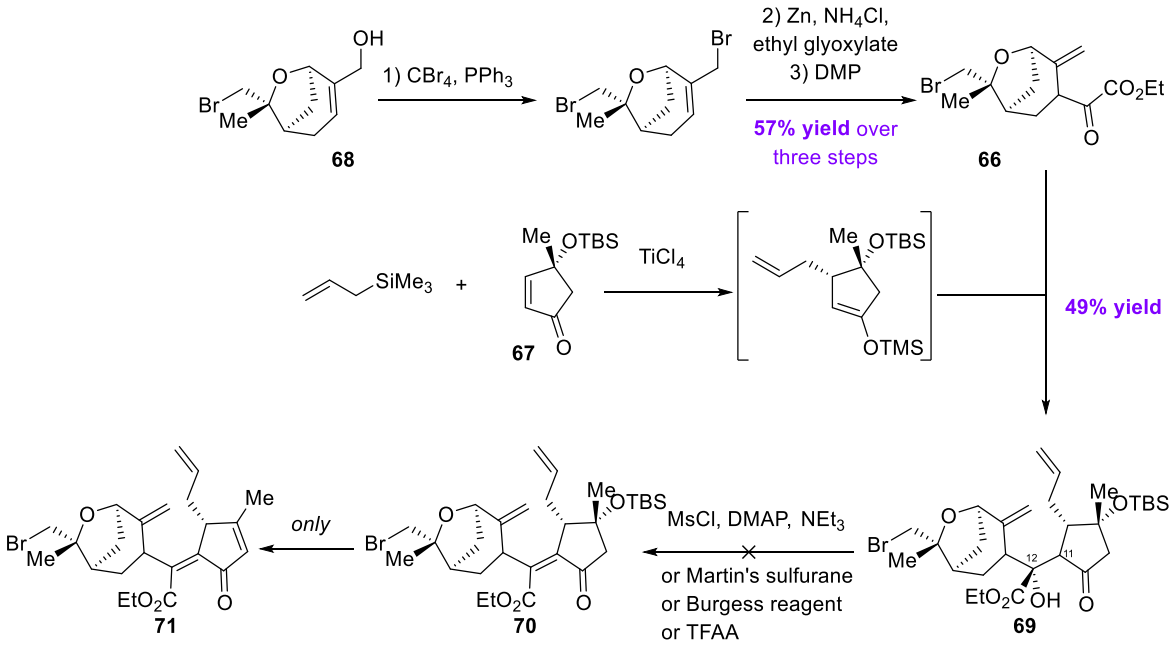


**Scheme 2.2.** Initial synthetic attempt to precursor of scabrolide B **34**.

The allylation/aldol sequence proceeded with 49% yield of a 2:1 C12 diastereoisomeric mixture of compound **69**, following conditions reported by the Danishefsky group.[46] Dehydration of **69** failed, resulting in either no reaction, or additional elimination of the C8 silyl ether to form enone **71**. Correction of the stereochemistry of C11 by hydrogenation, projected on enone **70**, would lead to chemoselectivity problems with **71**. It was therefore decided to fix the stereochemistry of that center at an earlier stage.

### 2.1.3 Revised retrosynthesis

Following the unsuccessful synthesis of the initially precursor planned for central ring-closure, revision of the retrosynthesis was necessary. RCM was proposed on diene **B**$_2$ to form the C5-C6 bond of the natural product, affording alkene **A**$_2$, which could in turn lead to the natural product after adjustment of the oxidation pattern and bromohydrin cleavage (Scheme 2.3).

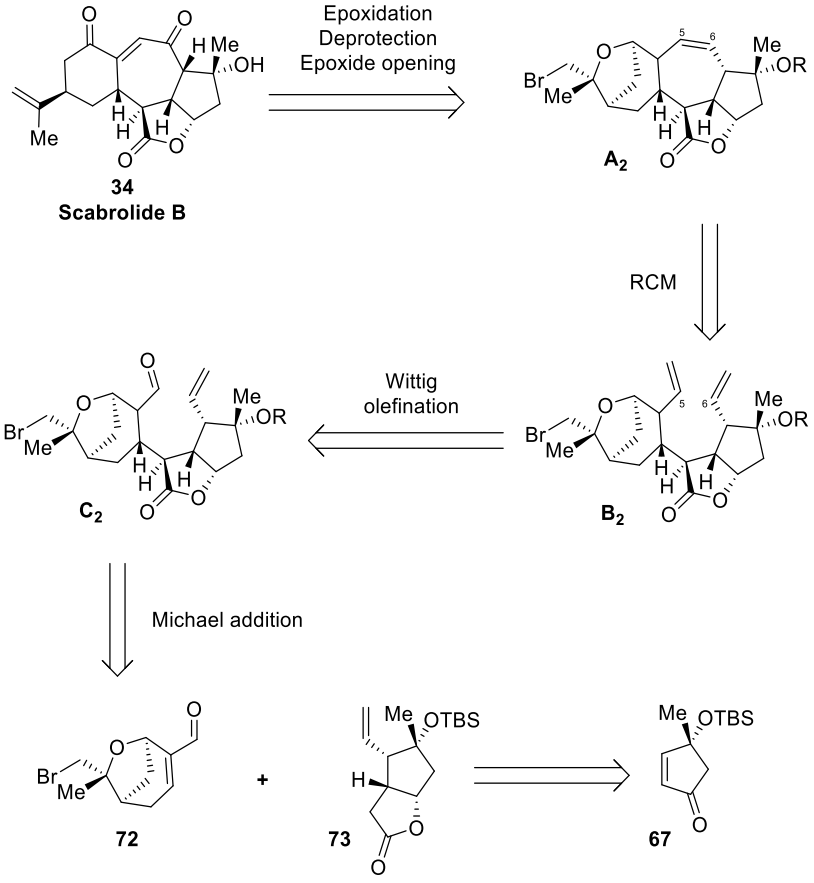


**Scheme 2.3.** Updated retrosynthetic analysis of scabrolide B **34**.

The bromohydrin not only protects the 1,1-disubstituted alkene during the RCM, but also avoids chemoselectivity issues during the epoxidation. Diene **B**$_2$ could be synthesized by Wittig olefination of **C**$_2$ which in turn could be traced back to bromohydrin **72**[45] and lactone **73** *via* Michael addition. **73** had already been synthesized in the total synthesis of putative scabrolide B from enone **67**.[14]

### 2.1.4 Second attempt

In a second approach, coupling of the [5,5]-bicyclic lactone **73** with the known bromohydrin **72** was investigated. The required lactone had already been synthesized in the total synthesis of scabrolide A **5**,[14] and a similar diastereoselective fragment coupling had been described by the Vanderwal group in their attempt to ineleganolide **2**.[39a] Indeed, fragment coupling of **73** and **72** proceeded under the described Mukaiyama-Michael conditions (with low yields, unoptimized). Deprotection of silyl enol ether **74** followed by Wittig reaction (which was accompanied by bromine extrusion) then formed epoxide **75**, which could equally serve as a masked alkene. Because installation of the final oxidation pattern of scabrolide B **34** was planned via a hydroxy-directed epoxidation analogous to the one described in the total synthesis of scabrolide A **5**,[14] silyl ether deprotection was undertaken at this stage. The attempts were unfortunately not fruitful, resulting in either no reaction, or in a mixture containing the desired product **76** alongside fluorohydrin **77** formed by epoxide opening by a fluoride source (Scheme 2.4).

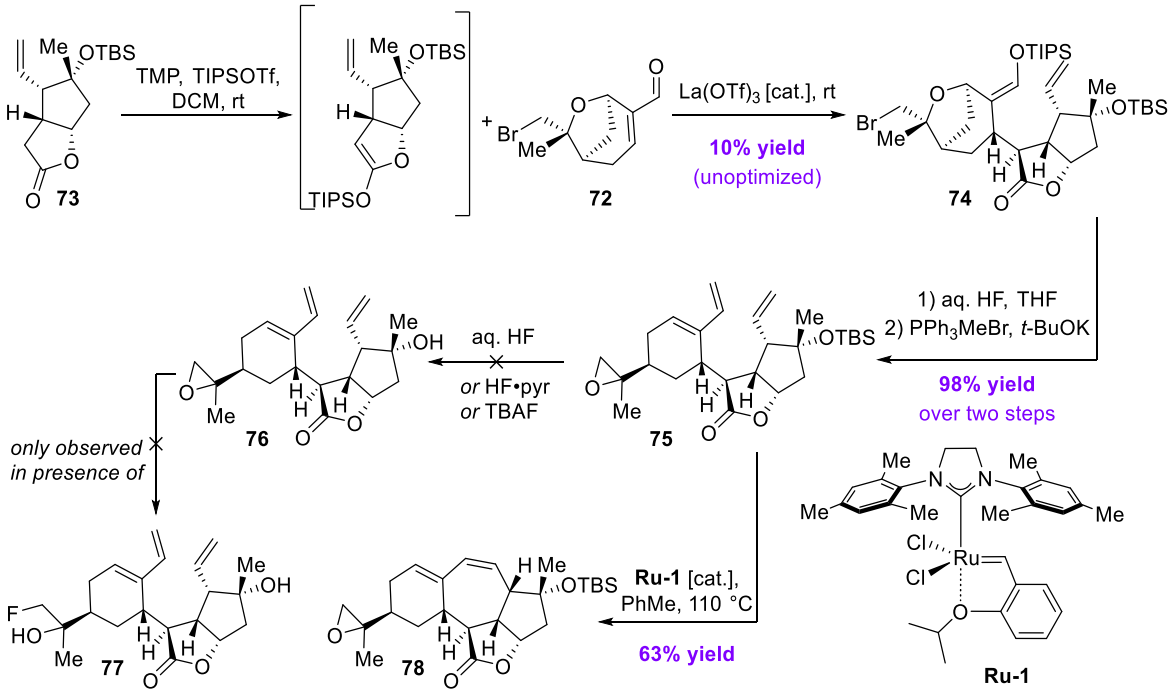


**Scheme 2.4.** Second synthetic approach to the synthesis of scabrolide B **34** – with a TBS protecting group.

Therefore, RCM was attempted on alkene **75**, using the second generation Hoveyda-Grubbs catalyst **Ru-1**. The reaction proceeded smoothly, proving ring-closed product **78** in 63% yield (unoptimized). The results suggest that the tertiary TBS silyl ether will not impede the ring closure.

To circumvent the deprotection issues, the TBS silyl ether was deprotected on lactone **73**. Alkene **79** was obtained following the same sequence (Scheme 2.5). To investigate the compatibility of the RCM with the 1,1-disubstituted alkene, **79** was successfully deoxygenated to give the tetraene **80**. Exposing **80** to **Ru-1** catalyst in refluxing toluene provided the ring-closed product **81** in 69% yield, with ruthenium impurities which could not be removed by chromatography. Remarkably, the 1,1-disubstituted alkene here did not interfere with the reaction.

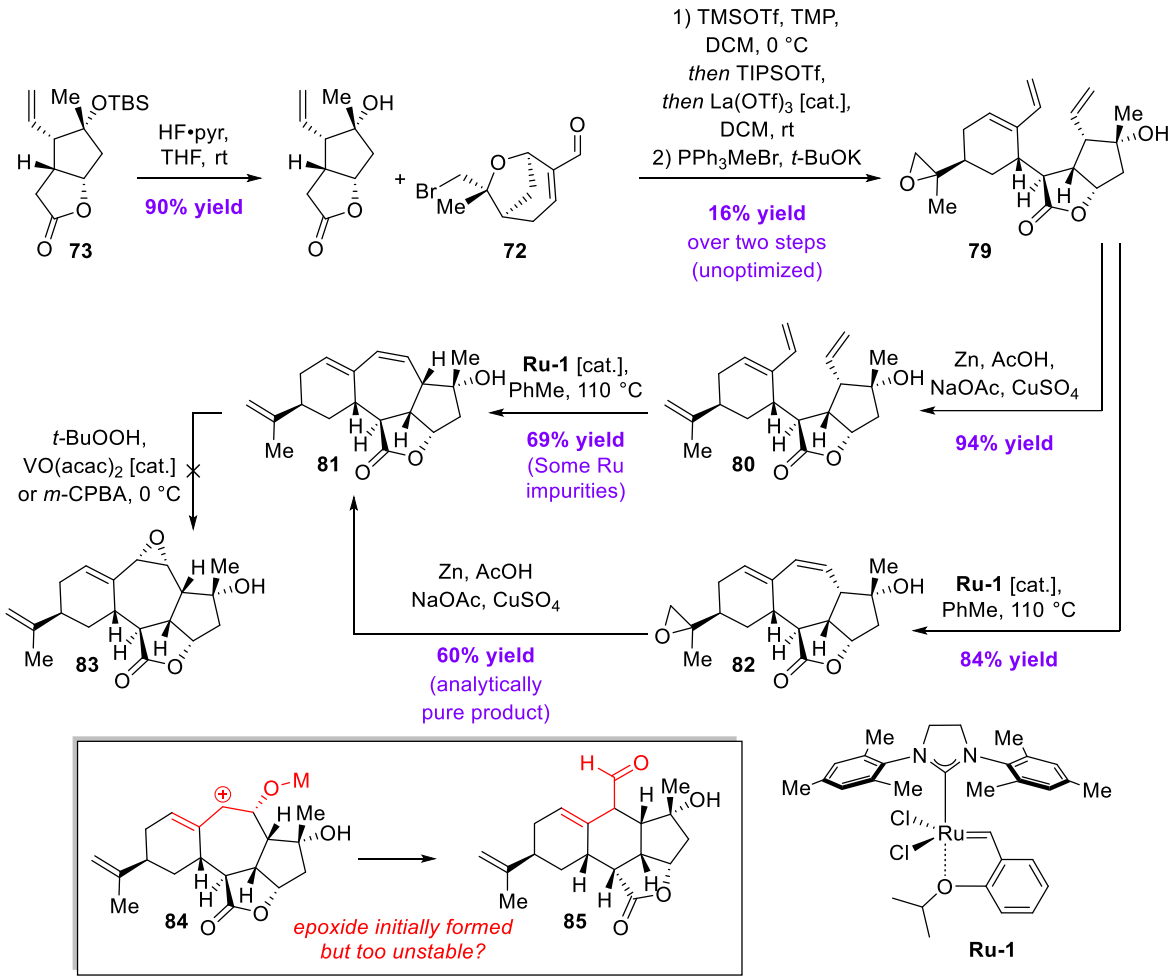


**Scheme 2.5.** Alternative synthetic attempt to scabrolide B **34** – with a TMS protecting group.

That mixture was subjected to vanadium-catalyzed hydroxy-directed epoxidation, but several side products were observed, potentially due to the trace metal impurities. To circumvent that issue, the order of the steps was changed. RCM on triene **79** gave analytically pure epoxide **82** which was then deoxygenated to give trace-metal-free product **81**.

To our dismay, epoxidation of this compound still featured the same disastrous reaction profile, regardless of reaction time and temperature. The analyses of the $^{1}$H NMR spectras of the complex crude mixtures revealed peaks in the aromatic and the aldehyde region. Possibly, the desired epoxide initially forms but then decomposes under the reaction conditions. That could be rationalized by a stabilized allylic cation **84** formed by opening of the epoxide, which may undergo ring-contraction to form aldehyde **85**. Other oxidants were attempted and similar results were observed. The route therefore needed to be redesigned.

## 2.2 Revised approach – retrosynthesis

Three key takeaways from the previous experiments led to a redesign of the retrosynthetic pathway: protection of the 1,1-disubstituted alkene is not necessary for the RCM reaction to be successful, RCM process to close the ring system via the C5–C6 bond is possible, and an alternative oxidation pattern around the C4 position is required. A new retrosynthetic analysis was therefore devised (Scheme 2.6). Scabrolide B **34** could be synthesized from alkene **A**$_3$ by an epoxidation/epoxide opening/oxidation sequence. **A**$_3$ could be traced back to triene **B**$_3$ *via* RCM reaction, which itself originates from ketone **C**$_3$ by various functional transformations. The required ketone **C**$_3$ could be obtained by substrate-controlled 1,4-addition of lactone **73** on a *(R)*-carvone derivative. Lactone **73** (eastern fragment) is literature-known, and is synthetized in nine steps from *(R)*-linalool.[14]

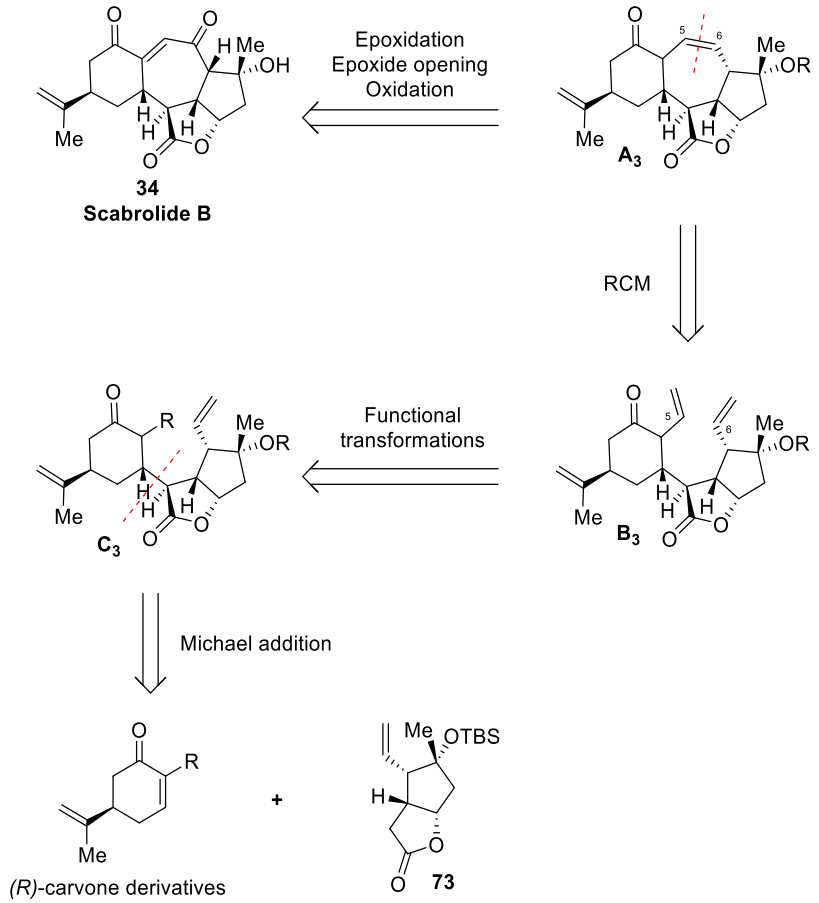


**Scheme 2.6.** Retrosynthetic analysis to the ring-closing precursor to scabrolide B **34**.

## 2.3 Fragment syntheses

### 2.3.1 Eastern fragment

The synthesis of the eastern fragment was reported in the total synthesis of scabrolide A **5**.[14] It begins with a RCM of (*R*)-linalool, followed by TBS protection and C–H oxidation to afford Maimone's enone **67**.[47] An $AlCl_3$-mediated counter-steric Diels-Alder cycloaddition with butadiene, followed by a face-selective reduction with L-selectride, provided alkene **86** (Scheme 2.7). The stereochemical outcome of the Diels-Alder reaction is proposed to arise from coordination of the tertiary silyl ether oxygen to the Lewis acid.[46]

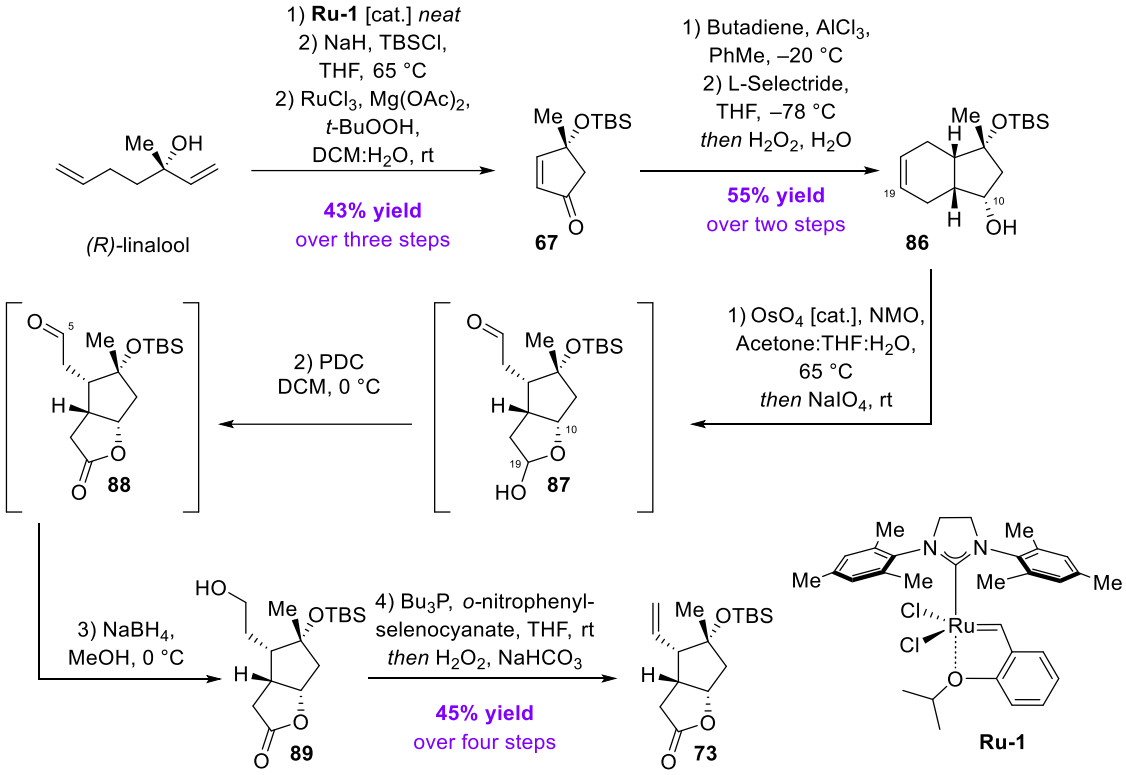


**Scheme 2.7.** Synthesis of the eastern fragment **73** from *(R)*-linalool.

Alkene **86** was then oxidized under Lemieux-Johnson conditions, as the original ozonolysis procedure used for alkene cleavage could not be reproduced.[14] This afforded lactol **87** through intramolecular addition of the C10-OH group to the aldehyde generated at C19 (scabrolide B numbering); oxidation of lactol **87** yielded lactone **88**, subsequent treatment with $NaBH_4$ reduced the aldehyde at C5 to the corresponding alcohol **89**. Dehydration of this alcohol under Grieco

conditions furnished lactone **73** with 11% overall yield over nine steps (Scheme 2.7).

With the eastern fragment in hand, our efforts then focused on the synthesis of the possible western fragments.

### 2.3.2 Possible western fragments: a collective synthesis

Note: the selenide **94** was initially prepared by Dr. Zhanchao Meng.

For exploratory purposes, we envisioned a divergent synthesis of the possible western fragments. To this end, we employed the bromohydrins used previously as a common intermediate.

*(L)*-Carveol (1:1 mixture of *cis* and *trans* isomers) was bromoetherified with NBS, and the resulting product was subjected to Riley oxidation with $SeO_2$ to give a mixture of bromohydrins **68** and **72** (Scheme 2.8).[45] The protection as a bromohydrin serves two purposes: it avoids chemoselectivity issues during the allylic oxidation, and masks the alcohol that could interfere with the projected functionalization chemistry.

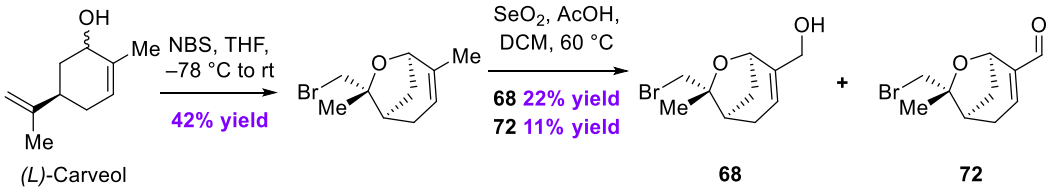


**Scheme 2.8.** Syntheses of bromohydrin **54** and **58**.

A sequence of functional-group interconversions on either the alcohol **68** or the aldehyde **72** enabled access to various targeted carvone derivatives (Scheme 2.9).

From alcohol **68**, OTBS-carvone **91** was obtained *via* TBS protection to give allyl ether **90**, followed by bromohydrin opening and DMP oxidation. Ester **93** was prepared by Jones oxidation of alcohol **68** followed by Fischer esterification to furnish unsaturated ester **92**, and subsequent bromohydrin opening and DMP oxidation.

For the synthesis of alkyl selenide **95**, aldehyde **72** was homologated *via* a Wittig reaction, and the resulting diene was hydroborated with 9-BBN. Introduction of the phenylselenide moiety afforded selenide **94**, whose bromohydrin was then opened. For this substrate, both DMP (slightly acidic) and Swern (slightly basic) oxidation led to decomposition upon solvent removal. Neutral oxidation

conditions were therefore needed, and $MnO_2$ provided the desired selenide **95** in 32% yield from **72**.

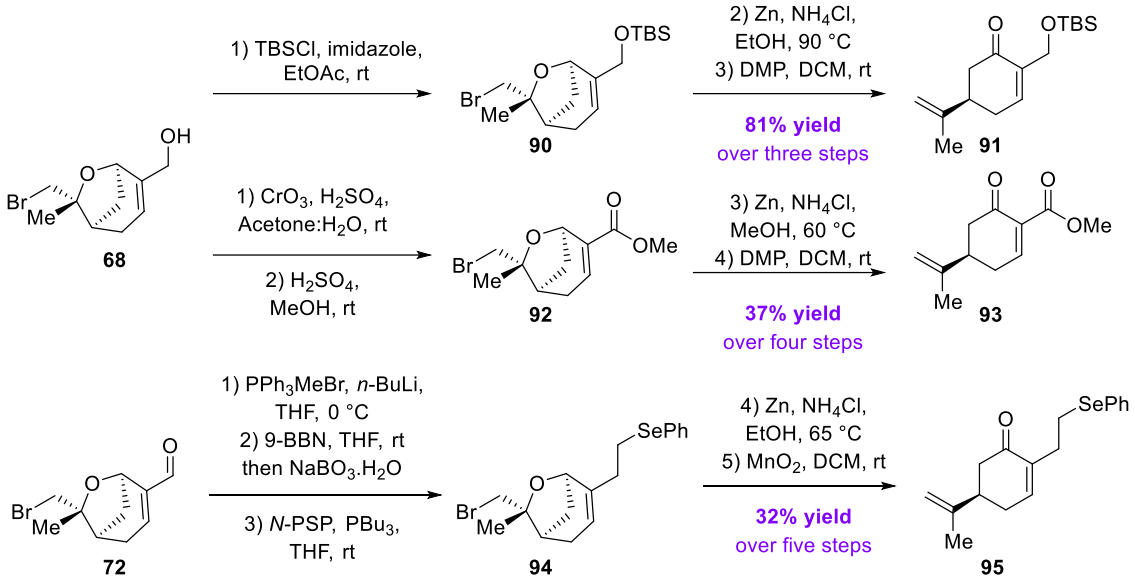


**Scheme 2.9.** Divergent synthesis of various *(R)*-carvone derivatives **91**, **93** and **95**.

### 2.3.3 De novo synthesis of *(R)*-norcarvone

The *de novo* synthesis of *(R)*-norcarvone **96** was performed by Dr. Georg Späth. This chapter represents a summary of his results.

In the literature, *(R)*-norcarvone **96** is synthesized by laborious routes, starting from *(R)*-carvone and proving **96**; seven steps are needed to remove a single carbon atom.[48] A more efficient route was therefore investigated here. Pleasingly, a recent set of conditions for the Rh-catalyzed enantioselective 1,4-addition to cyclohex-2-en-1-one could be utilized, providing **99** with 87% yield and *94% ee* on 2.5 g scale – that transformation has been reported on a preparative scale of 130 kg.[49] Subsequent kinetic deprotonation of this ketone with LiTMP gave the distal silyl enol ether **100** as the major isomer (distal:proximal=5:1). Saegusa-Ito oxidation of the crude mixture gave *(R)*-norcarvone **96** as a single isomer (Scheme 2.10).[50]

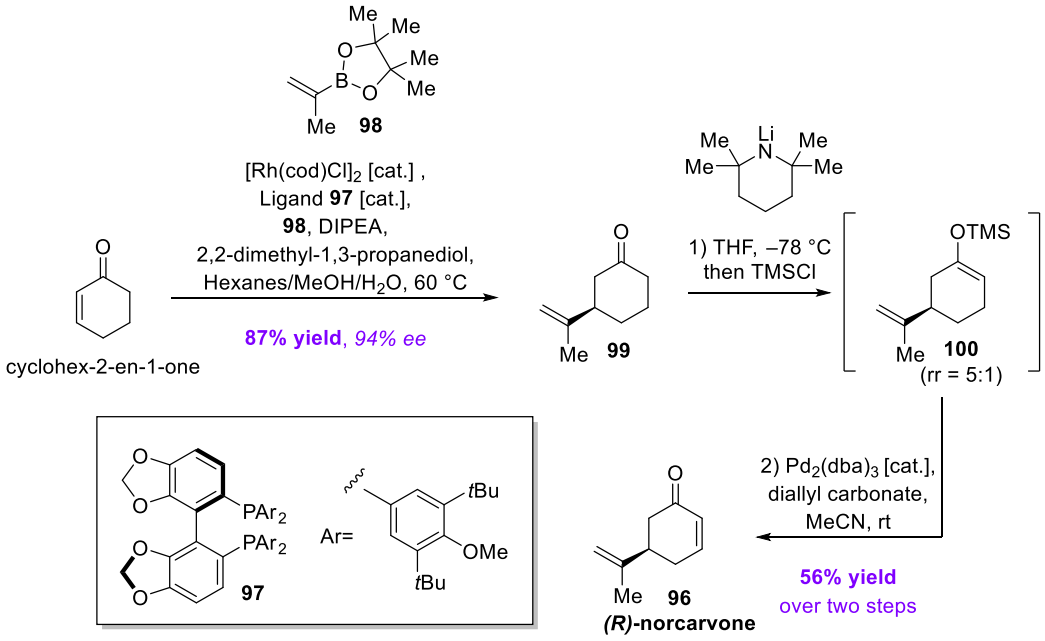


**Scheme 2.10.** Three steps synthesis of *(R)*-norcarvone **96** from cyclohex-2-en-1-one.

It should be noted that enone **96** is not chromatographically separable from the dibenzylideneacetone ligand, and purification of the product required a distillation of the crude material to leave back the ligand, followed by

chromatographic purification of the distillate. Despite this somewhat more laborious procedure, the reaction worked well on 1.5 g scale. Very interestingly, the described route here has already been proposed by the Vanderwal group, and pursued on a racemic substrate.[39b] However, the alkenylborate **98** or its trifluoroborate required for the enantioselective addition were not commercially available, and no solution was found for the purification of enone **82** from dibenzylideneacetone. For these reasons, this route had not been further explored in their studies.

### 2.3.4 Alternative synthetic approach to the selenide fragment 95

As selenide **95** will later appear as the only suitable western fragment to the desired RCM precursors, a more efficient and tailored route was envisioned.

Enantiopure limonene oxide was quantitatively opened with LDA to give allyl alcohol **101** (Scheme 2.11). At this stage, we could either perform an oxidation followed by cyclopropanation on the resulting enone **102** or carry out a hydroxy-directed cyclopropanation prior to oxidation. Because the enone **102** obtained by direct oxidation of alcohol **101** is known to dimerize *via* a hetero-Diels-Alder reaction to dimer **103**,[51] the latter sequence was chosen.

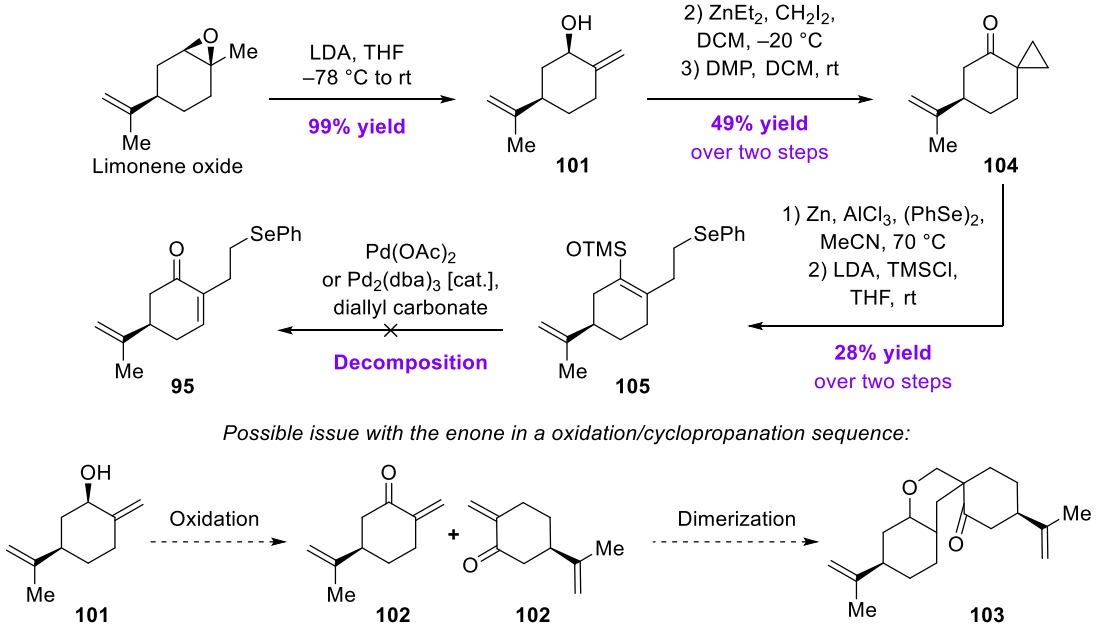


**Scheme 2.11.** Attempted synthesis of selenide **95** *via* cyclopropane opening.

Hydroxy-directed Simmons-Smith cyclopropanation on allyl alcohol **101** using the conditions of the Charette group,[52] followed by oxidation with DMP furnished cyclopropane **104**. Addition of a zinc selenolate then introduced the phenylselenide with concomitant cyclopropane opening,[53] and TMS-protection of the resulting ketone afforded silyl enol ether **105** with 28% yield over two steps (unoptimized). Compound **105**, however, proved unsuitable for Saegusa–Ito oxidation, decomposing under all conditions examined (Scheme 2.11). The route was therefore abandoned.

## 2.4 Fragment coupling

### 2.4.1 Coupling studies – unsaturated ketoester

Unsaturated keto-ester **93** turned out to be too unstable under any of the tested coupling conditions (Scheme 2.12).[39a, 54] When the silyl ketene acetal was formed *in-situ* with excess base, decomposition of ketoester **93** occurred at –78 °C. Exposure of **93** to pre-isolated silyl ketene acetal **107** in presence of a range of Lewis acid did not give any conversion either. It is to note that under these base-free conditions, decomposition of ketoester **93** only occurred when the reaction temperature was raised to –20 °C or higher. With a suitable Lewis acid, coupling with **93** could then *potentially* be suitable at –40 °C or below, but the investigations were not pursued further, due the inherent instability of **93** under the required conditions.

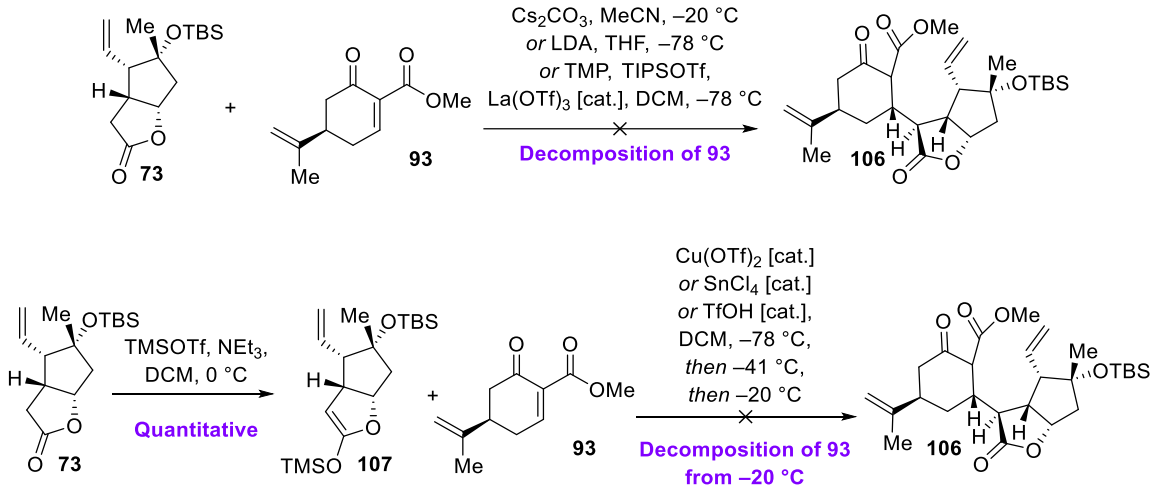


**Scheme 2.12.** Coupling attempts of **73** with unsaturated keto-ester **93**.

### 2.4.2 Coupling studies – protected hydroxycarvone

Coupling with the protected hydroxycarvone **91** was initially explored *via* in-situ formation of a TMS ketene acetal **107**, followed by activation with a Lewis acid. However, none of the conditions examined proved suitable for this transformation (Table 2.1).[39a, 54b, 55] $La(OTf)_3$ and $SnCl_4$ resulted in no reaction, while $TiCl_4$ provided only partial conversion to a 1:1 mixture of diastereomers—comprising the desired product **108** and a compound tentatively assigned as its C13 epimer. This outcome was unexpected, as a closely related precedent reported successful coupling using a TIPS silyl ketene acetal and $La(OTf)_3$ in the approach of the Vanderwal group to ineleganolide **2** (Scheme 2.13).[39a]

**Table 2.1.** Screening of Lewis acids for the Mukaiyama-Michael addition to enone **91** with TMS ketene acetal **107**.

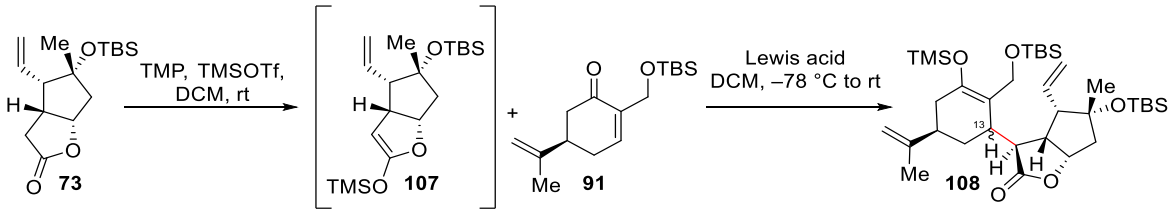


| Entry | Lewis acid | Results (qualitative, from crude $^1H$ NMR) |
|---|---|---|
| 1 | $La(OTf)_3$ (0.1 to 1.0 eq) | No reaction |
| 2 | $SnCl_4$ (0.1 eq) | No reaction |
| 3 | $TiCl_4$ (0.1 eq) | **35% conversion**<br>No diastereoselectivity |
| 4 | $TiCl_4$ (0.1 then 1.0 eq) | 0.1 eq: **30% conversion**<br>1.0 eq: decomposition of **108** |

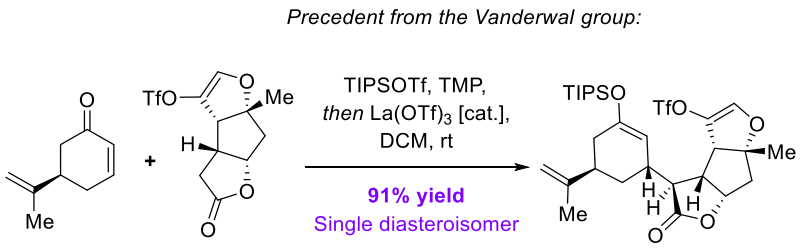


**Scheme 2.13.** Precedent on a similar diastereoselective Mukaiyama-Michael addition on a *(R)*-carvone derivative by the Vanderwal group.

Fragment coupling was therefore attempted using the corresponding TIPS silyl ketene acetal **109** under the reported conditions (Scheme 2.14). This approach afforded the desired product as a 1:1 mixture of diastereoisomers **110**, as previously observed with the TMS variant. However, the product proved unstable under all conditions examined for silyl ether deprotection.

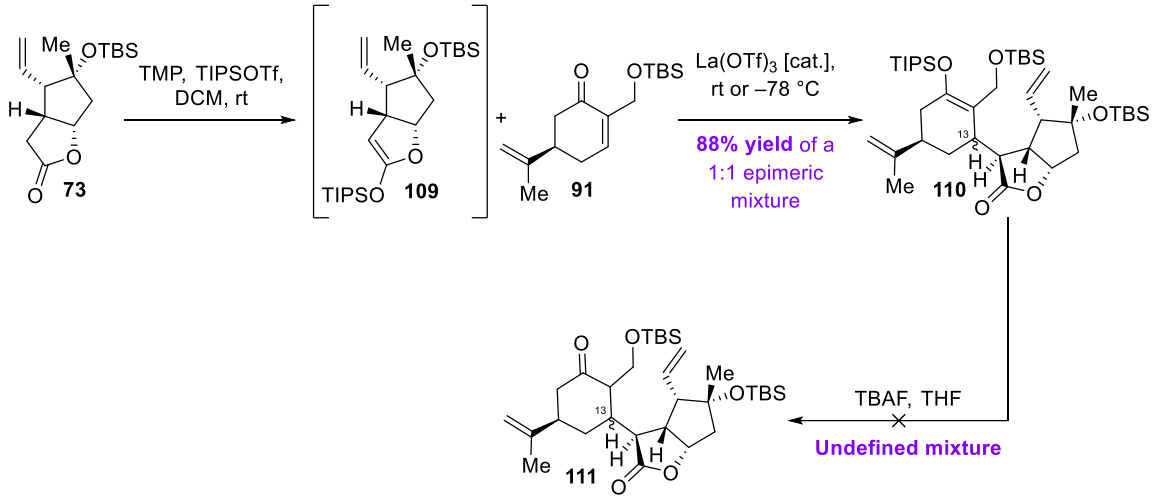


**Scheme 2.14.** Coupling attempts of enone **91** with TIPS ketene acetal **109**.

The contrasting reactivity observed with $La(OTf)_3$ is particularly surprising. Formation of the TMS silyl enol ether **107** from the lactone is rapid and essentially quantitative within minutes, yet no coupling occurs under these conditions. In contrast, generation of the TIPS silyl enol ether **109** is slow and incomplete—at best producing a ~1:1 mixture of silyl ketene acetal and unreacted lactone—yet this more sterically demanding mixture undergoes smooth Michael addition to enone **91**. These findings suggest that the transformation may not proceed *via* a classical Mukaiyama-type mechanism.

To determine whether the TBS silyl ether of **91** influenced the stereochemical outcome, the reaction was repeated using the corresponding TMS-protected derivative instead (Scheme 2.15). Thus, enone **91** was deprotected to hydroxycarvone **112**, which was then protected in situ as its TMS ether **113** and exposed to the coupling conditions. This modification did not alter the results: a 1:1 mixture of epimers was again obtained, and the product decomposed upon

attempted TMS-removal. These findings indicate that poor selectivity does not originate from the silyl ether on the western fragment.

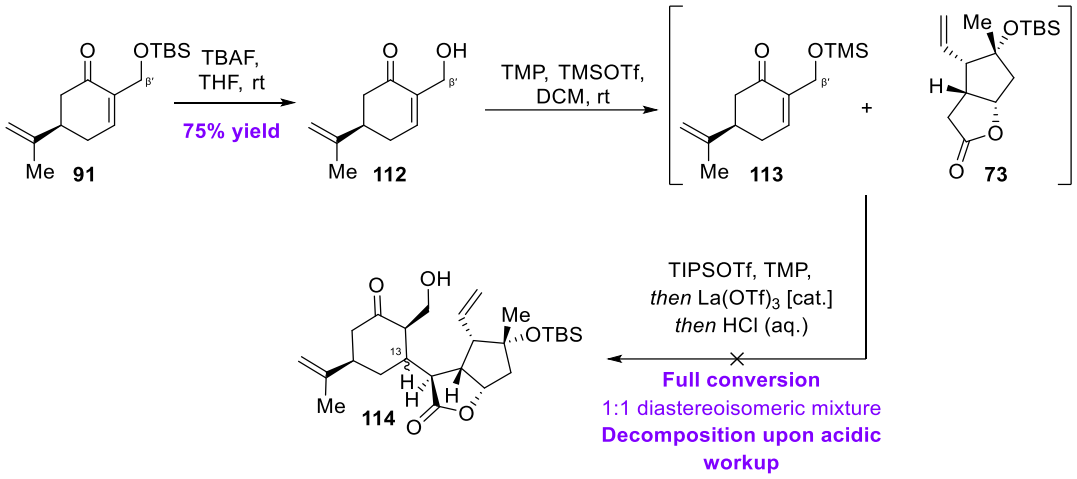


**Scheme 2.15.** Coupling attempts of lactone **73** with hydroxycarvone **112**.

To investigate the origin of the loss of selectivity, fragment coupling with unfunctionalized *(R)*-carvone was performed under the published conditions (Scheme 2.16). This reaction afforded silyl enol ether **115** as a single diastereoisomer in 93% yield, and subsequent deprotection proceeded smoothly to give ketone **116**. This result suggests that the decreased selectivity observed in our system may arise specifically from the β′-oxygen substituent on the modified carvone motif. A plausible explanation is the formation of a six-membered chelate with the Lewis acid, which could alter the preferred double-chair conformation and selectively block the approach from the *Si*-face (Figure 2.1).

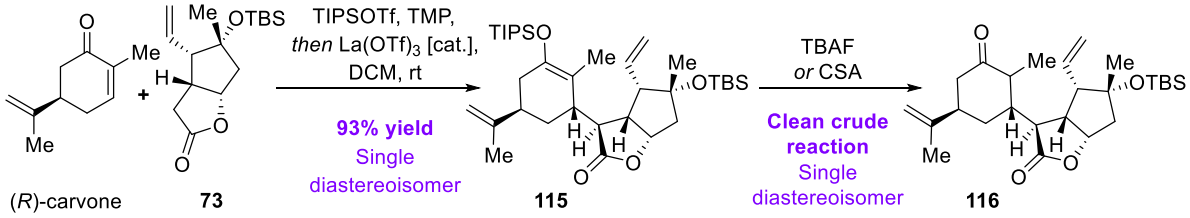


**Scheme 2.16.** Diastereoselective coupling of lactone **73** with *(R)*-carvone.

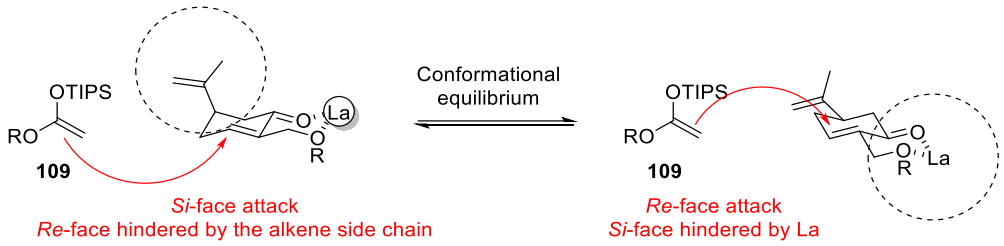


**Figure 2.1.** Possible explanation for the loss of face selectivity.

These results suggest that diastereoselective fragment coupling should be achievable with a substrate that cannot form such a chelate—that is, one lacking a coordinating heteroatom at the β′ position of the carvone motif. Two possibilities were therefore considered: either a substrate with no substituent at that position ((*R*)-norcarvone **96**) or one bearing an alkyl substituent.

### 2.4.3 Coupling studies – *(R)*-norcarvone 96

The coupling studies of lactone **73** and *(R)*-norcarvone **96** was performed by Dr. Georg Späth. This chapter represents a summary of his results.

Coupling of lactone **73** with *(R)*-norcarvone **96** under the conditions of the Vanderwal group gave adduct **117** as a single diastereoisomer with 63% yield after optimization (Scheme 2.17). A few routes were then investigated to install the alkene side chain required for the RCM.

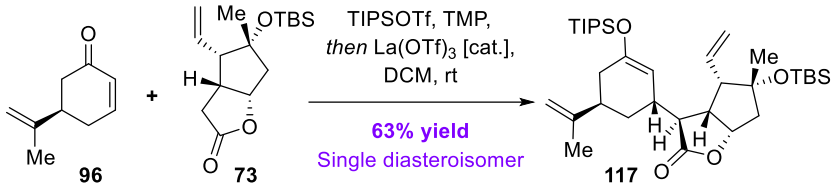


**Scheme 2.17.** Fragment coupling of lactone **73** with *(R)*-norcarvone **96**.

A direct alkenylation of TIPS enol ether **117** with bromopropene (commercially available as a 3:1 Z/E mixture) was attempted under conditions described by the Hartwig group[56] proceeding *via* formation of a tin enolate – note that this type of reaction is only described for TMS enol ethers (Scheme 2.18). Unfortunately, no conversion at all was observed under these conditions, only the starting material could be re-isolated. Due to scarce precedent of intermolecular Pd-catalyzed alkenylations, that approach was not investigated further.

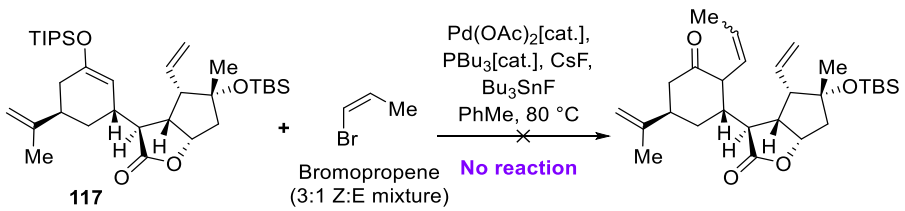


**Scheme 2.18.** Attempted functionalization of silyl enol ether **117** with bromopropene.

Alternatively, a Mukaiyama-aldol addition of TIPS enol ether **117** onto formaldehyde, oxidation of the resulting primary alcohol and subsequent Wittig olefination was envisaged. Since the intermediate aldehyde would certainly exist

in its enol form, Wittig olefination would only seem possible if the ketone was either protected or reduced before generation of the aldehyde functionality.

The main challenges from that approach turned out to be the activation of the rather unreactive TIPS enol ether and the employment of formaldehyde itself, especially at higher concentration. The use of an aqueous solution[57] gave inhomogeneous reaction mixtures and low yields (isolated yields: **118:** 27% and **119:** 30%). When anhydrous formaldehyde (obtained by pyrolysis of paraformaldehyde) was used, reproducibility issues were observed due to the strong tendency of anhydrous formaldehyde to repolymerize. After some optimization, aldol product **118** could be isolated in pure form in 38% yield, alongside a deprotected product **119** in 28% yield (Scheme 2.17).

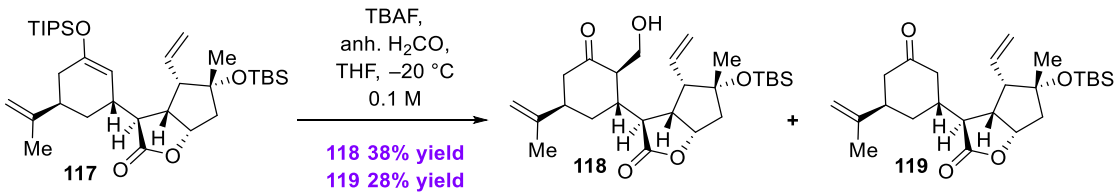


**Scheme 2.19.** Aldol addition of silyl enol ether **117** into formaldehyde.

Isolation of ketone **119** allowed the preparation of different silyl enol ethers, which had not been available yet by the Michael coupling as it had only worked with TIPS ketene acetal **109**. Treatment of **119** with $NEt_3$/TMSOTf or LDA/TMSCl quantitatively formed silyl enol ether **120** and **121** as a 1:1 or 1:3 mixture (Scheme 2.20); the TES silyl enol ethers were formed analogously. Unfortunately, aldol reaction with aqueous formaldehyde only resulted in hydrolytic cleavage to reform ketone **119**.

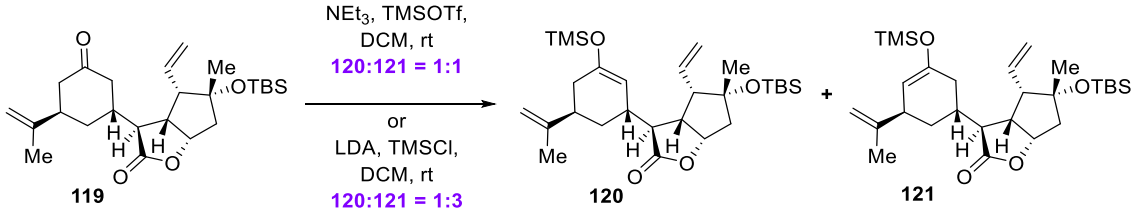


**Scheme 2.20.** Silylation attempts on ketone **119**.

With small amounts of ketone **118** in hand, the next steps to reach the RCM precursors were scouted qualitatively. Classical conditions for ketal formation with azeotropic removal of water were either not feasible on the small reaction scale, or did not work when a 1,3-diol and its orthoester **122** were employed. Only a mixture of concentrated sulfuric acid in DMSO/ethylene glycol/$CH_2Cl_2$ eventually formed the ketal **124**, albeit in equimolar amounts with the free ketone **118** (Scheme 2.18). Due to the low yield of the transformations after fragment coupling and the lengthy remaining sequence left to introduce the alkene side chain, this approach was not investigated further.

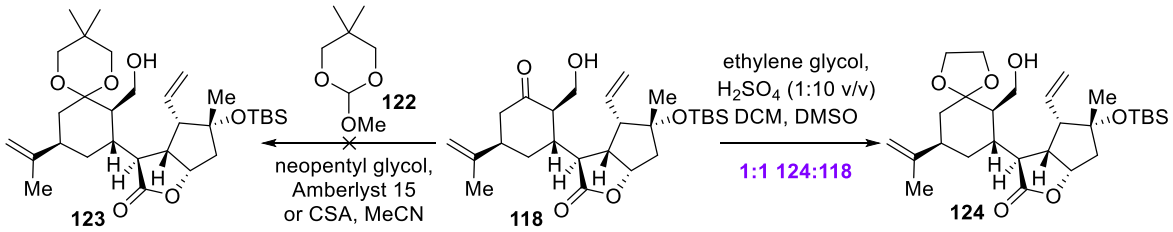


**Scheme 2.21.** Attempted ketalizations on ketone **118**.

### 2.4.4 Coupling studies – selenide 95

Fragment coupling between lactone **73** and selenide **95** was carried out under the conditions reported by the Vanderwal group,[39a] affording silyl enol ether **125** as a single diastereoisomer. Compound **125** proved unstable on silica, necessitating elaboration of the crude material without purification. Following deprotection and subsequent selenoxide elimination, alkene **127** could be obtained with 29% yield over three steps (unoptimized).

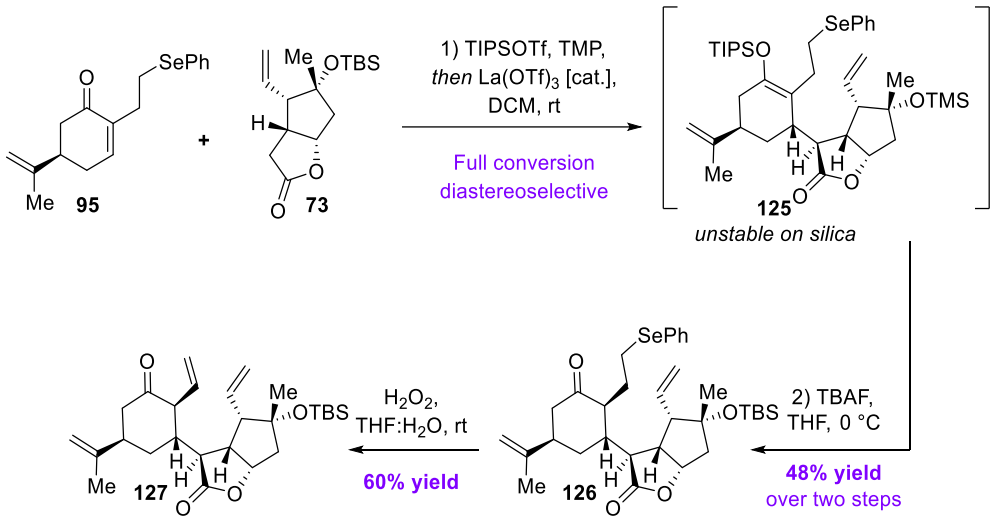


**Scheme 2.22.** Synthesis of alkene **127** *via* coupling of lactone **73** with alkyl selenide **95**.

### 2.4.5 Initial RCM attempts

The initial RCM reaction attempts of alkene **127** were performed by Dr. Georg Späth. This chapter represents a summary of his results.

Unfortunately, compound **127** did not undergo RCM either with Grubbs-II catalyst **Ru-2** or Hoveyda-Grubbs-II catalyst **Ru-1**, even after prolonged reaction time in refluxing toluene or $CH_2Cl_2$ (Scheme 2.23). It is of note that at least with **Ru-1**¸ a new carbene must have formed since the crude mixture contained the styrene derivative **130** derived from the catalyst, roughly estimated in the amount corresponding to the catalyst loading.

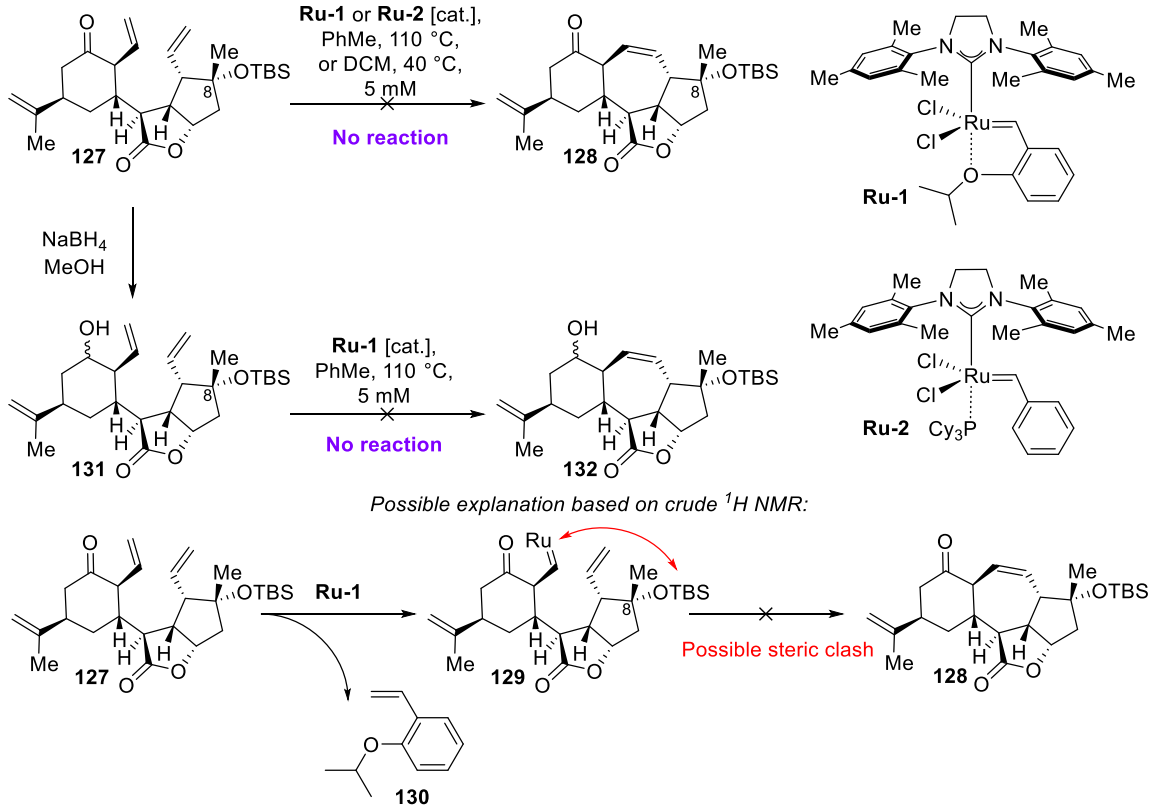


**Scheme 2.23.** Initial attempts to close the ring *via* RCM reaction.

A few hypotheses could explain that result. The steric bulk of the tertiary TBS on C8 could prevent initial carbene formation on the alkene on that side of the cyclization precursor. However, in an earlier approach, that tertiary TBS ether did not prevent alkene metathesis (Scheme 2.4). Due to the β-γ-positioning of the

alkene on the ketone side of the cyclization precursor, a rather stable and unreactive Ru carbene could be formed.[58] However, an epimeric mixture of alcohol **131** was also completely unreactive under the metathesis conditions in refluxing toluene. Under these conditions, a sufficient amount of non-coordinated carbene should be formed on the allylic alcohol side of the precursor to approach the second alkene, from the side of the C8 TBS ether. Finally, carbene formation at the 1,1-disubstituted alkene would be equally surprising due to our earlier precedent of a successful RCM reaction (Scheme 2.4), [59] but could at least explain why no further reaction occurred, since the cyclization products originating from this position would both be bridged bicycles with presumably high strain.

The cause for non-reactivity is therefore unclear at this stage. To exclude any doubt regarding the C8 TBS silyl ether, we planned to perform the RCM reaction with a fully deprotected substrate.

### 2.4.6 Deprotection issues

Late-stage deprotection was first attempted with compound **126** (Scheme 2.24). Treatment with TBAF resulted in decomposition, whereas HF afforded a 1:1 mixture of the desired product **133** and the corresponding hydrofluorinated product **134**.

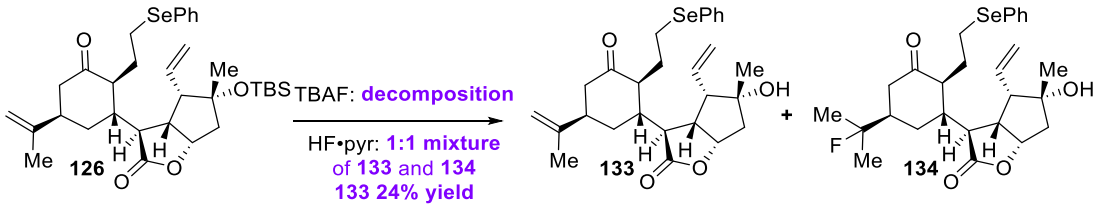


**Scheme 2.24.** Pre-ring-closing deprotection attempts on ketone **126**.

To our knowledge, this is the first example of HF-mediated alkene hydrofluorination. This outcome may arise from preactivation of the alkene by the phenylselenide substituent, enabling its subsequent displacement by fluoride to form product **134** (Figure 2.2).

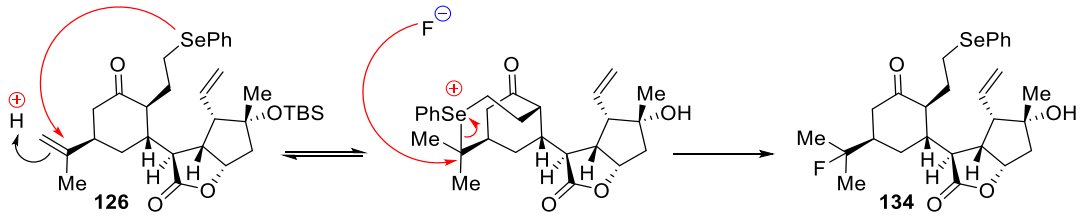


**Figure 2.2.** Possible mechanism for the formation of the hydrofluorinated product **134**.

These results suggest that a deprotection or a protecting group change need to be carried out at an earlier stage, i.e. possibly before fragment coupling.

## 2.5 Synthesis of the desired triene

The TBS protecting group of **73** was replaced by a TMS substituent. Lactone **135** was obtained in 77% yield over two steps *via* deprotection of **73** followed by TMS protection. At the end of the reaction, a brief treatment with TBAF was used to deprotect the doubly-protected product and improve material recovery. This takes advantage of the much faster deprotection of the silyl ketene acetal, which occurs *instantly* upon addition of TBAF at 0 °C, compared to the slower cleavage of the tertiary silyl ether.

Exposure of compound **135** to Mukaiyama-Michael conditions afforded silyl enol ether **136**. The crude material was then deprotected with TBAF and the phenylselenium group eliminated to give triene **137** in 32% yield over three steps (Scheme 2.25).

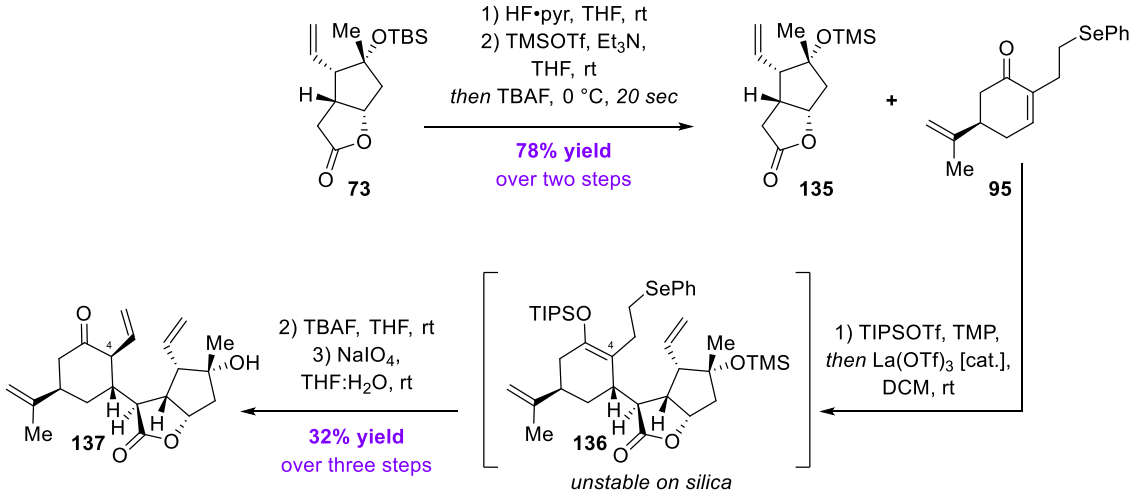


**Scheme 2.25.** Synthesis of deprotected triene **137**.

Quenching the reaction after deprotection of silyl enol ether **136** using aqueous solutions of varying pH (NaOH, $NH_4Cl$, $NaHCO_3$, HCl) had no effect on the C4 stereochemistry: the same diastereomer **137** was obtained in all cases.

## 2.6 RCM attempts

With the desired triene **137** in hand, ring closure *via* alkene metathesis was investigated (Scheme 2.26). Ru-based catalysts were chosen due to their high functional-group tolerance and well-documented use in the synthesis of highly functionalized natural products and pharmaceuticals.[60] In contrast W-, Mo-, or Ti-based catalyst are unsuitable for our substrate, as these metals react preferentially with carbonyls and alcohols rather than olefins, unlike Ru.[61]

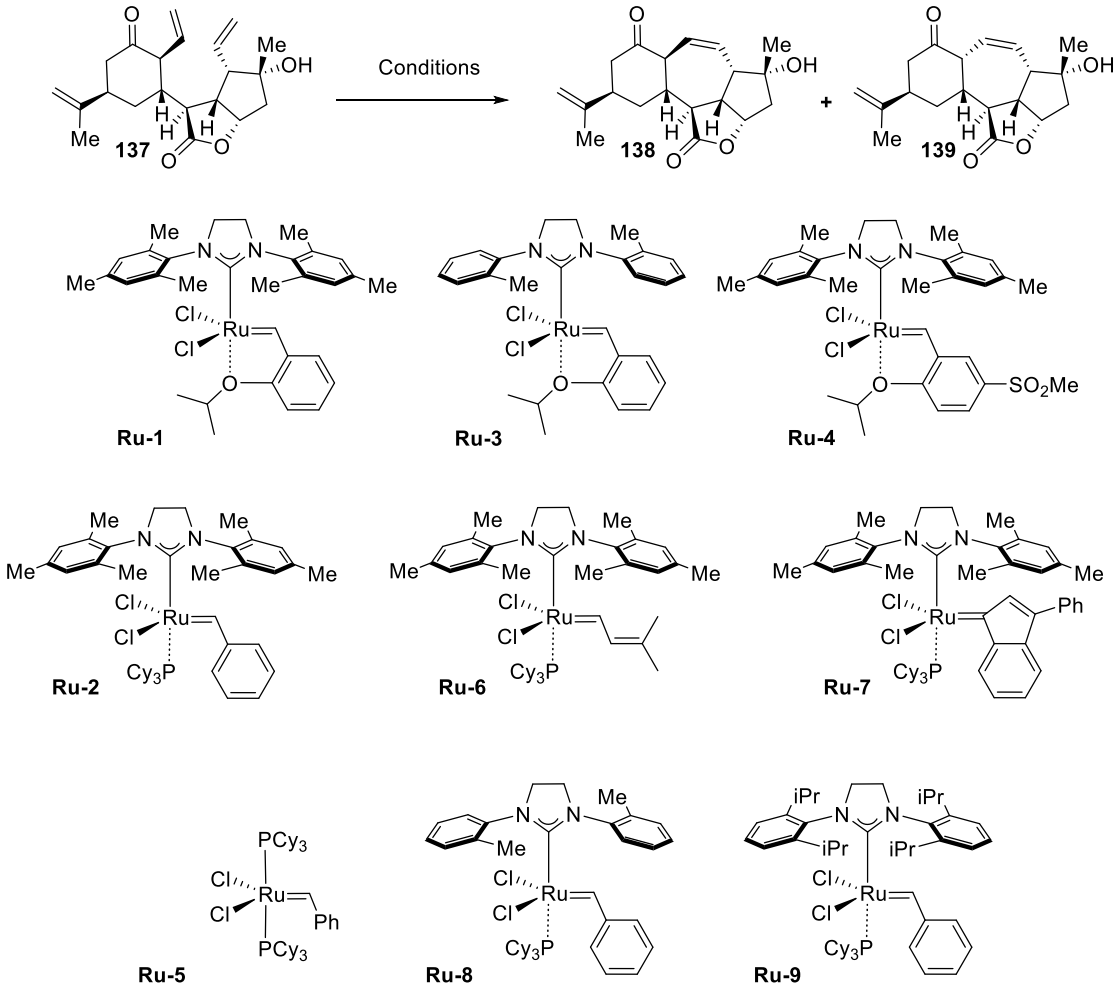


**Scheme 2.26.** Ring-closure attempts of triene **137** *via* RCM reaction and screened catalysts.

RCM was first attempted using Hoveyda-type catalysts (Table 2.2), following the precedent with scabrolide A **5**.[14] Neither the Hoveyda-Grubbs II catalyst **Ru-1** nor the less-hindered Stewart-Grubbs catalyst **Ru-3**[62] afforded any conversion at

100 °C in toluene, while the Zhan 1B catalyst **Ru-4** led to slow decomposition. Given these outcomes, other catalysts were subsequently investigated.

**Table 2.2.** Screening of Ru catalyst for the RCM reaction of triene **137** using Hoveyda-type catalysts; the reactions were carried out at a concentration of 4.5 mM; each batch of catalyst corresponds to 20 mol%.

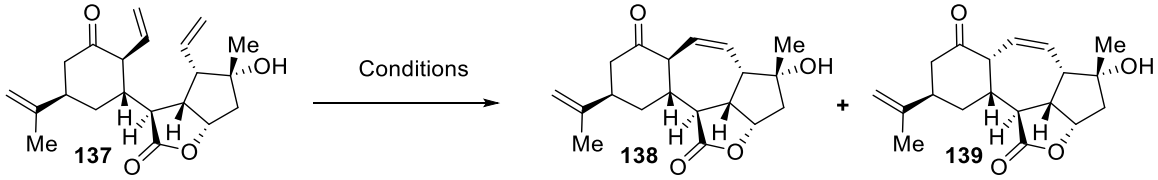


| Entry | Conditions | Results |
|---|---|---|
| **1** | **Ru-1**, toluene, 100 °C, 18 h | No reaction |
| **2** | **Ru-3**, $CH_2Cl_2$, 40 °C, 18 h | No reaction |
| **3** | **Ru-3** (x3), toluene, 100 °C, 96 h | No reaction |
| **4** | **Ru-4** (x5), toluene, 100 °C, 120 h | Slow decomposition |

RCM was then attempted with Grubbs-I catalyst **Ru-5** (Table 2.3). This attempt was motivated by the lower reactivity of that catalyst towards 1,1-disubstituted alkenes,[59] as undesired carbene formation at this site could account for the previously observed lack of reactivity. Nevertheless, no conversion was observed under any of the attempted conditions.

Our attempts then focused on Grubbs-II catalyst **Ru-2** (Table 2.4). This choice was motivated by its broad applicability in natural product synthesis, including substrates similar to triene **137**[63] and the observation in the literature that no single Ru catalyst universally outperforms others across all substrates.[64]

No reaction was observed either in $CH_2Cl_2$ at 40 °C of in 1,2-dichloroethane at 80 °C. In toluene at 100 °C, a trace amount of a ring-closed product **139** was detected in the crude $^1H$ NMR (assigned by NOE) and identified as the cyclized C4-epimer. The same result was obtained at a concentration of 0.45 mM, while increasing the temperature to 120 °C led only to decomposition. Although the stereochemistry at C4 will be lost in the target natural product (C4 is

sp²-hybridized in scabrolide B **34**), these results suggests that a *cis*-annulated ring system is less strained than a *trans*-annulated skeleton, highlighting the critical role of stereochemistry at this position for ring closure.

**Table 2.3.** Screening of conditions for the RCM reaction of triene **137** using Grubbs-I catalyst **Ru-5**; the reactions were carried out at a concentration of 4.5 mM; each batch of catalyst corresponds to 20 mol%.

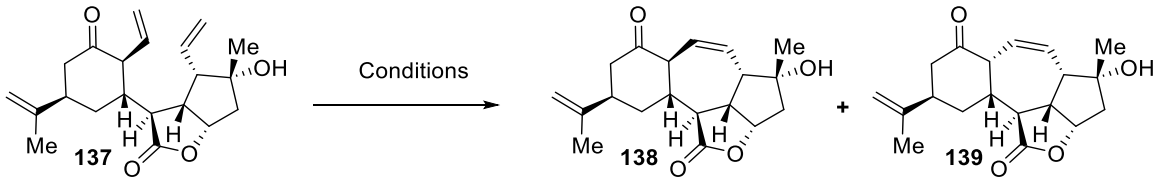


| Entry | Conditions | Results |
|---|---|---|
| **1** | **Ru-5**, $CH_2Cl_2$, 40 °C, 18 h | No reaction |
| **2** | **Ru-5**, Ti(O*i*Pr)$_4$, $CH_2Cl_2$, 40 °C, 18 h | No reaction |
| **3** | **Ru-5,** toluene, 100 °C, 72 h | No reaction |

The product may form via cyclization of the enol form of the ketone, which flattens the geometry around the alkene to enable ring closure (Scheme 2.5), Alternatively, enolization followed by epimerization and subsequent cyclization could account for the observed product. Attempts to favour the enol form using acids (Table 2.4, entries 6 and 7), a method commonly employed in RCM of alkenes with coordinating functional groups,[65] only led to decomposition.

In order to prevent a potential decomposition pathway *via* a ruthenium hydride,[66] or to destabilize a chelate formed between a Ru carbene and the alkene adjacent to the ketone,[67] the reaction was performed in the presence of benzoquinone or Ti(OiPr)$_4$. Benzoquinone led only to decomposition (Table 2.4, entry 8), while Ti(OiPr)$_4$ resulted in no reaction (Table 2.4, entry 9).

**Table 2.4.** Screening of conditions for the RCM reaction of triene **137** using Grubbs-II catalyst **Ru-2**; the reactions were carried out at a concentration of 4.5 mM unless stated otherwise; each batch of catalyst corresponds to 20 mol%.

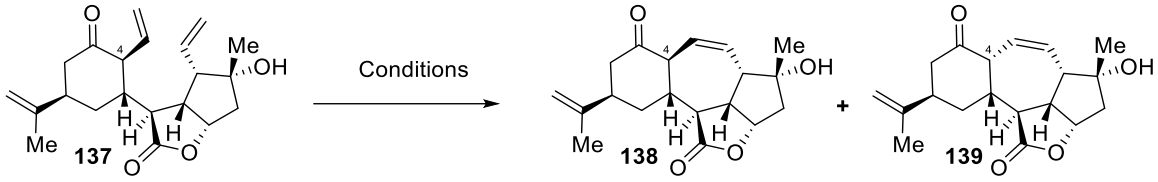


| Entry | Conditions | Results |
|---|---|---|
| **1** | **Ru-2**, $CH_2Cl_2$, 40 °C, 18 h | No reaction |
| **2** | **Ru-2**, 1,2-dichloroethane, 80 °C, 18 h | No reaction |
| **3** | **Ru-2** (x2), toluene, 100 °C, 40 h | Partial decomposition<br>**139** (≈ 12%, NMR) |
| **4** | **Ru-2** (x2), toluene, 120 °C, 18 h | Decomposition |
| **5** | **Ru-2** (x4), toluene, 100 °C, 96 h<br>c = 0.45 mM | Partial decomposition<br>**139** (≈ 13%, NMR) |
| **6** | **Ru-2**, TsOH, toluene, 100 °C, 17 h | Decomposition |
| **7** | **Ru-2** (x2), AcOH, toluene, 100 °C, 40 h | Decomposition |
| **8** | **Ru-2** (x2), benzoquinone, toluene, 100 °C, 40 h | Decomposition |
| **9** | **Ru-2** (x2), Ti(O*i*Pr)$_4$, toluene, 100 °C, 40 h | No reaction |

According to the established mechanism for RCM, both **Ru-1** and **Ru-2** catalysts generate the same propagating species. The styrene ligand influences initiation, whereas the *N*-hetereocyclic carbene (NHC) affects both initiation and propagation.[64a, 68] Our overall results therefore suggest that problems arise in both initiation and propagation. In the hope of obtaining isolable amounts of cycloheptene **139**, derivatives of Grubbs-II catalyst were screened. Catalysts with modified styrene ligands were examined, using the Umicore catalysts M207 **Ru-6** and M202 **Ru-7** (Table 2.5, entries 1 and 2), while NHC-modified variants were assessed using Umicore catalysts M205 **Ru-8** and M206 **Ru-9** (Table 2.5, entries 3 and 4). Notably, precedent exist for with *trans-cis* epimerization in RCM when

using **Ru-7**.[69] All these attempts, however, resulted in slow decomposition (Table 2.5).

**Table 2.5.** Screening of conditions for the RCM reaction of triene **137** using Grubbs-II catalyst derivatives; the reactions were carried out at a concentration of 4.5 mM; each batch of catalyst corresponds to 20 mol%.

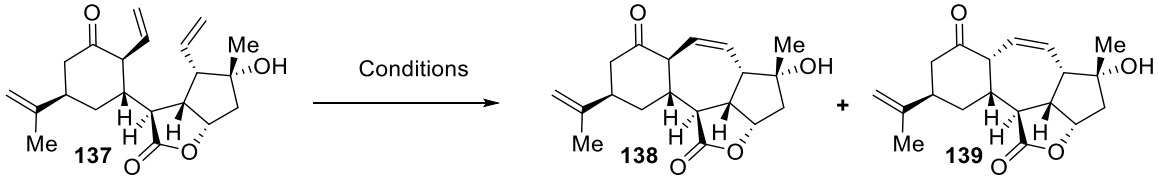


| Entry | Conditions | Results |
|---|---|---|
| **1** | **Ru-6** (x3), toluene, 100 °C, 96 h | Slow decomposition |
| **2** | **Ru-7** (x3), toluene, 100 °C, 96 h | Slow decomposition |
| **3** | **Ru-8** (x3), toluene, 100 °C, 96 h | Slow decomposition |
| **4** | **Ru-9** (x3), toluene, 100 °C, 96 h | Slow decomposition |

In summary, the RCM of triene **137** was extensively investigated, with the influences of catalyst, solvent, temperature, additive and concentration investigated. In all cases, either no reaction occurred, slow decomposition was observed, or only trace amounts of an epimeric cyclized product **139** was observed. A reasonable explanation is that the *trans*-cycloheptene **138** is too highly strained, and therefore, only the *cis*-cycloheptene **139** is accessible.

Taken together with the precedent showing a successful ring closure of a similar substrate possessing a flatter geometry surrounding that alkene attached to the C4 carbon (Scheme 2.4, Scheme 2.5), these observations suggest that the spatial orientation of the alkene attached to the C4 carbon, adjacent the six-membered ring, is crucial for the outcome of the reaction.

## 2.7 Modifications surrounding the C4 carbon to allow the RCM reaction

To enable the desired RCM reaction, modifications to the geometry around the ketone were attempted (Scheme 2.27). Deprotonation $\alpha$ to the β-γ-alkene was expected to afford the conjugated silyl enol ether **140** but the isomeric silyl enol ether **141** was formed exclusively instead. **141** proved to be an unsuitable substrate for RCM reaction as treatment with the **Ru-1** catalyst resulted either in no reaction or decomposition.

Silyl enol ether isomerization is literature-known, typically promoted by triflimide or $SnCl_4$.[70] Both conditions were evaluated but proved unsuccessful, giving either no reaction or simple deprotection back to ketone **137** (Scheme 2.27).

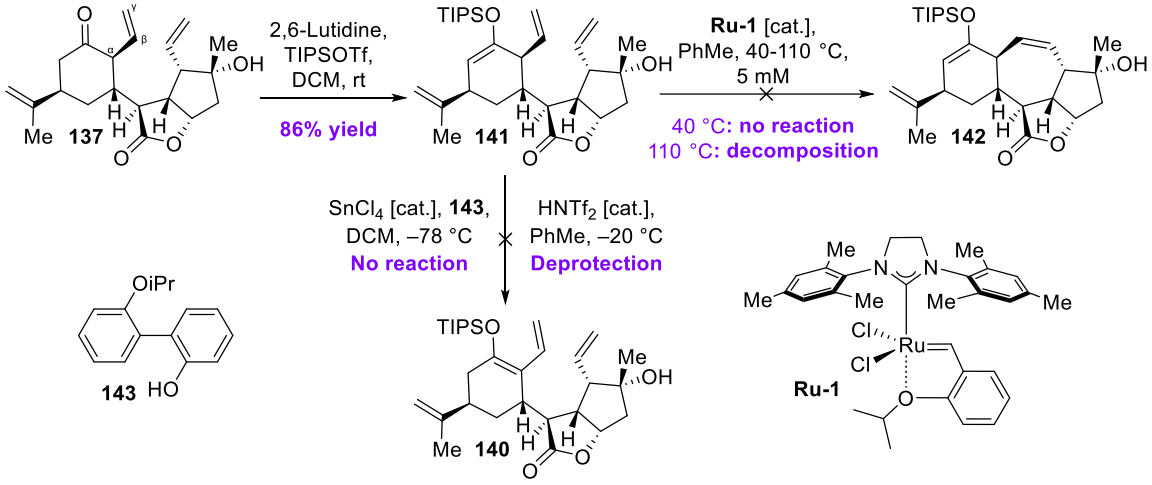


**Scheme 2.27.** Attempted modification of triene **137**.

In order to obtain the desired intermediate, direct selenoxide elimination was attempted on crude silyl enol ether **136** (Scheme 2.28). After optimization, *t*-BuOOH proved to be a suitable oxidant, affording the desired conjugated triene **144** in 30% yield from lactone **135**.[71] This modest yield is not surprising, as silyl enol ethers are known to be sensitive to oxidative conditions.

During this transformation, another product, identified as alcohol **145**, was isolated in 6% yield **135** after HPLC purification. Remarkably, both mono-substituted alkenes of **145** are *cis*-configured relative to each other, making it a potentially suitable RCM candidate. This compound likely arises *via* initial

epoxidation of the silyl enol ether, followed by eliminative epoxide opening on the opposite side of the silyl enol ether. Notably however, attempts to convert triene **144** into alcohol **145** under the same oxidative conditions, or in the presence of additional base (likely present in the crude silyl enol ether **136** mixture) resulted in no reaction. This observation suggests that formation of the epoxide must precede selenoxide elimination during the formation of alcohol **145** (Scheme 2.28).

Cyclization of conjugated silyl enol ether **144** was unsuccessful, as exposure to **Ru-1** catalyst led only to decomposition. This may stem from to the electron-rich character of the conjugated silyl enol ether, which renders it relatively unstable towards a Ru carbene. Our subsequent efforts therefore focused on alcohol **145**.

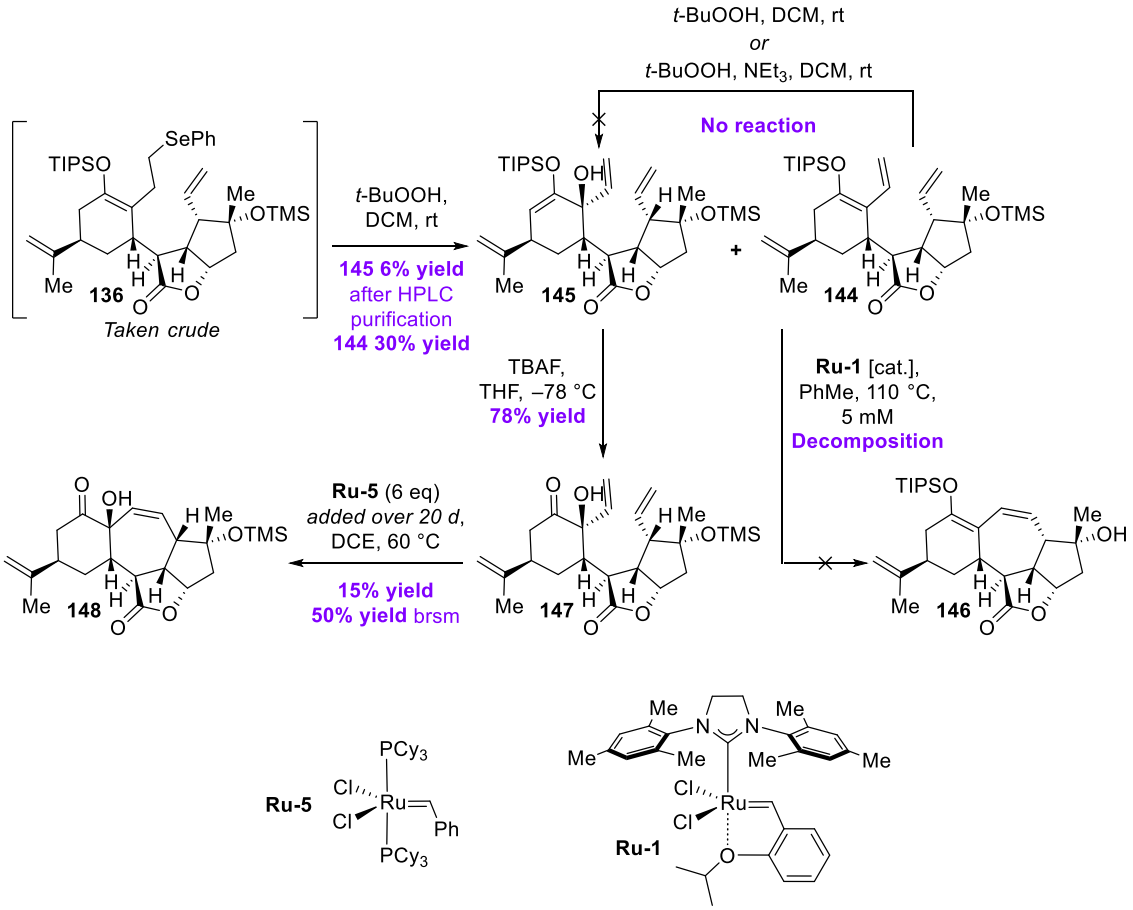


**Scheme 2.28.** Synthesis of a modified ring-closing substrate and successful ring-closure.

Exposure of silyl enol ether **145** to TBAF gave alcohol **147** in 78% yield. Ring-closure of **147** proved challenging, as only 30% conversion was achieved after

addition of six equivalents of catalyst over 20 days (Scheme 2.28). Nevertheless, the ring-closed product **148** was isolated in 15% yield (50% yield brsm, unoptimized). This successful ring closure confirms our hypothesis regarding the importance of the spatial orientation of the alkenes for the outcome of the RCM. Given the low yields obtained, however, this route is not suitable for the projected synthesis.

Yet, the following chapter details the identification of alcohol **148** as a key intermediate *en route* to (–)-scabrolide B **34**. In this way, the present chapter achieves a formal total synthesis of scabrolide B **34** by RCM reaction of the central seven-membered ring and lays the groundwork for further advancement toward the natural product.

# 3. Second approach: by enolate alkenylation to form the C4-C5 bond of Scabrolide B

## 3.1 Retrosynthesis

The retrosynthetic analysis for the second approach was proposed by Dr. Georg Späth prior to the RCM attempts, in the case such approach might prove unsuccessful. The following discussion represents a summary of his considerations regarding the key disconnection.

An alternative strategy to close the ring involves formation of the C4-C5 bond *via* intramolecular enolate alkenylation of ketone **C**$_4$. The resulting product **B**$_4$ would likely isomerize to the enone **A**$_4$ under the basic conditions typically employed for such transformations. Intermediate **C**$_4$ could be obtained by Michael addition of *Z*-vinyl iodide **149** to *(R)*-norcarvone **96**; vinyl iodide **149**, in turn, may be prepared by ozonolysis followed by Stork-Zhao olefination of lactones **73** or **135** (Scheme 3.1).

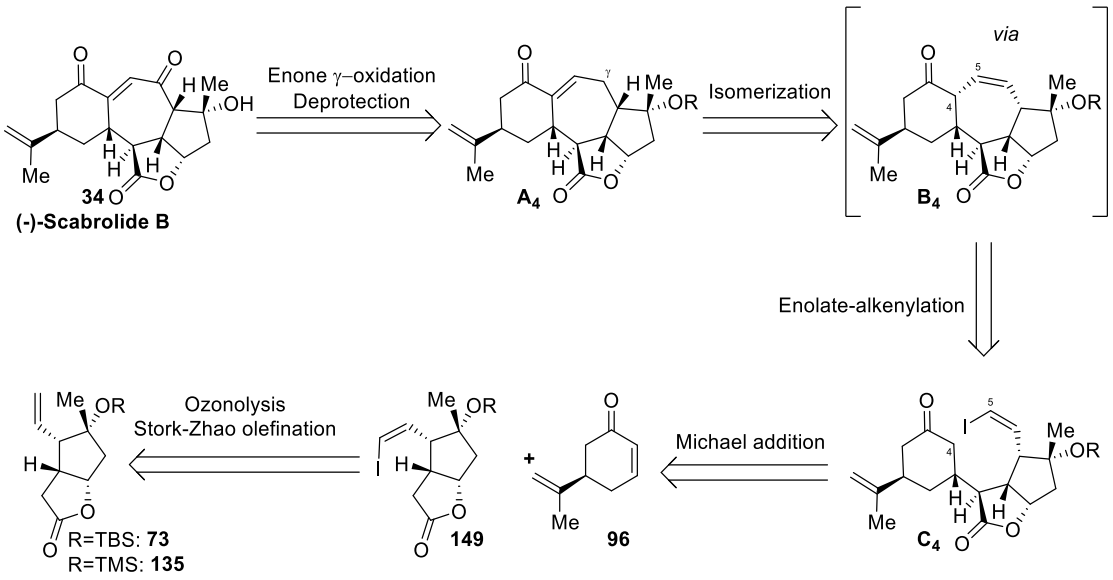


**Scheme 3.1.** Alternative retrosynthetic analysis of scabrolide B **34** - by intramolecular enolate alkenylation.

This retrosynthesis was also inspired by the fact that ketone **C**$_4$ would permit formation of the more accessible cis-fused ring prior to isomerization. Although

not particularly widespread, intramolecular enolate alkenylations have an established record of success for closing five- and six-membered rings.[72] However, precedence for larger or more hindered systems are extremely rare, limited essentially to the eight-membered ring of Taxol.[73] Furthermore, our ring-closing studies aiming at the formation of the central seven-membered ring by RCM reaction implied that the bridgehead alkene in **A**$_4$ is certainly highly congested. An additional challenge here lies in the cyclization of an almost symmetrical ketone with both C–H flanking the ketone being similarly accessible. This implies that enolization must be reversible; both enolates would form and be able to revert to ketone **C**$_4$, but only one of them is able to cyclize. If successful, the desired product **B**$_4$ might accumulate in a meaningful yield.

Finally, conversion of enone **A**$_4$ to scabrolide B **34** would require an enone $\gamma$-oxidation step, potentially facilitated by prior protection of the side-chain alkene as an epoxide.

## 3.2 Cyclization studies

Because the deprotection of TBS ethers after fragment coupling proved challenging (Scheme 2.4 and Scheme 2.24), the synthetic sequence was first conducted using the TMS-protected lactone **135**.

Vinyl iodide **149** was prepared in in 71% yield over two steps from alkene **135** *via* ozonolysis followed by Stork-Zhao olefination.[74] Coupling with *(R)*-norcarvone **96** furnished silyl enol ether **150**,[39a] which was subsequently deprotected to afford the desired protected ring closing precursor **151** in 69% yield over two steps (Scheme 3.2). The stereochemical assignment of ketone **151** was confirmed by a set of NOE correlations and by X-ray crystallography (Figure 3.1).

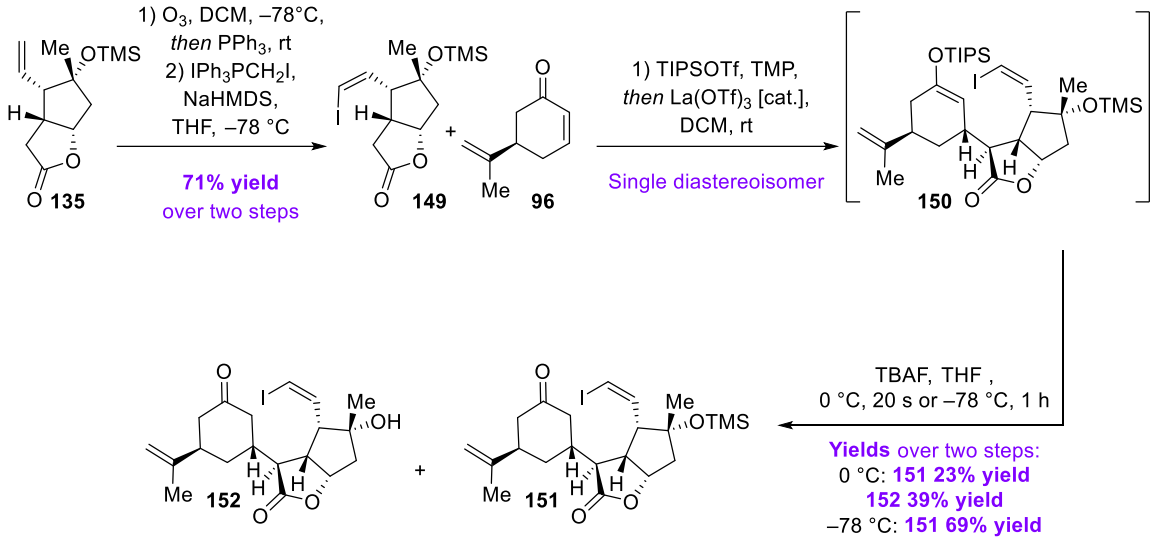


**Scheme 3.2.** Synthesis of cyclization precursors **151** and **152**.

Notably, selective mono-deprotection to ketone **151** required strict temperature control: the reaction had to be performed at –78 °C. Exposure of silyl enol ether **150** to TBAF at 0 °C for as little as 20 sec resulted in partial cleavage of the tertiary TMS ether, giving a mixture of **151** and the fully deprotected ketone **152** in 23% and 39% yield, respectively.

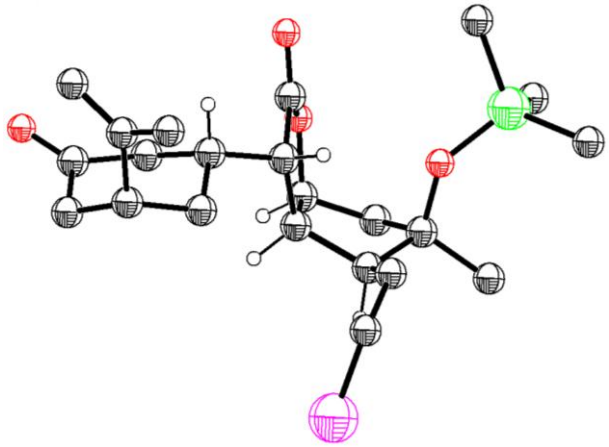

**Figure 3.1.** Structure of **151** in the solid state.

### 3.2.1 Investigations concerning the enolate alkenylation

As the TBS-protected intermediate **153** was readily accessible (prepared analogously to **150**), direct ring-closing was attempted. This strategy benefits from having an enol already at the desired position. However, all attempts were unsuccessful, and only decomposition was observed under both sets of conditions tested (Scheme 3.3).[75]

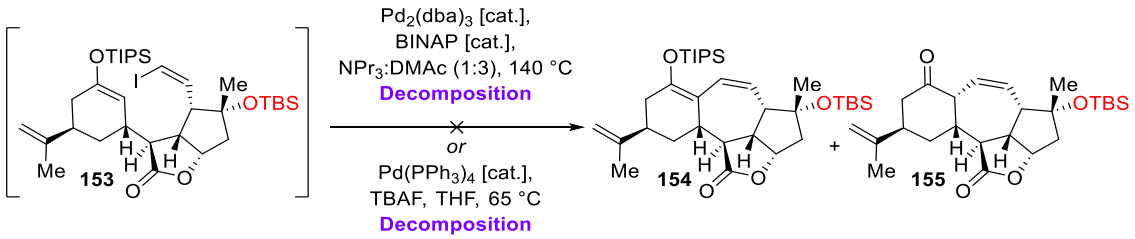


**Scheme 3.3.** Cyclization studies around silyl enol ether **153**.

Ring-closure was next attempted on the deprotected substrate **152**, as the free alcohol could later serve as a directing group for the redox manipulations required to access scabrolide B **34**. Unfortunately, the standard conditions led either to complete proto-deiodination to give alkene **156**, or to rapid elimination to alkyne **157** (Scheme 3.4).

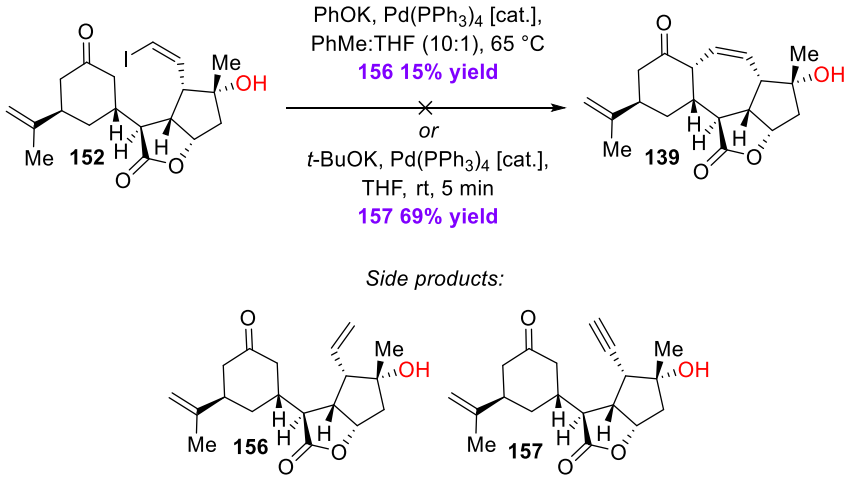


**Scheme 3.4.** Cyclization studies of deprotected ketone **152**.

Alkenylation to close the central seven-membered ring was therefore attempted with ketone **151** (Table 3.1). As expected, the reaction proved very challenging. Ketone **151** was very prone to proto-deiodination to furnish

alkene **158** (Table 3.1, entries 1, 2, 5, 6, 7 and 8), elimination to form alkyne **159** (Table 3.1, entries 1, 2 and 3), or homodimerization to form **161** (Table 3.1, entries 4, 5, 6, 7 and 8) under the usual conditions used for such transformation.[72a] It is of note that in the literature, the substrates undergoing successful ring-closure *via* enolate alkenylation to form the eight-membered ring of Taxol cannot eliminate as the sites flanking the vinyl halide are all carbon-substituted, unlike ketone **151**.[73] A first hit was obtained with phenol/*t*-BuOK (Table 3.1, entry 9), affording enone **162** in 27% yield; increasing the amounts of reagents or slightly changing catalyst and ligand gave similar results (Table 3.1, entries 10 and 11), while the omission of phenol, or use of THF instead of toluene as solvent were not tolerated (Table 3.1, entries 1 and 2). These observations seem to confirm the hypothesis regarding the required reversibility of the enolization.

**Table 3.1.** Initial screening of conditions for the intramolecular alkenylation of ketone **151**; the reactions were performed at a concentration of 10 mM.

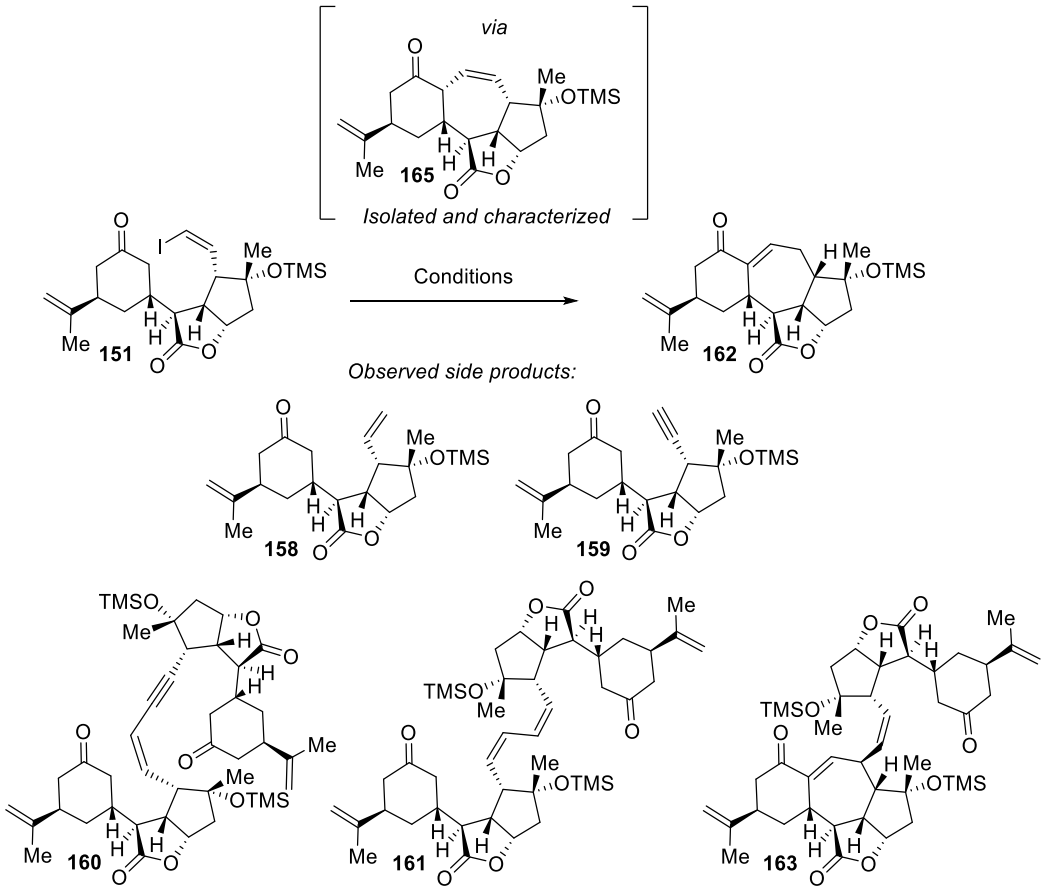

| Entry | Conditions | Results[1] |
|---|---|---|
| **1** | $Pd(PPh_3)_4$ (0.2 eq), *t*-BuOK (3.0 eq), toluene, 65 °C, 90 min | **158** and **159** |
| **2** | $Pd(PPh3)_4$ (0.2 eq), PhOH (3.5 eq), *t*-BuOK (3 eq), THF, 60 °C, 20 h | **158** and **159** |
| **3** | $Pd(PPh_3)_4$ (0.2 eq), *t*-BuOK (3.0 eq), THF, RT, 5 min | **160** |
| **4** | $Pd(PPh_3)_4$ (0.2 eq), $Cs_2CO_3$ (3.0 eq), toluene, 65 °C, 2.5 h | **161** |
| **5** | $PdCl_2(PPh_3)_2$ (0.2 eq), $Cs_2CO_3$ (3.0 eq), $NEt_3$ (3.0 eq), toluene, 90 °C, 24 h | **158** and **161** |
| **6** | $Pd(PPh_3)_4$ (0.2 eq), *t*-BuONa (3.0 eq), dioxane, 60 °C, 20 h | **158** and **161** |
| **7** | $PdCl_2$dppf (0.2 eq), $K_2CO_3$ (3.0 eq), MeOH, 60 °C, 2 h | **158** and **161** |
| **8** | $Pd(OAc)_2$ (0.05 eq), $PPh_3$ (0.3 eq), TBAB (1 eq), $K_2CO_3$ (4 eq), DMF:$H_2O$ (10:1), 90 °C, 20 h | **158** and **161** |
| **9** | $Pd(PPh_3)_4$ (0.2 eq), PhOH (1.7 eq), *t*-BuOK (1.5 eq), toluene, 65 °C, 2 h | **162** 27% yield |
| **10** | $Pd(PPh_3)_4$ (0.2 eq), PhOH (3.5 eq), *t*-BuOK (3.0 eq), toluene, 65 °C, 2 h | **162** 30% yield |
| **11** | $Pd_2(dba)_3$ (0.2 eq), SPhos (0.6 eq), PhOH (3.5 eq), *t*-BuOK (3 eq), toluene, 65 °C, 2 h | **162** 25% yield |

After the initial first hit, a set of different commercial phenol derivatives were screened (Table 3.2). 2,6-Dimethylphenol lead to the formation of the desired product, alongside dimer **163**, produced by the intermolecular alkenylation of enone **162** with the cyclization precursor **151**. This result was still encouraging, as the formation of that dimer also implies a rather efficient alkenylation. Usage of 2,6-diisopropylphenol **164** improved the ratio of enone **162** and dimer **163** to 46% and 13% respective yields (Table 3.2, entry 2), while 2,6-di-*tert*-butylphenol was likely too hindered to deprotonate the ketone, resulting in almost no conversion (Table 3.2, entry 3). Finally, diluting the reaction mixture to a concentration of 2 mM with 2,6-diisopropylphenol **164** as the phenol derivative led to the formation of enone **162** with 57% yield and 20% yield of dimer **163** on a scale of 1.9 g (Table 3.2, entry 4). The structure of enone **162** was confirmed by X-ray crystallography

[1] Yields of isolated products, for entries in which no yields are reported, the analysis is solely based on the inspection of the crude mixture by NMR.

(Figure 3.2).

**Table 3.2.** Further screening of conditions for the intramolecular alkenylation of ketone **151**; the reactions were performed at a concentration of 10 mM unless stated otherwise.

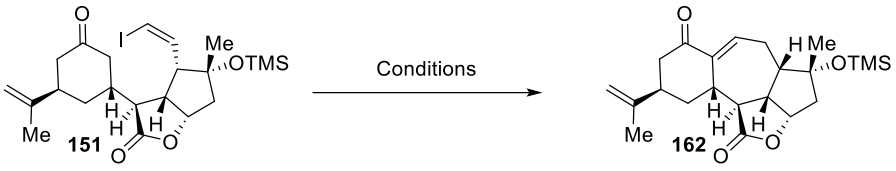


| Entry | Conditions | Results[1] |
|---|---|---|
| **1** | $Pd(PPh_3)_4$ (0.2 eq), 2,6-dimethylphenol (3.5 eq), *t*-BuOK (3.0 eq), toluene, 65 °C, 70 min | **162** 21% yield<br>**163** 32% yield |
| **2** | $Pd(PPh_3)_4$ (0.2 eq), 2,6-diisopropylphenol **164** (3.5 eq), *t*-BuOK (3.0 eq), toluene, 65 °C, 70 min | **162** 46% yield<br>**163** 13% yield |
| **3** | $Pd(PPh_3)_4$ (0.2 eq), 2,6-di-*tert*-butylphenol (3.5 eq), *t*-BuOK 3.0 eq, toluene, 65 °C, 70 min | **162** 7% yield<br>**163** 4% yield |
| **4** | $Pd(PPh_3)_4$ (0.2 eq), 2,6-diisopropylphenol **164** (3.5 eq), *t*-BuOK (3.0 eq), toluene, 65 °C, 70 min, c= 2mM | **162** 57% yield<br>**163** 20% yield |

[1] Yields of isolated products, for entries in which no yields are reported, the analysis is solely based on the inspection of the crude mixture by NMR.

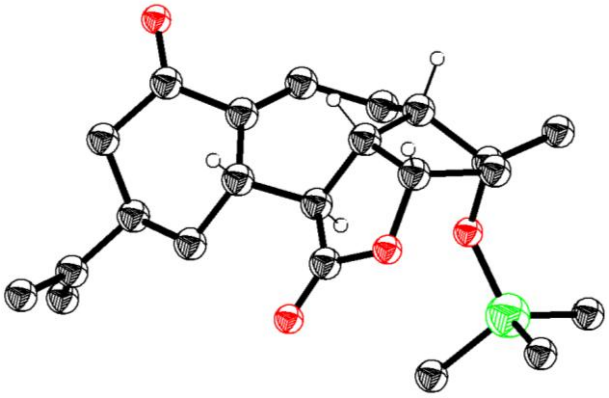

**Figure 3.2.** Solid state structure of enone **162**.

During the course of our investigations, the intermediate **165** formed upon alkenylation before isomerization to give enone **162** could be observed. Using the same conditions as the first hit (with phenol), **165** was isolated as a single diastereoisomer in 3% yield after HPLC purification, with a *cis*-configured seven-membered ring, in accordance with the hypothesis leading to that disconnection.

### 3.2.2 Alternative attempts *via* Conia-ene reaction

For exploratory purposes, and in case that the functionalization of enone **162** might prove unsuccessful, both protected and deprotected alkynes **157** and **159**, isolated from the previous screenings, were exposed to Conia-ene cyclization conditions.[76] Such reaction has been applied to the synthesis of natural products.[77] Unfortunately, none of the screened conditions turned successful on either of the substrates, as decomposition was observed in the majority of the cases (Table 3.3).[78] In one case where defined products were observed in the crude mixture, dimer **166** had formed in 40% yield (Table 3.3, entry 6).

**Table 3.3.** Screening of conditions for Conia-ene reaction; the reactions were performed at a concentration of 10 mM.

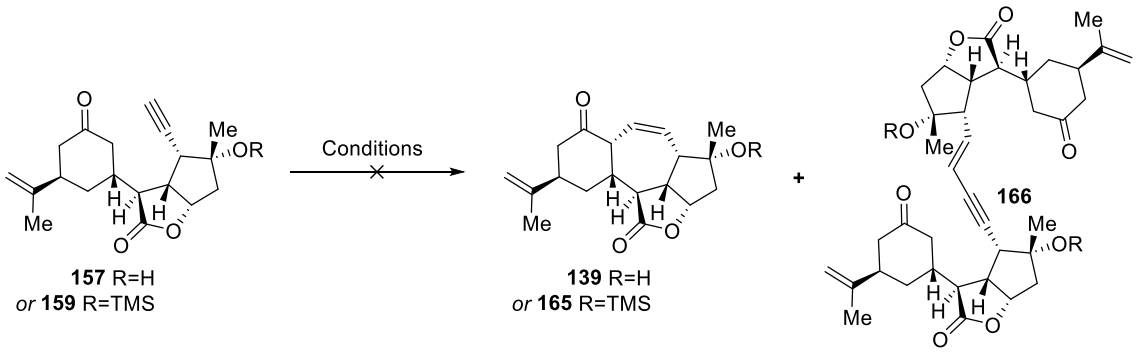


| Entry | R | Conditions | Results[1] |
|---|---|---|---|
| **1** | H | $PPh_3AuCl$ (0.3 eq), AgOTf (0.3 eq), $CH_2Cl_2$, RT | Decomposition |
| **2** | TMS | $PPh_3AuCl$ (0.3 eq), AgOTf (0.3 eq), $CH_2Cl_2$, RT | Decomposition |
| **3** | H | $Mn(OAc)_3 \cdot 2H_2O$ (10 eq), AcOH/EtOAc (1:9), 90 °C | Decomposition |
| **4** | TMS | $Mn(OAc)_3 \bullet 2H_2O$ (10 eq), AcOH/EtOAc (1:9), 60 °C | Decomposition |
| **5** | H | $Pd(OAc)_2$ (0.1 eq), 1,1'-Bis (diisopropylphosphin)-ferrocen (0.1 eq), toluene, 110 °C | Decomposition |
| **6** | TMS | $Pd(OAc)_2$ (0.1 eq), 1,1'-Bis (diisopropylphosphin)-ferrocen (0.1 eq), toluene, 60 °C | **166** 40% yield |
| **7** | H | PMP (0.4 eq), $ZnI_2$ (0.2 eq), $B(C_6F_5)_3$ (0.2 eq), $CH_2Cl_2$, RT | No reaction |

[1] Yields of isolated products, for entries in which no yields are reported, the analysis is solely based on the inspection of the crude mixture by NMR.

## 3.3 Completion of the first total syntheses of (-)-Scabrolide B and (-)-Sinuscalide C

### 3.3.1 Oxidation of enone 162

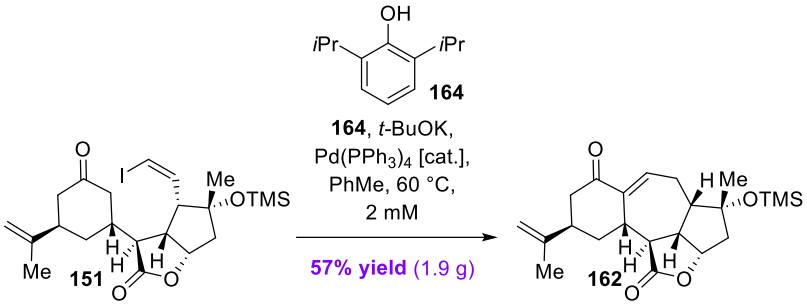


**Scheme 3.5.** Ring closure of ketone **151** after optimization.

With ample material **162** in hand (Scheme 3.5), C–H oxidation at the γ-position of the enone was attempted to form enedione **167** or alcohol **168** which could then potentially lead to scabrolide B **34**. Many oxidants were screened but none of them was successful, often leading to decomposition (Table 3.4).[79]

As the dimer **163** likely forms *via* a deprotonation at the γ-position of the enone of **162**, attempts to activate that position with subsequent trapping with an oxygen source were also made, without success (Table 3.4, entries 9, 10, 11, 12, 13 and 14) despite the successful use of such strategies in the synthesis of bioactive compounds.[79h, 79j, 79k] The use of oxaziridines as oxygen electrophiles (Table 3.4, entries 15 and 16) resulted either in no conversion, or in a complex mixture mainly containing products from deprotonation on the six-membered ring. Attempted formation of a vinylogous silyl enol ether from enone **162** for potential step-wise oxidation were also unsuccessful and gave similar results (Scheme 3.6).

As direct oxidation from enone **162** seemed to be of no avail, we resorted to a step-wise procedure. Enone **162** was converted into α-hydroxyketone **148** with conditions used by the Sarlah group in their total synthesis of scabrolide A **5** (Scheme 3.7).[43]

**Table 3.4.** Screening of conditions for the C–H oxidation of enone **162**.

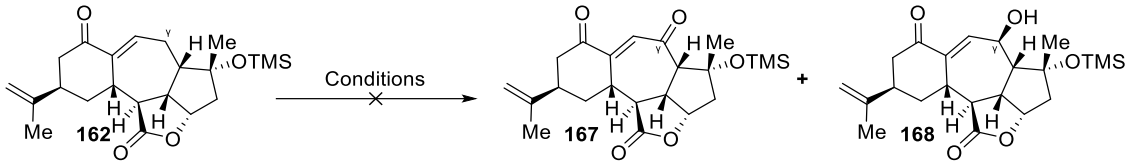


| Entry | Conditions | Results |
|---|---|---|
| **1**[2] | $Rh_2(cap)_4$ (0.2 eq), $K_2CO_3$ (1.5 eq), *t*-BuOOH (6 eq), $CH_2Cl_2$, 40 °C | Decomposition |
| **2** | $Pd(OH)_2$ (0.3 eq), $K_2CO_3$ (0.3 eq), *t*-BuOOH (5.0 eq), $CH_2Cl_2$, rt | Decomposition |
| **3** | $CrO_3$ (excess), 3,5-DMP (5.0 eq), $CH_2Cl_2$, RT | Decomposition |
| **4** | $CrO_3$ (excess), AcOH/$CH_2Cl_2$ (1:2) RT | Decomposition |
| **5** | $MnO_2$ (excess), $CH_2Cl_2$, RT | No reaction |
| **6** | TPAP (1.0 eq), NMO (4.0 eq), $CH_2Cl_2$, 40 °C | No reaction |
| **7** | $SeO_2$ (2.0 eq), 1,4-dioxane, 80 °C | Complex mixture |
| **8** | CuI (0.6 eq), *t*-BuOOH (5.0 eq), MeCN, RT | Decomposition |
| **9** | AIBN (0.4 eq), NBS (1.2 eq), 1,2-dichloroethane, 80 °C then NMO (3.0 eq), DMF | Complex mixture |
| **10**[2] | DABCO (1.0 eq), $CHCl_3$, air, 40 °C | No reaction |
| **11** | *t*-BuOK, *t*-BuOH, air, RT | No reaction |
| **12** | PTSA (7 eq), pyridine, air, 110 °C | TMS ether deprotection |
| **13** | $Na_2$-eosin Y (0.2 eq), $O_2$, 455 nm, MeCN, RT then thiourea (4 eq), MeOH, rt | Decomposition |
| **14** | $Na_2$-eosin Y (0.2 eq), $O_2$, 455 nm, EtOAc, RT then thiourea (4 eq), MeOH, RT | No reaction |
| **15** | KHMDS (1.5 eq), Davis oxaziridine (2.0 eq), THF, RT | Complex mixture |
| **16** | KHMDS (1.5 eq), (*1R*)-(-)-(10-Camphorsulfonyl)-oxaziridine, THF, RT | No reaction |

[2] Reaction carried out on TBS-protected substrate

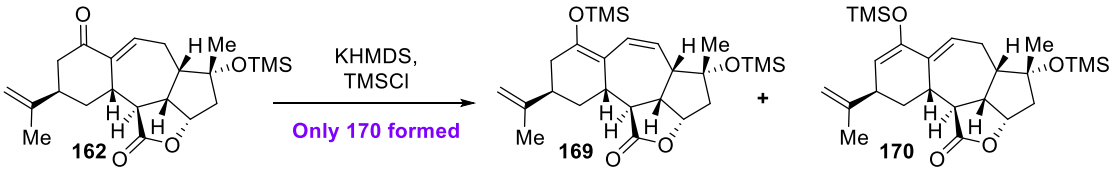


**Scheme 3.6.** Attempted formation of a silyl enol ether from enone **162**.

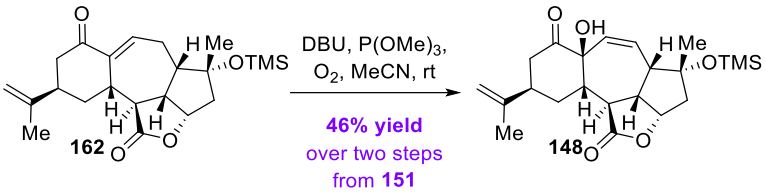


**Scheme 3.7.** $\alpha$-hydroxylation of enone **162**.

Alcohol **148** was isolated as a single diastereoisomer. The structure of the TMS-deprotected derivative **171**, isolated during the screening displayed in the next subchapter, was confirmed by X-ray crystallography and provided the same results as the Sarlah group (Figure 3.3). [41] Notably, alcohol **148** can also be prepared by RCM (see section 2.7 in the previous chapter).

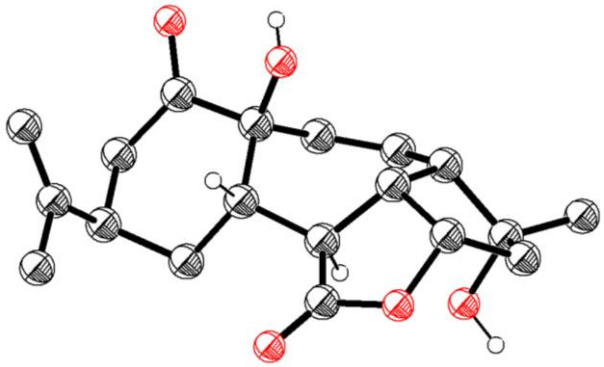

**Figure 3.3.** Solid state structure of alcohol **171**.

### 3.3.2 Allylic alcohol rearrangement

For the subsequent oxidative transposition, the Sarlah group used PCC or PDC in their total synthesis of scabrolide A **5**, which completely failed in our case, resulting either in decomposition or formation of an epoxide (Table 3.5). Note that the screening was initially carried out on y substrate bearing a TBS-protecting group due to material availability.

**Table 3.5.** Attempted oxidative rearrangement of a TBS-protected variant of **148**.

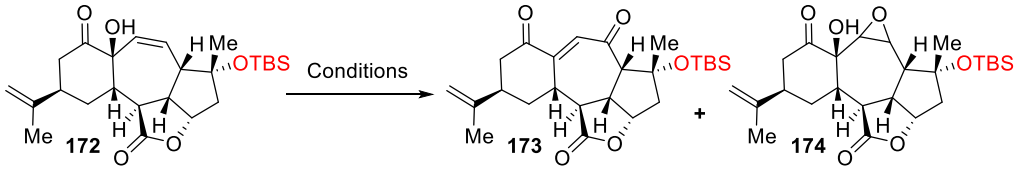


| Entry | Conditions | Results[1] |
|---|---|---|
| **1** | PCC/silica (excess), $CH_2Cl_2$, RT | Formation of **174** |
| **2** | PCC (excess), $CH_2Cl_2$, RT | Decomposition |
| **3**[3] | PCC (excess), $CH_2Cl_2$, RT | Decomposition |
| **4** | PDC (excess), $CH_2Cl_2$, RT | Decomposition |
| **5** | Bobbitt's salt (4.0 eq), MeCN, RT | No reaction |

[1] Yields of isolated products, for entries in which no yields are reported, the analysis is solely based on the inspection of the crude mixture by NMR.

We therefore resorted to a stepwise-procedure, starting with the rearrangement of an allylic alcohol. The allylic alcohol rearrangement is not a widespread reaction, with a very limited set of conditions, mainly based on the use of rhenium(VII) catalysts. This reaction is an equilibrium, usually driven either by the formation of a conjugated system (with an aromatic ring or a ketone to form an enone), or by trapping of the resulting alcohol into the formation of a cyclic system.[80] Despite that, it has found some applications in natural product synthesis.[80-81] Given the very limited information in the literature on possible

[3] Reaction carried out on TMS-protected substrate **148**

conditions for that transformation, we report our full screening results (Table 3.6, Table 3.7 and Table 3.8).

In an initial screening, recently published alternative methodologies resulted solely in deprotection of the tertiary TMS ether of alcohol **148** (Table 3.6, entries 1, 2 and 3).[82] Screening of rhenium(VII) catalysts showed that the most active systems reported in the literature afforded mainly the deprotected product **171** with only partial rearrangement to the desired alcohol **175** even after prolonged reaction times (Table 3.6, entries 4, 5, 6 and 7).[83] It should be emphasized—here and for all subsequent entries—that deprotection of the tertiary TMS ether consistently occurred prior to rearrangement. A further limitation is that these catalysts are reported only in dichloromethane or diethyl ether, two low boiling points solvents, which constitutes an important limitation. By contrast, methyltrioxorhenium(VII)—the least active of these catalysts—is reported exclusively in acetonitrile or benzene.[84] Because of the safety concerns associated with benzene, screening was pursued in toluene, a structurally related but less hazardous alternative.

As expected, methyltrioxorhenium(VII) performed poorly at room temperature (Table 3.6, entry 8). However, upon heating to 60 °C under an air atmosphere, full conversion to alcohol **175** was achieved after 30 h, alongside a first crop of the target natural product scabrolide B **34** (Table 3.6, entry 9) resulting from an oxidation of **175**. Notably, the reaction required the presence of air: running it under inert atmosphere resulted only in limited conversion (Table 3.6, entry 10), possibly because catalyst regeneration after deprotection is accelerated by the residual water present in air. Attempts to increase the amount of scabrolide B **34** formed by extending the reaction time or increasing the temperature resulted in dehydration, yielding predominantly triene **176** and the natural product sinuscalide C **35** as a minor product (Table 3.6, entries 11 and 12).[85] Conversely, running the reaction in the presence of added water to suppress dehydration lowered the mass recovery of alcohol **175** (Table 3.6, entry 13).

**Table 3.6.** Initial screening for the allylic rearrangement of alcohol **148**. The reactions were carried out on 20 μmol (≈ 10 mg), at c = 50 mM and under inert atmosphere unless otherwise specified.

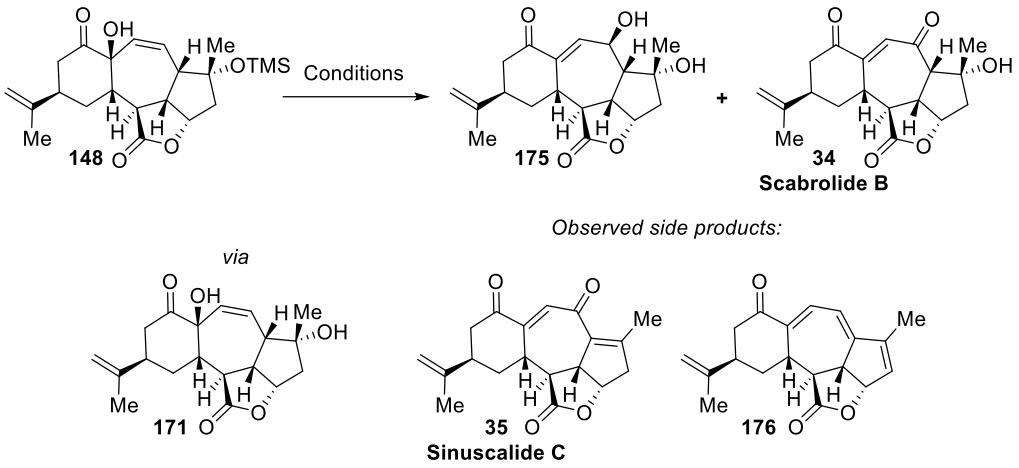


| Entry | Conditions | Product ratio in crude $^1$H NMR (148/171/175/34) |
|---|---|---|
| **1** | $H_2O$/1,4-dioxane (9:1), 80 °C, 43 h | 0/1/0/0 |
| **2** | Salicylic acid (0.2 eq), MeCN, 100 °C, 20 h | 0/1/0/0 |
| **3** | [Ir(cod)($PCy_3$)(py)]$PF_6$ (0.2 eq), $H_2$, 2-MeTHF, RT, 48 h | 0/1/0/0 |
| **4** | $Re_2O_7$ (10 eq), $CH_2Cl_2$, air, RT, 2 h | 0/10/1/0 |
| **5** | $Re_2O_7$ (0.2 eq), $CH_2Cl_2$, RT, 22 h | 0/3/2/0 |
| **6** | $Re_2O_7$ (0.2 eq), $Et_2O$, RT, 45 h | 0/2/1/0 |
| **7** | $Ph_3SiOReO_3$ (0.3 eq), $Et_2O$, RT, 80 h | 0/2/1/0 |
| **8** | $MeReO_3$ (0.3 eq), toluene, air, RT 67 h | 5/4/1/0 |
| **9** | $MeReO_3$ (0.3 eq), toluene, air, 60 °C, 30 h | 0/1/10/1 |
| **10** | $MeReO_3$ (0.3 eq), toluene, 60 °C, 30 h | 0/10/4/1 |
| **11** | $MeReO_3$ (0.3 eq), toluene, air 60 °C 90 h | **35**/**176** 1:4 |
| **12** | $MeReO_3$ (0.3 eq), toluene, air 100 °C 20 h | **35**/**176** 1:4 |
| **13** | $MeReO_3$ (0.3 eq), toluene/$H_2O$ (5:1), air, 60 °C, 30 h | **175** 19% yield |

These optimized conditions proved difficult to reproduce on larger scale. On 15 mg scale, alcohol **175** and natural product **34** were obtained in 52% and 7% yield, respectively; however, on 173 mg scale, the yield of **175** dropped to 21% while the yield of **34** increased to 18%, corresponding overall to a reduced mass balance**.** Further optimization was therefore required. Because the literature reports only a narrow set of conditions for rhenium(VII)-catalyzed rearrangements, solvent choice appeared to be a promising optimization axis (Table 3.7).

**Table 3.7.** Solvent screening for the allylic rearrangement of alcohol **148** with $MeReO_3$. The reactions were carried out on 20 μmol (≈ 10 mg), at c = 50 mM and under inert atmosphere unless otherwise specified. The reactions were stirred at room temperature for 24 h before being heated for entries where heating was carried out.

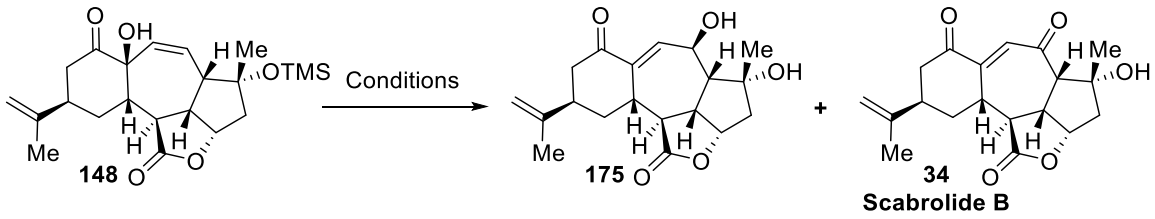


| Entry | Conditions | Product ratio in crude $^1$H NMR (148/171/175/34) |
|---|---|---|
| **1** | $MeReO_3$ (0.3 eq), MeCN, 80 °C, 20 h | 1/0/0/0 |
| **2** | $MeReO_3$ (0.3 eq), DMF, <u>air</u>, 100 °C, 20 h | 0/1/0/0 |
| **3** | $MeReO_3$ (0.3 eq), 1,2-dichloroethane, <u>air</u>, 60 °C, 30 h | 0/1/2/1 |
| **4** | $MeReO_3$ (0.3 eq), 1,4-dioxane, <u>air</u>, RT, 96 h | 0/1/2/0<br>Some decomposition |
| **5** | $MeReO_3$ (0.3 eq), 2-MeTHF, <u>air</u>, 60 °C, 19 h | Complex mixture<br>**175** and **176** in crude |
| **6** | $MeReO_3$ (0.3 eq), EtOAc, <u>air</u>, RT, 67 h | **176** |
| **7** | $MeReO_3$ (0.3 eq), fluorobenzene, <u>air</u>, 60 °C, 17 h | 1/6/2/0 |
| **8** | $MeReO_3$ (0.3 eq), $\alpha,\alpha,\alpha$-trifluorotoluene, <u>air</u>, 60 °C, 17 h | 0/3/2/1 |
| **9** | $MeReO_3$ (0.3 eq), chlorobenzene, <u>air</u>, 60 °C, 17 h | 0/2/10/1 |

Acetonitrile (under inert atmosphere) completely suppressed reactivity, and DMF did not allow rearrangement even at elevated temperatures (Table 3.7, entries 1 and 2). While 1,2-dichloroethane showed interesting results (Table 3.7, entry 3), 1,4-dioxane exhibited the best kinetic profile at room temperature (Table 3.7, entry 4), but also showed decomposition, making it unsuitable for scale-up. Both 2-MeTHF and EtOAc predominantly produced the double dehydrated product **176** (Table 3.7, entries 5 and 6). Among benzene derivatives, fluorobenzene and $\alpha,\alpha,\alpha$-trifluorotoluene slowed the reaction considerably (Table 3.7, entries 7 and 8), and chlorobenzene provided the most favourable performance among this subset (Table 3.7, entry 9).

**Table 3.8.** Scalability of the optimum conditions for the $MeReO_3$-catalyzed allylic alcohol rearrangement of alcohol **148**.

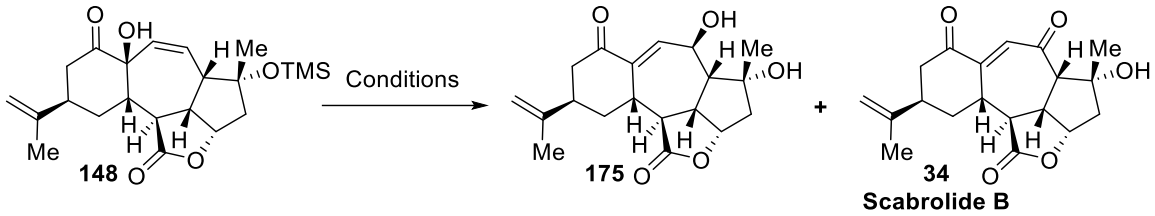


| Entry | Conditions | Scale (mg of **148**) | Isolated yields |
|---|---|---|---|
| **1** | $MeReO_3$ (0.3 eq), toluene, air, 60 °C, 30 h | 15 | **175 52%**<br>**34 7%** |
| **2** | $MeReO_3$ (0.3 eq), toluene, air, 60 °C, 30 h | 173 | **175 21%**<br>**34 18%**<br>**35 6%**<br>**17 5%** |
| **3** | $MeReO_3$ (0.3 eq), 1,2-dichloroethane, air, 60 °C, 30 h | 40 | Decomposition |
| **4** | $MeReO_3$ (0.3 eq), chlorobenzene, air, 60 °C, 42 h | 40 | **175 84%**<br>**34 6%** |
| **5** | $MeReO_3$ (0.3 eq), chlorobenzene, air, 60 °C, 48 h | 430 | **175 71%**<br>**34 15%** |

On a slightly larger scale, 1,2-dichloroethane proved completely unsuitable (

Table **3.8**, entry 3), whereas chlorobenzene gave a better mass balance than toluene, affording alcohol **175** in 84% yield and natural product **34** in 6% yield on 40 mg scale (Table 3.8, entry 4).

These conditions were further scaled up on 430 mg scale, successfully delivering alcohol **175** in 71% yield (corresponding to 250 mg of product), along with an initial crop of scabrolide B **34** in 15% yield. The structure of **175** was confirmed by NOE correlations and by X-ray crystallography, confirming the stereoretentive character of the rearrangement (Figure 3.4).[84]

After optimization, alcohol **175** was successfully oxidized to (-)-scabrolide B **34** using IBX in 74% yield[4], providing at least 110 mg of the natural product in a single run[5] (Scheme 3.8). The collected spectral data of scabrolide B **34** matched the reported spectral data, confirming the reassignment; an analysis by X-ray crystallography excluded any doubts (Figure 3.5). A comparison between the spectral data of synthetic **34** and the natural samples can be found in the experimental section. Similar comparisons were performed for all the other natural products synthesized in the present work.

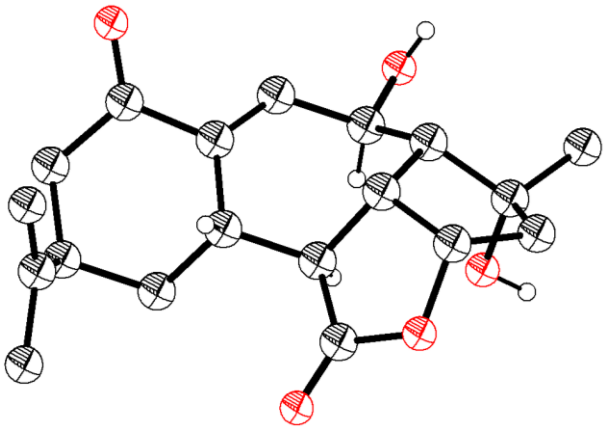

**Figure 3.4.** Solid state structure of **175**.

[4] The Sarlah group reported 90% yield for this oxidation with DMP. In our laboratory, these results could not be reproduced, giving scabrolide B **34** in 40% yield along with with sinuscalide C **35** in 10% yield.

[5] The stated amount includes the scabrolide B **34** isolated from the previous step. At the time, the bioactivity of **175** and **34** were unknown, so the oxidation was performed on only 80 mg out of the 250 mg of **175** available. Under the optimized conditions, it is estimated that 250 mg of **34** could be obtained in a single run.

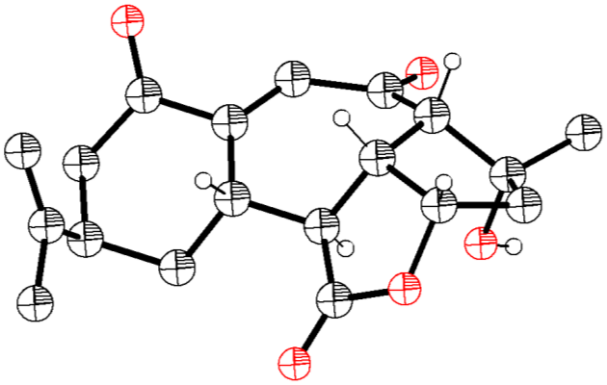

**Figure 3.5.** Solid state structure of (-)-scabrolide B **34**.

Scabrolide B **34** could be dehydrated with Burgess reagent to afford sinuscalide C **35**, [86] while fragilolide A **33** was obtained by Luche reduction of **34** as reported by the Sarlah group.[41] The spectral data of both natural products fully matched the reported data (Scheme 3.8).[28, 30]

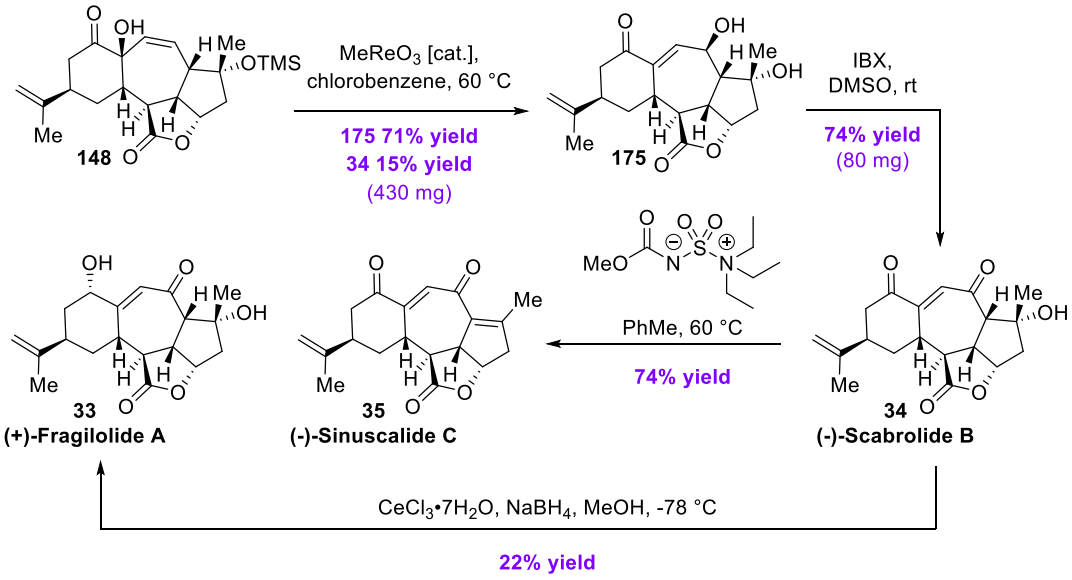


**Scheme 3.8.** Completion of the total syntheses of (-)-scabrolide B **34**, (-)-sinuscalide C **35** and (+)-fragilolide A **33**.

## 3.4 Total syntheses of Ineleganolide, Horiolide and Kavaranolide

With scabrolide B **34** in hand, its conversion into ineleganolide **2** was envisioned. Under basic conditions, the C12 carbon of scabrolide B **34** could undergo epimerization, allowing an oxa-Michael addition to take place, either in a one-pot or stepwise manner, to furnish **2**. That transformation, usually resulting in an equilibrium, could be favoured by its intramolecular character.[87]

Screening of bases showed that potassium bases led to rapid decomposition (Table 3.9, entries 1 and 2), as well as DBU in THF (Table 3.9, entry 3), whereas $NEt_3$ in THF or acetonitrile resulted in no reaction even when used in large excess (Table 3.9, entries 4 and 5). A first hit was obtained using an excess of $NEt_3$ in methanol, albeit with some decomposition.[14] Under these conditions, ineleganolide **2** was formed alongside with horiolide **3**, prolonged reaction times converted all of **2** into **3** with no remaining scabrolide B **34**, consistent with the proposed biosynthetic relationship between **2** and **3** (Table 3.9, entries 7 and 9).[24] The use of acetonitrile as a co-solvent to dilute methanol allowed isolation of ineleganolide **2** in 20% yield brsm (Table 3.9, entry 10). To maximize the amount of **2**, the reaction was deliberately stopped at incomplete conversion. While the net yield per batch remained modest, the spectral data of **2** matched the reported spectral data.[11] Extended reaction time enabled isolation of horiolide **3** in 20% yield (Table 3.9, entry 11).[32] This constitutes the first total synthesis of horiolide **3**.

After the publication of the work reported in this thesis, the Sarlah group reported that using DBU in acetonitrile converted scabrolide B **34** into ineleganolide **2** in 80% yield without formation of horiolide **3**.[41] This report prompted further investigations to improve the throughput of ineleganolide **2**.

**Table 3.9.** Screening of conditions for the formation of ineleganolide **2** from scabrolide B **2**.

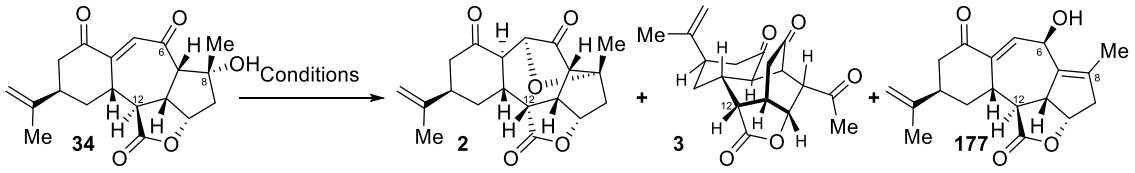


| Entry | Conditions | Results[1] |
|---|---|---|
| **1** | *t*-BuOK (5 eq), THF, RT, 1 min | Decomposition |
| **2** | $K_2CO_3$ (5 eq), MeOH, RT, 2 h | Decomposition |
| **3** | DBU (5 eq), THF, RT, 6 h | Decomposition |
| **4** | $NEt_3$ (20 eq), THF, 60 °C, 70 h | No reaction |
| **5** | $NEt_3$ (20 eq), MeCN, 60 °C, 20 h | No reaction |
| **6** | $NEt_3$ (20 eq), MeOH, RT, 20 h | **2** and **3** in traces |
| **7** | $NEt_3$ (20 eq), MeOH, 60 °C, 18 h | Presence of **3**,<br>**2** in traces |
| **8** | $NEt_3$ (20 eq), MeOH/MeCN (1:1),<br>60 °C, 17 h | Presence of **2** and **3** |
| **9** | $NEt_3$ (20 eq), MeOH/MeCN (1:1),<br>60 °C, 30 h | Presence of **3** only |
| **10** | $NEt_3$ (20 eq), MeOH/MeCN (1:4),<br>60 °C, 20 h | **2 20% yield brsm** |
| **11** | $NEt_3$ (20 eq), MeOH/MeCN (1:4),<br>60 °C, 44 h | **3** 20% yield,<br>**2** 8% yield |
| **12** | DBU (1.0 eq), MeCN, 0 °C, 1 h | **34**:**2** in a 5:1 ratio |
| **13** | DBU (1.0 eq), MeCN, 0 °C, 3 h | **2** 40% yield + 14% recovered **34** |
| **14** | DBU (2.0 eq), MeCN, 0 °C, 2 h | **2** 24% yield<br>**177** 26% yield |
| **15** | Quinuclidin (2 eq), MeCN, RT, 17 h<br>*then* 60 °C, 17 h | Partial conversion, formation of **177**,<br>**2** in traces |
| **16** | Spartein (2 eq), MeCN, RT, 17 h<br>*then* 60 °C, 17 h | Partial conversion, formation of **177** |
| **17** | TMG (2 eq), MeCN, RT, 17 h | **2**:**3** in a 4:1 ratio<br>**2** 43% yield |
| **18** | TMG (2 eq), MeCN, RT, 85 h | **2**:**3** in a 3:1 ratio |

[1] Yields of isolated products, for entries in which no yields are reported, the analysis is solely based on the inspection of the crude mixture by NMR.

Reproduction of these conditions unfortunately proved unsuccessful, providing at best 40% yield of ineleganolide **2** (Table 3.9, entries 12 and 13). Increasing the amount of DBU further diminished the yield of ineleganolide **2** (24% yield) and instead led to formation of the product **177** as the major component in 26% yield (Table 3.9, entry 14). Alcohol **177** seem to result from a dehydration of the alcohol at C8 and reduction of the carbonyl at C6. The potential hydride source that led to the reduction of the carbonyl at C6 is unclear.

These observations, together with the lack of reactivity observed with $NEt_3$ in acetonitrile (Table 3.9, entry 5) suggest that the $pK_a$ of the base in acetonitrile may dictate the balance between formation of ineleganolide **2** and formation of alcohol **177**. We therefore hypothesized that a base of intermediate basicity—stronger than $NEt_3$ but weaker than DBU—might enhance the formation of ineleganolide **2** while suppressing formation of **177**.

Selected commercially available bases with pKa values in acetonitrile between those of $NEt_3$ (pKa(MeCN)=18.8) and DBU (pKa(MeCN)=24.3) were therefore screened.[88] Quinuclidin (pKa(MeCN)=19.7) and sparteine (pKa(MeCN)=21.7) (Table 3.9, entries 15 and 16) were unsuitable, delivering mainly alcohol **177** with only traces of ineleganolide **2** and noticeable decomposition. TMG (pKa(MeCN)=23.3) gave ineleganolide **2** in 43% isolated yield (Table 3.9, entry 17), corresponding to the highest obtained yields obtained in this study The crude mixture also contained ~20% of horiolide **3**, which could not be isolated due to apparent chromatographic instability; extended reaction times marginally increased its proportion to ~25%, still without isolable material (Table 3.9, entry 18).

Several mechanistic pathways could account for the conversion of scabrolide B **34** into ineleganolide **2**. The one-pot character of this transformation suggests a biosynthetic relationship in which ineleganolide **2** can arise from scabrolide B **34**. One plausible sequence involves an initial oxa-Michael addition, followed by

epimerization at C12 through a retro-Michael/Michael addition process, with the resulting anion stabilized by resonance with the C6 carbonyl group (Scheme 3.9).

Notably, the observations reported by the Sarlah group seem to confirm this hypothesis: epimerization was observed only for scabrolide B **34**, whereas all related intermediates (enone **162,** alcohols **148** and **175**, in both protected and unprotected forms) could not be epimerized under the same conditions. [41]

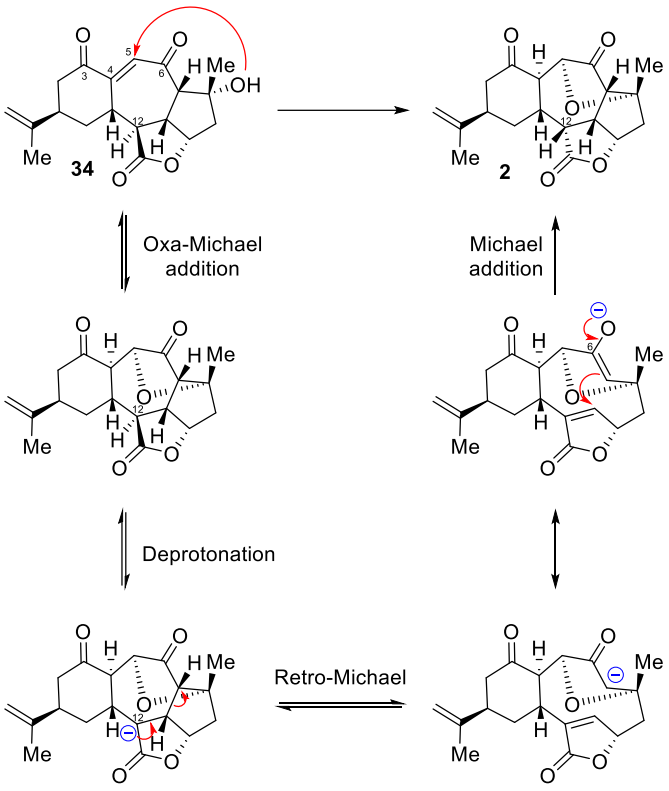


**Scheme 3.9.** Suggested mechanism for the formation of ineleganolide **2** from scabrolide B **34**.

In order to improve the yield of horiolide **3**, a more controlled transformation was attempted. Ineleganolide **2** was exposed to basic conditions (TBAF or DBU in methanol) and both conditions led to horiolide **3** (Scheme 3.10). Very interestingly, when no workup was carried out, the main product observed in the crude mixture was the natural product kavaranolide **18**.

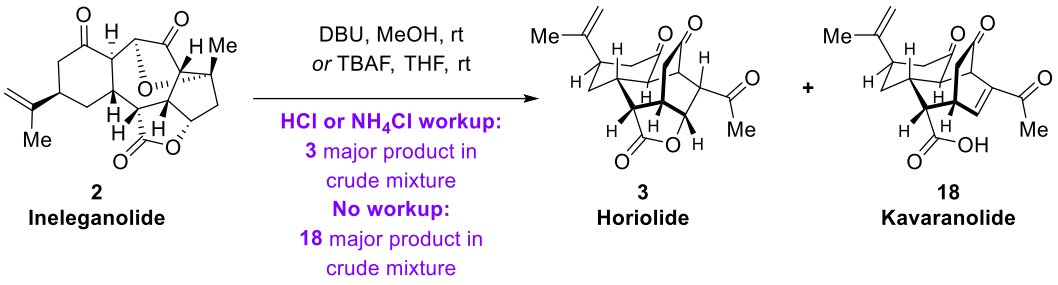


**Scheme 3.10.** Attempted conversion of ineleganolide **2** into horiolide **3**.

Taken together with the earlier observations that DBU in acetonitrile converts scabrolide B **34** selectively to ineleganolide **2**, whereas weaker bases in methanol favour the formation of horiolide **3** (Table 3.9), these results suggest that applying stronger bases in methanol directly to scabrolide B **34** might provide a direct access to downstream isomers such as horiolide **3** or kavaranolide **18**.

Consistent with the initial observations, omission of an aqueous workup again resulted in kavaranolide **18** (Table 3.10, entries 1, 2, 4 and 5). Importantly, although this transformation is formally an isomerization, a catalytic amount of base was not effective (Table 3.10, entry 3), whereas stoichiometric or excess base gave crude mixtures containing mainly kavaranolide **18** and the base employed. Remarkably, when an acidic workup was performed, horiolide **3** was obtained as the sole product (Table 3.10, entry 6).

Attempts in isolating base-free kavaranolide **18** from the base were really tedious, as neither extraction nor evaporation were successful, despite the volatility of DBN (Table 3.11, entries 1, 2, 3 and 4). When any acidic conditions were employed, horiolide **3** was observed in the resulting crude mixture (Table 3.11, entries 5 and 6), while purification by reverse phase HPLC without a pH modifier was messy, giving base-free kavaranolide **18** in 4% yield (Table 3.11, entry 7), with the major fraction containing kavaranolide **18** with DBN in equimolar proportions. Despite the low isolated amount, the recorded spectral data of **18** matched nicely with the reported data of the natural product.[33] Under the same

conditions and after acidic workup, horiolide **3** could be obtained in 46% yield after reverse phase HPLC purification (Scheme 3.11).

**Table 3.10.** Screening of conditions for the formation of horiolide **3** and kavaranolide **18** from scabrolide B **34**.

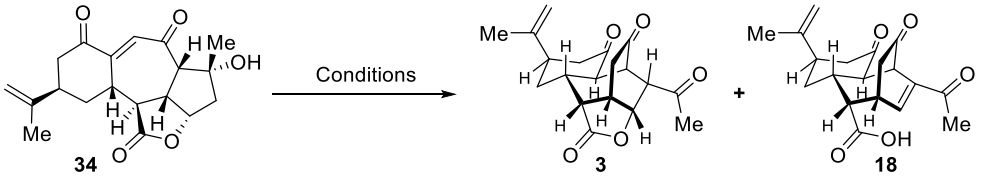


| Entry | Conditions | Results[1] |
|---|---|---|
| **1** | 2,8,9-Tri-iso-butyl-2,5,8,9-tetraaza-1-phosphabicyclo[3.3.3] undecane (0.2 eq), MeOH, 50 °C, 17 h<br>*No workup* | Presence of **18** (major product), **2** and **3** (minor products) |
| **2** | DBU (2.0 eq), MeOH, RT, 90 min,<br>*No workup* | Presence of **18** only |
| **3** | DBU (0.2 eq), MeOH 60 °C, 24 h<br>*No workup* | Low conversion<br>**2**, **3** and Sinuscalide C **35** in traces |
| **4** | TMG (2.0 eq), MeOH, RT, 2 h<br>*No workup* | Presence of **18** only |
| **5** | DBN (2.0 eq) RT, 4 h<br>*No workup* | Presence of **18** only |
| **6** | DBN (2.0 eq) RT, 17 h<br>*HCl workup* | Presence of **3** only |

[1] Yields of isolated products, for entries in which no yields are reported, the analysis is solely based on the inspection of the crude mixture by NMR.

**Table 3.11.** Attempts in obtaining analytically pure kavaranolide **18**.

| Entry | Conditions | Results (qualitative, from final $^1$H NMR) |
|---|---|---|
| **1** | 60 °C at 0.03 mbar for 6 h | No change from crude |
| **2** | Silica gel chromatography | Decomposition |
| **3** | Extraction with EtOAc or $CH_2Cl_2$ | **18** in aqueous phase<br>No change from crude |
| **4** | Organic washes of a solution in $H_2O$ with $CH_2Cl_2$ and EtOAc | No change from crude |
| **5** | SCX cartridge, eluting with $CH_2Cl_2$ then MeOH | Presence of horiolide **3** |
| **6** | HPLC with MeOH, $H_2O$ + 0.1% Formic acid | Formation of horiolide **3** during solvent removal |
| **7** | HPLC with MeOH, $H_2O$ | Mostly no change from crude<br>A clean minor fraction |

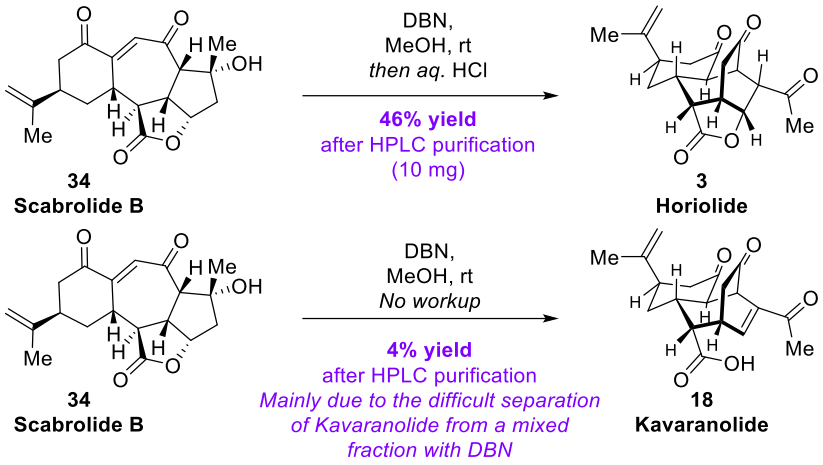


**Scheme 3.11.** Syntheses of horiolide **3** and kavaranolide **18** from scabrolide B **34**.

To showcase the rather clean transformation of scabrolide B **34** into kavaranolide **18**, its isolation as a methyl ester was attempted. Using the conditions that form **18**, an excess of (trimethylsilyl)-diazomethane was added to the reaction mixture when scabrolide B **34** was completely consumed. This procedure afforded product **178** – likely resulting from an additional [3+2]-cycloaddition of (trimethylsilyl)-diazomethane or diazomethane on the methyl ester of kavaranolide **18** – in 29% yield from scabrolide B **34** (Scheme 3.12).

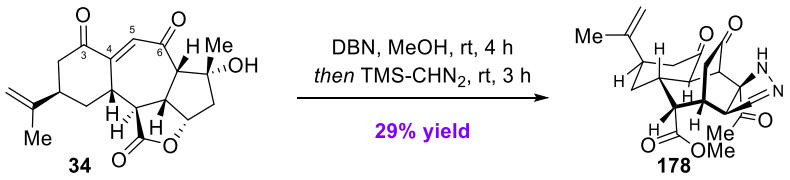


**Scheme 3.12.** Transformation of scabrolide B **34** into product **178**.

The formation of horiolide **3** from scabrolide B **34** *via* ineleganolide **2** likely proceeds *via* a retro-oxa-Michael reaction, giving intermediate **179**, which is the 12-epimer of scabrolide B **34**. Instead of reverting back to scabrolide B **34**, the compound **179** adopts a conformation that allows the C7–C8 σ orbital to overlap with the C6–O π* orbital. The ensuing retro-aldol reaction affords ketone **180**, which instantly succumbs to a proximity-driven intramolecular Michael addition

to form the new C5–C9 bond. The involved course of this step mirrors the proposed biosynthetic pathway (Scheme 1.2) (Scheme 3.13).[24]

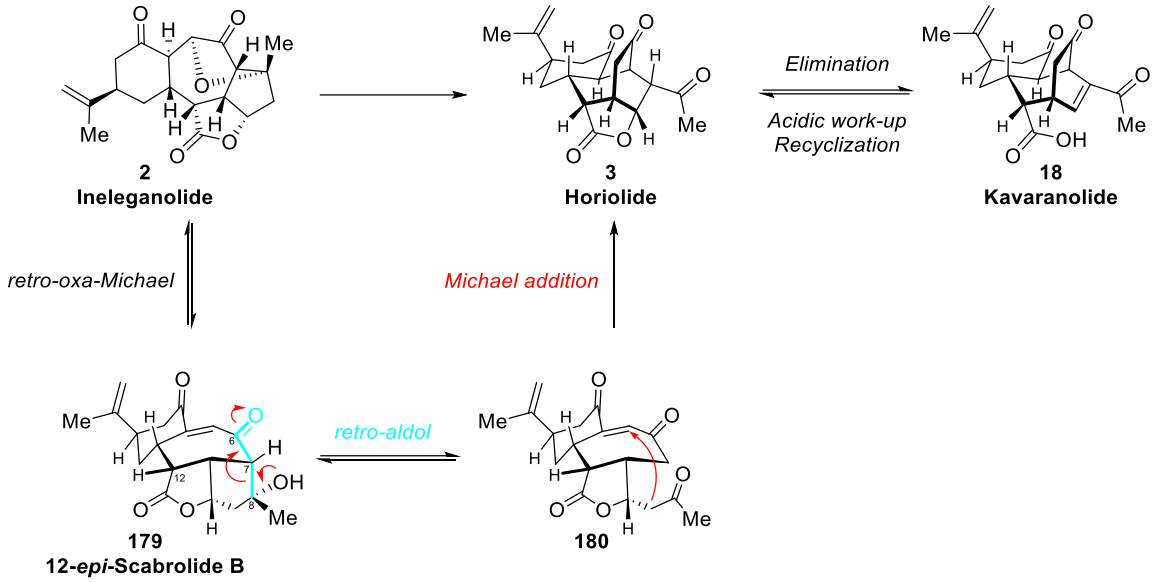


**Scheme 3.13.** Suggested mechanism for the formation of horiolide **3** and kavaranolide **18** from ineleganolide **2**.

From the course of the observed events, it seems that when the base is strong enough, the lactone moiety of horiolide **3** is eliminated to give kavaranolide **18**. Under acidic conditions, kavaranolide **18** recyclizes into horiolide **3**, likely via acid activation of the enone. Even without workup, kavaranolide **18** was never observed when $NEt_3$ was employed as a base (Table 3.9, entries 6-11).

Remarkably, in most reactions that produced horiolide **3**, methanol served as the solvent, suggesting that it facilitates the transformation, perhaps by opening the lactone ring.

We never observed any reactivity at the C5 position which is apparently conjugated with the C7 carbonyl. That could be rationalized by the solid-state structure of scabrolide B **34** (Figure 3.5), where the C6 carbonyl is almost perpendicular to the C4-C5 alkene, suggesting an absence of conjugation between these bonds. In contrast, the olefin at C4-C5 seem coplanar to the carbonyl group at C3, explaining the observed electrophilic character at C5.

## 3.5 Synthetic attempts to Pambanolides $B_1$ and $B_2$

The pambanolides are a family of diterpenoids that have also been isolated from *Sinularia inelegans* and present a very weak cytotoxicity against a series of human cancer cell lines (A549, DU145, HeLa and MCF-7).[31] Among them, pambanolide $B_1$ and $B_2$ **36** – the structure of the latter was confirmed by X-ray crystallography – feature the same cyclic backbone as many of the natural products studied in this report. The main difference is that the alkene of the bridgehead enone on the seven-membered ring is replaced by a methoxycarbonyl attached to the C4 carbon at the ring-junction and a methoxy group at the C5 position, the stereochemistry at this center being the point of difference between pambanolide $B_1$ and pambanolide $B_2$. Given the very close structural similarity of these compounds to sinuscalide C **35** and scabrolide B **34**, their syntheses were attempted *via* late-stage transformations.

It was envisioned that the pambanolides **36** could be obtained by oxa-Michael addition of methanol at C5 of scabrolide B **34** or sinuscalide C **35**. The intermediate could then be trapped, either by methoxycarbonylation, or with a halogen source, followed by a methoxycarbonylation under transition-metal catalysis (Scheme 3.14).

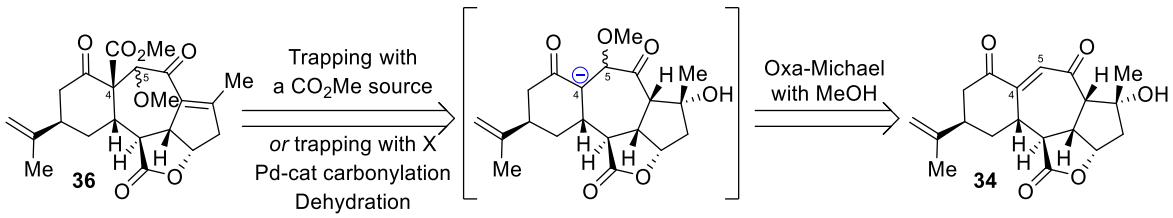


**Scheme 3.14.** Retrosynthetic analysis of the pambanolides $B_1$ and $B_2$ **36** from scabrolide B **34** or sinuscalide C **35**.

The oxa-Michael addition might be selective at C5 following the observations drawn in the previous subchapter. A major challenge in that approach is the low precedence of oxa-Michael reactions, especially with methoxide, due to the low nucleophilicity of alcohols, and the reversible character of the reaction. Moreover, the majority of literature precedents for oxa-Michael additions involve

intramolecular reactions.[87, 89] Therefore, when that reaction is attempted on scabrolide B **34**, the challenge would be to favour the intermolecular pathway over the intramolecular pathway that leads to ineleganolide **2** and horiolide **3**. These challenges could hopefully be overcome by trapping of the resulting oxa-Michael addition product with an electrophile, which could shift the reaction equilibrium towards the formation of the desired products.

Attempts focused on sinuscalide C **35** first, as in the case an oxa-Michael addition with trapping is successful, the desired natural products could directly be obtained. The desired product could also be obtained by Morita-Bailys-Hillman reaction with subsequent substitution of the initial nucleophile. Despite the dienone character of sinuscalide C **35**, the C5 position should be much more reactive than the C8 position for steric reasons.

A set of acids (CSA, tartaric acid, acetic acid), bases (imidazole, $NEt_3$, DBU, NaOMe, $Cs_2CO_3$) or nucleophiles (DABCO, $PPh_3$) in a mixture of methanol and dimethylcarbonate were screened; unfortunately, none of these turned successful, resulting in decomposition or in recovered starting material (Scheme 3.15).

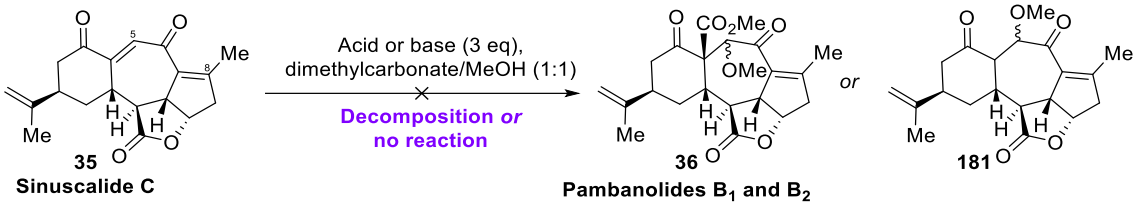


**Scheme 3.15.** Synthetic attempts to pambanolides $B_1$ and $B_2$ **36** from sinuscalide C **35**.

The transformation was then attempted with the substrate **175**, which will then require oxidation and dehydration. Treating it with base in methanol and dimethylcarbonate gave either no conversion, or methoxycarbonylation of the allylic alcohol to carbonate product **183** (Scheme 3.16). Acid catalysis with triflimide, or trapping with NBS in methanol were also attempted but both resulted in decomposition.

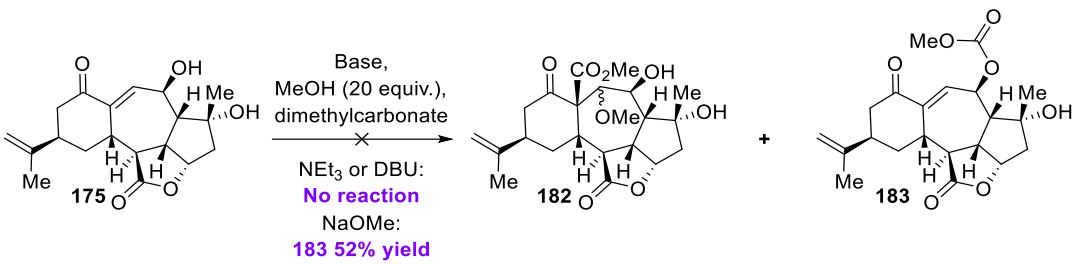


**Scheme 3.16.** Oxa-Michael addition attempts on allylic alcohol **175**.

Scabrolide B **34** was then the last remaining possible precursor. The major issue when attempting the transformation from **34** is that using methanol in presence of organic bases leads to the formation of ineleganolide **2** and horiolide **3** (Table 3.9). This narrows the possible conditions to alkaline bases, and to acid or neutral conditions with trapping with a halogen source.

Unfortunately, instant decomposition was observed when NaOMe was added to a solution of **34** in dimethylcarbonate; triflimide also led to decomposition. Halogenation was attempted, but only the formation of bromohydrin **185** was observed in 80% yield (3:1 diastereoisomeric mixture) from reaction with the 1,1-disubstituted alkene (Scheme 3.17).

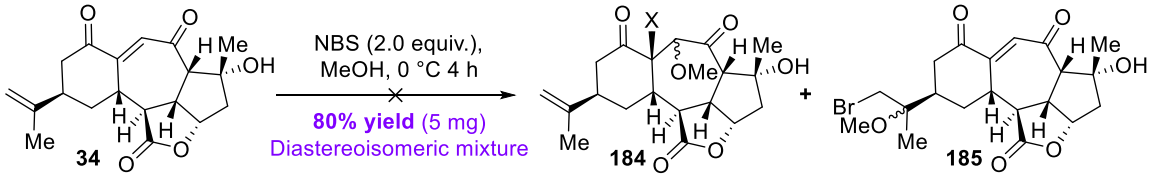


**Scheme 3.17.** Oxa-Michael addition with bromination attempt on scabrolide B **34.**

These unsuccessful attempts suggest that installation of the carboxyl moiety should take place at a much earlier stage. From our studies in sections 2.4.1 and 2.4.3, that installation could take place after Mukaiyama-Michael addition of lactone **135** on *(R)*-norcarvone **96**. This will also imply a revision of the end-game, as isomerization of the ring-closed alkene to the enone will no longer be possible. As the pambanolides $B_1$ and $B_2$ **36** could not be obtained *via* straightforward transformations on the late-stage intermediates *en route* to scabrolide B **34**, these targets were not pursued further.

## 3.6 Second generation synthesis of Scabrolide B

### 3.6.1 Considerations around the ring-closing strategy

Multiple points in the initial synthetic route to scabrolide B **34** might be further improved. One involves the lengthy sequence to install the vinyl iodide moiety. When inspecting the synthetic route, one could notice that three steps are necessary in order to remove a single carbon (Scheme 3.18, indicated in red). A direct formation of a Z-enol triflate **187** could therefore significantly shorten the synthetic route by two steps. This would also induce a reoptimization of the alkenylation.

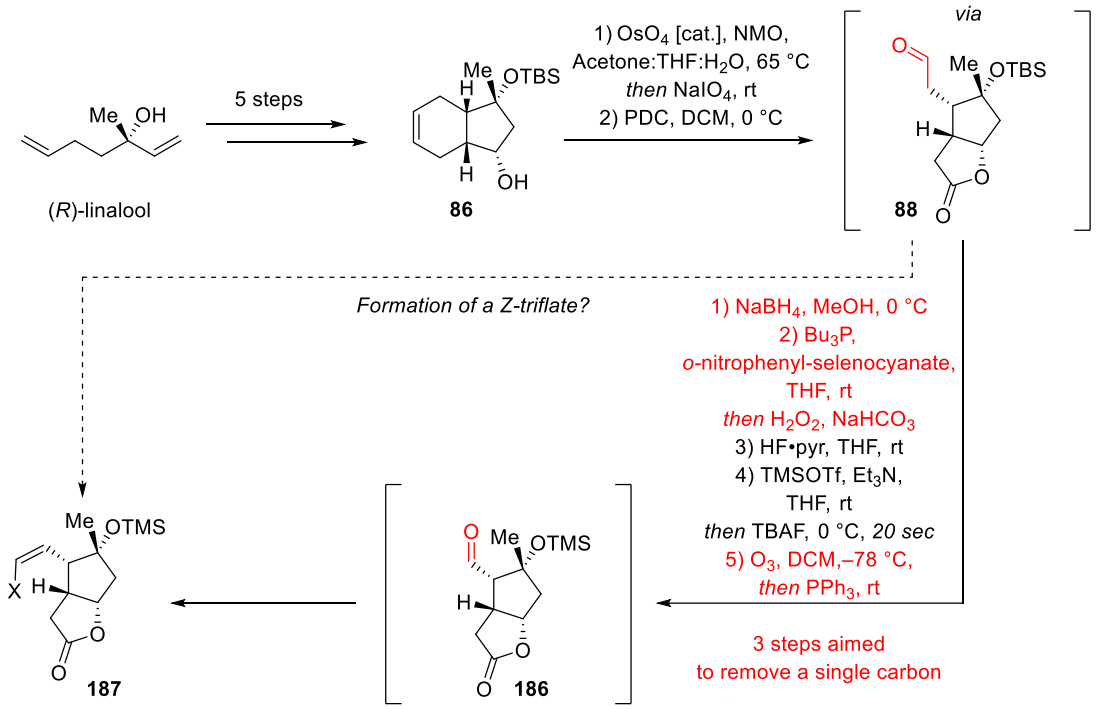


**Scheme 3.18.** Possible shortening of the synthesis *via* Z-vinyl-triflate **187**.

For exploratory purposes, aldehyde **88** was synthesized from alcohol **89**. Unfortunately, when subjecting aldehyde **88** to the reported Z-triflation conditions,[90] a complex mixture was observed, with the mass of the desired product **188** not even detected by mass spectrometric analysis of the crude mixture (Scheme 3.19). Since these were the only reported set of conditions for such a transformation, that approach was abandoned.

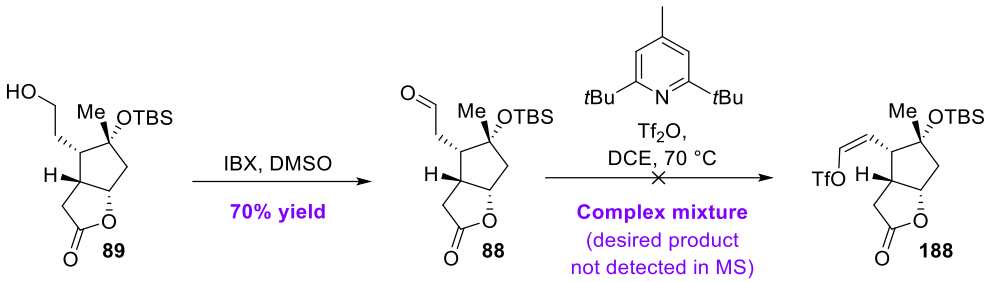


**Scheme 3.19.** Synthetic attempts towards Z-vinyl-triflate **188**.

### 3.6.2 Alternative protecting group strategy

After the synthesis described in the previous chapter was published, the Sarlah group disclosed their total synthesis of scabrolide B **34**.[41] As described in the introduction, the intermediates are very similar to those described in this thesis. One remarkable point was that a TBS-protecting group strategy was used, and a late stage deprotection was successful. That strategy had not been pursued in this study due to unsuccessful prior attempts (Scheme 2.4 and Scheme 2.24). It was therefore an opportunity to possibly shorten the route by a step or two, if TBS removal could occur under the conditions of the allylic alcohol rearrangement, analogously to the cleavage of the TMS group in the initial route.

Synthesis of the Z-vinyl iodide fragment **189** was achieved *via* ozonolysis/Stork Zhao olefination sequence, albeit with significantly reduced yields (44% yield over two steps instead of 70% yield with a TMS ether). This result may be due to a lower mass recovery during ozonolysis (75% instead of 100%), possibly arising from sensitivity of the aldehyde intermediate upon chromatography.[42] That issue surprisingly does not exist when the TMS silyl ether – a less hindering and more labile silyl ether than a TBS ether, is present on the tertiary alcohol (Scheme 3.20).

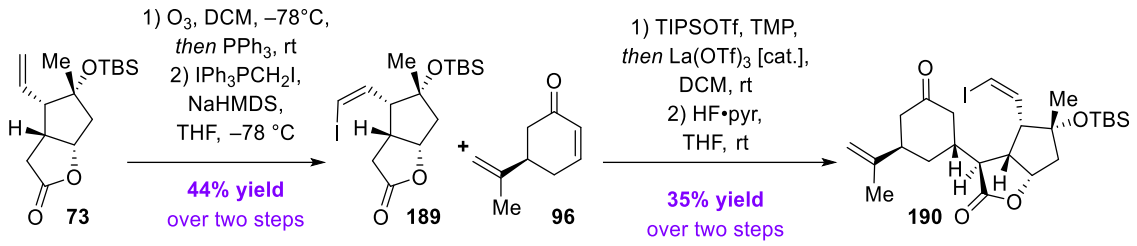


**Scheme 3.20.** Synthesis of TBS-protected vinyl iodide **189** and fragment coupling.

The Mukaiyama-Michael addition of fragment **189** to *(R)*-norcarvone **96**, followed by deprotection, afforded lactone **190** in 35% yield over two steps (yield with TMS: 69% over two steps). The lower yield mainly comes from the deprotection, which proved hardly scalable and would require further optimization (on 10 mg scale: quantitative yield, on 150 mg scale: 50% yield) (Scheme 3.20). Notably, a one-pot sequence without purification of the silyl ether

is not possible due to a difficult separation of **190** from *(R)*-norcarvone **96**, affording **190** in 20% yield over two steps in that case.

With the ketone **190** available, ring-closure could be attempted. To our dismay, the optimized conditions used for the ring-closure of compound **151**, with a TMS protecting group, could not be applied to the TBS-protected intermediate **190**, resulting mainly in proto-dehalogenation to give alkene **191** (Scheme 3.21).

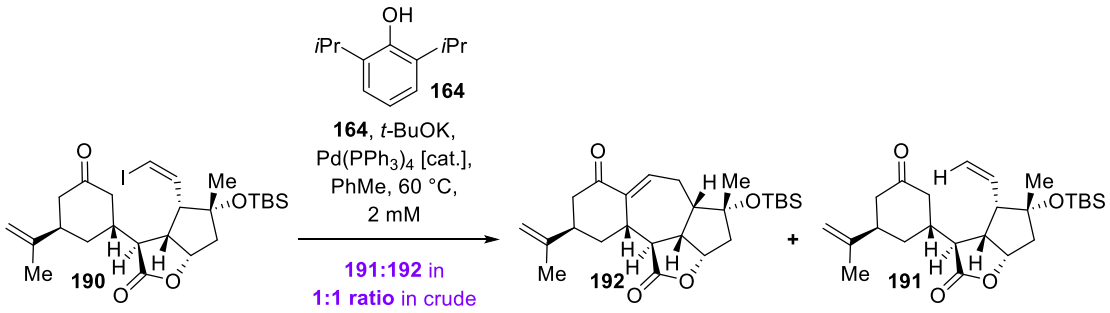


**Scheme 3.21.** Initial attempt in closing the ring of **190**.

As that pattern had already been observed with the TMS ether when a too bulky phenol was used (Table 3.2, entry 14), it was decided to screen a less bulky phenol, which successfully afforded enone **192** in 53% yield, alongside 16% of alcohol **193** (Table 3.12, entry 1).

Remarkably, the formation of alcohol **193** represents a formal C–H activation at the γ-position of the enone of **192**. Improving its formation would shorten the synthesis by two steps, requiring only deprotection then oxidation to reach scabrolide B **34**. The oxygen atom in the alcohol of **193** might come from various sources: traces of silica powder or water or oxygen in the reaction mixture. All these factors were investigated, but none of these gave better results than the initial entry (Table 3.12, entries 2-6). Notably, in this foray, unlike with a TMS ether, the dimeric product from intermolecular coupling between ketone **190** and enone **192** was not observed or only in traces, likely due to the higher steric hindrance with the TBS ether than with the TMS ether. Nevertheless, enone **192** could be α-hydroxylated the same way as in TMS series, producing alcohol **172** in 32% yields over two steps (Scheme 3.22). As with a TMS ether, the intermediate

**194** after alkenylation and before isomerization could be isolated as a single diastereoisomer, with a *cis*-configured seven-membered ring.

**Table 3.12.** Screening of conditions for the intramolecular alkenylation of ketone **190**; the reactions were performed at a concentration of 2 mM.

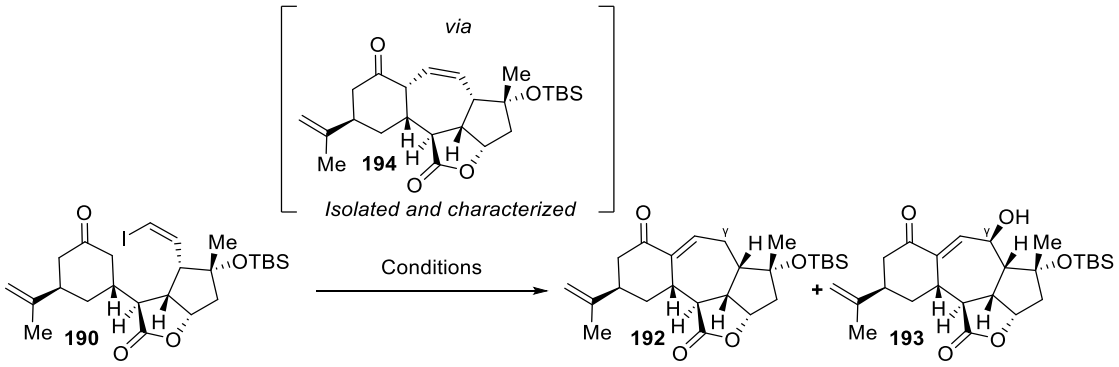


| Entry | Conditions (deviation from entry 1) | Results[1] |
|---|---|---|
| **1** | $Pd(PPh_3)_4$ 0.2 eq, 2,6-dimethylphenol 3.5 eq, *t*-BuOK 3.0 eq, toluene, 65 °C, 90 min | **192** 53% yield<br>**193** 16% yield |
| **2** | $Pd(PPh_3)_4$ 0.2 eq, 2,6-dimethylphenol 3.5 eq, *t*-BuOK 3.0 eq, toluene, 65 °C, 17 h, *then* $O_2$, 65 °C, 17 h *then* $SiO_2$, 65 °C, 17 h | **192** formed<br>Formation of **193** unconclusive |
| **3** | $Pd(PPh_3)_4$ 0.2 eq, 2,6-dimethylphenol 3.5 eq, *t*-BuOK 3.0 eq, $H_2O$ 10 eq., toluene, 65 °C, 90 min | **192:193** 10:1 |
| **4** | $Pd(PPh_3)_4$ 0.2 eq, 2,6-dimethylphenol 3.5 eq, *t*-BuOK 3.0 eq, toluene, 65 °C, 90 min *under air atmosphere* | **No reaction** |
| **5** | $Pd(PPh_3)_4$ 0.2 eq, 2,6-dimethylphenol 8 eq, *t*-BuOK 3.0 eq, toluene, 65 °C, 90 min | **192:193** 10:1 |
| **6** | $Pd(PPh_3)_4$ 0.2 eq, 2,6-dimethylphenol 3.5 eq, *t*-BuOK 3.0 eq, toluene, 85 °C, 20 h | **192:193** 10:1 |

[1] Yields of isolated products, for entries in which no yields are reported, the analysis is solely based on the inspection of the crude mixture by NMR.

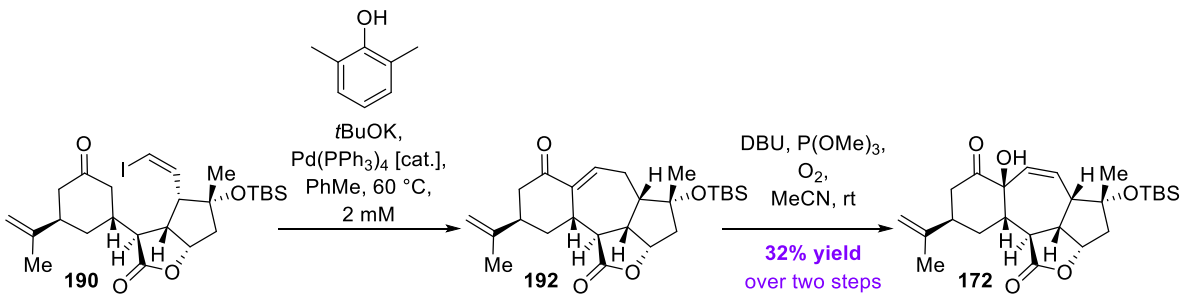


**Scheme 3.22.** Synthesis of allylic alcohol **172** from ketone **190**.

The Re-catalyzed allylic alcohol rearrangement of hydroxyketone **172** afforded alcohol **193** in 54% yield. Despite the long reaction time, no TBS-cleavage was observed unlike with TMS. The deprotection had therefore to carried out separately to form alcohol **175** in 60% yield (32% yield from **172** (Scheme 3.23)). As the yields are lower than when a TMS ether is used, it was decided to invert the order of the steps to potentially improve the yields.

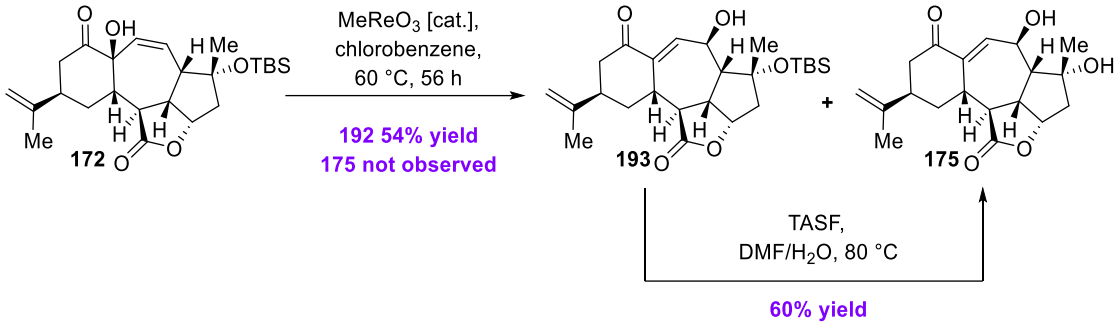


**Scheme 3.23.** Allylic rearrangement of the TBS-protected hydroxyketone **171**.

Alcohol **172** could be deprotected with TASF as described by the Sarlah group, affording **171** in 70% yield (lit. yield: 76%[41]). For comparison purposes, as this deprotection is meant to replace the two-step transsilylation sequence, the yield of the formation of TMS-protected ether **135** from TBS-protected ether **73** is 77%, which is in the range of the yield of the late-stage TBS removal.

Allylic rearrangement of compound **172** with $MeReO_3$ afforded alcohol **175** in 71% yield (90% yield brsm) alongside scabrolide B **34** in 8% yield (10% yield brsm) (Scheme 3.24).

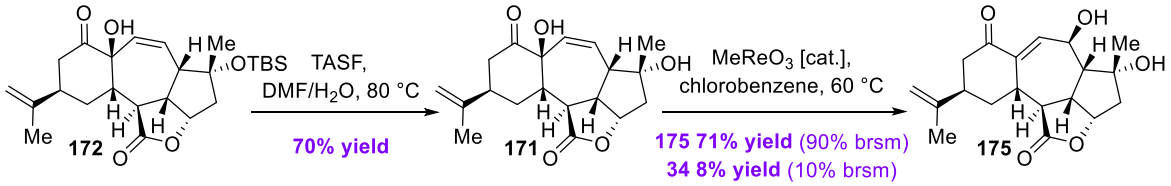


**Scheme 3.24.** Synthesis of allylic alcohol **175** *via* the deprotection/rearrangement sequence.

Overall, scabrolide B **34** could be synthesized from lactone **73** with no transsilylation sequence. The overall synthesis is one-step shorter with a TBS ether

but also much less mass efficient: 0.4% yield over 18 steps with a TBS ether, 1.2% yield over 19 steps with a TMS ether.

In conclusion, scabrolide B **34** was synthesized in 19 steps from *(R)*-linalool, and was successfully elaborated into sinuscalide C **35**, fragilolide A **33**, ineleganolide **1**, horiolide **3** and kavaranolide **18**, some of which were synthesized for the first time – with potentially biosynthetic implications. Key to success was a challenging intramolecular alkenylation of an almost symmetrical ketone, which allowed the congested central seven-membered ring with an inscribed bridgehead olefin to be forged, as well as an allylic alcohol rearrangement which allowed the oxidative pattern to be formed.

# 4. Conclusion and Outlook

Scabrolide B **34** is a furanobutenolide-derived norcembranoid first isolated from *Sinularia Scabra* in 2002. Initially misassigned, its structure features a highly oxygenated 6/7/5/5 ring system with seven stereocenters, six of which are contiguous.

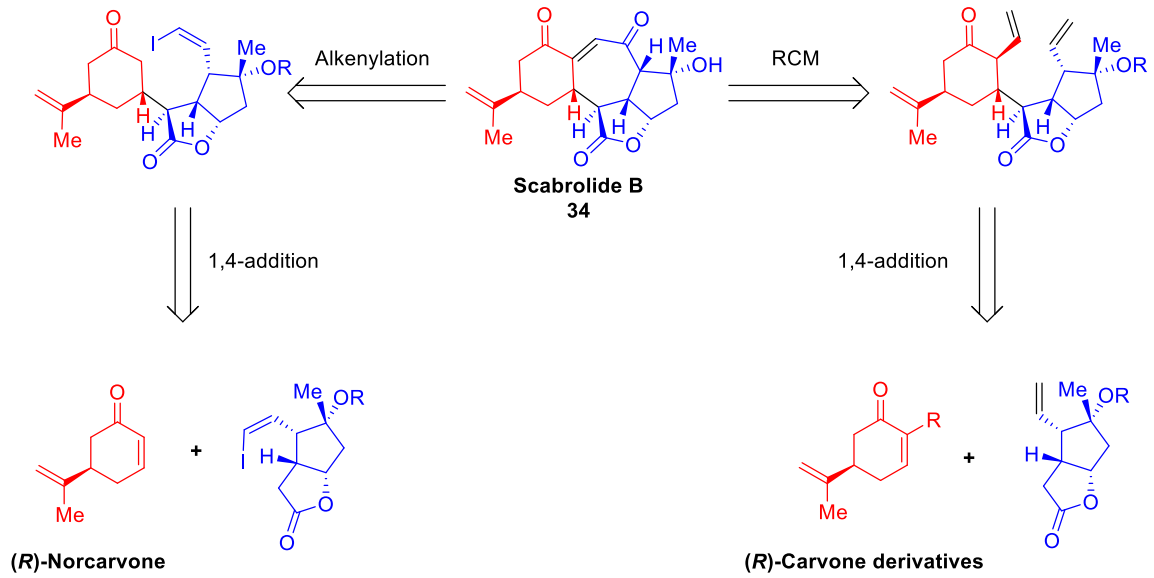


**Scheme 4.1.** Retrosynthetic analyses of scabrolide B **34**.

Two different retrosynthetic approaches to scabrolide B **34** were investigated: both rely on a 1,4-addition to connect two fragments: one is a carvone derivative, while the other one is a [5,5]-bicyclic lactone containing five of the stereocenters of **34**. The two approaches differ in the way the seven-membered ring is closed: either by RCM reaction or by enolate alkenylation (Scheme 4.1).

In the forward sense, for the RCM approach, the bicyclic lactone was synthesized in eleven steps from *(R)*-linalool, while several potential carvone derivatives were synthesized from *(L)*-carveol. Of all the investigated *(R)*-carvone derivatives, only the selenide derivative **95** provided the desired intermediate. However, the delicate β,γ-unsaturated ketone **137** could not be engaged in RCM even under forcing conditions; poor conversions into complex mixtures were observed, which contained at best traces of an isomeric cycloheptene **139** (Scheme

4.2). That result suggested the critical character of the stereochemistry at C4 for the outcome of the RCM reaction. When attempting to synthesize a cyclization precursor with a modified spatial orientation at that position, $\alpha$-hydroxyketone **147** was formed in small amount. **147** could be successfully closed by RCM under forcing conditions, affording the ring-closed product **148** (Scheme 4.2). While that route was not pursued further due to low material throughput, product **148** will also be synthesized using the alkenylation strategy, which ultimately provided scabrolide B **34**. This sequence therefore constitutes a formal total synthesis of **34** by RCM.

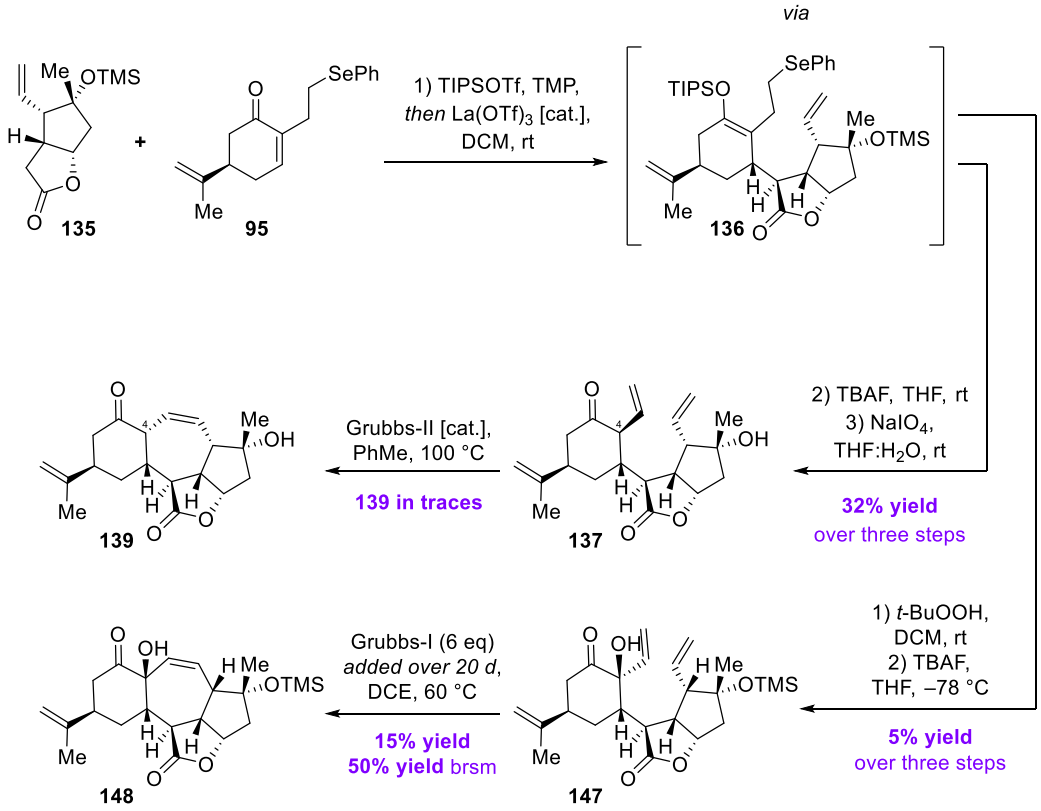


**Scheme 4.2.** Attempts to synthesize scabrolide B **34** by RCM reaction.

For the alkenylation approach, vinyl iodide **149** was obtained from lactone **135** in two steps. (*R*)-Norcarvone **96** was generated *de novo* in three steps. The two fragments were coupled via a Mukaiyama–Michael addition and the ring was subsequently closed by Pd-catalyzed enolate alkenylation. After $\alpha$-hydroxylation, Re-catalyzed transposition and oxidation, scabrolide B **34** was obtained in

1.2% yield over 19 steps (longest linear sequence) and 110 mg of combined isolated material from the final two steps in a single run (Scheme 4.3).

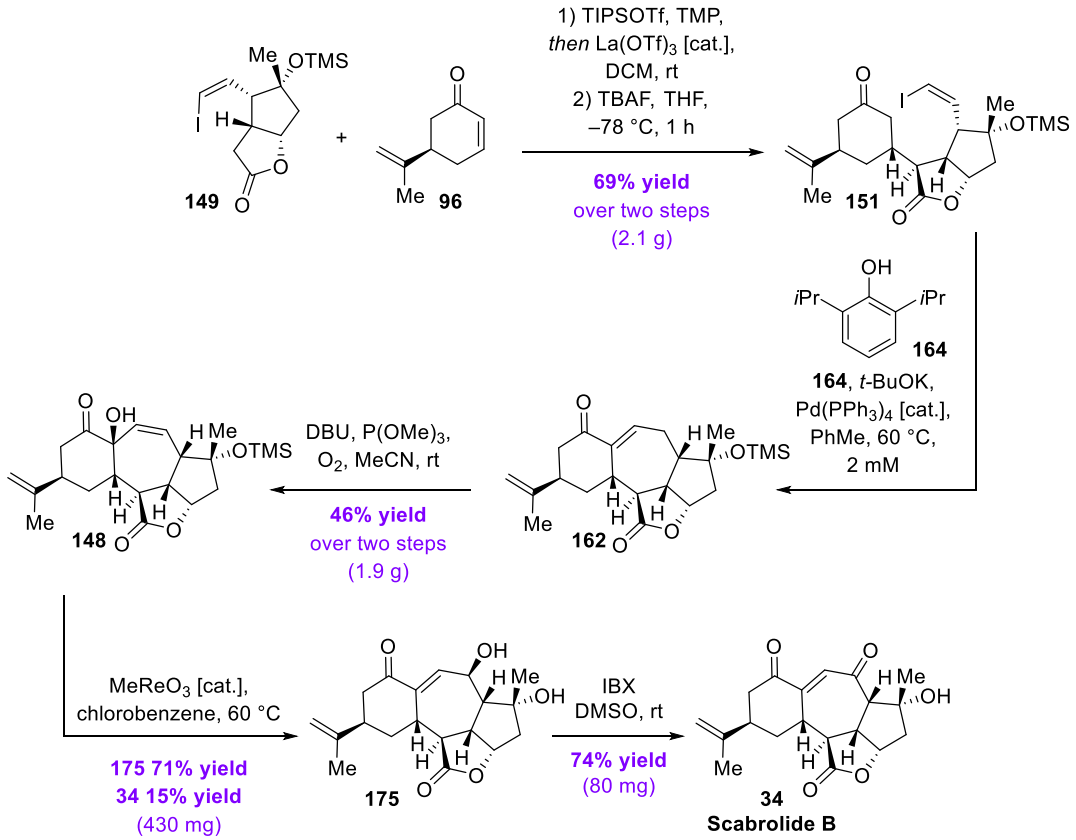


**Scheme 4.3.** Total synthesis of scabrolide B **34** by enolate alkenylation.

Scabrolide B **34** could then be transformed into sinuscalide C **35**, fragilolide A **33**, ineleganolide **2**, horiolide **3** and kavaranolide **18**. The one-pot formation of ineleganolide **2** under basic conditions from **34** reveals a previously unrecognized biosynthetic link between both natural products. Further, the successful formation of horiolide **2** and kavaranolide **18** *via* ineleganolide **2** confirms the proposed biosynthetic pathway between these compounds (Scheme 4.4).

The current foray allowed the total synthesis of a series of six related natural products in respectable amounts. As the biological activity of this family of natural products remains largely unexplored, submitting these compounds, alongside structurally similar intermediates such as **175** and the deprotected derivative of **162**, to biological assays might provide precious insights in their bioactivity.

Depending on the results of these assays, further analogues could then be synthesized.

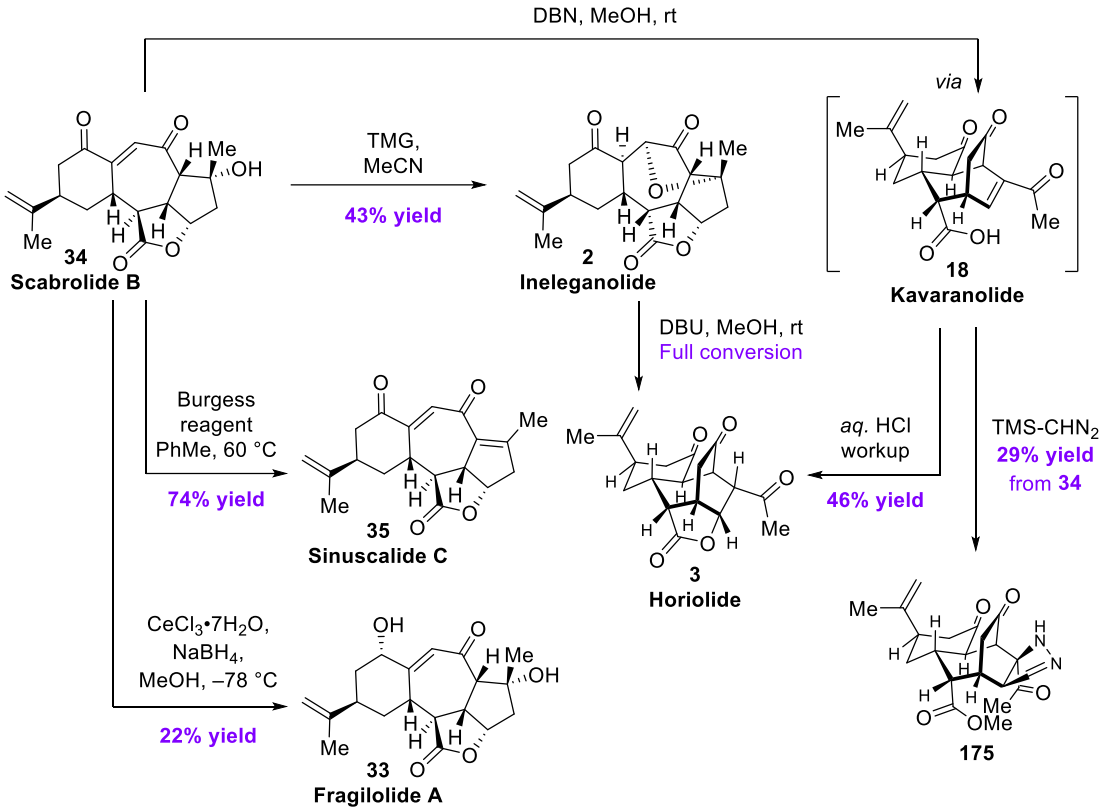


**Scheme 4.4.** Interconversion of scabrolide B **34** into other related norcembranoids.

These considerations, however, gain true significance only if the synthesized compounds prove to possess meaningful biological activity. The structural complexity of these norcembranoids suggests that their biosynthesis by *Sinularia* soft corals is likely biologically relevant. From an evolutionary perspective, the persistence of such complex molecules indicates they may provide a selective advantage in their natural environment. Clarifying the biological relevance of scabrolide B **34** and its congeners will therefore be essential not only for understanding their potential ecological roles but also to guide future synthetic, mechanistic, and potentially medicinal studies. The work presented herein provides a strong foundation for both the continued chemical exploration of these compounds and for investigating their biological properties.

# 5. Experimental section

## 5.1 General information

Unless stated otherwise, all reactions were carried out in flame-dried glassware using anhydrous solvents under argon atmosphere.

The solvents were purified by distillation over the indicated drying agents and were transferred under argon: THF, $Et_2O$ (Mg/anthracene); acetonitrile, 2,6-lutidine, $CH_2Cl_2$, 1,2-dichloroethane, nitromethane ($CaH_2$); toluene (Na/K alloy); MeOH (Mg, stored over MS 3 Å). DMSO, DMF, $Et_3N$, pentane and pyridine were dried by an adsorption solvent purification system based on molecular sieves.

Thin layer chromatography (TLC): Macherey-Nagel pre-coated plates (POLYGRAM®SIL/UV254). Detection was achieved under UV-light (254 nm) and by staining with cerium ammonium molybdenate. Flash chromatography: Merck silica gel 60 (40–63 μm) with predistilled or HPLC grade solvents.

NMR: spectra were recorded on Bruker AV 400, AV 500, AVIII 600 or AVneo 600 spectrometers in the indicated solvents; chemical shifts (δ) are given in ppm relative to TMS, coupling constants (*J*) in Hz. All spectra were recorded at 25 °C. The solvent signals were used as references and the chemical shifts converted to the TMS scale ($CDCl_3$: $\delta_C$ = 77.16 ppm; residual $CHCl_3$ in $CDCl_3$: $\delta_H$ = 7.26 ppm; $CD_2Cl_2$: $\delta_C$ = 53.84 ppm, residual $CDHCl_2$: $\delta_H$ = 5.32 ppm). Multiplicities are indicated by the following abbreviations: s: singlet, d: doublet, t: triplet, q: quartet, hept: heptet, m: multiplet, br. s: broad singlet.

$^{13}C$ NMR spectra were recorded in $^{1}H$ decoupled manner and the values of the chemical shifts are rounded to one decimal point. Signal assignments were established using HSQC, HMBC, COSY, NOESY and other 2D experiments.

IR: Spectra were recorded on an Alpha Platinum ATR instrument (Bruker), wave numbers ($\tilde{\nu}$) in $cm^{-1}$.

MS (ESI-MS): Finnigan MAT 8200 (70 eV), ESI-MS: ESQ3000 (Bruker), accurate mass determinations: Bruker APEX III FTMS (7 T magnet) or Mat 95 (Finnigan).

Optical rotations ($[\alpha]_D^{20}$) were measured with an A-Krüss Optronic Model P8000-t polarimeter at a wavelength of 589 nm.

Unless stated otherwise, commercially available compounds (Alfa Aesar, Sigma Aldrich, TCI, Strem Chemicals, ChemPUR) are used as received.

## 5.2 Experimental procedures

### 5.2.1 First approach: by RCM to form the C5-C6 bond of Scabrolide B

#### 5.2.1.1 Preliminary studies

**Ester 66**

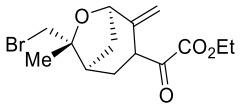


To a stirred solution of alcohol **68** (1.82 g, 7.36 mmol) and $CBr_4$ (2.56 g, 7.72 mmol) in dichloromethane (24.5 mL) was added $PPh_3$ (2.05 g, 7.82 mmol) at room temperature. After 2 h, the solvent was removed and the residue was purified by flash chromatography on silica, eluting with 10% *tert*-butyl methyl ether in petroleum ether to afford the bromide (2.0 g, 87.6%).

To a solution of the cyclic bromide (2.0 g, 6.45 mmol) in THF (13 mL) was added dropwise aldehyde (4.1 mL, 19.4 mmol), $NH_4Cl$ (345 mg, 6.45 mmol) and zinc metal (843 mg, 12.9 mmol). The mixture was stirred 3 h, filtered to remove excess zinc and precipitated salts, and the organic layers were separated. The aqueous layer was washed with diethyl ether (3 × 50 mL). The combined organics were dried over $Na_2SO_4$, filtered, and concentrated. The crude was purified by flash chromatography on silica, eluting with 20% EtOAc in Hexanes to afford the desired product (1.22 g, 57%).

DMP (2.26 g, 5.33 mmol) was added to a solution that ester in dichloromethane (18 mL). The mixture was stirred at room temperature for 1 h. The mixture was extracted with EtOAc (50 mL x 3), washed with brine (10 mL), dried over $Na_2SO_4$, filtered and concentrated. The crude was purified by flash chromatography on

silica, eluting with 10% EtOAc in Hexanes to afford the desired product **66** (930 mg, 57% yield over three steps).

$^1$H NMR (400 MHz, $CDCl_3$): δ = 4.91 (d, *J* = 2.6 Hz, 1H), 4.62 (d, *J* = 6.4 Hz, 1H), 4.52 (d, *J* = 2.4 Hz, 1H), 4.34 (q, *J* = 7.1 Hz, 3H), 3.76–3.54 (m, 1H), 3.50 (dd, *J* = 10.2, 0.7 Hz, 1H), 2.52 (dddd, *J* = 12.0, 6.5, 4.7, 2.6 Hz, 1H), 2.47–2.39 (m, 1H), 2.22 (ddt, *J* = 13.7, 8.2, 2.6 Hz, 1H), 2.11 –2.00 (m, 1H), 1.83 (d, *J* = 12.0 Hz, 1H), 1.44 (d, *J* = 0.9 Hz, 3H), 1.37 (t, *J* = 7.1 Hz, 3H); $^{13}$C NMR (101 MHz, $CDCl_3$): δ = 195.4, 161.5, 146.1, 110.0, 84.1, 82.2, 62.8, 45.7, 41.2, 37.0, 36.9, 27.5, 26.3, 14.1.

**Ketone 69**

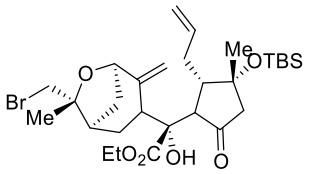


To a stirred solution of the enone **67** (1.27 g, 5.6 mmol) in dichloromethane (43 mL) was added $TiCl_4$ (1.0 M solution in dichloromethane, 5.3 mL, 5.3 mmol) dropwise at −78 °C and stirred at that temperature for 10 min. To the resulting solution was added allyltrimethylsilane (1.0 mL, 6.3 mmol) dropwise at −78 °C over 2 h. After stirring for additional 10 min at −78 °C, ester **66** (930 mg, 2.81 mmol) was added to the above mixture and stirred for 10 min before it was quenched with sat. aq. $NaHCO_3$ (50 mL). The mixture was partitioned between ether and brine. The organic layer was dried over $Na_2SO_4$ and the solvent was evaporated. The crude was purified by flash chromatography on silica, eluting with 20% EtOAc in Hexanes to afford the desired product **69** (820 mg, 49% yield, 2:1) as a white solid.

Polar isomer: $^1$H NMR (600 MHz, $CDCl_3$): δ = 5.83 (dddd, *J* = 17.1, 10.1, 8.6, 5.2 Hz, 1H), 5.04 (dq, *J* = 17.2, 1.0 Hz, 1H), 4.98 (ddt, *J* = 10.2, 2.0, 1.0 Hz, 1H), 4.72 (dd, *J* = 4.6, 2.6 Hz, 2H), 4.51 (d, *J* = 6.4 Hz, 1H), 4.33 (dq, *J* = 10.8, 7.2 Hz, 1H), 4.21 – 4.09 (m, 2H), 3.62 (d, *J* = 10.1 Hz, 1H), 3.56 – 3.46 (m, 1H), 2.62 – 2.54 (m, 1H), 2.53 – 2.46 (m, 3H), 2.41 (d, *J* = 1.4 Hz, 1H), 2.38 – 2.33 (m, 2H), 2.12 (td, *J* = 9.5, 2.2 Hz, 1H), 2.08 – 2.02 (m, 1H), 1.86 – 1.76 (m, 1H), 1.59 – 1.54 (m, 2H), 1.45 (s, 3H), 1.42 (d, *J* = 0.7 Hz, 3H), 1.30 (t, *J* = 7.2 Hz, 3H), 0.85 (s, 9H), 0.09 (d, *J* = 2.7 Hz, 6H);

$^{13}$C NMR (151 MHz, $CDCl_3$): δ = 213.4, 174.6, 148.9, 138.8, 115.8, 107.3, 84.3, 84.1, 79.0, 78.4, 62.4, 56.9, 55.5, 48.3, 42.0, 41.3, 37.9, 37.5, 32.6, 30.1, 26.5, 26.4, 26.0, 18.4, 14.3, -2.1, -2.5; HRMS (ESI): calcd for $C_{29}H_{47}BrO_6SiNa$ $[M+Na]^+$: 621.22176, found: 621.22177.

**Triene 75**

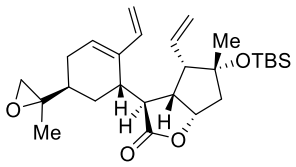


2,2,6,6-tetramethylpiperidine (90 $\mu$L, 0.533 mmol) was added to a solution of lactone **73** (81 mg, 0.273 mmol) in $CH_2Cl_2$ (1.4 mL).

The mixture was cooled to 0 °C before triisopropylsilyl trifluoromethanesulfonate (130 $\mu$L, 0.484 mmol) was added. The mixture was warmed to room temperature and stirred for 30 min. A solution of aldehyde **72** (78 mg, 0.30 mmol) in dichloromethane (0.4 mL) was added, and the resulting mixture was stirred for 5 min. The rubber septum was temporarily removed, and $La(OTf)_3$ (18 mg, 0.03 mmol) was added at -78 °C then followed by $La(OTf)_3$ (18 mg, 0.03 mmol). The mixture was to stirred for 1 h before it was quenched with sat. aq. $Na_2HCO_3$ (2 mL). The resulting mixture was extracted with EtOAc (5 mL x 3), washed with brine (2 mL), dried with $Na_2SO_4$, filtered and concentrated. The crude mixture was purified by flash chromatography on silica, eluting with 40% EtOAc in hexanes to give the desired product as a pair of isomers. The mixture was further subjected to preparative HPLC separation [(150 μm Kromasil-5-C18, 30.0 mm ∅, MeCN, 35 mL/min, $\lambda$ = 254 nm, t = 11 min)] to afford the title compound **74** as a colorless oil

HF solution (50% in $H_2O$, 0.05 mL, 1.44 mmol) was added to a solution of that product (16 mg, 23 μmol) in THF (0.5 mL) at 0 °C. The mixture was warmed to room temperature and stirred at this temperature before it was poured into sat. aq. $NaHCO_3$ (3 mL). The resulting mixture was extracted with EtOAc (3 x 5 mL), washed with brine (5 mL), dried over $Na_2SO_4$, filtered and concentrated. The crude product was purified over a pad of silica gel to provide the desired product.

*t*-BuOK (10 mg, 89 μmol) was added to a solution of methyltriphenylphosphonium bromide (33 mg, 92 μmol) in THF (0.46 mL). After stirring for 30 min, a solution of furanyl aldehyde (10 mg, 0.019 μmol) in THF (0.5 mL) was added at 0 °C, the mixture was stirred at that temperature for 15 min, then at room temperature for another 12 h. After water (0.1 mL) was added, the resulting solvent was removed, and the crude was purified by flash chromatography on silica (hexane/EtOAc 4:1) to afford the triene **75** (8.3 mg, 9% yield over three steps) as a colourless oil.

$^1$H NMR (400 MHz, $CDCl_3$): δ = 6.26 (dd, *J* = 17.6, 11.0 Hz, 1H), 6.01 – 5.89 (m, 2H), 5.28 (dd, *J* = 10.2, 2.2 Hz, 1H), 5.20 – 5.07 (m, 2H), 4.96 (dt, *J* = 10.9, 0.8 Hz, 1H), 4.90 –4.82 (m, 1H), 3.01 – 2.90 (m, 3H), 2.63 (dd, *J* = 4.8, 0.8 Hz, 1H), 2.51 (d, *J* = 4.7 Hz, 1H), 2.34 (d, *J* = 9.3 Hz, 1H), 2.31 – 2.24 (m, 1H), 2.24 – 2.18 (m, 1H), 1.99 – 1.86 (m, 2H), 1.81 – 1.71 (m, 2H), 1.62 – 1.53 (m, 1H), 1.28 – 1.24 (m, 6H), 0.84 (s, 9H), 0.09 (s, 3H), 0.06 (s, 3H); $^{13}$C NMR (101 MHz, $CDCl_3$): δ = 180.0, 138.4, 136.4, 134.7, 130.4, 119.8, 112.3, 83.5, 83.3, 58.9, 58.7, 53.0, 47.6, 47.4, 44.8, 36.3, 34.2, 31.1, 29.2, 27.5, 26.2, 26.2, 18.6, -1.8, -2.1.

**Diene 78**

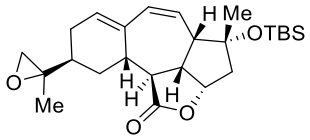


Hoveyda-Grubbs second-generation catalyst (1.0 mg, 1.6 μmol) was added to a solution of triene **75** (2 mg, 3.7 μmol) in toluene (1.0 mL) at room temperature. The resulting mixture was heated to 100 °C (bath temperature) and stirred at this temperature for 12 h. The mixture was cooled to room temperature, the solvent was removed under high vacuum, the crude was purified by flash chromatography on silica, eluting with a gradient of 20-35% EtOAc in hexanes to afford the desired product **78** (1.2 mg, 63% yield) as a colourless oil.

$^1$H NMR (600 MHz, $CDCl_3$): δ = 6.05 (dd, *J* = 12.9, 1.0 Hz, 1H), 5.77 (q, *J* = 4.3 Hz, 1H), 5.32 (dd, *J* = 12.8, 4.7 Hz, 1H), 4.93 (ddd, *J* = 8.9, 8.2, 2.4 Hz, 1H), 4.28 (s, 1H),

3.65 (t, *J* = 10.6 Hz, 1H), 2.97 (ddd, *J* = 10.6, 8.1, 6.8 Hz, 1H), 2.89 (dt, *J* = 13.7, 3.9 Hz, 1H), 2.64 (dd, *J* = 4.6, 0.9 Hz, 1H), 2.50 (dd, *J* = 4.6, 0.8 Hz, 1H), 2.44 (t, *J* = 5.7 Hz, 1H), 2.39 (m, 1H), 2.24 (dd, *J* = 15.9, 2.4 Hz, 1H), 2.17 (dd, *J* = 15.9, 8.9 Hz, 1H), 2.16 (m, 2H), 1.92 (m, 1H), 1.66 (ddd, *J* = 13.9, 11.6, 5.0 Hz, 1H), 1.43 (s, 3H), 1.38 (d, *J* = 0.7 Hz, 3H), 0.79 (s, 9H), 0.07 (s, 6H); $^{13}$C NMR (151 MHz, $CDCl_3$): δ = 177.7, 138.6, 134.9, 134.0, 121.1, 83.9, 79.6, 57.8, 53.6, 52.1, 51.2, 48.7, 42.5, 38.4, 34.6, 28.3, 28.1, 25.9, 25.2, 21.1, 18.2, -1.9, -2.4; HRMS (ESI): calcd for $C_{27}H_{42}O_4SiNa$ $[M+Na]^+$: 481.27446, found: 481.27422.

**Triene 79**

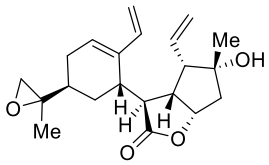


2,2,6,6-Tetramethylpiperidine (189 μL, 1.12 mmol) was added to a solution of lactone **135** (117.3 mg, 0.461 mmol) in dichloromethane (2 mL). The mixture was cooled to 0 °C before triisopropylsilyl trifluoromethanesulfonate (170 μL, 0.633 mmol) was added. The mixture was warmed to room temperature and stirred for 4 h. A solution of aldehyde **72** (360 mg, 1.47 mmol) in dichloromethane (1.0 mL) was added, followed by $La(OTf)_3$ (18 mg, 0.03 mmol). The resulting mixture was stirred at that temperature for 24 h before it was quenched with HCl (2 M, 5 mL). After stirring for 10 min, the aqueous phase was extracted with EtOAc (5 mL x 3), the combined extracts were washed with brine (2 mL), dried over $Na_2SO4$, and filtered. After evaporation of the solvent, the residue was quickly passed through a short plug silica, eluting with 25% Acetone: in hexanes to provide a rather unstable colourless oil.

*t*-BuOK (130 mg, 1.16 mmol) was added to a solution of methyltriphenylphosphonium bromide (418 mg, 1.17 mmol) in THF (5 mL) at 0 °C and the resulting mixture was stirred for 30 min. A solution of the crude aldehyde obtained in the previous step in THF (0.8 mL) was added. Stirring was continued at 0 °C for 15 min and then at room temperature for another 12 h. Water (0.1 mL)

was added to quench the mixture. All volatiles were removed and the crude material was purified by flash chromatography on silica, eluting with 20% acetone in hexanes to afford the title compound **79** as a colourless oil (26 mg, 16% yield over two steps).

$^{1}$H NMR (400 MHz, $CDCl_3$): δ = 6.27 (dd, *J* = 17.7, 11.0 Hz, 1H), 6.06–5.86 (m, 2H), 5.31 (dd, *J* = 10.2, 2.2 Hz, 1H), 5.24–5.09 (m, 2H), 4.98 (d, *J* = 11.0 Hz, 1H), 4.89 (dd, *J* = 7.6, 6.1 Hz, 1H), 3.04 (t, *J* = 3.5 Hz, 1H), 2.96 (ddd, *J* = 9.2, 7.6, 3.7 Hz, 2H), 2.67 – 2.55 (m, 1H), 2.53 (d, *J* = 4.7 Hz, 1H), 2.39 (t, *J* = 9.4 Hz, 1H), 2.28 – 2.09 (m, 4H), 1.98–1.85 (m, 2H), 1.84–1.77 (m, 1H), 1.77 – 1.71 (m, 1H), 1.25 (s, 3H), 1.22 (s, 3H); $^{13}$C NMR (101 MHz, $CDCl_3$): δ = 180.4, 138.3, 136.3, 133.6, 130.4, 120.6, 112.4, 83.1, 80.5, 58.9, 56.6, 53.0, 47.6, 47.4, 45.4, 36.4, 34.2, 29.6, 29.4, 27.6, 25.6, 18.6; HRMS (ESI): m/z: calcd. for $C_{21}H_{28}O_4Na$ [M+Na]$^+$: 367.18798, found: 367.18758.

**Tetraene 80**

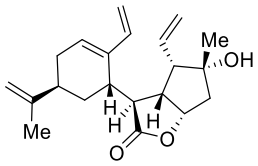


To a solution of compound **79** (22.4 mg, 0.065 mmol) in 1,4-dioxane and MeOH (1.2 mL, v/v = 1:1) were added zinc dust (85 mg, 1.30 mmol), $CuSO_4$ (10.0 mg, 0.0627 mmol), NaI (230 mg, 1.53 mmol), NaOAc (48.0 mg, 0.585 mmol), and HOAc (0.1 mL, 96 mmol). The resulting suspension was stirred at room temperature for 12 h before it was filtered through a pad of Celite®, rinsing with EtOAc (15 mL). The combined filtrates were washed with sat. aq. $NaHCO_3$ (2 mL) and brine (2 mL), dried over $Na_2SO_4$ and evaporated. The residue purified by flash chromatography on silica, eluting with a gradient of 13-18% acetone in hexane to afford the title compound **80** as a colourless oil (20.0 mg, 94% yield).

$^{1}$H NMR (400 MHz, $CDCl_3$): δ = 6.27 (dd, *J* = 17.6, 11.0 Hz, 1H), 6.08 – 5.85 (m, 2H), 5.30 (dd, *J* = 10.3, 2.1 Hz, 1H), 5.25 – 5.08 (m, 2H), 4.97 (d, *J* = 11.0 Hz, 1H), 4.86 (dd, *J* = 7.4, 6.1 Hz, 1H), 4.75 – 4.63 (m, 2H), 3.11 – 2.88 (m, 3H), 2.52 – 2.21 (m, 3H), 2.17 (d, *J* = 15.0 Hz, 1H), 2.04 – 1.87 (m, 2H), 1.81 (dd, *J* = 15.0, 6.2 Hz, 1H), 1.76 – 1.65

(m, 4H), 1.22 (s, 3H); $^{13}$C NMR (101 MHz, $CDCl_3$): δ = 180.8, 149.2, 138.4, 136.1, 133.7, 131.0, 120.5, 112.5, 109.2, 83.2, 80.5, 56.6, 47.4, 47.3, 45.9, 37.1, 35.5, 33.1, 31.1, 25.6, 20.7; HRMS (ESI): m/z: calcd for $C_{21}H_{28}O_3Na$ [M+Na]$^+$: 351.19306, found: 351.19329.

**Diene 82**

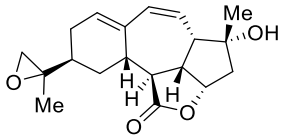


$^1$H NMR (400 MHz, $CDCl_3$): δ = 6.20 (dd, *J* = 12.8, 1.6 Hz, 1H), 5.88 – 5.81 (m, 1H), 5.31 (dd, *J* = 12.8, 5.0 Hz, 1H), 4.93 (ddd, *J* = 8.0, 6.9, 5.3 Hz, 1H), 3.52 (t, *J* = 10.8 Hz, 1H), 2.97 (ddd, *J* = 11.0, 8.0, 6.5 Hz, 1H), 2.89 – 2.80 (m, 1H), 2.65 – 2.57 (m, 2H), 2.52 – 2.49 (m, 1H), 2.46 – 2.36 (m, 1H), 2.25 – 2.18 (m, 3H), 2.17 – 2.12 (m, 1H), 2.00 – 1.90 (m, 1H), 1.85 – 1.75 (m, 1H), 1.38 (s, 6H); $^{13}$C NMR (101 MHz, $CDCl_3$): δ = 177.3, 138.2, 138.0, 135.8, 118.7, 81.1, 79.2, 57.7, 52.5, 51.8, 51.1, 47.1, 42.7, 38.1, 34.3, 28.8, 27.7, 25.4, 21.2.

**Triene 81**

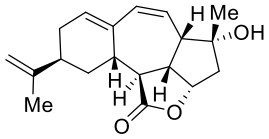


Second-generation Hoveyda-Grubbs catalyst (3.8 mg, 0.0061 mmol) was added to a solution of tetraene **80** (20.0 mg, 0.0609 mmol) in toluene (12.0 mL). The mixture was stirred at 100 °C (bath temperature) for 5 h. After cooling to ambient temperature, the solvent was removed under vacuum, and the residue was purified by flash chromatography on silica, eluting with 10% acetone in hexanes to afford the title compound **81** as a colourless oil (12.6 mg, 69%).

$^1$H NMR (400 MHz, $CDCl_3$): δ = 6.26 – 6.16 (m, 1H), 6.00 – 5.86 (m, 1H), 5.28 (dd, *J* = 12.8, 4.9 Hz, 1H), 4.91 (dt, *J* = 8.0, 6.0 Hz, 1H), 4.82 (q, *J* = 1.6 Hz, 1H), 4.60 (dt, *J* = 2.0, 1.0 Hz, 1H), 3.52 (t, *J* = 10.7 Hz, 1H), 2.97 (ddd, *J* = 11.0, 8.0, 6.6 Hz, 1H), 2.77–2.69 (m, 1H), 2.62–2.51 (m, 1H), 2.49–2.38 (m, 3H), 2.34–2.25 (m, 2H), 2.26–2.18 (m, 2H), 1.80–1.65 (m, 4H), 1.37 (s, 3H); $^{13}$C NMR (101 MHz, $CDCl_3$): δ = 177.4, 147.8,

138.7, 137.4, 135.5, 118.3, 109.8, 81.1, 79.2, 52.6, 51.9, 47.1, 42.5, 37.7, 37.0, 30.4, 28.8, 28.2, 22.3; HRMS (ESI): calcd for $C_{19}H_{24}O_3Na$ $[M+Na]^+$: 323.16176; found: 323.16199.

### 5.2.1.2 Fragment syntheses

#### 5.2.1.2.1 Eastern fragment

As a minor modification of the literature route to compound **73** reported,[14] the ozonolysis step was replaced by a catalytic dihydroxylation followed by periodate cleavage. This modified procedure is described below. All other steps followed exactly the literature.

**Lactone 89**

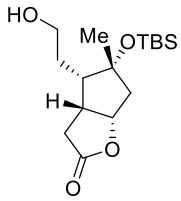


*N*-Methylmorpholine N-oxide (2.5 g, 21 mmol) and OsO4 (4% w/w in water, 134 μL, 21 μmol) were added to a suspension of cyclohexene **86** (2.0 g, 7 mmol)[14] in acetone/THF/water (12 mL each). The mixture was stirred at 65 °C for 65 h and then cooled to room temperature. $NaIO_4$ (7.5 g, 35 mmol) was added and stirring continued at ambient temperature for 20 min. For work-up, the mixture was cooled to 0 °C before sat. aq. sodium $Na_2S_2O_3$ (20 mL) was introduced. The aqueous phase was extracted with EtOAc (3 x 100 mL) and the combined organic layers were washed with brine (20 mL), dried over $MgSO_4$, filtered, and concentrated under reduced pressure. The residue was purified by flash chromatography on silica, eluting with a gradient of 0-30% EtOAc in hexanes to afford **87** an unstable colorless oil, which was immediately used in the next step.

MS 4 Å (3.8 g) and PDC (3.7 g, 9.8 mmol) were successively added to a solution of this compound in $CH_2Cl_2$ (30 mL) at 0 °C. The mixture was stirred at this temperature for 1 h before it was quickly passed through a pad of silica, eluting with hexane:acetone (1:0 to 2:1). Evaporation of the combined filtrates gave **88** as a yellow oil, which was dissolved in THF (25 mL).

$NaBH_4$ (400 mg, 10.6 mmol) was added in portions to this solution at 0 °C and the mixture was stirred at this temperature for 15 min before quenching with sat.

aq. $NH_4Cl$ (50 mL). The resulting mixture was extracted EtOAc (3 x 200 mL), the combined organic layers were washed with brine (50 mL), dried with MgSO4, filtered, and evaporated. The residue was purified by flash chromatography on silica gel (hexanes:acetone, 4:1 to 1:1) to afford the title compound **89** as a white solid (1.03 g, 46% over 3 steps).

The analytical and spectroscopic data fully matched the literature.[14]

#### 5.2.1.2.2 Possible western fragments: a collective synthesis

**Silyl ether 91**

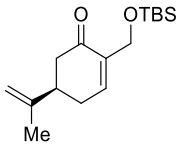


Imidazole (551 mg, 8.0 mmol) was added to a solution of alcohol **68** (1 g, 4.0 mmol) in dichloromethane (13 mL) at room temperature. The mixture was cooled to 0 °C, then TBSCl (1.2 g, 8.0 mmol) was added, the mixture was stirred at this temperature for 2 h. The mixture was adsorbed onto Celite®, dried *in vacuo*, then purified by flash chromatography on silica, eluting with a gradient of 0-12% EtOAc in hexanes to give the desired product as a yellow liquid.

$NH_4Cl$ (1.56 g, 29.1 mmol), then Zn dust (3.8 g, 58.4 mmol) was added to a solution of that product in EtOH (9.7 mL). The mixture was heated to 90 °C (bath temperature) for 17 h. It was cooled to room temperature, then filtered through Celite®, then concentrated. The residue was triturated with hexanes (10 mL), the remaining precipitate was filtered off, water (10 mL) was added to the resulting solution. The mixture was extracted with *tert*-butyl-methyl ether (3 x 30 mL), the combined organic layers were washed with brine (10 mL), dried over $MgSO_4$, filtered and concentrated under reduced pressure to give the desired product as an orange oil.

DMP (2.39 g, 5.6 mmol) was added to a solution of that product in dichloromethane (7 mL) at 0 °C. The mixture was stirred at room temperature for 1 h, then adsorbed onto Celite®, then purified by flash chromatography on silica,

eluting with a gradient of 0-6% EtOAc in hexanes to give the desired product **91** (670 mg, 81% yield over three steps) as a yellowish oil.

$^{1}$H NMR (400 MHz, $CDCl_3$) δ = 7.01 (dq, *J* = 6.5, 2.1 Hz, 1H), 4.82 (tt, *J* = 1.9, 1.0 Hz, 1H), 4.77 (tq, *J* = 1.7, 0.9 Hz, 1H), 4.36 (tt, *J* = 3.5, 1.9 Hz, 2H), 2.76 – 2.63 (m, 1H), 2.55 (ddt, *J* = 16.1, 4.3, 2.1 Hz, 2H), 2.37 (dd, *J* = 16.2, 13.5 Hz, 1H), 2.34 – 2.27 (m, 1H), 1.76 (s, 3H), 0.92 (s, 9H), 0.08 (s, 6H); $^{13}$C NMR (101 MHz, $CDCl_3$) δ = 199.1, 146.7, 143.2, 138.1, 110.6, 77.2, 60.0, 43.3, 42.2, 30.9, 26.0, 20.6, 18.4, -5.4.

**Ester 93**

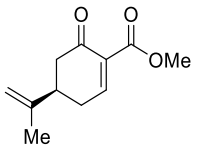


$H_2SO_4$ (0.78 mL, 14.6 mmol) was added dropwise to a solution of $CrO_3$ (728 mg, 7.3 mmol) in water (3.6 mL) at 0 °C. That solution was added over 4 h (1.2 mL every 80 min) to a solution of alcohol **68** (340 mg, 1.4 mmol) in acetone (12 mL) at 0 °C, stirring at that temperature between each addition. After the last addition, the mixture was stirred at room temperature for 17 h, then cooled to 0 °C, isopropanol (10 mL) was added and the aqueous layer was extracted with EtOAc (3 x 20 mL), the combined organic layers were washed with brine (12 mL), dried over MgSO4, filtered and concentrated under reduced pressure. The residue was purified by flash chromatography on silica, eluting with a gradient of 0-50% EtOAc in hexanes to give the desired product as a white solid.

$H_2SO_4$ (34 μL, 0.63 mmol) was added to a solution of that product in methanol (2 mL). The mixture was stirred for 72 h, then sat. aq. NaHCO3 (5 mL) was added, then $MgSO_4$ was added, the mixture was filtered, rinced with MeOH (3 x 2 mL) then concentrated until 2 mL of methanol remain.

$NH_4Cl$ (338 mg, 6.3 mmol) then Zn dust (826 mg, 12.6 mmol) was added to that solution, which was then heated to 60 °C (bath temperature) for 5 h. The resulting mixture was cooled to room temperature, then filtered through Celite®, then concentrated. Water (10 mL) was added to the resulting solution, the mixture was

extracted with EtOAc (3 x 20 mL), the combined organic layers were washed with brine (10 mL), dried over $MgSO_4$, filtered and concentrated under reduced pressure.

DMP (536 mg, 1.26 mmol) was added to a solution of that crude product in dichloromethane (1.6 mL) at 0 °C. The mixture was stirred at that temperature for 30 min, then sat. aq. $NaHCO_3$ (3 mL) then sat. aq. $Na_2S_2O_3$ (3 mL) were added, the mixture was extracted with dichloromethane (3 x 5 mL), the organics were combined, washed with brine (5 mL), dried over MgSO4, filtered and concentrated. That residue was suspended with *tert*-butyl methyl ether (5 mL), then washed with sat. aq. $NaHCO_3$ (3 x 3 mL) then dried on MgSO4, filtered and concentrated to give the desired product **93** (95 mg, 37% yield over four steps).

The spectral data fully matched the literature.[91]

**Alkyl selenide 95**

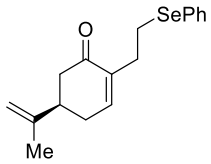


*n*-Butyllithium (1.6 M in hexanes, 7.0 mL, 11.1 mmol) was added to a solution of $PPh_3MeBr$ (4.24 g, 11.9 mmol) in THF (12 mL) at 0 °C. The resulting mixture was stirred for 5 min at this temperature and for 1 h at room temperature before it was cooled to 0 °C. A solution of aldehyde **72** (2.0 g, 7.91 mmol) in THF (12 mL) was added dropwise and stirring continued at that temperature for 1 h. Sat. aq. $NH_4Cl$ (10 mL) was introduced, the mixture was extracted with hexanes (3 x 100 mL), the combined organic layers were washed with brine (10 mL), dried over $MgSO_4$, filtered and concentrated under reduced pressure. The residue was triturated with hexanes, the remaining precipitate was filtered off, and the solution was concentrated. The residue was purified by flash chromatography on silica, eluting with a gradient of 0-5% *tert*-butyl methyl ether in hexanes to afford a colourless oil.

A solution of 9-BBN (0.5 M in THF, 9.0 mL, 4.5 mmol) was added dropwise over 5 min to a solution of that product in THF (42 mL) at 0 °C. The resulting

mixture was stirred at that temperature for 5 min and then for 4 h at room temperature. The mixture was cooled to 0 °C before water (1.0 mL) and $NaBO_3 \cdot H_2O$ (2.66 g, 13.3 mmol) were slowly added. After stirring for 17 h at room temperature, the mixture was poured into a sat. aq. sodium $Na_2S_2O_3$ (100 mL) at 0 °C. The aqueous layer was extracted with EtOAc (3 x 100 mL), the combined organics phases were washed with brine, dried over MgSO4, filtered and concentrated. The residue was purified by flash chromatography on silica, eluting with a gradient of 0-50% EtOAc in hexanes to afford the title compound as a colourless oil.

Tributylphosphine (2.3 mL, 9.36 mmol) was added to a suspension of N-(phenylseleno)-phtalimide (2.8 g, 9.36 mmol) in THF (6 mL). The mixture was stirred at room temperature for 5 min and then cooled to 0 °C before that alcohol (815 mg, 3.12 mmol) was added. Stirring was continued at room temperature for 17 h. The mixture was concentrated under a stream of argon and the residue purified by flash chromatography on silica, eluting with 0-6% acetone in hexanes to afford the desired selenide as a yellowish oil, which was directly used in the next step.

Zn powder (4.0 g, 61.2 mmol) and $NH_4Cl$ (1.6 g, 29.9 mmol) were added to a solution of this compound in EtOH (10 mL). The resulting mixture was stirred at reflux temperature for 150 min. The suspension was filtered through a pad of Celite®, rinsing with EtOAc (5 x 20 mL), and the combined filtrates were concentrated under reduced pressure. The residue was purified by flash chromatography on silica, eluting with a gradient of 0-30% *tert*-butyl methyl ether in hexanes to afford the title compound as a colourless oil.

$MnO_2$ (3.6 g, 41.4 mmol) was added to a solution of that alcohol in dichloromethane (10 mL) and the resulting suspension was stirred at room temperature for 17 h. The mixture was filtered through a pad of Celite®, rinsing with EtOAc (5 x 10 mL), and the combined filtrates were concentrated under reduced pressure to give the title compound **95** as a yellow oil (627 mg, 32% yield over five steps).

$[\alpha]_D^{20}$ = -16.9 (c = 0.8, $CHCl_3$). $^1H$ NMR (400 MHz, $CDCl_3$) δ = 7.52 – 7.47 (m, 2H), 7.30 – 7.20 (m, 3H) 6.77 (ddt, *J* = 6.1, 2.4, 1.1 Hz, 1H), 4.85 – 4.78 (m, 1H), 4.75 (s, 1H), 3.15 – 2.99 (m, 2H), 2.64 (t, *J* = 7.6 Hz, 2H), 2.60 – 2.55 (m, 1H), 2.52 (ddd, *J* = 15.8, 3.8, 1.7 Hz, 1H), 2.44 (dt, *J* = 18.4, 5.2 Hz, 1H), 2.30 – 2.21 (m, 2H), 1.75 (s, 3H); $^{13}C$ NMR (101 MHz, CDCl3) δ = 199.0, 146.6, 146.2, 137.7, 132.3, 132.2, 132.2, 130.5, 129.1, 126.6, 110.6, 43.2, 42.1, 31.2, 31.2, 26.4, 20.5; IR (film) ν/$cm^{-1}$: 3071, 2968, 2933, 1672, 1579, 1478, 1436, 1378, 1243, 1133, 1023, 897, 737, 691; HRMS (ESI): calcd for $C_{17}H_{20}OSeNa$ $[M+Na]^+$: 343.05716, found: 343.05715.

### 5.2.1.2.3 *De novo* synthesis of *(R)*-norcarvone

**_(R)_-3-(Prop-1-en-2-yl)cyclohexan-1-one 99**

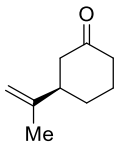


Catalyst solution: A mixture comprising $[Rh(cod)Cl]_2$ (27.5 mg, 55.8 μmol), *(R)*-DTBM SEGPHOS (136 mg, 0.115 mmol) and methanol (2.5 mL) was stirred for 20 min at room temperature to give a homogeneous dark orange solution. A 100-mL two-necked flask equipped with a reflux condenser was charged with 2,2-dimethyl-1,3-propanediol (2.13 g, 20.5 mmol), hexanes (15 mL), isopropenylboronic acid pinacol ester (3.8 mL, 20 mmol), *N,N*-diisopropylethylamine (1.6 mL, 9.2 mmol) and water (5.4 mL). Argon was bubbled through the mixture for five minutes before 2-cyclohexen-1-one (1.8 mL, 19 mmol) and the catalyst solution (see above, rinsing with an additional amount of methanol: 0.30 mL) were introduced. The resulting biphasic mixture was stirred at 60 °C (bath temperature) for 24 h. The mixture was cooled to room temperature, diluted with diethyl ether (15 mL), and the layers were separated. The organic layer was washed with aq. HCl (1 M, 20 mL) and water (2 × 15 mL), and the combined aqueous phases were extracted with diethyl ether (3 × 15 mL). The combined extracts were dried over $Na_2SO_4$, the drying agent was filtered off, and the solvent was carefully removed under reduced pressure (200 mbar, 36 °C). The

dark amber residue was purified by flash chromatography on silica, eluting with 11% diethyl ether in pentane to furnish the title compound **99** after careful evaporation of the solvents (150 mbar, 36 °C) as a yellow liquid (2.23 g, 87% yield, *94% ee*).

$[\alpha]_D^{20}$ = +18.2 (c = 1,1, $CH_2Cl_2$). $^1H$ NMR (400 MHz, $CDCl_3$): δ = 4.80 – 4.76 (m, 1H), 4.75 – 4.71 (m, 1H), 2.48 - 2.22 (m, 5H), 2.13 – 2.02 (m, 1H), 1.98 – 1.88 (m, 1H), 1.76 – 1.73 (m, 3H), 1.73 - 1.55 (m, 2H); $^{13}C$ NMR (101 MHz, $CDCl_3$): δ = 211.8, 147.6, 110.2, 46.9, 45.8, 41.4, 30.2, 25.3, 20.8; IR (film) ν/$cm^{-1}$ : 3079, 2938, 2865, 1710, 1645, 1448, 1423, 1376, 1346, 1316, 1271, 1251, 1223, 1182, 1102, 1056, 890, 754, 548, 473; HRMS (GC-EI): calcd. for C9H14O [M+]: 138.1039; found: 138.1042. The enantiomeric purity was determined by GC. The racemic sample needed for comparison was obtained by copper-catalyzed addition of isopropenylmagnesium bromide (CuI, THF, 0 °C) to 2-cyclohexen-1-one. The analytical data are in agreement with those reported in the literature. [92]

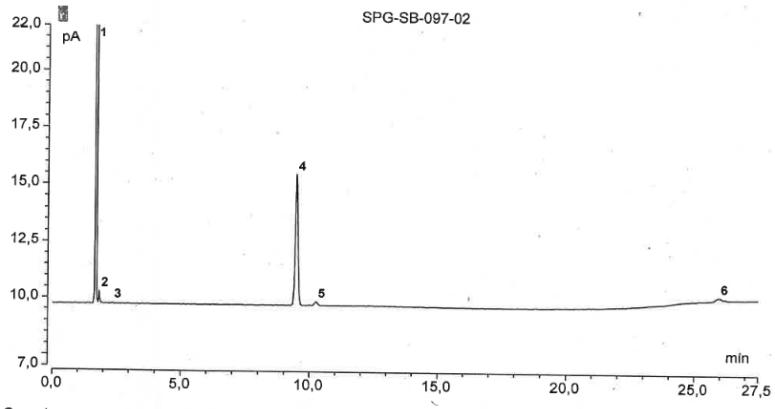


Sample: SPG-SB-097-02
Sequenz: 9299 SPG-SB PH
Sequenz date: 26.09.22

Instrument: GC_413
Measured: 26.09.22 14:00
Processing M.: MPI
Report-File: Verhältnis

Enantiomerenverhältnis
Zuordnung nach Razemat

| No. | Ret.Time min | Rel.Area % | Peak Name |
|---|---|---|---|
| 4 | 9,48 | 97,00 | |
| 5 | 10,25 | 3,00 | |

Instrument parameters:

| | | |
|---|---|---|
| Column: | 25,0 m | Hydrodex-beta-TBDAc-CD 0,25/?df G/681 |
| Temperature: | 220 / 120, 12 min iso 8/min 220, 3 min iso / 350 | |
| Gas: | 0,50 bar | Hydrogen |
| Sample size: | 0,2 µL | |

***(R)*-5-(Prop-1-en-2-yl)cyclohex-2-en-1-one *(R)*-norcarvone 96**

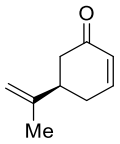


In a 100-mL two-necked flask, *n*-butyllithium (1.6 M in hexanes, 9.8 mL, 16 mmol) was added to a solution of 2,2,6,6-Tetramethylpiperidine (2.8 mL, 17 mmol) in THF (32 mL) at 0 °C, and the resulting solution was stirred at this temperature for 20 min before it was cooled to −78 °C. Trimethylsilyl chloride (2.4 mL, 18 mmol) was introduced, followed by slow addition of ketone **99** (1.79 g, 13.0 mmol). The resulting mixture was stirred for 30 min at −78 °C before half-saturated aqueous $NaHCO_3$ (50 mL) was added at this temperature and the mixture was warmed to ambient temperature. The mixture was diluted with diethyl ether (30 mL), the layers were separated, and the organic phase was washed with water (50 mL) and brine (20 mL). The aqueous layers were extracted with diethyl ether (3 × 25 mL), the combined organic phases were dried over $Na_2SO_4$, the drying agent was filtered off, and the solvent was removed under reduced pressure to give a mixture of the corresponding silyl enol ethers (ca. 5:1 by GC) which were directly used in the next step without further purification.

In a 100-mL two-necked flask, diallyl carbonate (2.4 mL, 17 mmol) and $Pd_2(dba)_3$ (949 mg, 1.04 mmol) were added to a solution of the crude material in acetonitrile (40 mL) at room temperature. The resulting dark suspension turned into a dark green, homogeneous mixture within a few minutes. Stirring was continued for 24 h at room temperature before diethyl ether (25 mL) and water (10 mL) were introduced. The mixture was filtered through a pad of Celite®, rinsing with diethyl ether. The organic layer was washed with water (3 × 25 mL) and brine (1 × 25 mL), the combined aqueous phases were extracted with diethyl ether (3 × 15 mL), the organic layers were dried over $Na_2SO_4$, the drying agent was filtered off, and the solvent was carefully removed under reduced pressure (100 mbar, 36 °C, ca. 10 min). The residue was then purified by distillation under

high vacuum ($2.5 \cdot 10^{-2}$ mbar, 65 °C) through a short-path connection into a receiving flask cooled to −78 °C, leaving behind an orange solid (dibenzylideneacetone). The colourless condensate was further purified by flash chromatography (silica; pentane/diethyl ether, 6:1) to furnish the title compound **96** as a colourless liquid after careful evaporation of the solvents at 150 mbar and 36 °C (998 mg, 56% yield).

$[\alpha]_D^{20}$ = -33.8 (c = 1.5, $CHCl_3$). $^1H$ NMR (400 MHz, $CDCl_3$): δ = 7.01 (ddd, *J* = 10.0, 5.7, 2.5 Hz, 1H), 6.04 (ddd, *J* = 10.0, 2.8, 1.1 Hz, 1H), 4.84 – 4.81 (m, 1H), 4.79 – 4.76 (m, 1H), 2.78 – 2.76 (m, 1H), 2.61 – 2.43 (m, 2H), 2.38 – 2.25 (m, 2H), 1.77 – 1.75 (m, 3H); $^{13}C$ NMR (101 MHz, $CDCl_3$): δ = 199.8, 149.8, 146.6, 129.7, 110.9, 43.2, 42.2, 31.1, 20.6; IR (film) ν/cm-1 : 2968, 1677, 1430, 1388, 1246, 892, 738; HRMS (GC-EI): calcd. for $C_9H_{12}O$ $[M]^+$: 136.0883; found: 136.0883.

The analytical data are in agreement with those reported in the literature for the enantiomer.[93]

### 5.2.1.3 Fragment coupling

#### 5.2.1.3.1 Coupling studies – protected hydroxycarvone

**Silyl enol ether 108**

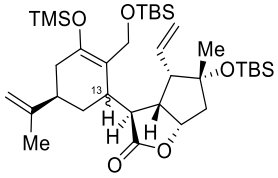


2,2,6,6-tetramethylpiperidine (22.5 μL, 0.13 mmol) was added to a solution of lactone **73** (19.8 mg, 67 μmol) in dichloromethane (0.7 mL). The mixture was cooled to 0 °C then trimethyl trifluoromethanesulfonate (20.5 μL, 0.11 mmol) was added, the mixture was stirred at that temperature for 5 min then at room temperature for 2 h. OTBS-Carvone **91** (19.7 mg, 70 μmol) was added, the mixture was cooled to -78 °C, then $TiCl_4$ solution (1M in dichloromethane, 6.7 μL, 7 μmol) was added, the mixture was stirred at - 78 °C for 1 h then at 0 °C for 1h, then at room temperature for 17 h. Sat. aq. $NaHCO_3$ (1 mL) was added to the mixture at 0 °C, the mixture was then extracted with *tert*-butyl-methyl ether (3 x 5 mL), the organic layers were combined, washed with brine (5 mL), dried on MgSO4 filtered and concentrated. It was purified by silica gel chromatography, eluting with a gradient of 0-10% *tert*-butyl-methyl ether in hexanes, to give as a yellowish oil **108** (5 mg 12% yield) as an unassigned single diastereoisomer.

$^1$H NMR (400 MHz, $CD_2Cl_2$) δ = 5.99 (dt, *J* = 17.1, 9.9 Hz, 1H), 5.22 (dd, *J* = 10.2, 2.3 Hz, 1H), 5.14 (ddd, *J* = 17.0, 2.3, 0.8 Hz, 1H), 4.86 (dd, *J* = 7.8, 6.9 Hz, 1H), 4.75 (q, *J* = 1.6 Hz, 1H), 4.69 (dt, *J* = 2.0, 1.0 Hz, 1H), 4.64 (d, *J* = 12.0 Hz, 1H), 3.18 (t, *J* = 4.2 Hz, 1H), 2.91 (td, *J* = 8.6, 4.6 Hz, 1H), 2.76 (d, *J* = 4.7 Hz, 1H), 2.41 – 2.35 (m, 1H), 2.33 (t, *J* = 9.2 Hz, 1H), 2.24 (d, *J* = 15.0 Hz, 1H), 2.20 – 2.11 (m, 1H), 2.03 – 1.95 (m, 1H), 1.82 (dd, *J* = 15.0, 6.9 Hz, 1H), 1.73 – 1.70 (m, 3H), 1.69 – 1.62 (m, 2H), 1.54 (s, 3H), 1.26 (s, 4H), 0.88 (s, 9H), 0.85 (s, 9H), 0.19 (s, 6H), 0.08 (s, 6H), 0.06 (s, 3H), 0.03 (s, 3H); $^{13}$C NMR (101 MHz, $CD_2Cl_2$) δ = 178.9, 148.7, 146.8, 135.1, 119.5, 116.3, 109.6, 84.1, 82.8, 59.2, 58.5, 48.3, 48.2, 43.6, 37.3, 36.6, 35.5, 30.5, 26.4, 26.4, 26.3, 22.8,

21.3, 20.9, 18.9, 18.8, 0.9, -1.8, -2.0, -5.0, -5.6.

**Silyl enol ether 110**

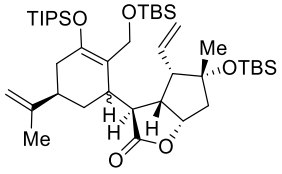


2,2,6,6-Tetramethylpiperidine (47.8 μL, 0.28 mmol) was added to a solution of lactone **73** (42.5 mg, 0.15 mmol) in dichloromethane (0.7 mL). The mixture that was cooled to 0 °C then triisopropylsilyl trifluoromethanesulfonate (68.5 μL, 0.26 mmol) was added, the mixture was stirred at that temperature for 5 min then at room temperature for 4 h. A solution of OTBS-Carvone **91** (42 mg, 0.14 mmol) in dichloromethane (0.4 ml) was added, the mixture was cooled to 0 °C, $La(OTf)_3$ (16.6 mg, 0.028 mmol) was added, and the mixture was stirred at room temperature for 4 h. Sat. aq. $NaHCO_3$ (2 mL) was added at 0 °C then the mixture was extracted with EtOAc (3 x 5 mL), the organic layers were combined, washed with brine, dried with MgSO4 and filtered. The residue was purified by flash chromatography on silica, eluting with a gradient of 0-10% *tert*-butyl methyl ether in hexanes to give a 1:1 diatereoisomeric mixture (104 mg, quantitative yield). In order to get analytically pure sample, an aliquot was purified by preparative HPLC [(MultoKrom 100-3 Si, 20.0 mm ∅, *tert*-butylmethyl ether in isohexane = 7:93 isocratic over 10 min, 15 mL/min, $\lambda$ = 220 nm, t = 4.71 and 5.69 min)] to give analytically pure diastereoisomers **110a** and **110b** as white solids.

Diastereoisomer **110a**: $^1$H NMR (600 MHz, $CD_2Cl_2$) δ = 5.96 (dt, *J* = 17.0, 9.9 Hz, 1H), 5.21 (dd, *J* = 10.2, 2.3 Hz, 1H), 5.13 (ddd, *J* = 17.1, 2.2, 0.7 Hz, 1H), 4.84 (td, *J* = 7.6, 0.7 Hz, 1H), 4.83 (d, *J* = 12.2 Hz, 1H), 4.74 (dqd, *J* = 2.1, 1.4, 0.6 Hz, 1H), 4.69 (ddd, *J* = 1.9, 1.2, 0.8 Hz, 1H), 3.94 (dddd, *J* = 12.1, 2.7, 1.9, 0.8 Hz, 1H), 3.08 (t, *J* = 4.3 Hz, 1H), 2.95 (ddd, *J* = 9.3, 7.9, 4.4 Hz, 1H), 2.86 (td, *J* = 5.9, 4.3 Hz, 1H), 2.40 (tt, *J* = 11.3, 5.8 Hz, 1H), 2.31 (t, *J* = 9.3 Hz, 1H), 2.24 (d, *J* = 15.0 Hz, 1H), 2.20 (dtd, *J* = 5.8, 1.0, -16.7 Hz, 1H), 2.05 (ddt, *J* = 16.7, 9.3, 1.7 Hz, 1H), 1.82 (ddd, *J* = 15.0, 6.8, 0.6 Hz, 1H), 1.75 (dtd, *J* = 13.4, 3.4, 1.0 Hz, 1H), 1.71 (dt, *J* = 1.2, 0.6 Hz, 3H), 1.61

(ddd, *J* = 13.3, 11.3, 5.9 Hz, 1H), 1.26 (s, 3H), 1.16 (m, 3H), 1.10 (m, 18H), 0.88 (s, 9H), 0.85 (s, 9H), 0.08 (s, 3H), 0.08 (s, 3H), 0.06 (s, 3H), 0.03 (s, 3H); $^{13}$C NMR (151 MHz, $CD_2Cl_2$) δ = 178.9, 148.8, 146.8, 135.2, 119.5, 115.1, 109.4, 84.0, 82.8, 59.2, 58.4, 48.1, 48.0, 44.1, 37.2, 36.5, 35.5, 31.2, 26.3, 26.3, 26.2, 21.1, 18.8, 18.6, 18.3, 18.3, 13.8, -1.9, -2.1, -5.1, -5.2.

Diastereoisomer **110b**: $^{1}$H NMR (600 MHz, $CD_2Cl_2$) δ = 5.96 (dtd, *J* = 17.1, 10.1, 2.8 Hz, 1H), 5.23 (dd, *J* = 10.1, 2.2 Hz, 1H), 5.06 (ddd, *J* = 17.1, 2.2, 0.6 Hz, 1H), 4.81 (ddd, *J* = 7.6, 6.4, 1.1 Hz, 1H), 4.73 (m, 1H), 4.73 (d, *J* = 11.5 Hz, 1H), 4.69 (dp, *J* = 1.8, 0.8 Hz, 1H), 4.00 (ddt, *J* = 12.2, 2.6, 1.3 Hz, 1H), 3.27 (dd, *J* = 3.8, 2.7 Hz, 1H), 3.13 (dtd, *J* = 12.0, 5.8, 2.9 Hz, 1H), 2.61 (ddd, *J* = 10.0, 7.6, 2.7 Hz, 1H), 2.27 (t, *J* = 9.8 Hz, 1H), 2.27 (d, *J* = 14.5 Hz, 1H), 2.21 (tdd, *J* = 12.0, 5.1, 2.4 Hz, 1H), 2.11 (m, 2H), 1.82 (ddd, *J* = 14.7, 6.4, 0.6 Hz, 1H), 1.72 (m, 3H), 1.72 (dtd, *J* = 6.0, 2.4, -12.2 Hz, 1H), 1.25 (s, 3H), 1.12 (m, 3H), 1.08 (m, 18H), 1.03 (td, *J* = 12.1, -12.2 Hz, 1H), 0.91 (s, 9H), 0.85 (s, 9H), 0.10 (br s, 3H), 0.08 (br s, 3H), 0.07 (br s, 3H), 0.06 (br s, *J* = 0.4 Hz, 3H); $^{13}$C NMR (151 MHz, $CD_2Cl_2$) δ = 179.9, 149.1, 147.9, 135.7, 119.4, 115.3, 109.1, 84.5, 83.8, 59.7, 58.0, 47.3, 44.9, 44.4, 41.1, 39.0, 36.6, 29.8, 26.7, 26.3, 26.1, 21.1, 18.8, 18.4, 18.3, 18.3, 13.6, -1.8, -2.1, -5.0, -5.1.

**Hydroxycarvone 112**

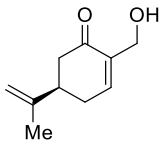


TBAF (1 M in THF, 5.4 mL, 5.4 mmol) was added to a solution of silyl ether **91** (763 mg, 2.7 mmol) in THF (9.0 mL) at room temperature. The solution was stirred for 5 min, then sat. aq. $NH_4Cl$ (10 mL) was introduced, the mixture was extracted with EtOAc (3 x 30 mL), the combined organic layers were washed with brine (10 mL), dried over MgSO4, filtered and concentrated under reduced pressure. The residue was purified by flash chromatography on silica, eluting with a gradient of 0-40% EtOAc in hexanes to give the desired product **112** as a yellow oil (380 mg, 84% yield).

The spectral data fully matched the literature.[94]

**Ketone 116**

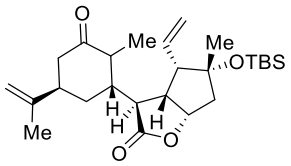


2,2,6,6-Tetramethylpiperidine (34 μL, 0.20 mmol) was added to a solution of lactone **73** (20 mg, 68 μmol) in dichloromethane (0.7 mL). The mixture that was cooled to 0 °C then triisopropylsilyl trifluoromethanesulfonate (36.3 μL, 0.13 mmol) was added, the mixture was stirred at that temperature for 5 min then at room temperature for 2 h. *(R)*-Carvone (10.6 μL, 68 μmol) was added, then the mixture was cooled to –78 °C, $La(OTf)_3$ (7.9 mg, 14 μmol) was added and the cold bath was removed and the mixture was stirred at room temperature for 30 min, then cooled to 0 °C, and sat. aq. $NaHCO_3$ (1 mL) was added. The mixture was extracted with *tert*-butyl-methyl ether (3 x 5 mL), the organic layers were combined, washed with brine (5 mL), dried over $MgSO_4$, filtered and concentrated. The residue was purified by flash chromatography on silica, eluting with a gradient of 0-10% EtOAc in hexane to give the desired product as a yellow oil and as single diastereoisomer.

Camphorsulfonic acid (9.2 mg, 40 μmol) was added to a solution of that compound in dichloromethane (0.4 mL). The mixture was stirred for 30 min, then the mixture was diluted with EtOAc (20 mL), cooled to 0 °C and sat. aq. $NaHCO_3$ (20 mL) was added. The mixture was extracted with EtOAc (3 x 10 mL), the organic layers were combined, washed with brine, dried over $Na_2SO_4$, filtered and concentrated. It was purified by flash chromatography on silica, eluting with 14% EtOAc in hexanes to give analytically pure **116** as a yellow oil.

$^1$H NMR (400 MHz, $CDCl_3$) δ = 5.88 (td, *J* = 19.8, 17.1 Hz, 1H), 5.27 (dd, *J* = 10.2, 2.1 Hz, 1H), 5.14 (ddd, *J* = 17.1, 2.0, 0.7 Hz, 1H), 4.95 (ddd, *J* = 7.7, 6.7, 0.8 Hz, 1H), 4.81 – 4.76 (m, 1H), 4.68 (td, *J* = 1.4, 0.8 Hz, 1H), 2.90 (dd, *J* = 5.5, 4.6 Hz, 1H), 2.81 (ddd, *J* = 9.2, 7.8, 4.6 Hz, 1H), 2.73 – 2.65 (m, 1H), 2.60 – 2.52 (m, 2H), 2.42 (t, *J* = 5.6 Hz, 1H), 2.36 – 2.27 (m, 3H), 2.02 – 1.98 (m, 2H), 1.80 (dd, *J* = 15.1, 6.7 Hz,

1H), 1.69 (dt, *J* = 1.4, 0.6 Hz, 3H), 1.26 (s, 3H), 1.12 (d, *J* = 7.0 Hz, 3H), 0.85 (s, 9H), 0.08 (d, *J* = 4.3 Hz, 6H).

#### 5.2.1.3.2 Coupling studies – norcarvone

**Silyl enol ether 117**

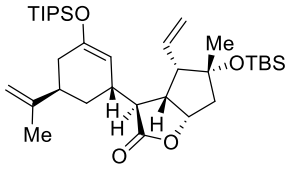


In a 10-mL Schlenk tube, triisopropylsilyl trifluormethanesulfonate (0.32 mL, 1.2 mmol) was added to a mixture of lactone **73** (87 mg, 0.29 mmol) and 2,2,6,6-tetramethylpiperidine (0.30 mL, 1.8 mmol) in dichloromethane (1.5 mL) at 0 °C (ice bath). After five minutes, the ice bath was removed, and the mixture was stirred at room temperature for additional 3 h. $La(OTf)_3$ (60.2 mg, 0.10 mmol) and (*R*)-norcarvone **96** (100 mg, 0.73 mmol) were introduced before the resulting suspension was stirred for 20 h at room temperature. The mixture was diluted with dichloromethane (2 mL) and filtered through a small plug of Celite®, which was rinsed with dichloromethane. The filtrate was concentrated under reduced pressure to give a light amber oil containing some solid. The residue was purified by flash chromatography on silica with hexanes/*tert*-butyl methyl ether (50:1) to furnish coupling product **117** as a pale yellowish gum (109 mg, 63% yield).

$^1$H NMR (400 MHz, $CD_2Cl_2$): δ = 5.96 – 5.82 (m, 1H), 5.22 (dd, *J* = 10.2, 2.2 Hz, 1H), 5.13 (ddd, *J* = 17.1, 2.3, 0.7 Hz, 1H), 4.81 – 4.73 (m, 2H), 4.70 – 4.66 (m, 1H), 4.44 – 4.39 (m, 1H), 2.98 (td, *J* = 8.6, 4.8 Hz, 1H), 2.82 (dd, *J* = 4.8, 3.8 Hz, 1H), 2.80 – 2.72 (m, 1H), 2.47 – 2.39 (m, 1H), 2.36 – 2.18 (m, 3H), 2.10 – 2.00 (m, 1H), 1.82 (dd, *J* = 15.1, 7.0 Hz, 1H), 1.76 – 1.72 (m, 3H), 1.70 – 1.61 (m, 1H), 1.56 – 1.48 (m, 1H), 1.26 (s, 3H), 1.10 – 1.04 (m, 21H), 0.85 (s, 9H), 0.09 (s, 6H); $^{13}$CNMR (101 MHz, $CD_2Cl_2$): δ = 179.9, 153.5, 148.3, 135.1, 119.5, 109.6, 101.6, 84.0, 83.3, 58.8, 47.9, 47.4, 45.9, 38.0, 35.3, 34.5, 31.3, 26.3, 26.3, 21.7, 18.7, 18.2, 18.2, 18.1, 13.0, 13.0, 12.9, -1.8, -2.2.

**Ketone 118**

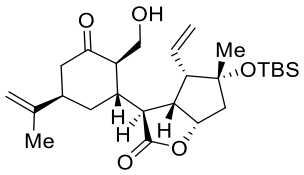


A solution of anhydrous formaldehyde was freshly prepared by pyrolysis of paraformaldehyde (55 mg, corresponding to 1.8 mmol of $CH_2O$, ~10 equiv. in case of quantitative yield) below 200 °C (heat gun) under a weak stream of argon, while passing the gas through 1.1 mL of anhydrous THF at −20 °C. Initially a homogeneous solution was obtained, which became turbid within a few minutes due to re-polymerization of formaldehyde, however, before the reaction below could be started. The already turbid solution was added to the neat silyl enol ether **117** (107 mg, 0.182 mmol) at −20 °C. TBAF (1.0 M in THF, 0.45 mL) was added dropwise to the resulting solution at −20 °C, and the mixture was stirred 30 min. For work-up, half-sat. aq. $NaHCO_3$ (10 mL) and EtOAc (5 mL) were introduced, the layers were separated, the organic layer was washed with brine (5 mL), and the aq. phases were extracted with EtOAc (4 × 10 mL). The combined org. layers were dried over $Na_2SO_4$, the drying agent was filtered off, and the solvent was removed under reduced pressure. The residue was purified by flash chromatography on silica, eluting with 25% EtOAc in hexanes to furnish aldol product **118** (31.9 mg, 38% yield, $R_f$ = 0.21) and ketone **119** (22.1 mg, 28% yield, $R_f$ = 0.29) as colourless gums.

$^1$H NMR (400 MHz, $CD_2Cl_2$): δ = 5.95 (ddd, *J* = 17.1, 10.3, 8.9 Hz, 1H), 5.27 (dd, *J* = 10.3, 2.1 Hz, 1H), 5.15 (ddd, *J* = 17.2, 2.1, 0.9 Hz, 1H), 4.97 (t, *J* = 7.7 Hz, 1H), 4.90 – 4.85 (m, 1H), 4.67 – 4.64 (m, 1H), 4.00 (ddd, *J* = 12, 6.2, 2.8 Hz, 1H), 3.66 (dt, *J* = 12, 6.1 Hz, 1H), 3.19 (dd, *J* = 5.4, 3.0 Hz, 1H), 2.97 (ddd, *J* = 11.3, 5.3, 2.7 Hz, 1H), 2.84 – 2.77 (m, 1H), 2.72 (td, *J* = 8.5, 5.4 Hz, 1H), 2.62 – 2.52 (m, 2H), 2.37 (t, *J* = 8.9 Hz, 1H), 2.32 – 2.22 (m, 1H), 2.29 (d, *J* = 15.3 Hz, 1H), 2.04 – 1.90 (m, 2H), 1.87 (dd, *J* = 15.3, 7.2 Hz, 1H), 1.80 – 1.68 (m, 4H), 1.29 (s, 3H), 0.86 (s, 9H), 0.10 (s, 3H), 0.09 (s, 3H); $^{13}$C NMR (101 MHz, $CD_2Cl_2$): δ = 213.5, 178.5, 146.5, 134.0, 119.9,

113.0, 83.9, 83.1, 59.1, 58.2, 49.2, 48.1, 45.1, 42.3, 40.3, 37.2, 28.4, 26.3, 26.2, 22.3, 18.7, -1.9, -2.1.

**Ketone 119**

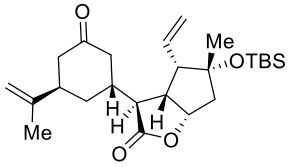


$^{1}$H NMR (400 MHz, $CD_2Cl_2$): δ = 5.90 (ddd, *J* = 17.1, 10.3, 9.3 Hz, 1H), 5.27 (dd, *J* = 10.3, 2.1 Hz, 1H), 5.17 (ddd, *J* = 17.1, 2.2, 0.8 Hz, 1H), 4.90 (t, *J* = 7.2 Hz, 1H), 4.88 – 4.86 (m, 1H), 4.64 – 4.61 (m, 1H), 2.87 (t, *J* = 5.0 Hz, 1H), 2.58 – 2.40 (m, 3H), 2.36 (t, *J* = 9.0 Hz, 1H), 2.26 (d, *J* = 15.3 Hz, 1H), 2.26 – 2.19 (m, 1H), 2.15 – 2.00 (m, 2H), 1.86 (dd, *J* = 15.3, 7.2 Hz, 1H), 1.75 – 1.71 (m, 3H), 1.71 – 1.61 (m, 1H), 1.27 (s, 3H), 0.85 (s, 9H), 0.09 (s, 6H); $^{13}$C NMR (101 MHz, $CD_2Cl_2$): δ = 210.3, 178.3, 147.0, 134.5, 119.9, 112.6, 83.9, 82.9, 58.3, 48.0, 47.6, 45.8, 44.8, 44.8, 40.5, 35.5, 30.0, 26.3, 26.2, 22.2, 18.7, -1.8, -2.2.

### 5.2.1.4 Coupling studies – selenide 95

**Selenide 126**

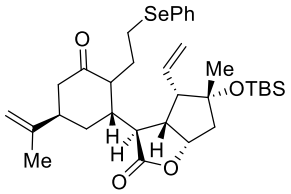


2,2,6,6-Tetramethylpiperidine (56.4 μL, 0.33 mmol) was added to a solution of lactone **73** (45.0 mg, 0.15 mmol) in dichloromethane (0.8 mL). The mixture was cooled to 0 °C before triisopropylsilyl trifluormethanesulfonate (81.6 μL, 0.30 μmol) was added. The mixture was warmed to room temperature and stirred for 4 h. Selenide **95** (53 mg, 0.17 mmol) was added and the mixture was cooled to 0 °C before $La(OTf)_3$ (18 mg, 0.03 mmol) was introduced. The resulting mixture was stirred at that temperature for 2 h. Sat. aq. $NaHCO_3$ (1.0 mL) was added, the aqueous phase was extracted with *tert*-butyl methyl ether (3 x 5 mL) the combined

organic layers were washed with brine (5 mL), dried over $MgSO_4$, filtered and concentrated under reduced pressure.

A solution of TBAF (1 M in THF, 0.3 mL, 0.30 mmol) was added to a solution of this crude product in THF (0.3 mL) at 0 °C and the resulting mixture was stirred at that temperature for 1 min, then sat. aq. $NH_4Cl$ (1.0 mL) was added. The aqueous phase was extracted with EtOAc (3 x 2 mL), the combined organic layers were combined, washed with brine (2 mL), dried over $MgSO_4$, filtered and concentrated. It was purified by flash chromatography on silica, eluting with a gradient of 0-15% EtOAc in hexanes to afford the desired product **126** as an orange oil (44.4 mg, 48% yield over two steps).

$[\alpha]_D^{20}$ = -23.4 (c = 0.6, $CHCl_3$). $^1H$ NMR (600 MHz, $CDCl_3$) δ = 7.53 (m, 2H), 7.26 (m, 2H), 7.21 (m, 1H), 5.88 (ddd, *J* = 17.2, 10.3, 9.1 Hz, 1H), 5.22 (dd, *J* = 10.3, 2.0 Hz, 1H), 5.15 (ddd, *J* = 17.2, 2.0, 0.8 Hz, 1H), 4.90 (dd, *J* = 8.4, 7.1 Hz, 1H), 4.86 (q, *J* = 1.2 Hz, 1H), 4.66 (dt, *J* = 1.7, 0.9 Hz, 1H), 3.05 (dd, *J* = 5.0, 3.4 Hz, 1H), 2.89 (dd, *J* = 18.9, 8.3 Hz, 1H), 2.88 – 2.85 (m, 2H), 2.74 (p, *J* = 4.6 Hz, 1H), 2.68 (td, *J* = 8.6, 5.0 Hz, 1H), 2.54 (ddd, *J* = 15.1, 5.0, 1.5 Hz, 1H), 2.44 (ddd, *J* = 15.0, 6.0, 0.9 Hz, 1H), 2.35 (t, *J* = 8.9 Hz, 1H), 2.31 (d, *J* = 15.3 Hz, 1H), 2.08 – 2.00 (m, 2H), 1.92 – 1.83 (m, 2H), 1.81 (dd, *J* = 15.1, 7.0 Hz, 1H), 1.80 – 1.78 (m, 1H), 1.71 (dt, *J* = 1.4, 0.7 Hz, 3H), 1.27 (s, 3H), 0.87 (s, 9H), 0.11 (m, 3H), 0.09 (s, 3H); $^{13}C$ NMR (151 MHz, $CDCl_3$) δ = 211.3, 178.0, 146.0, 133.6, 132.3, 130.6, 129.2, 126.7, 120.4, 112.7, 83.4, 82.7, 58.2, 52.2, 49.2, 47.9, 44.6, 42.9, 40.1, 39.8, 28.8, 28.2, 26.3, 26.2, 24.1, 22.0, 18.7, -1.8, -2.0; IR (film) ν/$cm^{-1}$ : 2952, 2929, 2856, 1757, 1704, 1438, 1377, 1321, 1257, 1193, 1177, 1117, 1091, 999, 898, 831, 805, 778, 736, 690; HRMS (ESI): calcd for $C_{33}H_{48}O_4SiSeNa$ $[M+Na]^+$: 639.23793; found: 639.23806.

**Triene 127**

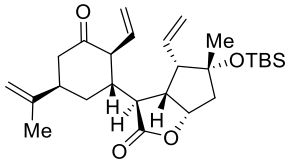


In a flask under air atmosphere a solution of $H_2O_2$ (35% in water, 50 μL, 0.58 mmol) was added to a solution of selenide **126** (9.0 mg, 0.015 mmol) in THF (0.3 mL) at room temperature. The mixture was stirred for 17 h, then sat. aq. $Na_2S_2O_3$ (1 mL) was added, the aqueous phase was then extracted with EtOAc (3 x 1 mL), the combined organic layers were washed with brine (1 mL), dried with $MgSO_4$, filtered and concentrated. The residue was purified by flash chromatography on silica, eluting with a gradient of 0-25% acetone in hexanes to afford the titled product **127** as a white gum (4.0 mg, 60% yield).

$[\alpha]_D^{20}$ = -63.7 (c = 0.2, $CHCl_3$). $^1$H NMR (400 MHz, $CD_2Cl_2$) δ = 5.86 (ddd, *J* = 17.2, 10.3, 9.0 Hz, 1H), 5.59 (ddd, *J* = 17.2, 10.3, 9.2 Hz, 1H), 5.29 (dd, *J* = 10.3, 2.0 Hz, 1H), 5.24 (dd, *J* = 10.3, 2.2 Hz, 1H), 5.16 (ddd, *J* = 8.4, 2.1, 0.7 Hz, 1H), 5.12 (ddd, *J* = 8.3, 2.1, 0.7 Hz, 1H), 4.92 (dd, *J* = 8.0, 7.2 Hz, 1H), 4.89 (h, *J* = 1.3 Hz, 1H), 4.67 (dt, *J* = 1.8, 0.9 Hz, 1H), 3.49 (t, *J* = 10.0 Hz, 1H), 3.12 (dd, *J* = 5.5, 2.3 Hz, 1H), 2.84 – 2.75 (m, 1H), 2.68 (td, *J* = 8.6, 5.4 Hz, 1H), 2.58 (dd, *J* = 3.4, 1.9 Hz, 1H), 2.56 (dd, *J* = 6.1, 0.9 Hz, 1H), 2.34 (t, *J* = 9.0 Hz, 1H), 2.27 (d, *J* = 15.2 Hz, 1H), 1.98 (ddd, *J* = 10.1, 3.9, 1.9 Hz, 1H), 1.83 (dd, *J* = 15.3, 7.2 Hz, 1H), 1.81 – 1.75 (m, 2H), 1.74 (dt, *J* = 1.3, 0.7 Hz, 3H), 1.26 (s, 3H), 0.84 (s, 9H), 0.08 (s, 3H), 0.06 (s, 3H); $^{13}$C NMR (101 MHz, $CD_2Cl_2$) δ = 210.3, 178.4, 146.5, 134.6, 134.3, 120.9, 119.7, 113.0, 83.7, 82.9, 58.5, 58.3, 54.4, 54.3, 54.1, 53.8, 53.6, 53.3, 49.3, 48.0, 44.8, 42.7, 41.3, 40.5, 28.3, 26.4, 22.3, 18.7, -1.8, -2.2; IR (film) ν/cm$^{-1}$ : 2953, 2929, 2856, 1757, 1709, 1471, 1376, 1322, 1255, 1193, 1118, 1053, 1000, 922, 902, 833, 807, 778, 691; HRMS (ESI): calcd for $C_{27}H_{42}O_4SiNa$ $[M+Na]^+$: 481.27446; found: 481.27448.

**Selenide 134**

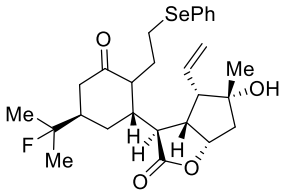


In a plastic vial, HF·pyr (70% w/w, 0.2 mL) was added to a solution of selenide **126** (11 mg, 18 μmol) in THF (0.2 mL) at 0 °C. The mixture was stirred at room temperature for 16 h before it was poured into sat. aq. $NaHCO_3$ (10 mL) at 0 °C. The aqueous phase was extracted with EtOAc (3 x 5 mL), the combined organic layers were washed with brine (5 mL), dried over $MgSO_4$, filtered and concentrated. The residue was purified by flash chromatography on silica, eluting with a gradient of 0-30% EtOAc in hexanes, to afford the corresponding selenide **134** as a colourless gum (2.2 mg, 24% yield).

$[\alpha]_D^{20}$ = +3.3 (c = 0.8, $CHCl_3$). $^1H$ NMR (400 MHz, $CDCl_3$) δ 7.56 – 7.52 (m, 2H), 7.32 – 7.29 (m, 1H), 7.28 – 7.25 (m, 2H), 5.75 (ddd, *J* = 17.0, 10.3, 9.1 Hz, 1H), 5.31 (dd, *J* = 10.3, 2.0 Hz, 1H), 5.23 (ddd, *J* = 17.0, 2.0, 0.8 Hz, 1H), 4.97 (dd, *J* = 7.7, 6.4 Hz, 1H), 2.91 (ddt, *J* = 6.9, 4.9, 2.2 Hz, 3H), 2.80 (td, *J* = 7.9, 3.8 Hz, 2H), 2.47 – 2.35 (m, 3H), 2.29 (ddd, *J* = 21.5, 9.3, 5.3 Hz, 1H), 2.21 (d, *J* = 15.1 Hz, 1H), 2.15 – 2.02 (m, 2H), 1.97 – 1.77 (m, 4H), 1.36 (dd, *J* = 21.5, 8.0 Hz, 6H), 1.26 (s, 3H); $^{13}C$ NMR (151 MHz, $CDCl_3$) δ = 212.0, 178.1, 132.9, 132.6, 130.0, 129.3, 127.0, 121.3, 96.9 (d, *J* = 170.4 Hz), 82.2, 80.4, 56.2, 51.3, 49.3, 47.5, 44.2, 41.8 (d, *J* = 1.3 Hz), 41.4 (d, *J* = 21.9 Hz), 40.3 (d, *J* = 3.7 Hz), 30.3, 25.6, 25.5 (d, *J* = 25.0 Hz), 25.2 (d, *J* = 3.1 Hz), 25.0 (d, *J* = 24.5 Hz), 25.0; $^{19}F$ NMR (565 MHz, $CDCl_3$) δ = -147.7 (h, *J* = 21.4 Hz); IR (film) ν/$cm^{-1}$ : 3470, 2961, 2926, 2855, 1748, 1702, 1579, 1478, 1437, 1375, 1321, 1188, 1115, 1073, 1020, 930, 898, 738, 692, 668; HRMS (ESI): calcd for $C_{27}H_{35}O_4FSeNa$ $[M+Na]^+$: 545.15785; found: 545.15768.

### 5.2.1.5 Synthesis of the desired RCM precursor

**Lactone 135**

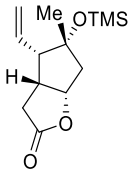


In a plastic vial, HF·pyr (70% w/w, 11 mL) was added to a solution of silyl ether **73** (3.0 g, 11.1 mmol)[14, 95] in THF (11 mL) at 0 °C. The mixture was stirred at room temperature for 7 h before it was poured into sat. aq. $NaHCO_3$ (100 mL) at 0 °C. The aqueous phase was extracted with EtOAc (5 x 200 mL), the combined organic layers were washed with brine (30 mL), dried over $MgSO_4$, filtered and concentrated. The residue was purified by flash chromatography on silica, eluting with a gradient of 0-40% EtOAc in hexanes, to afford the corresponding alcohol as a yellow solid.

Triethylamine (3.8 mL, 27.7 mmol) was added to a solution of this product in THF (46 mL). The mixture was cooled to 0°C before trimethylsilyl trifluoromethanesulfonate (3.7 mL, 20.3 mmol) was added and stirring continued at room temperature for 2 h. The mixture was cooled to 0 °C before TBAF (1 M in THF, 5.6 mL, 5.6 mmol) was added, and the resulting mixture stirred at that temperature *for 20 seconds*. The mixture was instantly quenched with saturated aqueous $NH_4Cl$ (100 mL), then extracted with EtOAc (3 x 200 mL), the combined organic layers were washed with brine (50 mL), dried over $MgSO_4$, filtered and concentrated under reduced pressure. The residue was purified by flash chromatography on silica, eluting with a gradient of 0-20% EtOAc in hexanes, to afford the title compound **135** as a yellow oil (2.0 g, 78% yield over two steps).

$[\alpha]_D^{20} = -12.6$ (c = 1.08, $CHCl_3$). $^1H$ NMR (400 MHz, $CDCl_3$): δ = 5.93 (ddd, *J* = 17.3, 10.4, 8.7 Hz, 1H), 5.25 (ddd, *J* = 10.4, 2.1, 0.6 Hz, 1H), 5.14 (ddd, *J* = 17.2, 2.0, 0.9 Hz, 1H), 5.04 (dd, *J* = 7.9, 6.8 Hz, 1H), 3.15–3.06 (m, 1H), 2.82 (dd, *J* = 18.6, 4.8 Hz, 1H), 2.44 (dd, *J* = 18.6, 12.0 Hz, 1H), 2.30 (d, *J* = 15.0 Hz, 1H), 2.23 (t, *J* = 8.7 Hz, 1H), 1.74

(ddd, *J* = 15.0, 6.9, 0.6 Hz, 1H), 1.28 (s, 3H) ppm, 0.11 (s, 9H) ppm; $^{13}$C NMR (101 MHz, $CDCl_3$): δ = 178.2, 134.3, 119.0, 84.0, 83.1, 57.2, 47.3, 42.7, 30.8, 25.1, 2.1 ppm IR (film) ν/$cm^{-1}$: 3077, 2959, 2898, 1766, 1638, 1453, 1415, 1377, 1364, 1321, 1251, 1194, 1172, 1112, 1005, 890, 841, 754; HRMS (GC-EI): calcd for $C_{13}H_{22}O_3Si$ $[M]^+$: 254.13327; found: 254.13286.

**Triene 137**

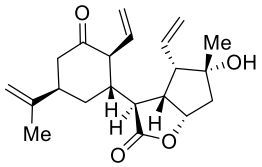


2,2,6,6-Tetramethylpiperidine (189 μL, 1.12 mmol) was added to a solution of lactone **135** (94.8 mg, 0.37 mmol) in dichloromethane (2 mL). The mixture was cooled to 0 °C before triisopropylsilyl trifluormethanesulfonate (200 μL, 0.74 mmol) was added. The mixture was warmed to room temperature and stirred for 4 h. Selenide **95** (178 mg, 0.56 mmol) was added and the mixture was cooled to 0 °C before $La(OTf)_3$ (44 mg, 0.073 mmol) was introduced. The resulting mixture was stirred at that temperature for 1 h. Sat. aq. $NaHCO_3$ (2 mL) was added, the aqueous phase was extracted with *tert*-butyl methyl ether (3 x 5 mL), the combined organic layers were washed with brine (5 mL), dried over MgSO4, filtered and concentrated under reduced pressure. The residue was triturated with hexanes (10 mL), the remaining precipitate was filtered off, and the solution concentrated under reduced pressure to give an orange oil.

A solution of TBAF (1 M in THF, 2 mL, 2 mmol) was added to a solution of this crude product in THF (2 mL) at 0 °C and the resulting mixture was stirred at room temperature for 2 h. Sat. aq. $NH_4Cl$ (5 mL) was introduced at 0 °C, the aqueous phase was extracted with EtOAc (3 x 10 mL), the combined organic layers were washed with brine (5 mL), dried over $MgSO_4$, filtered and concentrated under reduced pressure. The residue was purified by silica gel chromatography, eluting with 15% EtOAc in hexanes to afford desired product as a yellow oil; for the limited stability, the compound was immediately used without further characterization.

In a round bottomed-flask under air, $H_2O$ (1.5 mL) and $NaIO_4$ (347 mg, 1.6 mmol) were successively added to a solution of that product in THF (3 mL). The resulting mixture was stirred at room temperature for 17 h before sat. aq. $Na_2S_2O_3$ (3 mL) was introduced. The aqueous phase was extracted with EtOAc (3 x 20 mL), the combined organic layers were washed with brine (10 mL), dried over $MgSO_4$, filtered and concentrated under reduced pressure. The residue was purified by flash chromatography, on silica, eluting with a gradient of 0-15% EtOAc in toluene to afford the title compound **137** as a yellow gum (40 mg, 32% over 3 steps).

$[\alpha]_D^{20}$ = -10.3 (c = 1.02, $CHCl_3$). $^1$H NMR (600 MHz, $CD_2Cl_2$) δ = 5.83 (ddd, *J* = 17.1, 10.3, 9.1 Hz, 1H), 5.65 (ddd, *J* = 17.3, 10.3, 9.1 Hz, 1H), 5.31 (ddd, *J* = 10.2, 2.0, 0.5 Hz, 1H), 5.28 (ddd, *J* = 10.3, 2.0, 0.5 Hz, 1H), 5.19 (ddd, *J* = 16.9, 1.9, 0.8 Hz, 1H), 5.16 (ddd, *J* = 17.2, 1.9, 0.7 Hz, 1H), 4.93 (ddd, *J* = 7.9, 6.8, 0.5 Hz, 1H), 4.89 (h, *J* = 1.4 Hz, 1H), 4.68 (dp, *J* = 1.7, 0.8 Hz, 1H), 3.41 (dd, *J* = 11.3, 8.8 Hz, 1H), 3.19 (dd, *J* = 4.9, 3.0 Hz, 1H), 2.81 (h, *J* = 4.6 Hz, 1H), 2.71 (td, *J* = 8.3, 4.9 Hz, 1H), 2.61 (ddd, *J* = 14.8, 3.4, 2.0 Hz, 1H), 2.53 (ddd, *J* = 14.8, 6.3, 1.0 Hz, 1H), 2.40 (t, *J* = 8.9 Hz, 1H), 2.13 (d, *J* = 15.2 Hz, 1H), 1.99 (dddd, *J* = 13.3, 4.1, 3.1, 2.0 Hz, 1H), 1.88 (ddd, *J* = 15.2, 6.7, 0.5 Hz, 1H), 1.83 (tt, *J* = 11.8, 3.0 Hz, 1H), 1.77 (dd, *J* = 13.2, 4.5 Hz, 1H), 1.75 (dt, *J* = 1.5, 0.7 Hz, 3H), 1.22 (s, 3H); $^{13}$C NMR (151 MHz, $CD_2Cl_2$) δ = 210.1, 178.7, 146.6, 135.0, 133.3, 120.5, 120.3, 113.0, 82.5, 80.7, 58.2, 56.4, 49.0, 47.8, 44.8, 43.3, 41.2, 40.5, 28.6, 25.7, 22.3; IR (film) ν/cm$^{-1}$: 3476, 3077, 2964, 2928, 1749, 1707, 1643, 1452, 1375, 1192, 1116, 1018, 923; HRMS (ESI): calcd for $C_{21}H_{28}O_4Na$ $[M+Na]^+$: 367.18798; found: 367.18791.

**Diene 139**

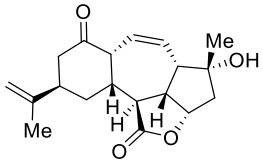


A solution of Grubbs second generation catalyst (0.5 mM in toluene, 0.5 mL, 0.2 μmol) was added to a solution of triene **137** (0.8 mg, 2.3 μmol) in toluene (0.5 mL). The mixture was heated to 100 °C (bath temperature) for 3 h then cooled to room temperature and concentrated. The residue was purified by flash chromatography on silica, eluting with a gradient of 0-50% EtOAc in hexanes to give the titled product **139** as a white gum (~0.2 mg, ~25% yield).

$^{1}$H NMR (600 MHz, $CDCl_3$) δ = 5.76 (dt, *J* = 11.3, 2.4 Hz, 1H), 5.53 (ddd, *J* = 11.3, 5.5, 2.6 Hz, 1H), 4.90 (td, *J* = 8.2, 3.1 Hz, 1H), 4.87 (q, *J* = 1.3 Hz, 1H), 4.71 (dt, *J* = 1.7, 0.9 Hz, 1H), 3.52 (t, *J* = 11.1 Hz, 1H), 3.42 – 3.36 (m, 2H), 3.16 (dt, *J* = 11.3, 7.9 Hz, 1H), 2.77 (p, *J* = 4.7 Hz, 2H), 2.70 – 2.66 (m, 1H), 2.63 (dd, *J* = 14.4, 6.5 Hz, 1H), 2.64 – 2.56 (m, 1H), 2.42 – 2.34 (m, 1H), 2.18 – 2.15 (m, 2H), 1.82 (dt, *J* = 1.5, 0.7 Hz, 3H), 1.76 (ddd, *J* = 13.9, 11.0, 4.7 Hz, 1H), 1.41 (s, 3H); $^{13}$C NMR (151 MHz, $CDCl_3$) δ = 212.1, 178.3, 146.6, 127.0, 127.2, 112.3, 81.9, 80.3, 52.2, 52.0, 47.2, 45.8, 43.7, 43.1, 40.6, 37.7, 29.7, 28.6, 22.1; HRMS (GC-EI): calcd for $C_{19}H_{24}O_4$ $[M]^+$: 316.16702; found: 316.16691.

### 5.2.1.6 Modifications surrounding the C4 carbon to allow the RCM

**Alkene 141**

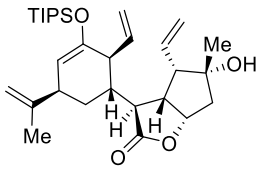


2,6-lutidine (2.1 μL, 18 μmol) was added to a solution of triene **137** (4.5 mg, 13 μmol) in dichloromethane (0.1 mL) at room temperature. The mixture was cooled to 0 °C, triisopropylsilyl trifluoromethanesulfonate (4.6 μL, 17 μmol) was added. The resulting mixture was stirred at room temperature for 17 h. Sat. aq. $NaHCO_3$ (0.2 mL) was added, then the mixture was extracted with EtOAc (3 x 1 mL). The combined organic layers were washed with brine (1 mL), dried with $MgSO_4$, filtered and concentrated. The residue was purified by flash chromatography on silica, eluting with a gradient of 0-20% EtOAc in hexanes to afford the titled product **141** as a grey oil (5.6 mg, 86% yield).

$[\alpha]_D^{20}$ = +25.9 (c = 0.13, $CHCl_3$). $^1$H NMR (600 MHz, $CDCl_3$) δ = 5.87 (ddd, *J* = 17.1, 10.3, 9.2 Hz, 1H), 5.58 (ddd, *J* = 17.1, 10.1, 8.9 Hz, 1H), 5.26 (ddd, *J* = 10.3, 2.0, 0.4 Hz, 1H), 5.19 (ddd, *J* = 17.1, 1.9, 0.8 Hz, 1H), 5.17 (ddd, *J* = 17.0, 2.0, 0.8 Hz, 1H), 5.19 – 5.14 (m, 1H), 4.93 (dd, *J* = 7.8, 6.5 Hz, 1H), 4.85 – 4.82 (m, 1H), 4.77 (dd, *J* = 2.1, 1.1 Hz, 1H), 4.72 (ddd, *J* = 4.9, 1.4, 0.5 Hz, 1H), 3.14 (t, *J* = 4.3 Hz, 1H), 3.11 (t, *J* = 8.4 Hz, 1H), 2.91 (q, *J* = 5.0 Hz, 1H), 2.70 (td, *J* = 8.3, 4.2 Hz, 1H), 2.38 (t, *J* = 9.0 Hz, 1H), 2.17 (d, *J* = 15.1 Hz, 1H), 1.86 (dd, *J* = 15.1, 6.6 Hz, 1H), 1.75 (dt, *J* = 1.1, 0.6 Hz, 3H), 1.71 – 1.65 (m, 1H), 1.65 – 1.58 (m, 1H), 1.55 (dt, *J* = 12.8, 3.5 Hz, 1H), 1.23 (s, 3H), 1.16 (hept, *J* = 7.3 Hz, 3H), 1.06 (d, *J* = 7.3 Hz, 9H), 1.06 (d, *J* = 7.3 Hz, 9H); $^{13}$C NMR (151 MHz, $CDCl_3$) δ = 178.8, 151.6, 148.5, 139.4, 133.1, 120.4, 118.1, 112.2, 104.0, 82.1, 80.5, 56.6, 49.4, 47.8, 47.7, 42.9, 40.2, 39.9, 26.7, 25.8, 22.0, 18.3, 18.3, 12.9; IR (film) ν/cm$^{-1}$: 3463, 2945, 2866, 1748, 1662, 1639, 1464, 1374, 1324, 1244, 1186, 1129,

1112, 1018, 995, 917, 883, 685; HRMS (ESI): calcd for $C_{30}H_{48}O_4SiNa$ $[M+Na]^+$: 523.32158; found: 523.32141.

**Alkenes 144 and 145**

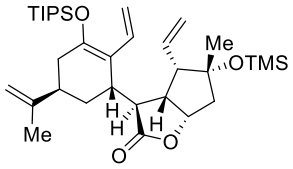


2,2,6,6-Tetramethylpiperidine (120 μL, 0.71 mmol) was added to a solution of lactone **135** (60.0 mg, 0.24 mmol) in dichloromethane (1.2 mL). The mixture was cooled to 0 °C before triisopropylsilyl trifluoromethanesulfonate (127 μL, 0.47 mmol) was added. The mixture was warmed to room temperature and stirred for 4 h. Selenide **95** (113 mg, 0.35 mmol) was added and the mixture was cooled to 0 °C before $La(OTf)_3$ (27.6 mg, 0.047 mmol) was introduced. The resulting mixture was warmed to room temperature and stirred for 17 h. Sat. aq. $NaHCO_3$ (1.5 mL) was added, the aqueous phase was extracted with *tert*-butyl methyl ether (3 x 5 mL) the combined organic layers were washed with brine (5 mL), dried over $MgSO_4$, filtered and concentrated under reduced pressure. The residue was triturated with hexanes (10 mL), the remaining precipitate was filtered off, and the solution concentrated under reduced pressure to give an orange oil.

A solution of *t*-BuOOH (5-6 M in decane, 100 μL, 0.6 mmol) was added to a solution of that crude mixture in dichloromethane (2 mL) at room temperature. The mixture was stirred for 24 h, after which a solution of *t*-BuOOH (5-6 M in decane, 100 μL, 6 mmol) was added to that solution at room temperature. The mixture was stirred for 15 h, then sat. aq. $Na_2S_2O_3$ (10 mL) was added. The aqueous phase was extracted with *tert*-butyl methyl ether (3 x 5 mL), the combined organic layers were washed with brine (5 mL), dried over $MgSO_4$, filtered and concentrated under reduced pressure. The residue was purified by flash chromatography on silica, eluting with a gradient of 0-10% *tert*-butyl methyl ether in pentane to afford the conjugated alkene **144** as an orange gum (41 mg, 30% yield over two steps) and

a fraction containing unpure alcohol **145**. That latter fraction was purified by preparative HPLC (250 mm YMC PVA-Sil 5 μm, 20.0 mm ∅, *tert*-butyl methyl ether in hexanes = 1:99 isocratic over 45 min, 15 mL/min, $\lambda$ = 220 nm, t = 17.30 min) to give alcohol **145** as an orange gum (9.1 mg, 7% yield over two steps) (the data of the alcohol are compiled below).

**Alkene 144:**

$[\alpha]_D^{20}$ = +42.3 (c = 0.8, $CH_2Cl_2$). $^1$H NMR (600 MHz, $CDCl_3$) δ = 6.92 (dd, *J* = 18.1, 11.4 Hz, 1H), 5.92 (dt, *J* = 17.2, 9.8 Hz, 1H), 5.23 (dd, *J* = 10.2, 2.2 Hz, 1H), 5.13 (dd, *J* = 17.2, 2.2 Hz, 1H), 4.98 (d, *J* = 18.1 Hz, 1H), 4.94 (d, *J* = 11.4 Hz, 1H), 4.81 (dd, *J* = 7.7, 6.2 Hz, 1H), 4.74 (t, *J* = 1.6 Hz, 1H), 4.70 (s, 1H), 3.16 – 3.12 (m, 1H), 2.97 (ddd, *J* = 9.2, 7.7, 3.9 Hz, 1H), 2.87 (t, *J* = 3.5 Hz, 1H), 2.56 – 2.46 (m, 1H), 2.25 (dd, *J* = 12.1, 2.7 Hz, 2H), 2.23 (q, *J* = 5.5 Hz, 1H), 2.07 (dd, *J* = 17.6, 11.1 Hz, 1H), 1.92 (d, *J* = 13.2 Hz, 1H), 1.71 (s, 3H), 1.67 – 1.59 (m, 2H), 1.23 (s, 3H), 1.22 – 1.13 (m, 3H), 1.10 (dd, *J* = 7.3, 1.9 Hz, 18H), 0.09 (s, 9H); $^{13}$C NMR (151 MHz, $CDCl_3$) δ = 181.4, 150.8, 148.8, 135.1, 131.8, 119.4, 114.9, 111.2, 109.3, 83.5, 83.3, 58.5, 47.5, 46.9, 46.2, 36.5, 36.1, 35.9, 34.2, 25.2, 20.7, 18.2, 18.2, 13.4, 2.23; IR (film) ν/cm$^{-1}$: 2945, 2867, 1760, 1634, 1463, 1429, 1366, 1249, 1192, 1154, 1115, 1001, 920, 883, 841, 784, 681; HRMS (ESI): calcd for $C_{33}H_{56}O_4SiNa$ $[M+Na]^+$: 595.36123; found: 595.36093.

**Alcohol 145:**

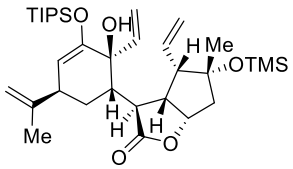


$[\alpha]_D^{20}$ = +60.6 (c = 1.4, $CH_2Cl_2$). $^1$H NMR (600 MHz, $CDCl_3$) δ = 6.11 (dd, *J* = 17.0, 10.6 Hz, 1H), 6.00 (ddd, *J* = 17.1, 10.2, 9.4 Hz, 1H), 5.33 (dd, *J* = 17.1, 1.7 Hz, 1H), 5.24 – 5.19 (m, 2H), 5.08 (ddd, *J* = 17.2, 2.3, 0.7 Hz, 1H), 4.85 – 4.83 (m, 1H), 4.86 – 4.80 (m, 1H), 4.77 (dt, *J* = 2.0, 1.0 Hz, 1H), 4.69 (dd, *J* = 4.7, 1.2 Hz, 1H), 3.07 (t, *J* = 4.5 Hz, 1H), 3.07 – 3.01 (m, 1H), 2.90 (s, 1H), 2.80 (t, *J* = 5.7 Hz, 1H), 2.25 – 2.19 (m, 2H), 2.16 (ddd, *J* = 13.6, 4.0, 2.6 Hz, 1H), 1.91 (td, *J* = 13.8, 7.0 Hz, 1H), 1.76 – 1.74 (m, 3H), 1.69 (ddd, *J* = 14.8, 6.7, 0.6 Hz, 1H), 1.60 – 1.56 (m, 1H), 1.24 (s, 3H), 1.22 – 1.15 (m, 3H),

1.07 (d, *J* = 7.5 Hz, 9H), 1.05 (d, *J* = 7.4 Hz, 9H), 0.08 (s, 9H); $^{13}$C NMR (151 MHz, $CDCl_3$) δ = 178.4, 151.3, 147.6, 139.3, 135.2, 118.7, 114.7, 112.4, 104.1, 83.3, 82.1, 77.0, 58.3, 49.4, 47.3, 43.3, 42.6, 40.0, 26.5, 25.7, 22.4, 18.3, 18.2, 12.8, 2.3; IR (film) ν/cm$^{-1}$: 3476, 2955, 2927, 2854, 1761, 1714, 1453, 1376, 1322, 1250, 1192, 1138, 1102, 1007, 902, 842, 753; HRMS (ESI): calcd for $C_{33}H_{56}O_5Si_2Na$ [M+Na]$^+$: 611.35623; found: 611.35585.

**Alcohol 147**

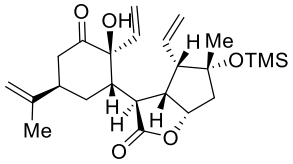


TBAF (1 M in THF, 30 μL, 30 μmol) was added to a solution of silyl enol ether **145** (8 mg, 14 μmol) in THF (0.3 mL) at -78 °C. The mixture was stirred at that temperature for 1 h, then sat. aq. $NH_4Cl$ (0.5 mL) was added. The mixture was warmed to room temperature then the aqueous phase was extracted with EtOAc (3 x 2 mL), the combined organic layers were washed with brine (2 mL), dried over $MgSO_4$, filtered and concentrated. The residue was purified by flash chromatography on silica, eluting with a gradient of 0-15% EtOAc in cyclohexane to afford the desired product **147** as a colourless gum (4.6 mg, 78% yield).

$[\alpha]_D^{20}$ = -20.4 (c = 0.5, $CHCl_3$). $^1$H NMR (600 MHz, $CD_2Cl_2$) δ = 6.48 (dd, *J* = 16.7, 10.5 Hz, 1H), 6.02 (ddd, *J* = 17.2, 10.3, 9.3 Hz, 1H), 5.48 (dd, *J* = 16.7, 1.6 Hz, 1H), 5.26 (ddd, *J* = 10.5, 1.6, 0.8 Hz, 1H), 5.21 (ddd, *J* = 10.2, 2.3, 0.3 Hz, 1H), 5.11 (ddd, *J* = 17.2, 2.4, 0.8 Hz, 1H), 4.92 (qt, *J* = 1.6, 1.1 Hz, 1H), 4.83 (ddd, *J* = 7.8, 7.0, 0.6 Hz, 1H), 4.70 (dq, *J* = 1.5, 0.8 Hz, 1H), 3.99 (s, 1H), 3.19 (dd, *J* = 5.4, 2.7 Hz, 1H), 2.92 (td, *J* = 8.5, 5.4 Hz, 1H), 2.88 – 2.82 (m, 1H), 2.79 (dd, *J* = 14.6, 6.8 Hz, 1H), 2.74 (dt, *J* = 14.6, 2.3 Hz, 1H), 2.23 (t, *J* = 9.1 Hz, 1H), 2.21 (ddd, *J* = 13.6, 3.0, -14.6 Hz, 1H), 2.19 (d, *J* = 15.0 Hz, 1H), 2.01 (dt, *J* = 13.6, 3.0 Hz, 1H), 1.85 (ddt, *J* = 14.6, 3.3, 2.5 Hz, 1H), 1.74 (dt, *J* = 1.4, 0.7 Hz, 3H), 1.72 (ddd, *J* = 15.0, 6.9, 0.6 Hz, 1H), 1.24 (s, 3H), 0.07 (s, 9H); $^{13}$C NMR (151 MHz, $CD_2Cl_2$) δ = 209.9, 178.3, 146.3, 135.6, 135.3, 118.9, 117.0, 113.3, 83.7, 83.0, 82.4, 58.3, 49.8, 47.5, 47.4, 43.2, 41.3, 40.8, 27.9, 25.4, 22.6, 2.2;

IR (film) ν/cm$^{-1}$: 3581, 2946, 2867, 1764, 1664, 1463, 1375, 1249, 1195, 1101, 1005, 916, 883, 840, 750, 681; HRMS (ESI): calcd for $C_{24}H_{36}O_5SiNa$ $[M+Na]^+$: 455.22275; found: 455.22242.

**Alcohol 148**

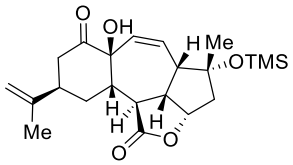


A solution of Grubbs first generation catalyst (0.012 M in 1,2-dichloroethane, 2.2 mL, 57 μmol) was *added over 22 days* to a solution of ketone **147** (2.1 mg, 4.9 μmol) in 1,2-dichloroethane (2.0 mL) at 60 °C (bath temperature). The mixture was cooled to room temperature, then Celite® (10 mg) was added and the mixture was stirred at that temperature for 30 min before being filtered filtered over silica, then rinced with EtOAc (5 x 5 mL) and the combined filtrates were concentrated. The residue was purified by flash chromatography on silica, eluting with a gradient of 15 % EtOAc in pentane to give recovered starting material **147** as a colourless gum (1.5 mg, 71% recovery) and the desired product **148** as a colourless gum (0.3 mg, 53% yield brsm).

$[\alpha]_D^{20}$ = +35.5 (c = 0.79, $CHCl_3$). $^1$H NMR (600 MHz, $CD_2Cl_2$) δ = 5.90 (ddd, *J* = 11.6, 2.3, 0.6 Hz, 1H), 5.60 (dd, *J* = 11.7, 2.6 Hz, 1H), 4.88 (q, *J* = 1.5 Hz, 1H), 4.86 (td, *J* = 8.7, 2.0 Hz, 1H), 4.69 (dp, *J* = 1.7, 0.8 Hz, 1H), 4.39 (s, 1H), 4.09 (ddd, *J* = 11.2, 8.7, 7.2 Hz, 1H), 3.60 (dd, *J* = 11.2, 10.4 Hz, 1H), 2.85 – 2.82 (m, 2H), 2.81 – 2.76 (m, 1H), 2.68 – 2.61 (m, 1H), 2.61 (dt, *J* = 7.3, 2.5 Hz, 1H), 2.27 (ddd, *J* = 15.8, 2.0, 0.6 Hz, 1H), 2.18 (td, *J* = 10.8, 4.5 Hz, 1H), 2.08 (dd, *J* = 15.8, 8.7 Hz, 1H), 1.80 (dt, *J* = 1.5, 0.7 Hz, 3H), 1.65 (ddd, *J* = 14.8, 11.3, 4.0 Hz, 1H), 1.43 (s, 3H), 0.13 (s, 9H); $^{13}$C NMR (151 MHz, $CD_2Cl_2$) δ = 212.9, 179.0, 146.2, 134.8, 127.9, 112.5, 84.7, 81.0, 78.6, 48.0, 45.2, 44.7, 43.7, 41.4, 40.5, 32.1, 27.9, 22.1, 2.2; IR (film) ν/cm$^{-1}$: 3461, 2962, 1761, 1712, 1644, 1449, 1378, 1338, 1263, 1250, 1178, 1142, 1101, 1010, 895, 840, 756; HRMS (ESI): calcd for $C_{22}H_{32}O_5SiNa$ $[M+Na]^+$: 427.19112; found: 427.19102.

## 5.2.2 Second approach: by alkenylation to form the C4-C5 bond of Scabrolide B

### 5.2.2.1 Cyclization studies

**Vinyl iodide 149**

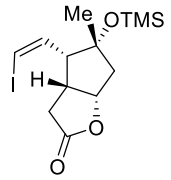


$O_3$ was bubbled through a solution of alkene **135** (2.0 g, 7.9 mmol) in dichloromethane (50 mL) at –78 °C for 10 min until a deep blue color persisted. The mixture was warmed to 0 °C, argon was bubbled through it for 15 min, followed by addition of triphenylphosphine (6.0 g, 22.9 mmol). The mixture was stirred at room temperature for 3 h before it was concentrated under reduced pressure and the residue purified by flash chromatography on silica, eluting with a gradient of 0-40% EtOAc in hexanes, to afford the corresponding aldehyde as a yellow oil, which was used in the next step without delay.

Sodium bis(trimethylsilyl)amide (NaHMDS, 1.7 g, 9.5 mmol) was added to a suspension of $[PPh_3CH_2I]I$ (5.4 g, 10.42 mmol) in THF (80 mL), the resulting mixture was stirred at room temperature for 15 min and then cooled to –78 °C. A solution of the aldehyde in THF (15 mL) was added dropwise over 4 min (rinsing the flask with THF (2 x 15 mL)) at -78 °C and stirring continued at this temperature for 30 min. Sat. aq. $NH_4Cl$ (50 mL) was added, the mixture was warmed to room temperature, extracted with *tert*-butyl methyl ether (3 x 100 mL), the combined organic layers were washed with brine (20 mL), dried over MgSO4, filtered and concentrated. The residue was purified by flash chromatography on silica, eluting with a gradient of 0-20% *tert*-butyl methyl ether in hexanes, to afford the title compound **149** as a yellow oil (2.13 g, 71% yield over two steps)

$[\alpha]_D^{20}$ = +76.9 (c = 1.09, $CHCl_3$). $^1H$ NMR (400 MHz, $CDCl_3$) δ = 6.53 (dd, *J* = 7.5, 0.7 Hz, 1H), 6.47 (t, *J* = 7.9 Hz, 1H), 5.09 (dd, *J* = 7.9, 6.6 Hz, 1H), 3.41 – 3.31 (m, 1H),

2.69 – 2.57 (m, 2H), 2.46 (dd, *J* = 18.6, 11.9 Hz, 1H), 2.36 (d, *J* = 15.1 Hz, 1H), 1.82 (ddd, *J* = 15.1, 6.6, 0.5 Hz, 1H), 1.30 (s, 3H), 0.13 (s, 9H) ppm; $^{13}$C NMR (101 MHz, $CDCl_3$) δ = 177.8, 138.1, 85.9, 84.0, 83.3, 57.9, 47.0, 40.6, 31.1, 25.4, 2.1 ppm; IR (film) ν/cm$^{-1}$: 2958, 2897, 1766, 1608, 1450, 1414, 1377, 1366, 1301, 1252, 1190, 1174, 1113, 1004, 891, 840, 754; HRMS (ESI): calcd for $C_{13}H_{21}IO_3SiNa$ [M+Na]$^+$: 403.01969; found: 403.02000.

**Vinyl iodide 151**

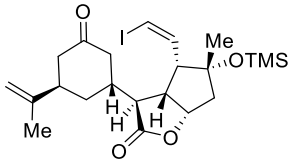


2,2,6,6-Tetramethylpiperidine (5.7 mL, 33.6 mmol) was added to a solution of lactone **149** (2.13 g, 5.6 mmol) in dichloromethane (28 mL). The mixture was cooled to 0 °C before triisopropylsilyl trifluoromethansulfonate (6.0 mL, 22.4 mmol) was added. The mixture was warmed to room temperature and stirred for 4 h. $La(OTf)_3$ (657 mg, 1.1 mmol) and *(R)*-norcarvone **96** (1.47 g, 10.8 mmol) were successively added and stirring continued at room temperature for 17 h. The mixture was filtered through a pad of Celite®, rinsing with dichloromethane (5 x 50 mL), and the combined filtrates were concentrated under reduced pressure. The residue was triturated with hexanes (40 mL), the resulting precipitate was filtered off, and the remaining solution was concentrated under reduced pressure. The crude product was purified by flash chromatography on silica, eluting with a gradient of 0-3% *tert*-butyl methyl ether in hexanes, to afford the silyl enol ether **150** as a grey solid.

TBAF (1 M in THF, 11.0 mL, 11.0 mmol) was added dropwise over 5 min to a solution of this product in THF (30 mL) at -78 °C. The mixture was stirred at this temperature for 1 h before sat. aq. $NH_4Cl$ (30 mL) was added and the mixture warmed to room temperature. The mixture was extracted with EtOAc (3 x 100 mL), the combined organic layers were washed with brine (50 mL), dried over $MgSO_4$, filtered and concentrated under reduced pressure. The residue was purified by flash chromatography on silica, eluting with a gradient of 0-25% *tert*-butyl methyl

ether in hexanes, to give the title compound **151** as a white solid (2.0 g, 69% yield over two steps).

$[\alpha]_D^{20}$ = +142.8 (c = 1.64, $CHCl_3$). $^1H$ NMR (600 MHz, $CDCl_3$) δ = 6.57 (dd, *J* = 7.5, 0.9 Hz, 1H), 6.46 (dd, *J* = 8.0, 7.5 Hz, 1H), 4.96 (dd, *J* = 7.9, 6.5 Hz, 1H), 4.89 (p, *J* = 1.2 Hz, 1H), 4.66 (dt, *J* = 1.6, 0.8 Hz, 1H), 3.04 (td, *J* = 8.5, 4.5 Hz, 1H), 2.79 (p, *J* = 4.8 Hz, 1H), 2.64 (td, *J* = 8.5, 0.9 Hz, 1H), 2.60 (t, *J* = 4.5 Hz, 1H), 2.59 (ddt, *J* = 15.0, 3.5, 1.9 Hz, 1H), 2.51 (ddd, *J* = 15.1, 12.2, 1.0 Hz, 1H), 2.44 (ddd, *J* = 15.2, 6.2, 1.0 Hz, 1H), 2.34 (d, *J* = 15.0 Hz, 1H), 2.30 (ddt, *J* = 15.0, 4.1, 2.0 Hz, 1H), 2.09 (tq, *J* = 12.1, 4.1 Hz, 1H), 1.97 (dtt, *J* = 13.6, 3.9, 1.9 Hz, 1H), 1.81 (ddd, *J* = 15.1, 6.7, 0.5 Hz, 1H), 1.74 (dt, *J* = 1.4, 0.7 Hz, 3H), 1.67 (ddd, *J* = 13.6, 11.9, 4.7 Hz, 1H), 1.29 (s, 3H), 0.12 (s, 9H); $^{13}C$ NMR (151 MHz, $CDCl_3$) δ = 210.4, 178.0, 145.9, 137.8, 113.3, 87.1, 82.9, 82.6, 58.3, 47.0, 46.4, 45.4, 44.6, 44.6, 40.2, 35.6, 29.5, 25.5, 22.4, 2.2; IR (film) ν/$cm^{-1}$: 2957, 1757, 1710, 1645, 1449, 1377, 1301, 1260, 1185, 1117, 1003, 902, 842, 754; HRMS (ESI): calcd for $C_{22}H_{33}IO_4SiNa$ $[M+Na]^+$: 539.10851; found: 539.10879.

**Vinyl iodide 152**

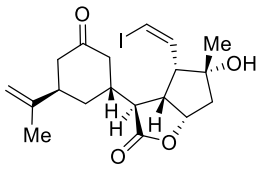


2,2,6,6-Tetramethylpiperidine (324 μL, 1.92 mmol) was added to a solution of lactone **149** (135 mg, 0.32 mmol) in dichloromethane (1.5 mL). The mixture was cooled to 0 °C before triisopropylsilyl trifluoromethansulfonate (343 μL, 1.28 mmol) was added. The mixture was warmed to room temperature and stirred for 4 h. $La(OTf)_3$ (37 mg, 0.064 mmol) and *(R)*-norcarvone **96** (108 mg, 0.80 mmol) were successively added and stirring continued at room temperature for 17 h. The mixture was filtered through a pad of Celite®, rinsing with dichloromethane (5 x 5 mL), and the combined filtrates were concentrated under reduced pressure. The residue was triturated with cyclohexane (5 mL), the resulting precipitate was filtered off, and the remaining solution was concentrated under reduced pressure. The crude product was purified by flash chromatography on silica, eluting with a

gradient of 0-3% *tert*-butyl methyl ether in hexanes, to afford the silyl enol ether **150** as a grey solid.

A solution of TBAF (1 M in THF, 0.7 mL, 0.7 mmol) was added dropwise *over 20 seconds* to a solution of this crude product in THF (2.5 mL) at 0 °C and the resulting mixture was stirred at that temperature *for 10 seconds*, then sat. aq. $NH_4Cl$ (5.0 mL) was added. The aqueous phase was extracted with EtOAc (3 x 5 mL), the combined organic layers were combined, washed with brine (5 mL), dried over $MgSO_4$, filtered and concentrated. It was purified by flash chromatography on silica, eluting with a gradient of 0-50% EtOAc in hexanes to afford the vinyl iodide **151** as a white oil (43 mg, 23% yield over two steps) and a second fraction comprised of deprotected vinyl iodide **152** as a yellow solid (61 mg, 39% yield over two steps).

$[\alpha]_D^{20}$ = +106.7 (c = 0.65, $CHCl_3$). $^1H$ NMR (400 MHz, $CDCl_3$) δ = 6.62 (d, *J* = 7.6 Hz, 1H), 6.57 (t, *J* = 7.6 Hz, 1H), 5.03 (dd, *J* = 7.8, 6.3 Hz, 1H), 4.92 (q, *J* = 1.2 Hz, 1H), 4.69 (dd, *J* = 1.7, 0.9 Hz, 1H), 3.10 (ddd, *J* = 9.1, 7.8, 4.1 Hz, 1H), 2.85 – 2.80 (m, 1H), 2.75 (t, *J* = 8.4 Hz, 1H), 2.71 (t, *J* = 4.3 Hz, 1H), 2.62 (ddt, *J* = 15.2, 3.5, 1.9 Hz, 1H), 2.50 (ddd, *J* = 12.1, 2.8, 1.0 Hz, 1H), 2.46 (ddd, *J* = 15.3, 5.8, 1.4 Hz, 1H), 2.36 (ddd, *J* = 13.1, 4.4, 2.2 Hz, 1H), 2.26 (d, *J* = 15.2 Hz, 1H), 2.12 (ddt, *J* = 12.0, 8.1, 4.1 Hz, 1H), 2.03 – 1.98 (m, 1H), 1.99 (dd, *J* = 15.2, 6.5 Hz, 1H), 1.77 (s, 3H), 1.70 (ddd, *J* = 13.6, 11.8, 4.6 Hz, 1H), 1.30 (s, 3H); $^{13}C$ NMR (101 MHz, $CDCl_3$) δ = 210.1, 178.3, 145.7, 136.9, 113.2, 87.7, 82.3, 80.0, 56.5, 47.6, 46.6, 45.5, 44.5, 44.5, 40.0, 35.7, 29.5, 25.6, 22.2; IR (film) ν/cm$^{-1}$: 3443, 2962, 2925, 2855, 1748, 1707, 1450, 1376, 1316, 1263, 1189, 1114, 1011, 937, 889, 808, 754, 665, 621; HRMS (ESI): calcd for $C_{19}H_{25}O_4INa$ $[M+Na]^+$: 467.06898; found: 467.06890.

**Ketone 156**

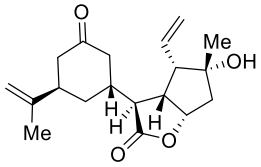


Potassium *tert*-butoxide (20 mg, 0.19 mmol) was added to a solution of phenol (19 mg, 0.21 mmol) in toluene (4 mL). The resulting suspension was stirred for 5 min before a solution of alkenyl iodide **152** (55 mg, 0.12 mmol) in 3:1 toluene/THF (6.5 mL) then $Pd(PPh_3)_4$ (29 mg, 0.025 mmol) were successively added. The mixture was heated to 65 °C for 22 h, then $Pd(PPh_3)_4$ (58 mg, 0.05 mmol) was added over 40 h under heating at 65 °C (bath temperature). The mixture was cooled to room temperature, then diluted with water (5 mL) and extracted with EtOAc (3 x 5 mL), the combined organic layers were washed with brine (5 mL), dried over MgSO4, filtered and concentrated. The residue was purified by flash chromatography on silica, eluting with a gradient of 0-50% EtOAc in hexanes, to afford the title compound **156** as a white solid (6 mg, 15% yield).

$^1$H NMR (400 MHz, $CDCl_3$) δ = 5.93 (ddd, *J* = 17.1, 10.3, 9.2 Hz, 1H), 5.35 (dd, *J* = 10.3, 2.0 Hz, 1H), 5.24 (ddd, *J* = 17.1, 1.9, 0.8 Hz, 1H), 4.97 (dd, *J* = 7.7, 6.5 Hz, 1H), 4.90 (q, *J* = 1.3 Hz, 1H), 4.68 (dt, *J* = 1.6, 0.9 Hz, 1H), 2.92 – 2.88 (m, 1H), 2.82 (td, *J* = 8.2, 4.1 Hz, 2H), 2.62 (ddt, *J* = 15.2, 3.6, 1.8 Hz, 1H), 2.50 – 2.38 (m, 4H), 2.38 – 2.30 (m, 1H), 2.22 (d, *J* = 15.2 Hz, 2H), 2.18 – 2.02 (m, 3H), 1.91 (dd, *J* = 15.2, 6.5 Hz, 1H), 1.76 (d, *J* = 0.8 Hz, 3H), 1.70 (ddd, *J* = 13.7, 11.6, 4.6 Hz, 1H); HRMS (ESI): calcd for $C_{19}H_{26}O_4Na$ $[M+Na]^+$: 341.17235; found: 341.17233.

**Alkyne 157**

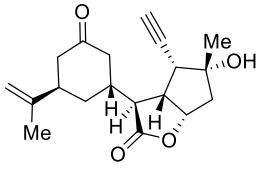


A solution of alkenyl iodide **152** (51. mg, 11.5 μmol) in THF (0.5 mL) and $Pd(PPh_3)_4$ (2.6 mg, 2.3 μmol) were successively added to a solution of potassium *tert*-butoxide (1.9 mg, 17 μmol) in THF (5 mL). The mixture was stirred for 5 min

then sat. aq. $NH_4Cl$ (5 mL) was added, then extracted with EtOAc (3 x 5 mL), the combined organic layers were washed with brine (5 mL), dried over $MgSO_4$, filtered and concentrated. The residue was purified by flash chromatography on silica, eluting with a gradient of 0-50% EtOAc in hexanes, to afford the title compound **157** as a white solid (2.5 mg, 69% yield).

$^1$H NMR (400 MHz, $CDCl_3$) δ = 4.94 (dd, *J* = 7.1, 6.1 Hz, 1H), 4.90 (d, *J* = 1.3 Hz, 1H), 4.68 (dt, *J* = 1.7, 0.8 Hz, 1H), 3.05 (dd, *J* = 5.0, 3.4 Hz, 1H), 2.90 – 2.79 (m, 3H), 2.62 (ddt, *J* = 15.2, 3.6, 1.8 Hz, 1H), 2.54 – 2.43 (m, 3H), 2.40 (d, *J* = 2.1 Hz, 1H), 2.33 (d, *J* = 15.1 Hz, 1H), 2.24 – 2.14 (m, 1H), 2.12 (dtt, *J* = 13.7, 3.8, 2.1 Hz, 1H), 1.84 – 1.69 (m, 6H), 1.39 (s, 3H); $^{13}$C NMR (101 MHz, $CDCl_3$) δ = 210.1, 177.6, 145.9, 113.1, 82.0, 80.1, 79.7, 75.8, 48.1, 46.8, 45.8, 45.2, 44.8, 44.5, 40.0, 35.8, 29.8, 25.5, 22.2; HRMS (ESI): calcd for $C_{29}H_{24}O_4Na$ $[M+Na]^+$: 339.15668; found: 339.15660.

*Products 158-161 were isolated during the optimization of the alkenylation/isomerization step.*

**Ketone 158**

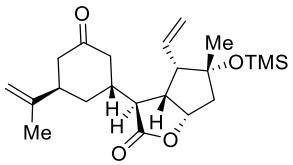


$^1$H NMR (400 MHz, $CDCl_3$) δ = 5.87 (ddd, *J* = 17.2, 10.3, 9.0 Hz, 1H), 5.28 (dd, *J* = 10.3, 2.1 Hz, 1H), 5.17 (ddd, *J* = 17.3, 2.1, 0.8 Hz, 1H), 4.90 (dd, *J* = 7.7, 6.7 Hz, 1H), 4.87 (s, 1H), 4.65 (s, 1H), 2.82 – 2.74 (m, 3H), 2.59 (ddt, *J* = 15.3, 3.6, 1.8 Hz, 1H), 2.47 – 2.38 (m, 2H), 2.36 – 2.25 (m, 3H), 2.12 (tt, *J* = 7.4, 3.5 Hz, 1H), 2.05 (dtt, *J* = 13.7, 3.8, 1.9 Hz, 1H), 1.78 – 1.67 (m, 5H), 1.27 (s, 3H), 0.10 (s, 9H); $^{13}$C NMR (101 MHz, $CDCl_3$) δ = 210.5, 178.4, 146.1, 134.0, 119.9, 113.0, 83.1, 82.6, 57.7, 47.6, 47.4, 46.0, 44.8, 44.7, 44.6, 42.1, 40.4, 40.2, 35.7, 30.9, 29.9, 25.1, 22.3, 21.3, 2.3, 2.2, 1.2; HRMS (ESI): calcd for $C_{22}H_{34}O_4NaSi$ $[M+Na]^+$: 413.21186; found: 413.21210.

**Alkyne 159**

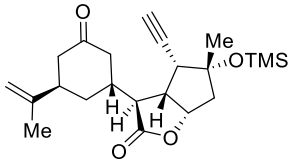


$^{1}$H NMR (400 MHz, $CDCl_3$) δ = 4.94 – 4.86 (m, 2H), 4.68 (s, 1H), 3.08 (t, *J* = 4.6 Hz, 1H), 2.89 – 2.79 (m, 2H), 2.69 – 2.57 (m, 2H), 2.52 – 2.35 (m, 3H), 2.28 – 2.11 (m, 4H), 1.75 (s, 3H), 1.71 (dd, *J* = 14.7, 6.7 Hz, 2H), 1.44 (s, 3H), 0.13 (s, 9H); $^{13}$C NMR (101 MHz, $CDCl_3$) δ = 210.6, 178.1, 146.1, 113.1, 83.1, 82.1, 80.8, 73.8, 48.0, 47.9, 47.0, 46.0, 44.8, 44.7, 40.2, 35.5, 30.0, 29.9, 25.1, 22.3, 2.2; HRMS (ESI): calcd for $C_{22}H_{32}O_4NaSi[M+Na]^+$: 411.19621; found: 411.19635.

**Dimer 161**

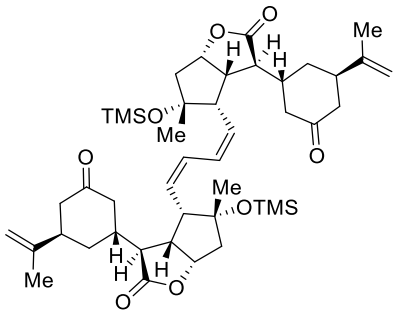


$^{1}$H NMR (400 MHz, $CDCl_3$) δ = 6.44 (dd, *J* = 7.7, 2.2 Hz, 1H), 5.61 (t, *J* = 8.7 Hz, 1H) 4.97 (t, *J* = 6.9 Hz, 1H), 4.82 (q, *J* = 1.2 Hz, 1H), 4.64 (dt, *J* = 1.7, 0.9 Hz, 1H), 2.89 – 2.77 (m, 2H), 2.77 – 2.70 (m, 2H), 2.56 – 2.24 (m, 5H), 2.06 – 1.97 (m, 2H), 1.86 – 1.75 (m, 2H), 1.72 (s, 3H), 1.25 (s, 3H), 0.11 (s, 9H); $^{13}$C NMR (101 MHz, $CDCl_3$) δ = 210.5, 177.9, 146.5, 128.6, 127.7, 112.4, 83.8, 82.6, 50.7, 47.9, 47.4, 45.5, 44.9, 44.8, 40.0, 36.5, 30.3, 25.3, 22.1, 2.2; HRMS (ESI): calcd for $C_{44}H_{66}O_8NaSi_2$ $[M+Na]^+$: 801.41884; found: 801.41915.

**Enone 162**

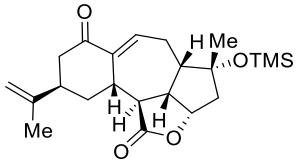


**Intramolecular Alkenylation/Isomerization**: Potassium *tert*-butoxide (1.3 g, 11.6 mmol) was added to a solution of 2,6-diisopropylphenol (2.5 mL, 13.6 mmol) in toluene (2 L) at 60 °C (bath temperature). The resulting suspension was stirred at that temperature for 90 min before alkenyl iodide **151** (1.86 g, 3.6 mmol) and $Pd(PPh_3)_4$ (900 mg, 0.77 mmol) were successively added. Stirring was continued at 60 °C (bath temperature) for 75 min before the mixture was cooled to room temperature and filtered through a pad of silica, rinsing with EtOAc (10 x 250 mL). The combined filtrates were concentrated under reduced pressure and the residue was purified by flash chromatography on silica, eluting with a gradient of 0-30% EtOAc in hexanes, to afford enone **162** (793 mg, 57% yield) as a red solid and a second fraction containing dimer **163** (280 mg, 20% yield) as an orange solid (the data of the dimer are compiled below). For analytical purposes, an aliquot was purified by HPLC [(150 mm YMC Triart C18 5 μm, 20.0 mm ∅, MeOH in $H_2O$ = 80:20 isocratic over 20 min, 15 mL/min, $\lambda$ = 210 nm, t = 9.91 min)] to give analytically pure **162**, which analysed as follows: colourless gum;

$[\alpha]_D^{20}$ = +3.8 (c = 0.8, $CHCl_3$). $^1$H NMR (600 MHz, $CDCl_3$) δ = 6.67 (ddd, *J* = 9.6, 3.9, 1.9 Hz, 1H), 4.86 (td, *J* = 8.3, 1.3 Hz, 1H), 4.83 (s, 1H), 4.70 (s, 1H), 3.60 (dd, *J* = 11.9, 9.8 Hz, 1H), 2.90 (dtd, *J* = 13.7, 5.4, 1.4 Hz, 1H), 2.82 (dt, *J* = 9.7, 8.4 Hz, 1H), 2.76-2.69 (m, 2H), 2.68-2.59 (m, 2H), 2.45 (dd, *J* = 15.6, 5.0 Hz, 1H), 2.35 (ddd, *J* = 15.5, 1.4, 0.6 Hz, 1H), 2.28 (ddd, *J* = 16.0, 9.6, 7.5 Hz, 1H), 2.16 (dt, *J* = 10.0, 7.8 Hz, 1H), 1.91 (dd, *J* = 15.5, 8.1 Hz, 1H), 1.78 (s, 3H), 1.76 (ddd, *J* = 13.7, 11.9, 6.7 Hz, 1H), 1.28 (s, 3H), 0.15 (s, 9H); $^{13}$C NMR (151 MHz, $CDCl_3$) δ = 203.3, 177.8, 147.3, 141.8, 134.5, 111.5, 82.7, 80.4, 50.7, 48.6, 47.6, 44.0, 42.1, 40.4, 38.7, 31.2, 26.6, 21.4, 21.3, 2.2; IR (film) ν/cm$^{-1}$: 2959, 1763, 1695, 1611, 1451, 1377, 1301, 1251, 1232, 1194, 1109, 1011,

890, 841, 754; HRMS (ESI): calcd for $C_{22}H_{32}O_4SiNa$ $[M+Na]^+$: 411.19620; found: 411.19654.

**Hydroxyketone 148**

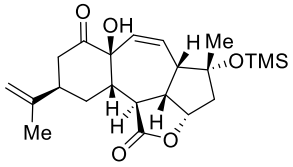


**Hydroxylation**: 1,8-Diazabicyclo[5.4.0]undec-7-ene (1.0 mL, 7.2 mmol) was added to a solution of trimethyl phosphite (0.6 mL, 5.4 mmol) in acetonitrile (36 mL). The solution was purged with $O_2$ for 40 min. This solution was then transferred *via* canula into the reaction flask that had been charged with the crude enone **162** and purged with $O_2$ for 30 min. The resulting mixture was stirred at room temperature under $O_2$ atmosphere (balloon) for 70 h. The mixture was poured into sat. aq. $NaHCO_3$ (100 mL) at 0 °C, which was extracted with EtOAc (3 x 100 mL). The combined organic layers were washed with brine (50 mL), dried over $MgSO_4$, filtered and concentrated under reduced pressure. The residue was purified by flash chromatography on silica, eluting with a gradient of 0-20% EtOAc in hexanes, to afford the desired product **148** as a yellowish gum (635 mg, 44% yield over two steps).

$[\alpha]_D^{20}$ = +35.5 (c = 0.79, $CHCl_3$). $^1$H NMR (600 MHz, $CD_2Cl_2$) δ = 5.90 (ddd, *J* = 11.6, 2.3, 0.6 Hz, 1H), 5.60 (dd, *J* = 11.7, 2.6 Hz, 1H), 4.88 (q, *J* = 1.5 Hz, 1H), 4.86 (td, *J* = 8.7, 2.0 Hz, 1H), 4.69 (dp, *J* = 1.7, 0.8 Hz, 1H), 4.39 (s, 1H), 4.09 (ddd, *J* = 11.2, 8.7, 7.2 Hz, 1H), 3.60 (dd, *J* = 11.2, 10.4 Hz, 1H), 2.85 – 2.82 (m, 2H), 2.81 – 2.76 (m, 1H), 2.68 – 2.61 (m, 1H), 2.61 (dt, *J* = 7.3, 2.5 Hz, 1H), 2.27 (ddd, *J* = 15.8, 2.0, 0.6 Hz, 1H), 2.18 (td, *J* = 10.8, 4.5 Hz, 1H), 2.08 (dd, *J* = 15.8, 8.7 Hz, 1H), 1.80 (dt, *J* = 1.5, 0.7 Hz, 3H), 1.65 (ddd, *J* = 14.8, 11.3, 4.0 Hz, 1H), 1.43 (s, 3H), 0.13 (s, 9H); $^{13}$C NMR (151 MHz, $CD_2Cl_2$) δ = 212.9, 179.0, 146.2, 134.8, 127.9, 112.5, 84.7, 81.0, 78.6, 48.0, 45.2, 44.7, 43.7, 41.4, 40.5, 32.1, 27.9, 22.1, 2.2; IR (film) ν/cm$^{-1}$: 3461, 2962, 1761, 1712, 1644, 1449, 1378, 1338, 1263, 1250, 1178, 1142, 1101, 1010, 895, 840, 756; HRMS (ESI): calcd for $C_{22}H_{32}O_5SiNa$ $[M+Na]^+$: 427.19112; found: 427.19102.

**Dimer 163**

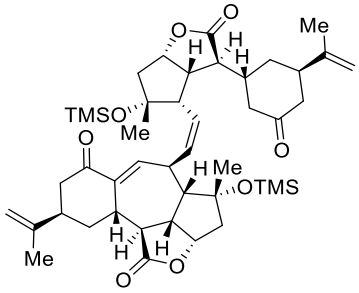


$[\alpha]_D^{20}$ = +18.8 (c = 0.4, $CHCl_3$). $^1H$ NMR (400 MHz, $CDCl_3$) δ = 6.38 (dd, *J* = 3.3, 2.0 Hz, 1H), 5.90 (dd, *J* = 11.1, 8.2 Hz, 1H), 5.71 (ddd, 1H), 4.94 – 4.85 (m, 3H), 4.85 – 4.83 (m, 1H), 4.70 (s, 1H), 4.66 (s, 1H), 3.86 – 3.78 (m, 1H), 3.56 (dd, *J* = 12.1, 9.5 Hz, 1H), 2.97 – 2.82 (m, 3H), 2.81 - 2.63 (m, 5H), 2.61 – 2.49 (m, 3H), 2.47 – 2.38 (m, 2H), 2.36 – 2.20 (m, 4H), 2.09 (t, *J* = 8.4 Hz, 1H), 1.96 (dd, *J* = 16.0, 8.3 Hz, 1H), 1.92 – 1.85 (m, 1H), 1.83 – 1.77 (m, 5H), 1.75 - 1.69 (m, 4H), 1.33 (s, 3H), 1.31 (s, 3H), 0.15 (s, 9H), 0.13 (s, 9H); $^{13}C$ NMR (101 MHz, $CDCl_3$) δ = 210.3, 201.7, 178.2, 177.2, 146.9, 146.1, 141.2, 140.5, 139.9, 126.5, 112.9, 111.5, 83.2, 83.1, 82.8, 79.8, 57.7, 51.5, 48.9, 47.1, 47.0, 46.3, 46.1, 44.3, 43.7, 43.2, 42.5, 40.5, 40.0, 38.4, 35.1, 32.5, 30.8, 30.7, 27.9, 25.9, 22.2, 21.0, 2.4, 2.2; IR (film) ν/$cm^{-1}$: 2954, 1763, 1712, 1603, 1450, 1377, 1320, 1251, 1194, 1117, 1007, 902, 841, 756; HRMS (ESI): calcd for $C_{44}H_{64}NaO_8Si_2$ $[M+Na]^+$: 799.40319; found: 799.40293.

**Alkene 165**

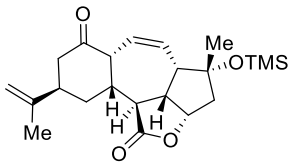


Potassium *tert*-butoxide (13.0 mg, 116 μmol) was added to a solution of phenol (12.4 mg, 132 μmol) in toluene (4 mL) at room temperature. The resulting suspension was stirred for 5 min before a solution of alkenyl iodide **151** (40 mg, 77 μmol) in toluene (4 mL) (rinsing the flask with toluene (2 x 0.5 mL)) and $Pd(PPh_3)_4$ (18 mg, 16 μmol) were successively added. The mixture was heated to 60 °C (bath temperature) for 90 min before the mixture was cooled to 0 °C, water (2 mL) was added and the mixture was extracted with EtOAc (5 x 10 mL), the

organic layers were combined, washed with brine (5 mL), dried over $MgSO_4$, filtered and concentrated. The residue was purified by flash chromatography on silica, eluting with a gradient of 0-20% EtOAc in pentane, to afford afford a crude mixture containing alkene **165** as a red solid.

To afford an analytically pure sample, that crude was purified by HPLC, [(150 mm YMC Triart C18 5 μm, 10.0 mm ∅, MeOH in $H_2O$ = 70:30 isocratic over 20 min, 4.7 mL/min, $\lambda$ = 192 nm, t = 9.0 min)] to give pure alkene **165** as a white solid (1.0 mg, 3% yield).

$^1$H NMR (600 MHz, $CDCl_3$) δ = 5.71 (dt, *J* = 11.2, 2.2 Hz, 1H), 5.38 (dddd, *J* = 11.2, 5.4, 2.7, 0.6 Hz, 1H), 4.92 – 4.85 (m, 2H), 4.69 (dt, *J* = 1.8, 0.9 Hz, 1H), 3.60 (t, *J* = 11.0 Hz, 1H), 3.36 – 3.32 (m, 1H), 3.16 (dt, *J* = 10.9, 8.1 Hz, 1H), 2.80 – 2.75 (m, 1H), 2.72 – 2.64 (m, 3H), 2.54 (dq, *J* = 7.5, 2.5 Hz, 1H), 2.34 – 2.27 (m, 1H), 2.25 (ddd, *J* = 15.8, 1.5, 0.5 Hz, 1H), 1.97 (dd, *J* = 15.7, 8.6 Hz, 1H), 1.81 (dt, *J* = 1.4, 0.7 Hz, 3H), 1.57 (td, *J* = 13.9, 4.5 Hz, 1H), 1.42 (s, 3H), 0.13 (s, 9H); $^{13}$C NMR (151 MHz, $CDCl_3$) δ = 212.5, 178.8, 146.5, 130.8, 124.5, 112.5, 84.5, 80.9, 53.8, 51.5, 47.2, 44.7, 44.0, 42.6, 40.5, 37.1, 29.2, 27.4, 22.3; HRMS (ESI): calcd for $C_{22}H_{32}O_4NaSi$ $[M+Na]^+$: 411.19621; found: 411.19654.

**Dimer 166**

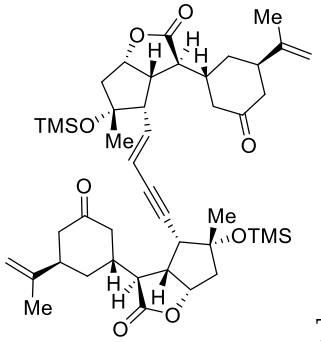


To a solution of alkyne **159** (2.0 mg, 5.1 μmol) in toluene (0.1 mL) at room temperature were added successively 1,1'-bis-(diisopropylphosphin)-ferrocen (0.4 mg, 1 μmol) and palladium(II)-acetate (0.4 mg, 1 μmol). The mixture was heated to 60 °C (bath temperature) for 17 h, then cooled to room temperature, filtered over Celite®, rinced with EtOAc (5 x 0.2 mL)

and the solution was concentrated. The residue was purified by flash chromatography on silica, eluting with 50% EtOAc in hexanes to give the dimer **166** as a colourless gum (0.8 mg, 40% yield).

$[\alpha]_D^{20}$ = +39.6 (c = 0.15, $CHCl_3$). $^1H$ NMR (600 MHz, $CDCl_3$) δ = 6.16 (dd, *J* = 16.0, 9.3 Hz, 1H), 5.65 (ddd, *J* = 16.0, 1.9, 0.8 Hz, 1H), 4.92 (ddd, *J* = 7.7, 6.4, 1.1 Hz, 2H), 4.90 – 4.87 (m, 2H), 4.68 (dt, *J* = 1.7, 0.8 Hz, 1H), 4.66 (dd, *J* = 1.6, 0.8 Hz, 1H), 3.04 (dd, *J* = 5.0, 4.2 Hz, 1H), 2.87 – 2.75 (m, 5H), 2.62 – 2.57 (m, 2H), 2.53 (ddd, *J* = 15.3, 11.7, 0.9 Hz, 1H), 2.48 – 2.43 (m, 3H), 2.40 – 2.24 (m, 4H), 2.32 (d, *J* = 15.0 Hz, 1H), 2.26 (d, *J* = 14.8 Hz, 1H), 2.23 – 2.15 (m, 1H), 2.13 – 2.05 (m, 3H), 1.79 – 1.75 (m, 2H), 1.75 – 1.72 (m, 7H), 1.67 (ddd, *J* = 14.1, 12.2, 5.0 Hz, 1H), 1.46 (s, 3H), 1.29 (s, 3H), 0.14 (s, 9H), 0.12 (s, 9H); $^{13}C$ NMR (151 MHz, $CDCl_3$) δ = 210.5, 210.3, 178.1, 178.0, 146.1, 146.0, 139.0, 114.3, 113.1, 113.0, 86.6, 84.0, 83.5, 83.4, 82.6, 82.2, 57.0, 48.8, 48.1, 48.0, 47.3, 47.2, 46.7, 46.1, 45.0, 44.8, 44.7, 44.6, 40.2, 40.2, 36.0, 35.9, 30.0, 29.9, 25.3, 25.3, 22.3, 22.3, 2.4, 2.3; IR (film) ν/$cm^{-1}$: 2959, 2925, 2854, 1765, 1715, 1456, 125, 1190, 1123, 1094, 1006, 843; HRMS (ESI): calcd for $C_{44}H_{64}O_8Si_2Na$ $[M+Na]^+$: 799.40281; found: 799.40319.

### 5.2.2.2 Completion of the first total syntheses of (-)-Scabrolide B and (-)-Sinuscalide C

**Allylic alcohol 175** (from **148**)

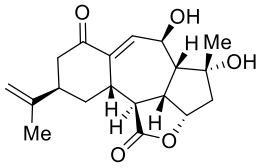


*Note: It proved necessary to perform the reaction in air*

In a round-bottomed-flask under air atmosphere methyltrioxorhenium(VII) (80 mg, 0.32 mmol) was added to a solution of alcohol **148** (430 mg, 1.1 mmol) in chlorobenzene (21 mL). The mixture was stirred at 60 °C (bath temperature) for 48 h before it was cooled to room temperature, and filtered through a plug of Celite®, rinsing with EtOAc (5 x 10 mL). The combined filtrates were concentrated under reduced pressure, and the residue was purified by flash chromatography on silica, eluting with a gradient of 30-50% EtOAc in hexanes, to afford the desired product as a white solid (250 mg, 71% yield), and a second fraction comprised of (-)-scabrolide B **34** as a white solid (53 mg, 15% yield).

$[\alpha]_D^{20}$= -73.6 (c = 0.07, $CHCl_3$). $^1$H NMR (600 MHz, $CD_2Cl_2$) δ = 6.37 (dd, *J* = 2.9, 1.9 Hz, 1H), 5.11 (dq, *J* = 10.0, 3.5 Hz, 1H), 4.84 (td, *J* = 1.4, 0.7 Hz, 1H), 4.78 (ddd, *J* = 8.3, 7.6, 6.2 Hz, 1H), 4.69 (tt, *J* = 1.3, 0.7 Hz, 1H), 3.20 (t, *J* = 11.5 Hz, 1H), 2.86 (dtd, *J* = 13.6, 5.5, 1.5 Hz, 1H), 2.83 (dt, *J* = 11.3, 8.6 Hz, 1H), 2.74 – 2.69 (m, 1H), 2.68 (tddd, *J* = 11.8, 5.3, 3.2, 2.0 Hz, 1H), 2.67 – 2.65 (m, 1H) 2.61 (d, *J* = 4.9 Hz, 1H), 2.44 (dd, *J* = 15.1, 4.3 Hz, 1H), 2.28 (t, *J* = 9.5 Hz, 1H), 2.25 (dd, *J* = 14.4, 7.7 Hz, 1H), 2.17 (dd, *J* = 14.4, 6.3 Hz, 1H), 2.14 (s, 1H), 1.81 (ddd, *J* = 13.8, 11.9, 6.7 Hz, 1H), 1.78 (dt, *J* = 1.3, 0.6 Hz, 3H), 1.42 (s, 3H); $^{13}$C NMR (151 MHz, $CD_2Cl_2$) δ = 201.8, 176.9, 147.8, 140.6, 139.2, 111.3, 79.8, 79.5, 67.6, 56.1, 47.4, 47.0, 44.2, 42.6, 40.5, 38.9, 31.5, 31.3, 21.1; IR (film) ν/cm$^{-1}$: 3423, 2961, 2925, 1760, 1689, 1616, 1450, 1378, 1310, 1240, 1215, 1196, 1111, 1049, 1020, 895, 757; HRMS (ESI): calcd for $C_{19}H_{24}O_5Na$ $[M+Na]^+$: 355.15159; found: 355.15169.

**Allylic alcohol 175** (from **171**)

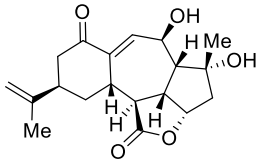

*Note: It proved necessary to perform the reaction in air*

In a round-bottomed-flask under air atmosphere methyltrioxorhenium(VII) (6.5 mg, 24 μmol) was added to a solution of alcohol **171** (27 mg, 81 μmol) in chlorobenzene (1.5 mL). The mixture was stirred at 60 °C (bath temperature) for 36 h before it was cooled to room temperature, and filtered through a plug of Celite®, rinsing with EtOAc (5 x 2 mL). The combined filtrates were concentrated under reduced pressure, and the residue was purified by flash chromatography on silica, eluting with a gradient of 30-60% EtOAc in hexanes, to afford recovered starting material as a white solid (6.0 mg, 21% recovered), the desired product **175** as a white solid (19.2 mg, 71% yield, 90% yield brsm), and a fraction comprised of scabrolide B **34** as a white solid (2.1 mg, 8% yield, 10% yield brsm).

**Tetraene 176**

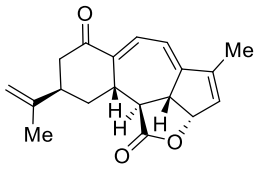

In a round-bottomed-flask under air atmosphere methyltrioxorhenium(VII) (43 mg, 0.17 mmol) was added to a solution of alcohol **148** (173 mg, 0.43 mmol) in toluene (9 mL). The mixture was heated to 60 °C (bath temperature) for 30 h before it was cooled to room temperature, and filtered through a plug of Celite®, rinsing with EtOAc (5 x 10 mL). The combined filtrates were concentrated under reduced pressure, and the residue was purified by flash chromatography on silica, eluting with a gradient of 0-60% EtOAc in hexanes, to afford **175** as a white solid (30 mg, 21% yield), a fraction comprised of (-)-scabrolide B **34** as a white solid (25 mg, 18% yield) and a fraction of mixture of tetraene **176** and (-)-sinuscalide C **35**.

That residue was purified by preparative HPLC (150 mm YMC Triart C18 5 μm, 20.0 mm ∅, MeOH in $H_2O$ = 65:35 isocratic over 20 min, 15.0 mL/min, $\lambda$ = 220 nm, t = 7.0 and 11.6 min) to give sinuscalide C **35** as a white solid (7.5 mg, 5.6% yield) and a fraction comprised of **176** as a yellow solid (5.9 mg, 4.7% yield).

$[\alpha]_D^{20}$= -578 (c = 0.59, $CHCl_3$). $^1$H NMR (600 MHz, $CDCl_3$) δ = 7.34 (dt, *J* = 4.9, 1.5 Hz, 1H), 6.16 – 6.14 (m, 1H), 6.12 (ddt, *J* = 4.9, 1.8, 0.8 Hz, 1H), 5.32 – 5.27 (m, 1H), 4.81 (td, *J* = 1.4, 0.7 Hz, 1H), 4.72 (td, *J* = 1.3, 0.7 Hz, 1H), 3.55 (dddd, *J* = 11.2, 5.8, 2.3, 1.1 Hz, 1H), 3.50 (dd, *J* = 12.5, 11.1 Hz, 1H), 3.16 (ddd, *J* = 12.5, 5.8, 2.8 Hz, 1H), 2.81 (dq, *J* = 14.3, 2.4 Hz, 1H), 2.69 (ddd, *J* = 17.7, 4.3, 2.5 Hz, 1H), 2.63 – 2.57 (m, 1H), 2.38 (dd, *J* = 17.7, 11.2 Hz, 1H), 1.94 (t, *J* = 1.2 Hz, 3H), 1.83 (ddd, *J* = 14.3, 11.3, 6.2 Hz, 1H), 1.79 (dt, *J* = 1.3, 0.6 Hz, 3H); $^{13}$C NMR (151 MHz, $CDCl_3$) δ = 199.49, 176.24, 154.51, 147.70, 146.88, 139.50, 139.16, 134.99, 118.90, 110.39, 81.95, 56.73, 44.74, 44.66, 37.28, 37.15, 30.03, 21.09, 12.65; HRMS (ESI): calcd for $C_{19}H_{20}O_3Na$ $[M+Na]^+$: 319.13047; found: 319.13055.

**(-)-Scabrolide B 34**

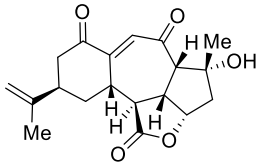

In a loosely caped vial under air 2-iodoxybenzoic acid (134 mg, 0.48 mmol) was added to a solution of alcohol **175** (80 mg, 0.24 mmol) in dimethylsulfoxide (2.4 mL). The mixture was stirred at room temperature for 3 h, then water (2 mL) was added, the mixture was filtered and rinced with EtOAc (3 x 5 mL). The aqueous phase of the combined filtrate was extracted with EtOAc (3 x 20 mL), the combined organic layers were washed with water (3 x 5 mL) then brine (5 mL), dried with $MgSO_4$, filtered and concentrated. The residue was purified by flash chromatography on silica, eluting with a gradient of 30-50% EtOAc in hexanes, to give (-)-scabrolide B **34** as a white solid (59 mg, 74% yield).

$[\alpha]_D^{20}$ = -56.4 (c = 0.5, $CHCl_3$), $[\alpha]_D^{25}$ = -33.2 (c = 0.34, MeOH) (lit: $[\alpha]_D^{29}$ = -80.0 (c = 0.33, $CHCl_3$)[26]; $[\alpha]_D^{25}$ = -60.0 (c = 0.10, MeOH)[30]). $^1$H NMR (600 MHz, $CDCl_3$) δ = 6.34 (d, *J* = 2.8 Hz, 1H), 4.98 (ddd, *J* = 9.2, 8.1, 2.3 Hz, 1H), 4.94 (q, *J* = 1.2, 1H), 4.71 (dt, *J* = 1.6, 0.8 Hz, 1H), 3.44 (dd, *J* = 11.0, 10.2 Hz, 1H), 3.30 (dtd, *J* = 13.8, 4.1, 2.3 Hz, 1H), 3.14 (dt, *J* = 10.2, 8.1 Hz, 1H), 2.93 (d, *J* = 8.1, 1H), 2.90 (ddd, *J* = 16.2, 3.9, 2.3 Hz, 1H), 2.81 (m, 1H), 2.78 (dddd, *J* = 12.3, 11.0, 4.1, 2.8 Hz, 1H), 2.58 (dd, *J* = 16.2, 6.3 Hz, 1H), 2.40 (d, *J* = 2.0 Hz, 1H), 2.36 (dd, *J* = 16.2, 2.3 Hz, 1H), 2.19 (ddd, *J* = 16.2, 9.2, 2.0 Hz, 1H), 1.82 (dt, *J* = 1.2, 0.8 Hz, 3H), 1.71 (ddd, *J* = 13.8, 12.3, 5.2 Hz, 1H), 1.62 (s, 3H); $^{13}$C NMR (151 MHz, $CDCl_3$) δ = 202.6, 202.3, 176.0 , 150.9, 146.5, 130.6, 112.8, 81.4, 79.6, 62.5, 47.5, 45.4, 45.4, 45.1, 41.7, 39.0, 30.5, 30.1, 22.0; IR (film) ν/cm$^{-1}$: 3498, 2964, 2927, 1763, 1697, 1667, 1451, 1376, 1334, 1210, 1191, 1166, 1110, 1054, 1018, 943, 899, 755; HRMS (ESI): calcd for $C_{19}H_{23}O_5$ $[M+H]^+$: 331.15400; found: 331.15415.

**(-)-Sinuscalide C 35**

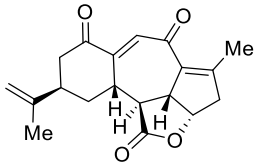

In an MS vial, Burgess reagent (4.3 mg, 18 μmol) was added to a solution of scabrolide B **34** (3.0 mg, 9.1 μmol) in toluene (0.2 mL). The mixture was stirred at 60 °C (bath temperature) for 2 h before it was concentrated under reduced pressure. The residue was purified by flash chromatography on silica, eluting with 30% EtOAc in hexanes, to afford (-)-sinuscalide C **35** as a yellowish solid (2.1 mg, 74% yield).

$[\alpha]_D^{20}$ = -42.1 (c =0.2, $CHCl_3$) (lit: $[\alpha]_D^{25}$ = -40.0 (c = 0.10, MeOH)[30])[6]. $^1$H NMR (600 MHz, $CDCl_3$) δ = 6.47 (d, *J* = 2.8 Hz, 1H), 5.15 (td, *J* = 8.8, 5.3 Hz, 1H), 4.95 (s, 1H), 4.75 (dt, *J* = 1.6, 0.8 Hz, 1H), 3.52 (ddp, *J* = 10.5, 8.7, 1.5 Hz, 1H), 3.25 (dtdd, *J* = 13.7, 4.2, 2.5, 0.5 Hz, 1H), 3.14 (ddq, *J* = 20.1, 8.8, 1.2 Hz, 1H), 2.95 (ddd, *J* = 16.0, 3.6, 2.5 Hz, 1H), 2.90 (dddd, *J* = 12.4, 11.3, 4.1, 2.6 Hz, 1H), 2.82 (m, 1H), 2.79 (dddd, *J* = 20.1, 6.6, 3.2, 1.4 Hz, 1H), 2.64 (dd, *J* = 11.3, 10.5 Hz, 1H), 2.60 (dd, *J* = 16.0, 6.4 Hz, 1H), 2.14 (q, *J* = 1.5 Hz, 3H), 1.84 (dt, *J* = 1.4, 0.7 Hz, 3H), 1.72 (ddd, *J* = 13.7, 12.4, 5.0 Hz, 1H); $^{13}$C NMR (151 MHz, $CDCl_3$) δ = 202.8, 187.5, 175.7, 153.1, 149.9, 146.2, 134.7, 132.8, 113.1, 77.6, 50.9, 48.8, 46.2, 45.5, 39.7, 38.9, 31.0, 22.0, 16.0; IR (film) ν/cm$^{-1}$: 2924, 2855, 1770, 1698, 1647, 1611, 1428, 1355, 1212, 1137, 1030, 959, 888; HRMS (GC-EI): calcd for $C_{19}H_{20}O_4$ [M]$^+$: 312.13561; found: 312.13562.

[6] The optical rotation for Sinuscalide C **35** is reported in MeOH. We were not able to dissolve our sample in MeOH, even at higher dilution. We therefore report an optical rotation in $CHCl_3$.

**(+)-Fragilolide A 33**

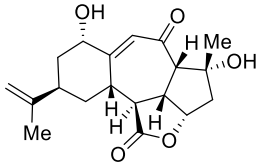


$CeCl_3 \cdot 7H_2O$ (11.0 mg, 30 μmol) was added to a solution of scabrolide B **34** (10.3 mg, 31 μmol) in MeOH (0.6 mL). The solution was cooled to –78 °C and $NaBH_4$ (1.7 mg, 45 μmol, 1.5 equiv.) was added before the mixture was stirred for 30 min. Water (500 μL) was then added and the solution was transferred to a separatory funnel with EtOAc. The aqueous layer was extracted with EtOAc (3 × 10 mL) and the combined organic extracts were washed with brine (5 mL), dried over $MgSO_4$, filtered, and concentrated. The residue was purified by flash chromatography on silica, eluting with a gradient of 0-50% acetone in pentane to give (+)-fragilolide A **33** (2.3 mg, 22% yield) as a white solid.

$[\alpha]_D^{20}$ = +64.0 (c = 0.08, MeOH) (litt: $[\alpha]_D^{20}$ = +16.0 (c = 0.1, MeOH)[28]). $^1$H NMR (600 MHz, $CDCl_3$) δ = 6.25 (td, *J* = 1.3, 0.7 Hz, 1H), 5.01 – 4.99 (m, 2H), 4.95 (ddd, *J* = 9.2, 8.4, 2.6 Hz, 1H), 4.32 (ddd, *J* = 11.3, 4.7, 1.0 Hz, 1H), 3.35 (t, *J* = 10.8 Hz, 1H), 3.33 (dq, *J* = 13.8, 3.1 Hz, 1H), 3.10 (dt, *J* = 10.6, 8.5 Hz, 1H), 2.92 (d, *J* = 7.4 Hz, 1H), 2.61 – 2.56 (m, 1H), 2.55 (ddt, *J* = 12.7, 4.8, 2.3 Hz, 1H), 2.46 (dddd, *J* = 12.7, 11.0, 3.6, 2.0 Hz, 1H), 2.35 (ddd, *J* = 16.2, 2.6, 0.6 Hz, 1H), 2.20 (dd, *J* = 16.2, 9.2 Hz, 1H), 1.85 (p, *J* = 0.8 Hz, 3H), 1.62 (td, *J* = 12.4, 5.3 Hz, 1H), 1.60 (s, 3H), 1.32 (ddd, *J* = 13.7, 12.4, 5.0 Hz, 1H); $^{13}$C NMR (151 MHz, $CDCl_3$) δ = 203.7, 176.9, 160.4, 145.4, 122.1, 111.7, 81.1, 79.7, 69.3, 62.8, 47.5, 45.4, 45.1, 41.6, 40.1, 38.5, 34.7, 30.7, 22.6; IR (film) ν/cm$^{-1}$: 3461, 2923, 2853, 1754, 1692, 1611, 1462, 1378, 1306, 1225, 1195, 1163, 1121, 1014, 942, 891, 665; HRMS (ESI): calcd for $C_{19}H_{24}O_5$ $[M+Na]^+$: 355.15159; found: 355.15153.

### 5.2.2.3 Total syntheses of Ineleganolide, Horiolide and Kavaranolide

**Alcohol 177**

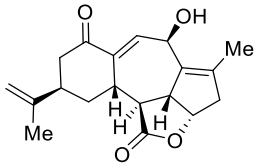


1,8-Diazabicyclo[5.4.0]undec-7-ene (9.1 uL, 61 μmol) was added to a solution of scabrolide B **34** (20.0 mg, 61 μmol) in acetonitrile (1.0 mL) at 0 °C. The mixture was stirred at this temperature for 1 h, then 1,8-diazabicyclo[5.4.0]undec-7-ene (9.1 μL, 61 μmol) was added to the solution, and stirring was continued at 0 °C for 1 h. Aq. HCl (2 M, 2 mL) was then added at 0 °C. The mixture was warmed to room temperature, then extracted with EtOAc (3 x 10 mL). The combined organic layers were washed with brine (5 mL), dried with $MgSO_4$, filtered and concentrated. The residue was purified by flash chromatography on silica, eluting with a gradient of 0-50% EtOAc in pentane to afford ineleganolide **2** as a white solid (4.8 mg, 24% yield) and alcohol **177** as a white solid (5 mg, 26% yield).

$[\alpha]_D^{20}$ = +47.9 (c = 0.15, $CHCl_3$). $^1$H NMR (600 MHz, $CDCl_3$) δ = 6.34 (dd, *J* = 2.8, 1.9 Hz, 1H), 5.60 (h, *J* = 1.6 Hz, 1H), 5.34 – 5.28 (m, 1H), 4.86 (h, *J* = 1.3 Hz, 1H), 4.72 (tq, *J* = 6.4, 3.0 Hz, 1H), 4.71 (h, *J* = 1.5 Hz, 1H), 3.04 – 2.96 (m, 3H), 2.76 (ddd, *J* = 16.0, 7.5, 1.4 Hz, 1H), 3.71 – 2.64 (m, 3H) 2.47 (dd, *J* = 16.0, 5.2 Hz, 1H), 1.95 – 1.91 (m, 4H), 1.79 (dt, *J* = 1.2, 0.6 Hz, 3H), 1.76 (ddd, *J* = 13.6, 11.4, 6.6 Hz, 1H); $^{13}$C NMR (151 MHz, $CDCl_3$) δ = 202.2, 176.4, 148.1, 146.9, 140.0, 139.2, 125.2, 111.9, 84.5, 69.9, 56.2, 45.5, 44.2, 42.5, 39.5, 38.7, 31.3, 21.2, 16.2; IR (film) ν/cm$^{-1}$: 3448, 2941, 2888, 1764, 1695, 1624, 1438, 1381, 1339, 1240, 1189, 1155, 1109, 1038, 1006, 896, 758; HRMS (GC-EI): calcd for $C_{19}H_{22}O_4$ $[M]^+$ : 314.15126; found: 314.15141.

**(+)-Ineleganolide 2**

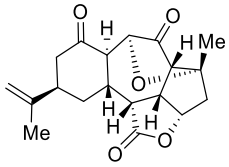

1,1,3,3-Tetramethylguanidin (12 μL, 97 μmol) was added to a solution of scabrolide B **34** (16.0 mg, 48 μmol) in acetonitrile (1.0 mL) at room temperature. The mixture was stirred for 17 h then aq. HCl (2 M, 2 mL) was added at 0 °C. The mixture was warmed to room temperature, then extracted with EtOAc (3 x 10 mL). The combined organic layers were washed with brine (5 mL), dried with $MgSO_4$, filtered and concentrated. The residue was purified by flash chromatography on silica, eluting with a gradient of 0-60% EtOAc in pentane to afford (+)-ineleganolide **2** as a white solid (6.8 mg, 43% yield).

$[\alpha]_D^{25}$ = +75.2 (c =0.11, $CHCl_3$) (lit: $[\alpha]_D^{25}$ = +26.4 (c = 0.05, $CHCl_3$)[11]). $^1$H NMR (600 MHz, $CDCl_3$) δ = 5.13 (t, *J* = 7.5 Hz, 1H), 5.07 (d, *J* = 1.2 Hz, 1H), 4.94 (qd, *J* = 1.4, 0.7 Hz, 1H), 4.62 (p, *J* = 1.4 Hz, 1H), 3.42 (ddd, *J* = 12.0, 9.3, 7.6 Hz, 1H), 3.02 (dd, *J* = 12.0, 2.4 Hz, 1H), 3.01 (ddd, *J* = 14.0, 12.1, 5.3 Hz, 1H), 2.78 (m, 1H), 2.70 (dt, *J* = 12.4, 1.1 Hz, 1H), 2.67 (dt, *J* = 15.2, 2.4 Hz, 1H), 2.59 (d, *J* = 9.3 Hz, 1H), 2.58 (ddd, *J* = 15.2, 6.5, 1.0 Hz, 1H), 2.52 (d, *J* = 15.5 Hz, 1H), 2.25 (tt, *J* = 12.3, 3.2 Hz, 1H), 2.10 (dd, *J* = 15.5, 7.3 Hz, 1H), 1.78 (dq, *J* = 13.9, 2.9 Hz, 1H), 1.71 (dt, *J* = 1.4, 0.7 Hz, 3H), 1.28 (s, 3H); $^{13}$C NMR (151 MHz, $CDCl_3$) δ = 212.2, 206.5, 176.1, 146, 113.8, 91.1, 83.1, 77.5, 62.5, 49.8, 47.1, 45.5, 44.4, 43.8, 40.4, 33.2, 32.7, 22.7, 20.2; IR (film) ν/cm$^{-1}$: 2964, 2929, 1756, 1707, 1464, 1376, 1322, 1216, 1184, 1171, 1066, 1024, 898, 837, 754; HRMS (ESI): calcd for $C_{19}H_{22}O_5Na$ [M+Na$^+$]: 353.13594; found: 353.13577.

**(+)-Horiolide 3**

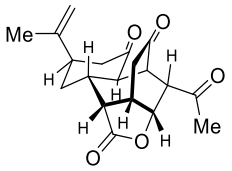


1,5-Diazabicyclo[4.3.0]non-5-ene (5.8 μL, 48 μmol) was added to a solution of scabrolide B **34** (8.0 mg, 24 μmol) in methanol (0.5 mL) at room temperature. The mixture was stirred for 17 h before aq. HCl (2 M, 2 mL) was added. The mixture was extracted with EtOAc (5 x 5 mL). The combined organic layers were washed with brine (5 mL), dried with $MgSO_4$, filtered and concentrated. The residue was purified by preparative HPLC (150 mm YMC Triart C18 5 μm, 20.0 mm ∅, MeOH in $H_2O$ = 40:60 isocratic over 20 min, 15.0 mL/min, $\lambda$ = 220 nm, t = 9.25 min) to give (+)-horiolide **3** as a white solid (3.7 mg, 46% yield).

$[\alpha]_D^{20}$ = +71.5 (c =0.08, MeOH) (lit: $[\alpha]_D$ = +81 (c = 0.037, MeOH)[32] – temperature not specified). $^1$H NMR (600 MHz, $CDCl_3$) δ = 5.42 (ddd, *J* = 8.3, 6.2, 1.5 Hz, 1H), 4.88 (q, *J* = 0.7 Hz, 1H), 4.60 (dq, *J* = 0.7, 0.7 Hz, 1H), 4.12 (dd, *J* = 3.0, 0.9 Hz, 1H), 3.37 (dddd, *J* = 8.5, 8.3, 4.6, 2.6 Hz, 1H), 3.00 (dd, *J* = 6.2, 3.0 Hz, 1H), 2.80 (bm, 1H), 2.74 (ddd, *J* = 15.2, 2.5, 2.3 Hz, 1H), 2.72 (dd, *J* = 8.5, 4.0 Hz, 1H), 2.65 (ddd, *J* = 13.6, 0.9, 0.9 Hz, 1H), 2.52 (dd, *J* = 19.7, 2.6 Hz, 1H), 2.51 (ddd, *J* = 15.2, 6.7, 0.9 Hz, 1H), 2.47 (dd, *J* = 19.7, 4.6 Hz, 1H), 2.31 (s, 3H), 2.20 (ddd, *J* = 14.0, 11.9, 4.9 Hz, 1H), 2.03 (dddd, *J* = 14.0, 3.0, 2.7, 2.5 Hz, 1H), 1.97 (dddd, *J* = 13.6, 11.9, 3.8, 3.0 Hz, 1H), 1.70 (ddd, *J* = 1.4, 0.7, 0.7 Hz, 3H); $^{13}$C NMR (151 MHz, $CDCl_3$) δ = 206.8, 204.4, 201.9, 175.3, 145.8, 114.0, 76.4, 51.7, 50.0, 47.0, 43.7, 43.7, 40.4, 36.1, 36.1, 35.4, 31.7, 29.0, 22.6; IR (film) ν/cm$^{-1}$: 2922, 1772, 1725, 1707, 1453, 1366, 1293, 1222, 1164, 1097, 1067, 1011, 993, 915, 899, 741; HRMS (GC-EI): calcd for $C_{19}H_{22}O_5$[$M^+$]: 330.14618; found: 330.14600.

**(+)-Kavaranolide 18**

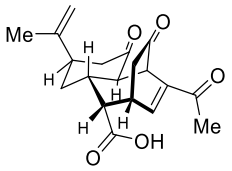


1,5-Diazabicyclo[4.3.0]non-5-ene (5.1 μL, 42 μmol) was added to a solution of scabrolide B **34** (7.0 mg, 21 μmol) in methanol (0.4 mL) at room temperature. The mixture was stirred for 4 h, then concentrated under reduced pressure. The residue was partitioned between dichloromethane (1 mL) and water (1 mL), the phases were separated and the aqueous layer was washed with dichloromethane (5 x 1 mL), EtOAc (3 x 2 mL) and ethanol (0.1 mL) was added and the crude was concentrated under reduced pressure. The residue was purified by preparative HPLC (150 mm YMC Triart C18 5 μm, 20.0 mm ∅, MeOH in $H_2O$ = 40:60 isocratic over 10 min, 4.7 mL/min, $\lambda$ = 220 nm, t = 2.2 min) to give (+)-kavaranolide **18** as a white solid (0.3 mg, 4% yield), and a mixed fraction (3 mg) containing a 1:1 mixture of **18** and DBN.

$[\alpha]_D^{20}$ = +105.6 (c = 0.08, MeOH) (lit: $[\alpha]_D^{25}$ = +14.5 (c = 0.5, MeOH)[33]). $^1$H NMR (600 MHz, [$D_6$]-DMSO) δ = 7.36 (dd, *J* = 7.6, 1.6 Hz, 1H), 4.75 (q, *J* = 1.4Hz, 1H), 4.44 (td, *J* = 1.6, 0.8 Hz, 1H), 4.33-4.29 (m, 1H), 3.18-3.12 (m, 1H), 3.15 (d, *J* = 12.8 Hz, 1H), 2.64 (td, *J* = 6.2, 3.4 Hz, 1H), 2.50-2.42 (m, 2H), 2.36 (dt, *J* = 14.8, 2.6 Hz, 1H), 2.27-2.23 (m, 2H), 2.20 (s, 3H), 2.20 (m, 1H), 1.86 (tt, *J* = 11.7, 4.1 Hz, 1H), 1.64 (dd, *J* = 1.4, 0.7 Hz, 3H), 1.54 (dq, *J* = 14.0, 2.9 Hz, 1H); $^{13}$C NMR (151 MHz, [$D_6$]-DMSO) δ = 211.5, 208.0, 195.7, 173.7, 149.7, 147.4, 139.9, 111.6, 50.7, 49.2, 44.2, 43.6, 40.1, 39.4, 36.4, 35.0, 32.0, 25.0, 22.1; IR (film) ν/cm$^{-1}$: 3398, 2920, 2852, 1764, 1716, 1664, 1575, 1407, 1378, 1234, 1197, 1151, 1106, 1013, 843; HRMS (ESI): calcd for $C_{19}H_{21}O_5$ $[M-H]^-$ :329.13980; found: 329.13945.

**Compound 178**

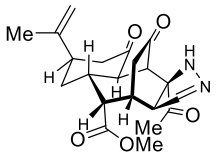

1,5-Diazabicyclo[4.3.0]non-5-ene (3.5 μL, 29 μmol) was added to a solution of scabrolide B **34** (4.8 mg, 15 μL) in methanol (0.3 mL). The mixture was stirred for 4 h, then (trimethylsilyl)-diazomethane (10% in Hexane, 120 μL, 73 μmol) was added and the mixture was stirred for 3 h. Acetic acid (1.75 M, 1 mL) was added and the mixture was concentrated. The residue was purified by flash chromatography on silica, eluting with 60% EtOAc in pentane to give the desired product **178** as a yellow oil (1.6 mg, 32% yield).

$^{1}$H NMR (600 MHz, $CD_2Cl_2$) δ = 6.58 (dd, *J* = 1.9, 1.2 Hz, 1H), 5.91 (s, 1H), 4.86 – 4.84 (m, 1H), 4.48 – 4.44 (m, 1H), 4.18 (s, 1H), 3.79 (s, 3H), 3.80 – 3.77 (m, 1H), 2.92 (dd, *J* = 6.5, 5.4 Hz, 1H), 2.76 – 2.70 (m, 2H), 2.66 (dt, *J* = 15.4, 2.5 Hz, 1H), 2.68 – 2.63 (m, 1H), 2.48 (ddd, *J* = 15.6, 6.3, 0.9 Hz, 1H), 2.22 – 2.20 (m, 2H), 2.19 (s, 3H), 2.06 (ddd, *J* = 13.6, 11.6, 4.6 Hz, 1H), 1.88 (tdd, *J* = 12.8, 5.4, 3.3 Hz, 1H), 1.78 (dtd, *J* = 13.6, 3.3, 2.4 Hz, 1H), 1.67 (dt, *J* = 1.4, 0.7 Hz, 3H); $^{13}$C NMR (151 MHz, $CD_2Cl_2$) δ = 207.7, 206.4, 202.3, 173.3, 146.7, 145.9, 113.3, 74.7, 52.2, 51.3, 49.7, 48.2, 47.0, 44.2, 40.3, 38.8, 35.5, 33.9, 31.0, 24.8, 22.4; HRMS (ESI): calcd for $C_{21}H_{26}O_5N_2Na$ $[M+Na]^+$: 409.17332; found: 409.17339.

### 5.2.2.4 Synthetic attempts to Pambanolides $B_1$ and $B_2$

**Ester 183**

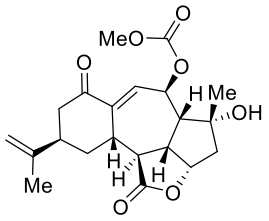


MeONa (25 wt% in methanol, 12.5 μL, 45 μmol) was added to a solution of alcohol **175** (5 mg, 15 μmol) in a (10:1) dimethylcarbonate/methanol mixture (0.15 mL). The mixture was stirred for 20 h. Sat. aq. $NaHCO_3$ (0.2 mL) was added, the mixture was then extracted with EtOAc (3 x 0.5 mL), the combined organic layers were washed with brine (3 x 5 mL), dried over $MgSO_4$, filtered and concentrated under reduced pressure. The residue was purified by flash chromatography on silica, eluting with 70% EtOAc in hexanes, to afford the desired product **183** as a white solid (3 mg, 52% yield).

$^1$H NMR (600 MHz, $CDCl_3$) δ = 6.31 (dd, *J* = 2.8, 2.1 Hz, 1H), 6.10 (dt, *J* = 9.0, 3.0 Hz, 1H), 4.89 (td, *J* = 8.6, 2.2 Hz, 1H), 4.86 (q, *J* = 1.1 Hz, 1H), 4.70 (q, *J* = 1.1 Hz, 1H), 3.83 (s, 3H), 3.45 (dd, *J* = 12.0, 10.2 Hz, 1H), 2.95 – 2.88 (m, 1H), 2.90 (td, *J* = 10.2, 9.0 Hz, 1H), 2.76 (ddd, *J* = 15.8, 6.9, 1.5 Hz, 1H), 2.71 (t, *J* = 5.9 Hz, 1H), 2.66 (ttt, *J* = 12.0, 3.0, 1.8 Hz, 1H), 2.50 (dd, *J* = 15.7, 5.0 Hz, 1H), 2.47 (t, *J* = 8.5 Hz, 1H), 2.29 (ddd, *J* = 16.0, 2.2, 0.6 Hz, 1H), 2.19 (dd, *J* = 16.0, 8.6 Hz, 1H), 1.89 (s, 1H), 1.87 (ddd, *J* = 13.6, 12.0, 6.3 Hz, 1H), 1.79 (dt, *J* = 1.3, 0.6 Hz, 3H), 1.33 (s, 3H); $^{13}$C NMR (151 MHz, $CDCl_3$) δ = 201.9, 176.7, 155.8, 146.9, 140.7, 135.9, 111.9, 79.6, 79.6, 72.9, 55.5, 54.1, 48.7, 47.4, 44.3, 42.1, 40.5, 38.8, 30.8, 28.7, 21.4; HRMS (ESI): calcd for $C_{21}H_{27}O_7Na$ $[M+Na]^+$: 413.15707; found: 413.15709.

### 5.2.2.5 Second generation synthesis of Scabrolide B

**Lactone 88**

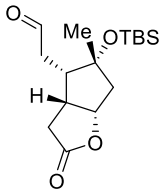


In a loosely caped vial under air, 2-iodoxybenzoic acid (30 mg, 0.10 mmol) was added to a solution of alcohol **89** (17 mg, 54 μmol)[14, 95] in dimethylsulfoxide (0.5 mL). The mixture was stirred at room temperature for 5 h, then water (1 mL) was added, the mixture was filtered and then rinced with EtOAc (3 x 2 mL). The aqueous phase of the combined filtrate was extracted with EtOAc (3 x 2 mL), the combined organic layers were washed with water (3 x 2 mL) and brine (2 mL), dried with $MgSO_4$, filtered and concentrated to give the desired product **88** as a colourless gum (10 mg, 59% yield).

$^1$H NMR (400 MHz, $CDCl_3$) δ = 9.89 (s, 1H), 5.06 (t, *J* = 7.7 Hz, 1H), 3.32 (dtd, *J* = 11.8, 8.5, 5.8 Hz, 1H), 2.79 (dd, *J* = 18.8, 4.7 Hz, 1H), 2.70 (ddd, *J* = 18.8, 9.2, 1.1 Hz, 1H), 2.62 (dd, *J* = 18.4, 5.9 Hz, 1H), 2.42 (dd, *J* = 18.4, 11.8 Hz, 1H), 2.32 (d, *J* = 15.4 Hz, 1H), 2.21 (td, *J* = 9.0, 4.7 Hz, 1H), 1.89 (dd, *J* = 15.4, 7.3 Hz, 1H), 1.31 (s, 3H), 0.88 (s, 9H), 0.13 (d, *J* = 1.7 Hz, 6H); $^{13}$C NMR (101 MHz, $CDCl_3$) δ = 201.1, 177.5, 83.8, 83.0, 47.4, 46.7, 40.8, 40.7, 30.5, 26.6, 26.2, 18.5, -1.7, -2.3; HRMS (ESI): calcd for $C_{16}H_{28}O_4SiNa$ $[M+Na]^+$: 335.16478; found: 335.16491.

**Lactone 189**

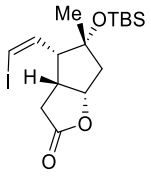


$O_3$ was bubbled through a solution of alkene **73** (485 mg, 1.64 mmol) in dichloromethane (8 mL) at –78 °C for 15 min until a deep blue color persisted. The mixture was warmed to 0 °C, argon was bubbled through it for 15 min, followed by addition of triphenylphosphine (1.3 g, 4.9 mmol). The mixture was stirred at

room temperature for 90 min before it was concentrated under reduced pressure and the residue purified by flash chromatography on silica, eluting with a gradient of 0-40% EtOAc in pentane, to afford the corresponding aldehyde as a yellow oil, which was used in the next step without delay.

Sodium bis(trimethylsilyl)amide (NaHMDS, 255 mg, 1.4 mmol) was added to a suspension of $[PPh_3CH_2I]I$ (797 mg, 1.5 mmol) in THF (16 mL), the resulting mixture was stirred at room temperature for 30 min and then cooled to –78 °C. A solution of the aldehyde in THF (2.5 mL) was added dropwise over 2 min (rinsing the flask with THF (2.5 x 2 mL)) at -78 °C and stirring continued at this temperature for 30 min. Saturated aqueous $NH_4Cl$ (10 mL) was added, the mixture was warmed to room temperature, the aqueous layer was extracted with *tert*-butyl methyl ether (3 x 25 mL), the combined organic layers were washed with brine (20 mL), dried over $MgSO_4$, filtered and concentrated. The residue was purified by flash chromatography on silica, eluting with a gradient of 0-20% *tert*-butyl methyl ether in pentane, to afford the title compound **189** as a yellow oil (305 mg, 44% yield over two steps).

$[\alpha]_D^{20}$ = +33.0 (c = 0.51, $CHCl_3$). $^1H$ NMR (400 MHz, $CDCl_3$) δ = 6.55 (dd, *J* = 7.5, 0.7 Hz, 1H), 6.49 (dd, *J* = 8.2, 7.6 Hz, 1H), 5.09 (ddd, *J* = 8.0, 7.1, 0.7 Hz, 1H), 3.35 (dtd, *J* = 11.7, 8.4, 5.3 Hz, 1H), 2.76 – 2.63 (m, 2H), 2.47 (dd, *J* = 18.6, 11.8 Hz, 1H), 2.36 (d, *J* = 15.3 Hz, 1H), 1.94 (dd, *J* = 15.3, 7.1 Hz, 1H), 1.31 (s, 3H), 0.87 (s, 9H), 0.13 (d, *J* = 5.0 Hz, 6H); $^{13}C$ NMR (101 MHz, $CDCl_3$) δ = 177.5, 137.9, 86.2, 84.1, 83.7, 58.2, 47.5, 40.7, 31.0, 26.7, 26.0, 18.4, -1.8, -2.3; IR (film) ν/cm$^{-1}$: 2953, 2929, 2859, 1770, 1470, 1377, 1365, 1302, 1259, 1189, 1175, 1113, 1000, 890, 836, 772; HRMS (ESI): calcd for $C_{16}H_{27}O_3ISiNa$ $[M+Na]^+$: 445.06664; found: 445.06670.

**Alkenyl iodide 190**

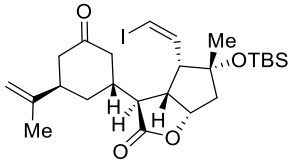


2,2,6,6-Tetramethylpiperidine (320 μL, 1.92 mmol) was added to a solution of lactone **189** (135 mg, 0.32 mmol) in dichloromethane (1.8 mL). The mixture was cooled to 0 °C before triisopropylsilyl trifluoromethansulfonate (340 μL, 1.28 mmol) was added. The mixture was warmed to room temperature and stirred for 4 h. $La(OTf)_3$ (18.7 mg, 0.032 mmol) and *(R)*-norcarvone **96** (109 mg, 0.80 mmol) were successively added and stirring continued at room temperature for 17 h. The mixture was filtered through a pad of Celite®, then rinsed with dichloromethane (5 x 5 mL), and the combined filtrates were concentrated under reduced pressure. The residue was triturated with cyclohexane (5 mL), the resulting precipitate was filtered off, and the remaining solution was concentrated under reduced pressure. The crude product was purified by flash chromatography on silica, eluting with a gradient of 0-2% *tert*-butyl methyl ether in cyclohexane, to afford the silyl enol ether as a grey solid.

In a plastic vial, HF·pyr (70% w/w, 1 mL) was added to a solution of this product in THF (3 mL) at room temperature. The resulting mixture was stirred for 4 h before it was poured into a sat. aq. $NaHCO_3$ (50 mL) at 0 °C then warmed to room temperature. The aqueous phase was extracted with EtOAc (3 x 25 mL), the combined organic layers were washed with brine (15 mL), dried over $MgSO_4$, filtered and concentrated. The residue was purified by flash chromatography on silica, eluting with 7.5% acetone in hexanes, to give the title compound **190** as a yellow oil (81 mg, 35% yield over two steps).

$[\alpha]_D^{20}$ = +57.8 (c = 0.58, $CHCl_3$). $^1H$ NMR (600 MHz, $CDCl_3$) δ = 6.59 (dd, *J* = 7.5, 0.9 Hz, 1H), 6.48 (dd, *J* = 8.2, 7.5 Hz, 1H), 4.98 (ddd, *J* = 8.0, 7.3, 0.7 Hz, 1H), 4.89 (q, *J* = 1.2 Hz, 1H), 4.66 (dt, *J* = 1.6, 0.8 Hz, 1H), 3.03 (td, *J* = 8.6, 5.6 Hz, 1H), 2.82 – 2.75 (m, 1H), 2.71 (dd, *J* = 5.7, 4.3 Hz, 1H), 2.73 – 2.67 (m, 1H), 2.66 (ddd, *J* = 15.1, 12.3,

0.9 Hz, 1H), 2.59 (ddt, *J* = 15.1, 3.3, 1.9 Hz, 1H), 2.45 (ddd, *J* = 15.2, 6.2, 1.0 Hz, 1H), 2.34 (d, *J* = 15.3 Hz, 1H), 2.28 (ddt, *J* = 15.1, 4.1, 2.0 Hz, 1H), 2.04 (tq, *J* = 12.0, 4.3 Hz, 1H), 1.98 (dtt, *J* = 13.6, 3.8, 2.0 Hz, 1H), 1.93 (ddd, *J* = 15.3, 7.2, 0.5 Hz, 1H), 1.74 (dt, *J* = 1.4, 0.7 Hz, 3H), 1.69 (ddd, *J* = 13.5, 11.9, 4.7 Hz, 1H), 1.30 (s, 3H), 0.86 (s, 9H), 0.12 (s, 3H), 0.11 (s, 3H); $^{13}$C NMR (151 MHz, $CDCl_3$) δ = 210.6, 177.7, 145.8, 137.3, 113.3, 87.4, 83.4, 82.4, 58.6, 47.6, 45.8, 45.5, 45.0, 44.6, 40.2, 35.2, 28.9, 26.7, 26.2, 22.5, 18.5, -1.7, -2.2; IR (film) ν/ cm$^{-1}$: 2953, 2930, 2856, 1759, 1712, 1470, 1378, 1303, 1259, 1224, 1187, 1116, 1101, 1001, 901, 836, 779; HRMS (ESI): calcd for $C_{25}H_{39}IO_4SiNa$ $[M+Na]^+$ : 581.15542; found: 581.15546.

**Alcohol 172**

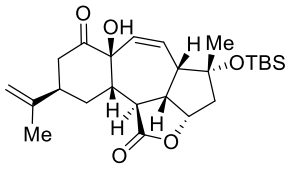


**Intramolecular alkenylation/isomerization**: Potassium *tert*-butoxide (41 mg, 0.37 mmol) was added to a solution of 2,6-dimethylphenol (52 mg, 0.43 mmol) in toluene (60 mL) at room temperature. The resulting suspension was stirred for 1 h before a solution of alkenyl iodide **190** (68 mg, 0.12 mmol) in toluene (2 mL) (rinsing the flask with toluene (2 x 2 mL)) and $Pd(PPh_3)_4$ (28 mg, 0.024 mmol) were successively added. The mixture was heated to 60 °C (bath temperature) for 90 min before the mixture was cooled to room temperature and filtered through a pad of silica, rinsing with EtOAc (5 x 20 mL). The combined filtrates were concentrated under reduced pressure and the residue was purified by flash chromatography on silica, eluting with a gradient of 0-30% EtOAc in pentane, to afford enone **192** as a red solid and alcohol **193** (8.6 mg, 16% yield) as a beige gum.

**Hydroxylation**: 1,8-Diazabicyclo[5.4.0]undec-7-ene (73 μL, 0.487 mmol) was added to a solution of trimethyl phosphite (43.1 μL, 0.365 mmol) in acetonitrile (2 mL). The solution was purged with $O_2$ for 5 min. This solution was then transferred *via* canula into the reaction flask that had been charged with the crude enone **192** and purged with $O_2$ for 5 min. The resulting mixture was stirred at room

temperature under $O_2$ atmosphere (balloon) for 42 h. The mixture was poured into a sat. aq. HCl (1 mL) at 0 °C, which was extracted with EtOAc (3 x 10 mL). The combined organic layers were washed with brine (10 mL), dried over $MgSO_4$, filtered and concentrated under reduced pressure. The residue was purified by flash chromatography on silica, eluting with a gradient of 0-20% EtOAc in pentane, to afford the desired product **172** as a colourless gum (17.6 mg, 32% yield over two steps).

$[\alpha]_D^{20}$ = +53.4 (c = 0.22, $CHCl_3$). $^1$H NMR (600 MHz, $CDCl_3$) δ = 5.93 (ddd, *J* = 11.6, 2.2, 0.7 Hz, 1H), 5.59 (dd, *J* = 11.6, 2.7 Hz, 1H), 4.88 (td, *J* = 8.8, 2.2 Hz, 1H), 4.88 (q, *J* = 1.2 Hz, 1H), 4.69 (dt, *J* = 1.7, 0.8 Hz, 1H), 4.43 (s, 1H), 4.13 (ddd, *J* = 12.1, 9.2, 7.9 Hz, 1H), 3.46 (dd, *J* = 11.3, 10.4 Hz, 1H), 2.86 (dd, *J* = 11.8, 2.6 Hz, 1H), 2.81 – 2.75 (m, 2H), 2.76 – 2.71 (m, 1H), 2.68 (dt, *J* = 7.5, 2.4 Hz, 1H), 2.31 (ddd, *J* = 16.0, 2.2, 0.6 Hz, 1H), 2.25 (td, *J* = 11.0, 4.4 Hz, 1H), 2.14 (dd, *J* = 15.9, 8.8 Hz, 1H), 1.80 (dt, *J* = 1.4, 0.6 Hz, 3H), 1.66 (ddd, *J* = 14.9, 11.5, 3.8 Hz, 1H), 1.43 (s, 3H), 0.87 (s, 9H), 0.15 (s, 3H), 0.11 (s, 3H); $^{13}$C NMR (151 MHz, $CDCl_3$) δ = 212.5, 178.6, 145.4, 134.9, 127.4, 112.9, 84.4, 80.7, 78.3, 54.2, 47.9, 45.0, 44.6, 43.3, 41.4, 40.2, 31.6, 28.9, 26.0, 22.2, 18.3, -2.0, -2.5; IR (film) ν/cm$^{-1}$: 3468, 2954, 2929, 2857, 1765, 1713, 1644, 1471, 1378, 1338, 1257, 1198, 1142, 1099, 1012, 899, 834, 775, 684; HRMS (ESI): calcd for $C_{25}H_{38}O_5SiNa$ $[M+Na]^+$ : 469.23850; found: 469.23807.

**Alcohol 193**

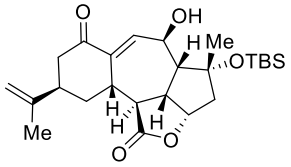


$^1$H NMR (400 MHz, $CDCl_3$) δ = 6.43 (dd, *J* = 2.9, 1.9 Hz, 1H), 5.07 (dq, *J* = 9.6, 3.2 Hz, 1H), 4.88 (t, *J* = 1.5 Hz, 1H), 4.79 (ddd, *J* = 8.4, 7.5, 6.6 Hz, 1H), 4.73 (q, *J* = 1.1 Hz, 1H), 3.18 (t, *J* = 11.6 Hz, 1H), 3.00 (dtd, *J* = 13.6, 5.1, 1.6 Hz, 1H), 2.87 – 2.64 (m, 5H), 2.57 – 2.44 (m, 1H), 2.33 – 2.19 (m, 3H), 1.81 (s, 3H), 1.80 – 1.74 (m, 1H), 1.46 (s, 3H), 0.93 (s, 9H), 0.21 (d, *J* = 1.0 Hz, 6H); HRMS (ESI): calcd for $C_{25}H_{38}O_5SiNa$ $[M+Na]^+$: 469.23850; found: 469.23819.

**Enone 192**

For analytical purposes, **192** and **194** were prepared as follow:

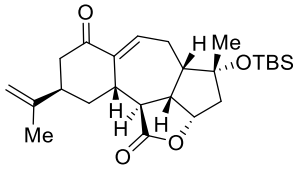


Potassium *tert*-butoxide (4.5 mg, 40 μmol) was added to a solution of phenol (4.3 mg, 46 μmol) in toluene (13 mL) at room temperature. The resulting suspension was stirred for 30 min before a solution of alkenyl iodide **190** (14 mg, 25 μmol) in toluene (0.5 mL) (rinsing the flask with toluene (2 x 0.5 mL)) and $Pd(PPh_3)_4$ (7 mg, 6.1 μmol) were successively added. The mixture was heated to 60 °C (bath temperature) for 90 min before the mixture was cooled to room temperature and filtered through a pad of silica, rinsing with EtOAc (5 x 10 mL). The combined filtrates were concentrated under reduced pressure and the residue was purified by flash chromatography on silica, eluting with a gradient of 0-20% EtOAc in pentane, to afford enone **192** as a red solid and alkene **194** as a red solid.

To afford analytically pure samples, both compounds were purified separately.

The enone fraction was purified by HPLC [(150 mm YMC Triart C18 5 μm, 10.0 mm ∅, MeOH in $H_2O$ = 80:20 isocratic over 20 min, 4.7 mL/min, $\lambda$ = 220 nm, t = 11.4 min)] to give pure enone **192** as a white solid (1.2 mg, 11% yield). The alkene fraction was purified by HPLC [(150 mm YMC Triart C18 5 μm, 10.0 mm ∅, MeOH in $H_2O$ = 80:20 isocratic over 20 min, 4.7 mL/min, $\lambda$ = 220 nm, t = 12.5 min)] to give pure alkene **194** as a white solid (0.3 mg, 3% yield) (the data of the alkene are compiled below).

$[\alpha]_D^{20}$ = +19.9 (c = 0.12, $CHCl_3$). $^1H$ NMR (600 MHz, $CDCl_3$) δ = 6.64 (ddd, *J* = 9.6, 3.9, 1.8 Hz, 1H), 4.87 (td, *J* = 8.5, 1.8 Hz, 1H), 4.84 (h, *J* = 1.4 Hz, 1H), 4.70 (tt, *J* = 1.3, 0.7 Hz, 1H), 3.60 (dd, *J* = 11.9, 10.2 Hz, 1H), 2.95 (dtd, *J* = 13.6, 5.2, 1.4 Hz, 1H), 2.83 (dt, *J* = 10.2, 8.3 Hz, 1H), 2.79 (ddt, *J* = 15.9, 10.1, 3.8 Hz, 1H), 2.72 (ddd, *J* = 15.7, 7.3,

1.4 Hz, 1H), 2.68 – 2.61 (m, 2H), 2.45 (dd, *J* = 15.7, 5.1 Hz, 1H), 2.35 (ddd, *J* = 15.8, 1.8, 0.5 Hz, 1H), 2.30 (ddd, *J* = 15.8, 9.5, 7.5 Hz, 1H), 2.21 (dt, *J* = 10.1, 7.8 Hz, 1H), 2.02 (dd, *J* = 15.7, 8.4 Hz, 1H), 1.78 (dt, *J* = 1.3, 0.6 Hz, 3H), 1.72 (ddd, *J* = 13.6, 11.9, 6.7 Hz, 1H), 1.30 (s, 3H), 0.89 (s, 9H), 0.14 (s, 3H), 0.14 (s, 3H); $^{13}$C NMR (151 MHz, $CDCl_3$) δ = 203.3, 177.7, 147.3, 142.0, 134.0, 111.6, 82.8, 80.3, 51.2, 48.5, 47.9, 44.1, 42.0, 40.2, 38.8, 31.3, 27.8, 26.0, 21.5, 21.3, 18.4, -1.8, -2.5; IR (film) ν/cm$^{-1}$ : 2956, 2928, 2856, 1764, 1711, 1461, 1377, 1335, 1256, 1221, 1194, 1164, 1140, 1100, 1011, 892, 836, 775, 679; HRMS (ESI): calcd for $C_{25}H_{38}O_4SiNa$ [M+Na]$^+$: 453.24316; found: 453.24299.

**Alkene 194**

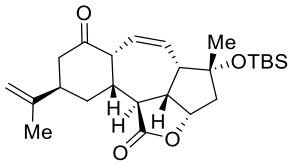


$[\alpha]_D^{20}$ = +24.0 (c = 0.03, $CHCl_3$). $^1$H NMR (600 MHz, $CDCl_3$) δ = 5.75 (dt, *J* = 11.1, 2.2 Hz, 1H), 5.39 (ddd, *J* = 11.2, 5.5, 2.8 Hz, 1H), 4.90 (td, *J* = 8.7, 1.7 Hz, 1H), 4.87 (q, *J* = 1.3 Hz, 1H), 4.69 (dt, *J* = 1.8, 0.9 Hz, 1H), 3.50 (t, *J* = 11.0 Hz, 1H), 3.37 – 3.32 (m, 1H), 3.16 (dt, *J* = 11.1, 8.1 Hz, 1H), 2.77 (br m, 1H), 2.71 – 2.62 (m, 3H), 2.60 (dq, *J* = 7.7, 2.6 Hz, 1H), 2.36 – 2.28 (m, 1H), 2.26 (dd, *J* = 16.0, 1.8 Hz, 1H), 2.06 (dd, *J* = 16.0, 8.9 Hz, 1H), 1.81 (dt, *J* = 1.5, 0.8 Hz, 3H), 1.58 (td, *J* = 13.2, 4.5 Hz, 1H), 1.42 (s, 3H), 0.87 (s, 9H), 0.14 (s, 3H), 0.11 (s, 3H); $^{13}$C NMR (151 MHz, $CDCl_3$) δ = 212.5, 178.6, 146.5, 131.2, 124.3, 112.5, 84.7, 81.0, 54.4, 51.4, 47.3, 44.8, 44.0, 42.6, 40.5, 37.3, 29.0, 28.5, 25.9, 22.2, 18.3, -1.9, -2.5; IR (film) ν/cm$^{-1}$ : 2956, 2928, 2856, 1764, 1711, 1461, 1377, 1335, 1256, 1221, 1194, 1164, 1140, 1100, 1011, 892, 836, 775, 679; HRMS (ESI): calcd for $C_{25}H_{38}O_4SiNa$ [M+Na]$^+$: 453.24316; found: 453.24299.

**Alcohol 171**

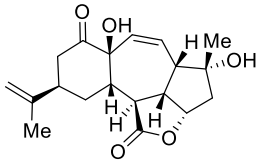


Water (6.7 μL, 0.37 mmol) was added to a solution of tris(dimethylamino)sulfonium difluorotrimethylsilicate (14.5 mg, 52 μmol) in *N,N*-dimethylformamide (0.4 mL). Then that solution was added to a solution of alcohol **172** (16.5 mg, 37 μmol) in *N,N*-dimethylformamide (0.4 mL) at room temperature. The resulting mixture was heated to 80 °C (bath temperature) for 90 min, then cooled to room temperature. Sat. aq. of $NaHCO_3$ (1 mL) was added to the mixture, which was then extracted with EtOAc (3 x 5 mL). The combined organic layers were washed with brine (3 x 5 mL), dried over $MgSO_4$, filtered and concentrated under reduced pressure. The residue was purified by flash chromatography on silica, eluting with 50% EtOAc in pentane, to afford the desired product **171** as a white solid (8.6 mg, 70% yield).

$[\alpha]_D^{20}$ = +35.1 (c = 0.13, $CHCl_3$). $^1$H NMR (600 MHz, $CDCl_3$) δ = 5.92 (dd, *J* = 11.6, 2.3 Hz, 1H), 5.69 (dd, *J* = 11.6, 2.6 Hz, 1H), 4.92 – 4.88 (m, 1H), 4.89 (ddd, *J* = 8.6, 6.5, 4.8 Hz, 1H), 4.71 (s, 1H), 4.47 (s, 1H), 4.17 (ddd, *J* = 11.6, 8.6, 7.2 Hz, 1H), 3.54 (dd, *J* = 11.6, 10.2 Hz, 1H), 2.93 – 2.87 (m, 1H), 2.81 – 2.73 (m, 4H), 2.28 (ddd, *J* = 11.4, 10.1, 4.1 Hz, 1H), 2.24 – 2.21 (m, 2H), 1.82 (dd, *J* = 1.4, 0.7 Hz, 3H), 1.67 (ddd, *J* = 14.2, 10.7, 3.4 Hz, 1H), 1.44 (s, 3H); $^{13}$C NMR (151 MHz, $CDCl_3$) δ = 212.3, 178.7, 145.3, 133.0, 129.6, 113.0, 81.9, 80.2, 78.3, 52.2, 48.0, 44.8, 44.6, 43.8, 41.2, 40.3, 32.1, 29.0, 22.3; IR (film) ν/cm$^{-1}$: 3464, 2960, 2923, 2853, 1753, 1711, 1644, 1452, 1378, 1313, 1265, 1238, 1200, 1173, 1158, 1173, 1011, 985, 899, 801, 756; HRMS (ESI): calcd for $C_{19}H_{24}O_5Na$ $[M+Na]^+$: 355.15159; found: 355.15158.

## 5.3 Comparison of spectral data of natural products and synthetic samples

### 5.3.1 (-)-Scabrolide B

Note: In both of the reported data for scabrolide B, the respective protons of C11 and C12, were interchanged.[26, 30] This was confirmed by COSY. The positions were corrected in our table.

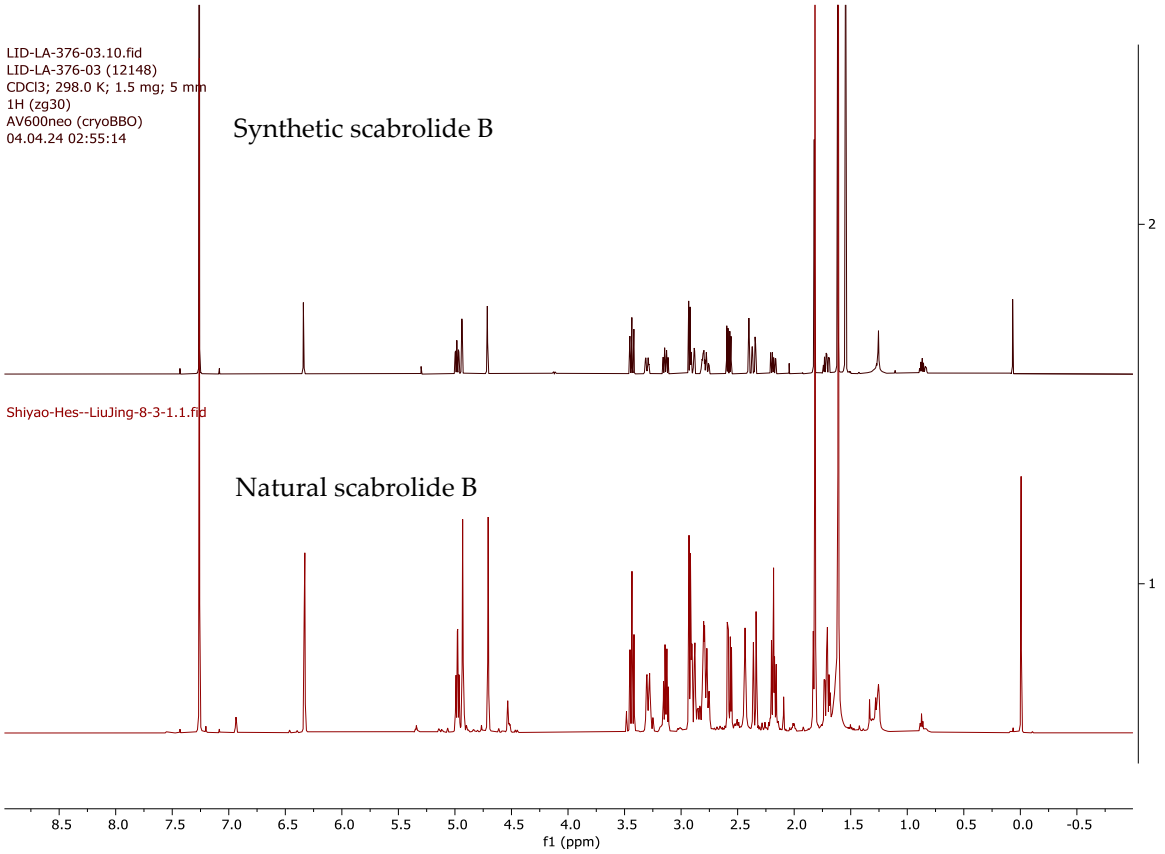


**Figure 5.1.** Visual comparison of $^{1}H$ NMR between natural and synthetic scabrolide B. Top: synthetic scabrolide B– bottom: natural scabrolide B measured by He *et al.*[30]

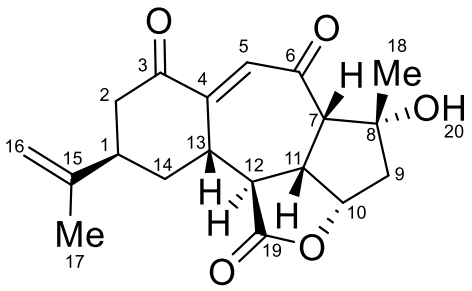


**Table 5.1.** Comparison of the $^{1}H$ NMR data ($CDCl_3$) of natural and synthetic scabrolide B; numbering scheme as shown in the insert.

| Position | Reported[26] δ (ppm) [*J* (Hz), 400 MHz] | Reported[30] | This work | Δδ (ppm) |
|---|---|---|---|---|
| | | δ (ppm) [*J* (Hz), 600 MHz] | | |
| **1** | 2.81 (m) | 2.80 (m) | 2.81 (m) | 0.01 |
| **2a** | 2.90 (ddd, 16.0, 4.0, 2.5) | 2.89 (dt, 16.4, 3.6) | 2.90 (ddd, 16.2, 3.9, 2.3) | 0.01 |
| **2b** | 2.60 (dd, 16.0, 6.0) | 2.57 (dd, 16.2, 6.3) | 2.58 (dd, 16.2, 6.3) | 0.01 |
| **3** | | | | |
| **4** | | | | |
| **5** | 6.34 (d, 3.0) | 6.33 (d, 2.7) | 6.34 (d, 2.8) | 0.00 |
| **6** | | | | |
| **7** | 2.93 (d, 7.2) | 2.92 (d, 7.5) | 2.93 (d, 8.1) | 0.01 |
| **8** | | | | |
| **9a** | 3.36 (dd, 16.0, 2.5) | 2.35 (dd, 16.2, 2.3) | 2.36 (dd, 16.2, 2.3) | 0.01 |
| **9b** | 2.21 (dd, 16.0, 9.0, 1.5) | 2.19 (m) | 2.19 (ddd, 16.2, 9.2, 2.0) | 0.00 |
| **10** | 4.98 (td, 9.0, 2.5) | 4.98 (td, 8.8, 2.3) | 4.98 (ddd, 9.2, 8.1, 2.3) | 0.00 |
| **11** | 3.14 (dt, 10.5, 7.8) | 3.13 (m) | 3.14 (dt, 10.2, 8.1) | 0.01 |
| **12** | 3.45 (t, 10.5) | 3.43 (t, 10.6) | 3.44 (dd, 11.0, 10.2) | 0.01 |
| **13** | 2.75 (m) | 2.76 (m) | 2.78 (dddd, 12.3, 11.0, 4.1, 2.8) | 0.02 |
| **14a** | 3.30 (dtd, 10.0, 4.0, 2.5) | 3.29 (dq, 13.9, 2.3) | 3.30 (dtd, 13.8, 4.1, 2.3) | 0.01 |
| **14b** | 1.71 (tdd, 10.0, 5.0, 1.2) | 1.71 (td, 13.5, 5.2) | 1.71 (ddd, 13.8, 12.3, 5.2) | 0.00 |
| **15** | | | | |
| **16a** | 4.95 (s) | 4.93 (s) | 4.94 (q, 1.2) | 0.01 |
| **16b** | 4.72 (s) | 4.71 (s) | 4.71 (dt, 1.6, 0.8) | 0.00 |
| **17** | 1.83 (s) | 1.82 (s) | 1.82 (dt, 1.2, 0.8) | 0.00 |
| **18** | 1.63 (s) | 1.61 (s) | 1.62 (s) | 0.01 |
| **19** | | | | |
| **20** | | | 2.40 (d, 2.0) | |

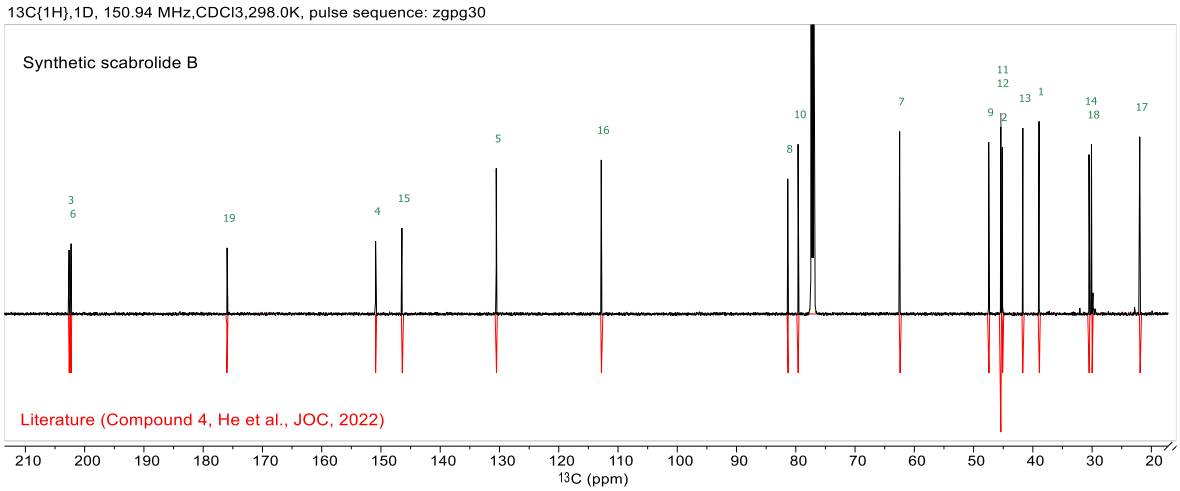


**Figure 5.2.** Visual comparison of $^{13}C$ NMR between natural and synthetic scabrolide B. Top: synthetic scabrolide B; bottom: spectrum generated (MestReNova) by converting the literature data[30] into a formal spectrum.

**Table 5.2.** Comparison of the $^{13}C$ NMR data ($CDCl_3$) of natural and synthetic scabrolide B.

| **Position** | **Reported**[26] δ (ppm) [75 MHz] | **Reported**[30] δ (ppm) [150 MHz] | **This work** δ (ppm) [151 MHz] | **Δδ** (ppm) |
|---|---|---|---|---|
| **1** | 38.9 | 38.9 | 39.0 | 0.1 |
| **2** | 45.0 | 45.1 | 45.1 | 0.0 |
| **3** | 202.2 | 202.3 | 202.6 | 0.3 |
| **4** | 130.5 | 150.9 | 150.9 | 0.0 |
| **5** | 150.8 | 130.5 | 130.6 | 0.1 |
| **6** | 202.5 | 202.6 | 202.3 | 0.3 |
| **7** | 62.4 | 62.4 | 62.5 | 0.1 |
| **8** | 81.3 | 81.3 | 81.4 | 0.1 |
| **9** | 47.4 | 47.4 | 47.5 | 0.1 |
| **10** | 79.5 | 79.6 | 79.6 | 0.0 |
| **11** | 45.3 | 45.4 | 45.4 | 0.0 |
| **12** | 45.3 | 45.4 | 45.4 | 0.0 |
| **13** | 41.6 | 41.7 | 41.7 | 0.0 |
| **14** | 30.5 | 30.5 | 30.5 | 0.0 |
| **15** | 146.4 | 146.4 | 146.5 | 0.1 |
| **16** | 112.7 | 112.8 | 112.8 | 0.0 |
| **17** | 21.8 | 21.9 | 22.0 | 0.1 |
| **18** | 30.0 | 30.0 | 30.1 | 0.1 |
| **19** | 175.9 | 176.0 | 176.0 | 0.0 |

### 5.3.2 (-)-Sinuscalide C

Note: In the reported data for sinuscalide C, the carbons C7 and C8 were interchanged.[30] These positions were corrected in our table.

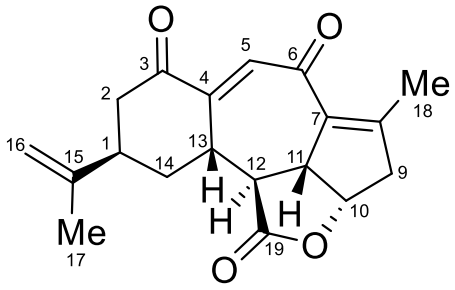


**Table 5.3.** Comparison of the $^{1}H$ NMR data ($CDCl_3$) of natural and synthetic sinuscalide C; numbering scheme as shown in the insert**.**

| Position | Reported[30] | This work | Δδ (ppm) |
|---|---|---|---|
| | δ (ppm) [*J* (Hz), 600 MHz] | | |
| **1** | 2.82 (m) | 2.82 (m) | 0 |
| **2a** | 2.95 (dt, 16.0, 3.0) | 2.95 (ddd, 16.0, 3.6, 2.5) | 0 |
| **2b** | 2.60 (dd, 16.2, 6.5) | 2.60 (dd, 16.0, 6.4) | 0 |
| **3** | | | |
| **4** | | | |
| **5** | 6.47 (d, 2.6) | 6.47 (d, 2.8) | 0 |
| **6** | | | |
| **7** | | | |
| **8** | | | |
| **9a** | 3.14 (m) | 3.14 (ddq, 20.1, 8.8, 1.2) | 0 |
| **9b** | 2.79 (m) | 2.79 (dddd, 20.1, 6.6, 3.2, 1.4) | 0 |
| **10** | 5.16 (td, 8.8, 5.3) | 5.15 (td, 8.8, 5.3) | -0.01 |
| **11** | 3.52 (t, 8.3) | 3.52 (ddp, 10.5, 8.7, 1.5) | 0 |
| **12** | 2.64 (t, 11.1) | 2.64 (dd, 11.3, 10.5) | 0 |
| **13** | 2.90 (m) | 2.90 (dddd, 12.4, 11.3, 4.1, 2.6) | 0 |
| **14a** | 3.25 (dq, 13.8, 3.5) | 3.25 (dtdd, 13.7, 4.2, 2.5, 0.5) | 0 |
| **14b** | 1.72 (td, 13.2, 4.9) | 1.72 (ddd, 13.7, 12.4, 5.0) | 0 |
| **15** | | | |
| **16a** | 4.95 (s) | 4.95 (s) | 0.01 |
| **16b** | 4.75 (s) | 4.75 (dt, 1.6, 0.8) | 0 |
| **17** | 1.85 (s) | 1.84 (dt, 1.4, 0.7) | -0.01 |
| **18** | 2.15 (s) | 2.14 (q, 1.5) | -0.01 |
| **19** | | | |

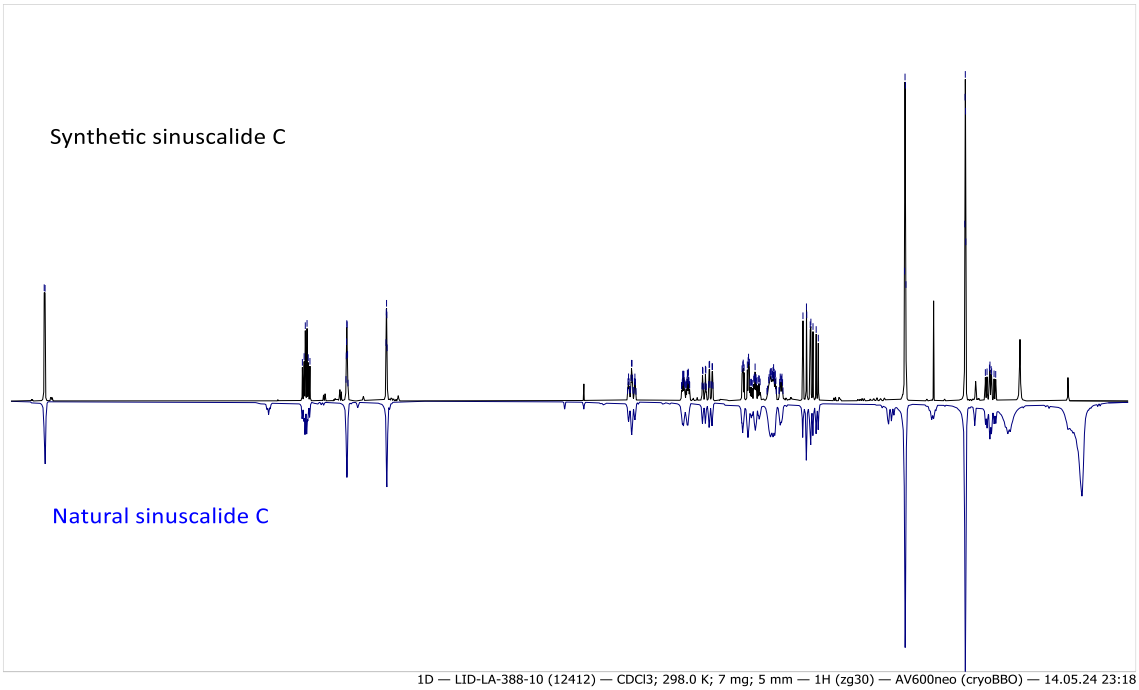


**Figure 5.3.** Visual comparison of $^{1}H$ NMR between natural and synthetic sinuscalide C. Top: synthetic sinuscalide C– bottom: $^{1}H$ NMR measured by He *et al.*[30]

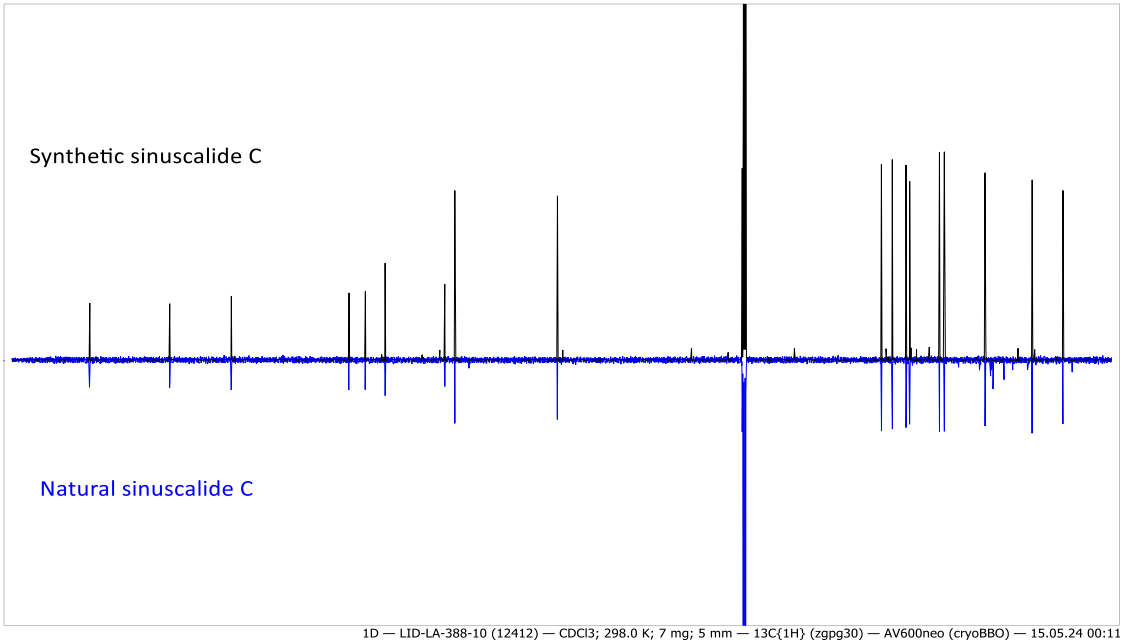


**Figure 5.4.** Visual comparison of $^{13}C$ NMR between natural and synthetic sinuscalide C. Top: synthetic sinuscalide C– bottom: $^{13}C$ NMR measured by He *et al.*[30]

**Table 5.4.** Comparison of the $^{13}C$ NMR data ($CDCl_3$) of natural and synthetic sinuscalide C.

| Position | Reported[30] δ (ppm) [150 MHz] | This work δ (ppm) [151 MHz] | Δδ (ppm) |
|---|---|---|---|
| **1** | 38.8 | 38.9 | 0.1 |
| **2** | 45.5 | 45.5 | 0 |
| **3** | 202.9 | 202.8 | 0.1 |
| **4** | 150.0 | 149.9 | 0.1 |
| **5** | 132.8 | 132.8 | 0 |
| **6** | 187.5 | 187.5 | 0 |
| **7** | 134.7 | 134.7 | 0 |
| **8** | 153.1 | 153.1 | 0 |
| **9** | 46.2 | 46.2 | 0 |
| **10** | 77.6 | 77.6 | 0 |
| **11** | 50.9 | 50.9 | 0 |
| **12** | 48.8 | 48.8 | 0 |
| **13** | 39.7 | 39.7 | 0 |
| **14** | 31.0 | 31.0 | 0 |
| **15** | 146.1 | 146.2 | 0.1 |
| **16** | 113.1 | 113.1 | 0 |
| **17** | 22.0 | 22.0 | 0 |
| **18** | 16.0 | 16.0 | 0 |
| **19** | 175.7 | 175.7 | 0 |

### 5.3.3 (+)-Fragilolide A

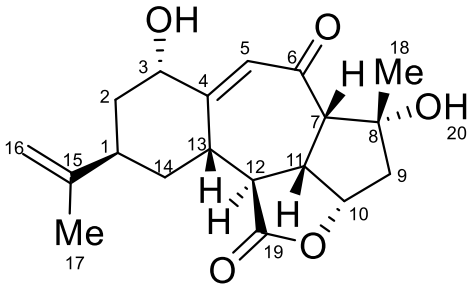


**Table 5.5.** Comparison of the $^{1}H$ NMR data ($CDCl_3$) of natural and fragilolide A; numbering scheme as shown in the insert.

| Position | Reported[28] δ (ppm) [*J* (Hz), 500 MHz] | Reported[41] δ (ppm) [*J* (Hz), 600 MHz] | This work δ (ppm) [*J* (Hz), 600 MHz] | Δδ (ppm) |
|---|---|---|---|---|
| **1** | 2.59 (m) | 2.52 - 2.59 (m) | 2.61 – 2.56 (m) | 0.1 |
| **2a** | 2.58 (m) | 2.52 - 2.59 (m) | 2.55 (ddt, 12.7, 4.8, 2.3) | 0.3 |
| **2b** | 1.64 (m) | 1.63 (m) | 1.62 (td, 12.4, 5.3) | 0.2 |
| **3** | 4.35 (dd, 12.0, 4.4) | 4.32 (m) | 4.32 (ddd, 11.3, 4.7, 1.0) | 0.3 |
| **4** | | | | |
| **5** | 6.27 (s) | 6.27 (s) | 6.25 (td, 1.3, 0.7) | 0.2 |
| **6** | | | | |
| **7** | 2.94 (d, 7.2) | 2.92 (d, 7.4) | 2.92 (d, 7.4) | 0.2 |
| **8** | | | | |
| **9a** | 2.38 (d, 16.0) | 2.35 (dd, 16.2, 2.6) | 2.35 (ddd, 16.2, 2.6, 0.6) | 0.3 |
| **9b** | 2.22 (dd, 16.0, 9.1) | 2.20 (ddd, 16.2, 9.2, 1.9) | 2.20 (dd, 16.2, 9.2) | 0.2 |
| **10** | 4.98 (dd, 9.1, 8.5) | 4.95 (ddd, 9.1, 8.4, 2.6) | 4.95 (ddd, 9.2, 8.4, 2.6) | 0.3 |
| **11** | 3.12 (ddd, 10.0, 8.5, 7.7) | 3.10 (dt, 10.9, 7.9) | 3.10 (dt, 10.6, 8.5) | 0.2 |
| **12** | 3.38 (dd, 11.0, 10.5) | 3.35 (m) | 3.35 (t, 10.8) | 0.3 |
| **13** | 2.48 (dd, 11.9, 10.7) | 2.46 (dddd, 12.7, 11.1, 3.5, 2.0) | 2.46 (dddd, 12.7, 11.0, 3.6, 2.0) | 0.2 |
| **14a** | 3.35 (d, 16.0) | 3.32 (m) | 3.33 (dq, 13.8, 3.1) | 0.3 |
| **14b** | 1.34 (m) | 1.33 (m) | 1.32 (ddd, 13.7, 12.4, 5.0) | 0.2 |
| **15** | | | | |
| **16a** | 5.02 (s) | 5.00 (m) | 5.01 – 4.99 (m) | 0.2 |
| **16b** | 5.02 (s) | 5.00 (m) | 5.01 – 4.99 (m) | 0.2 |
| **17** | 1.87 (s) | 1.85 (s) | 1.85 (p, 0.8) | 0.2 |
| **18** | 1.63 (s) | 1.60 (s) | 1.60 (s) | 0.3 |
| **19** | | | | |

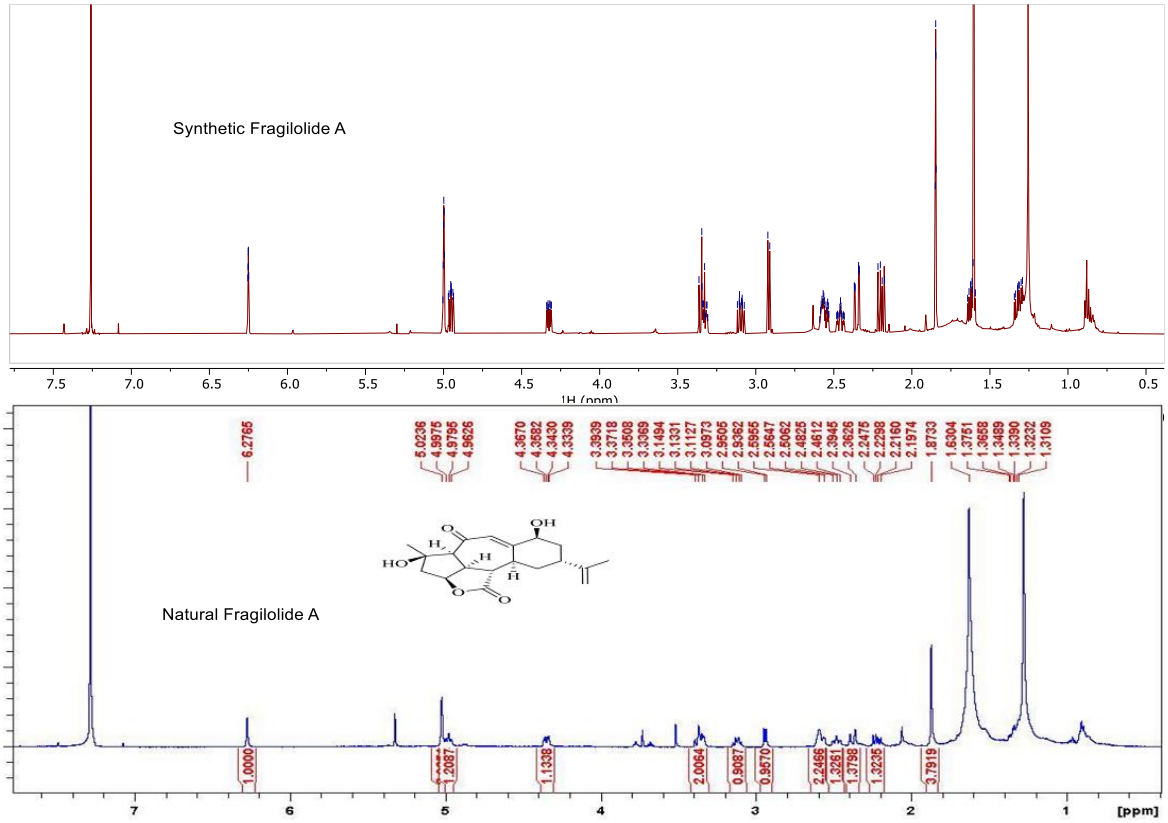


**Figure 5.5.** Visual comparison of $^{1}H$ NMR between natural and synthetic fragilolide A. Top: synthetic fragilolide A– bottom: $^{1}H$ NMR measured by Cheng *et al*.[28]

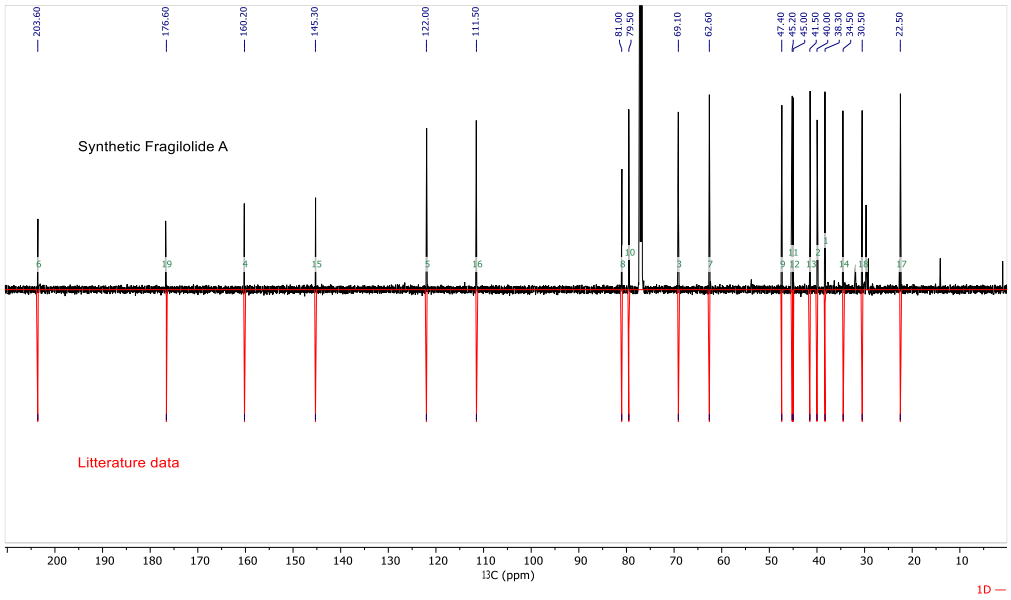


**Figure 5.6.** Visual comparison of $^{13}C$ NMR between natural and synthetic fragilolide A. Top: synthetic fragilolide A; bottom: spectrum generated (MestReNova) by converting the literature data Cheng *et al*.[28] into a formal spectrum.

**Table 5.6.** Comparison of the $^{13}C$ NMR data ($CDCl_3$) of natural and synthetic fragilolide A.

| Position | Reported[28] δ (ppm) [125 MHz] | Reported[41] δ (ppm) [151 MHz] | This work δ (ppm) [151 MHz] | Δδ (ppm) |
|---|---|---|---|---|
| **1** | 38.3 | 38.5 | 38.5 | 0.2 |
| **2** | 40 | 40.1 | 40.1 | 0.1 |
| **3** | 69.1 | 69.3 | 69.3 | 0.2 |
| **4** | 160.2 | 160.4 | 160.4 | 0.2 |
| **5** | 122 | 122.1 | 122.1 | 0.1 |
| **6** | 203.6 | 203.7 | 203.7 | 0.1 |
| **7** | 62.6 | 62.8 | 62.8 | 0.2 |
| **8** | 81 | 81.1 | 81.1 | 0.1 |
| **9** | 47.4 | 47.5 | 47.5 | 0.1 |
| **10** | 79.5 | 79.7 | 79.7 | 0.2 |
| **11** | 45.2 | 45.4 | 45.4 | 0.2 |
| **12** | 45 | 45.1 | 45.1 | 0.1 |
| **13** | 41.5 | 41.6 | 41.6 | 0.1 |
| **14** | 34.5 | 34.7 | 34.7 | 0.2 |
| **15** | 145.3 | 145.4 | 145.4 | 0.1 |
| **16** | 111.5 | 111.7 | 111.7 | 0.2 |
| **17** | 22.5 | 22.6 | 22.6 | 0.1 |
| **18** | 30.5 | 30.7 | 30.7 | 0.2 |
| **19** | 176.6 | 176.9 | 176.9 | 0.3 |

### 5.3.4 (+)-Ineleganolide

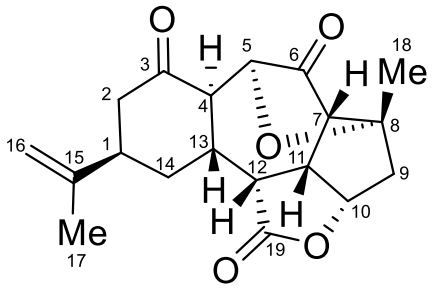

**Table 5.7.** Comparison of the $^{1}H$ NMR data ($CDCl_3$) of natural and synthetic ineleganolide; numbering scheme as shown in the insert.

| Position | Reported[11] | Reported[15] | Reported[16] | This work |
|---|---|---|---|---|
| | δ (ppm) [*J* (Hz), 400 MHz] | | | δ (ppm) [*J* (Hz), 600 MHz] |
| **1** | 2.78 (br s) | 2.79 (br s) | 2.78 (br s) | 2.78 (m) |
| **2a** | 2.63 (m) | 2.64 (m) | 2.64 (m) | 2.67 (dt, 15.2, 2.4) |
| **2b** | 2.63 (m) | 2.64 (m) | 2.64 (m) | 2.58 (ddd, 15.2, 6.5, 1.0) |
| **3** | | | | |
| **4** | 2.70 (d, 13.0) | 2.70 (d, 13.1) | 2.70 (d, 13.0) | 2.70 (dt, 12.4, 1.1) |
| **5** | 5.07 (s) | 5.07 (s) | 5.07 (s) | 5.07 (d, 1.2) |
| **6** | | | | |
| **7** | 2.59 (d, 9.3) | 2.59 (d, 9.3) | 2.59 (d, 9.3) | 2.59 (d, 9.3) |
| **8** | | | | |
| **9a** | 2.10 (dd, 15.6, 7.2) | 2.10 (dd, 15.7, 7.3) | 2.10 (dd, 15.5, 7.3) | 2.10 (dd, 15.5, 7.3) |
| **9b** | 2.51 (d, 15.6) | 2.52 (d, 15.5) | 2.52 (d, 15.6) | 2.52 (d, 15.5) |
| **10** | 5.13 (t, 7.2) | 5.12 (t, 7.3) | 5.12 (t, 7.4) | 5.13 (t, 7.5) |
| **11** | 3.42 (ddd, 12.3, 9.3, 7.2) | 3.42 (ddd, 12.2, 9.3, 7.5) | 3.42 (ddd, 12.1, 9.2, 7.6) | 3.42 (ddd, 12.0, 9.3, 7.6) |
| **12** | 3.02 (dd, 12.3, 2.5) | 3.02 (dd, 12.2, 2.5) | 3.02 (dd, 12.0, 2.4) | 3.02 (dd, 12.0, 2.4) |
| **13** | 2.24 (tt, 13.0, 2.5) | 2.25 (tt, 12.6, 2.7) | 2.25 (tt, 12.4, 2.8) | 2.25 (tt, 12.3, 3.2) |
| **14a** | 3.00 (m) | 3.00 (m) | 3.00 (m) | 3.01 (ddd, 14.0, 12.1, 5.3) |
| **14b** | 1.79 (m) | 1.79 (dq, 13.0, 2.6) | 1.78 (dq, 13.0, 2.8) | 1.78 (dq, 13.9, 2.9) |
| **15** | | | | |
| **16a** | 4.62 (s) | 4.62 (s) | 4.62 (s) | 4.62 (p, 1.4) |
| **16b** | 4.94 (s) | 4.94 (s) | 4.94 (s) | 4.94 (qd, 1.4, 0.7) |
| **17** | 1.71 (s) | 1.71 (s) | 1.71 (s) | 1.71 (dt, 1.4, 0.7) |
| **18** | 1.28 (s) | 1.28 (s) | 1.28 (s) | 1.28 (s) |
| **19** | | | | |

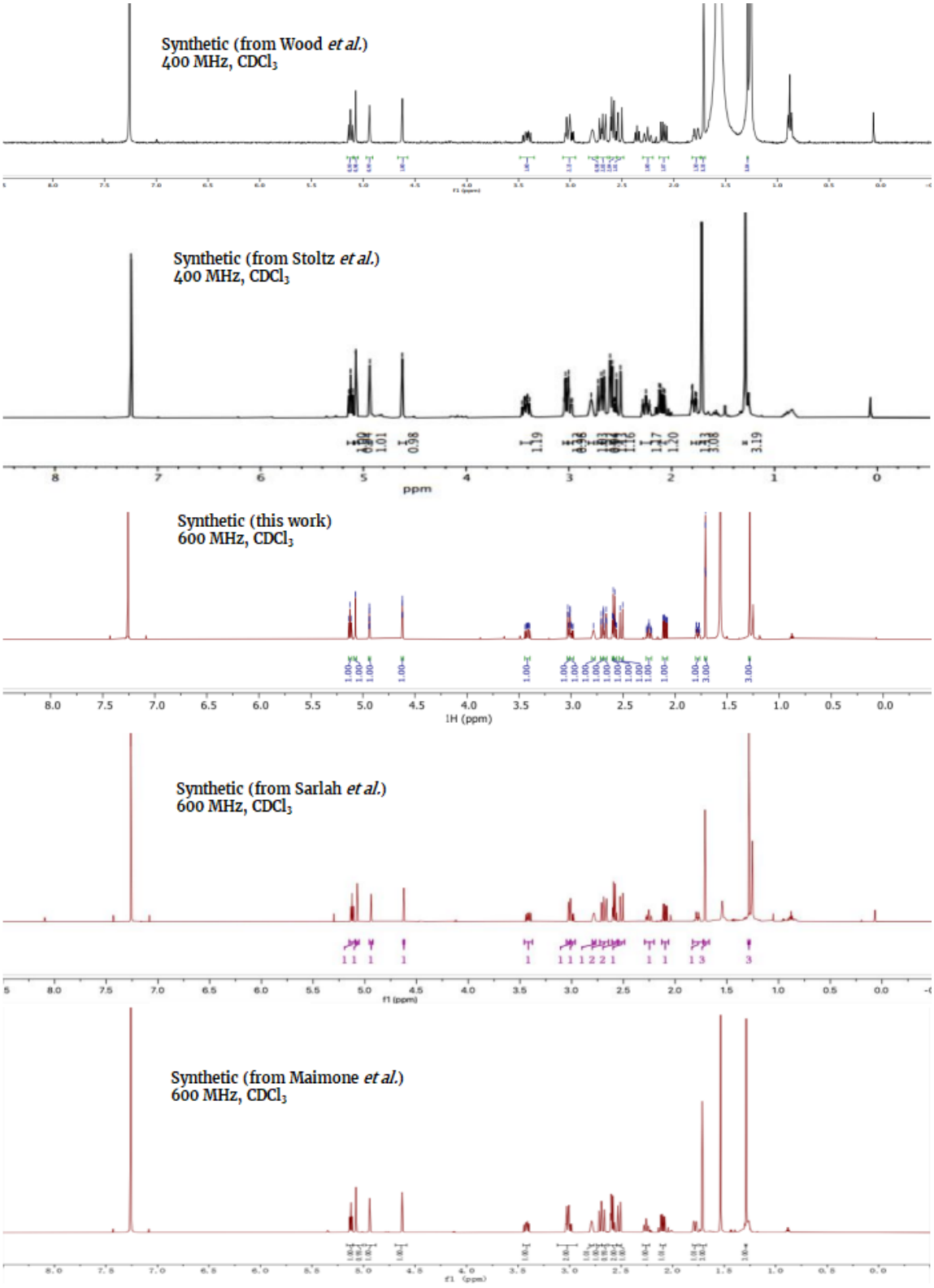


**Figure 5.7.** Comparison of the $^1$H NMR spectra of synthetic (+)-ineleganolide, adapted from Maimone *et al*.[44]

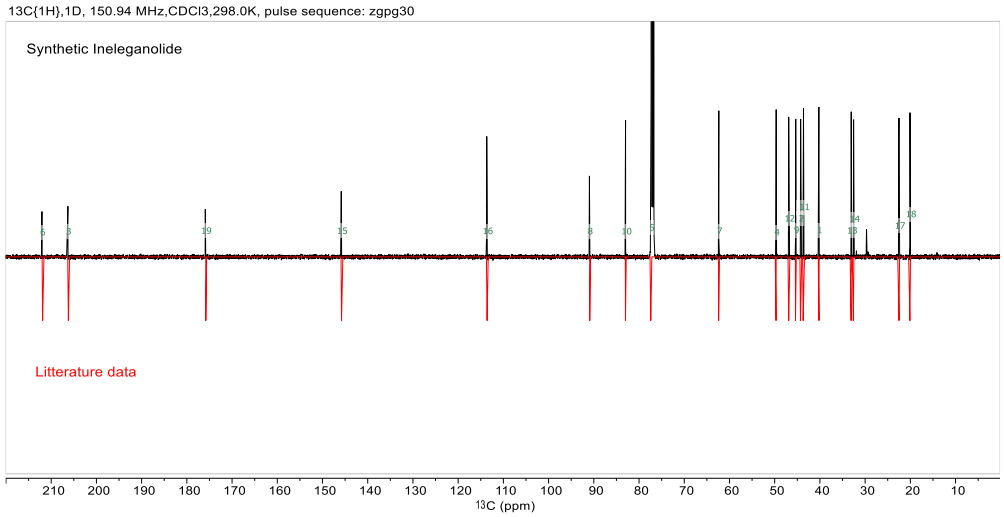


**Figure 5.8.** Visual comparison of $^{13}C$ NMR between natural and synthetic ineleganolide. Top: synthetic ineleganolide; bottom: spectrum generated (MestReNova) by converting the literature data[11] into a formal spectrum.

**Table 5.8.** Comparison of the $^{13}C$ NMR data ($CDCl_3$) of natural and synthetic ineleganolide.

| Position | Reported[11] δ (ppm) [100.6 MHz] | Reported[15] | Reported[16] | This work δ (ppm) [151 MHz] |
|---|---|---|---|---|
| | | δ (ppm) [100 MHz] | | |
| **1** | 40.2 | 40.3 | 40.4 | 40.4 |
| **2** | 44.3 | 44.3 | 44.4 | 44.4 |
| **3** | 206.2 | 206.3 | 206.4 | 206.5 |
| **4** | 49.7 | 49.7 | 49.8 | 49.8 |
| **5** | 77.4 | 77.3 | 77.4 | 77.5 |
| **6** | 211.9 | 212.1 | 212.2 | 212.2 |
| **7** | 62.4 | 62.4 | 62.5 | 62.5 |
| **8** | 90.9 | 91.0 | 91.1 | 91.1 |
| **9** | 45.4 | 45.4 | 45.5 | 45.5 |
| **10** | 83.0 | 83.0 | 83.1 | 83.1 |
| **11** | 43.7 | 43.6 | 43.8 | 43.8 |
| **12** | 46.9 | 46.9 | 47 | 47.1 |
| **13** | 33.1 | 33.1 | 33.2 | 33.2 |
| **14** | 32.6 | 32.6 | 32.7 | 32.7 |
| **15** | 145.8 | 145.9 | 146.0 | 146.0 |
| **16** | 113.6 | 113.7 | 113.8 | 113.8 |
| **17** | 22.5 | 22.5 | 22.7 | 22.7 |
| **18** | 20.1 | 20.1 | 20.2 | 20.2 |
| **19** | 175.8 | 175.9 | 176.1 | 176.1 |

### 5.3.5 (+)-Horiolide

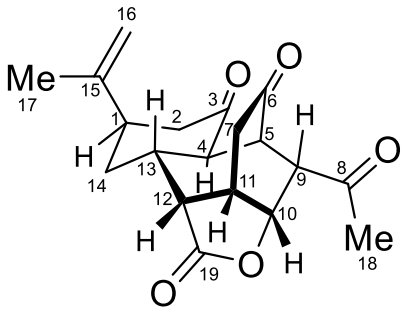


**Table 5.9.** Comparison of the $^{1}H$ NMR data ($CDCl_3$) of natural and synthetic horiolide; numbering scheme as shown in the insert**.**

| **Position** | **Reported**[32] δ (ppm) [*J* (Hz), 500 MHz] | **This work** δ (ppm) [*J* (Hz), 600 MHz] | **Δδ** (ppm) |
|---|---|---|---|
| 1 | 2.78 | 2.80 (bm) | 0.02 |
| 2a | 2.46 | 2.51 (ddd, 15.2, 6.7, 0.9) | 0.05 |
| 2b | 2.71 | 2.74 (ddd, 15.2, 2.5, 2.3) | 0.03 |
| 3 | | | |
| 4 | 2.61 | 2.65 (ddd, 13.6, 0.9, 0.9) | 0.04 |
| 5 | 4.08 | 4.12 (dd, 3.0, 0.9) | 0.04 |
| 6 | | | |
| 7a | 2.20 | 2.52 (dd, 19.7, 2.6) | 0.32 |
| 7b | 2.44 | 2.47 (dd, 19.7, 4.6) | 0.03 |
| 8 | | | |
| 9 | 2.99 (dd, 6, 3) | 3.00 (dd, 6.2, 1.5) | 0.01 |
| 10 | 5.40 (dd, 8, 8) | 5.42 (ddd, 8.3, 6.2, 1.5) | 0.02 |
| 11 | 3.34 | 3.37 (dddd, 8.5, 8.3, 4.6, 2.6) | 0.03 |
| 12 | 2.69 | 2.72 (dd, 8.5, 3.8) | 0.03 |
| 13 | 1.96 | 1.97 (dddd, 13.6, 11.9, 3.8, 3.0) | 0.01 |
| 14a | 2.16 | 2.20 (ddd, 14.0, 11.9, 4.9) | 0.04 |
| 14b | 1.99 | 2.03 (dddd, 14.0, 3.0, 2.7, 2.5) | 0.04 |
| 15 | | | |
| 16a | 4.57 | 4.60 (dq, 0.7, 0.7) | 0.03 |
| 16b | 4.85 | 4.88 (q, 0.7) | 0.03 |
| 17 | 1.65 | 1.70 (ddd, 1.4, 0.7, 0.7) | 0.05 |
| 18 | 2.30 | 2.31 (s) | 0.01 |
| 19 | | | |

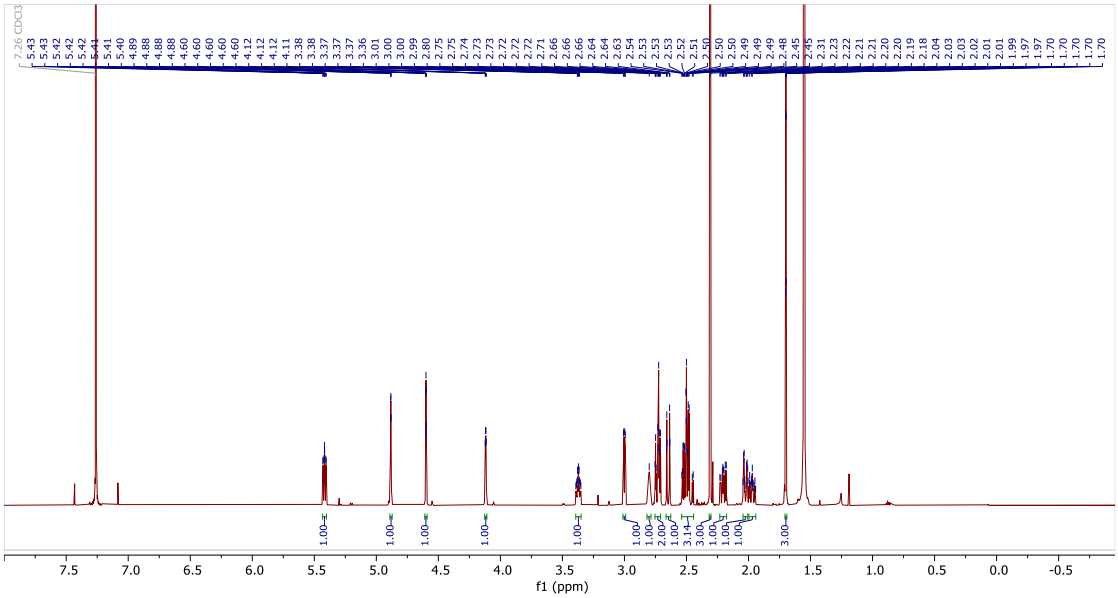


**Figure 5.9.** Copy of the $^{1}H$ NMR spectra of synthetic horiolide in $CDCl_3$.

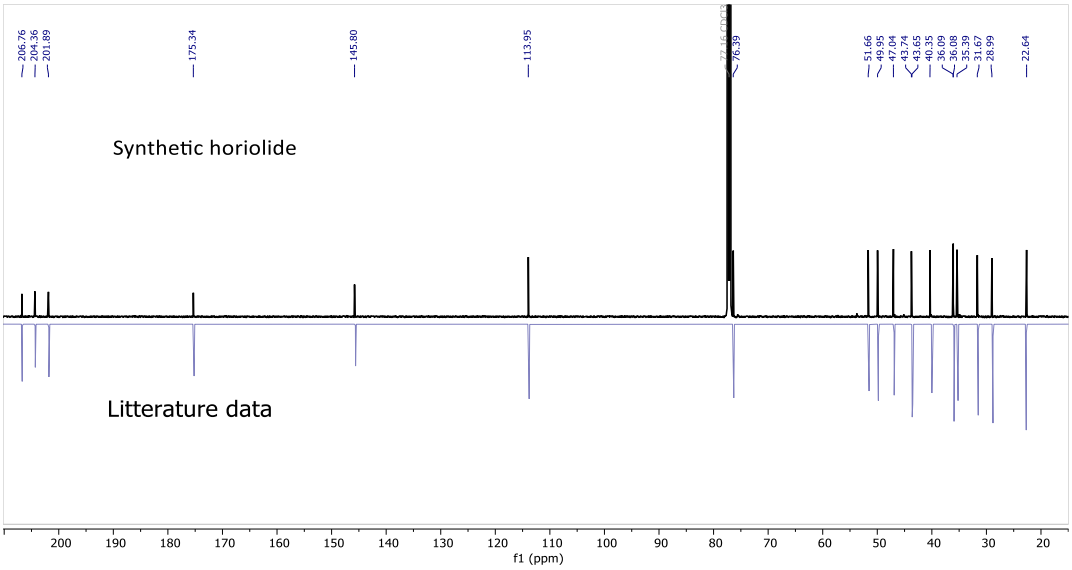


**Figure 5.10.** Visual Comparison of the $^{13}C$ NMR spectra of natural and synthetic horiolide. Top: synthetic horiolide; bottom: spectrum generated (MestReNova) by converting the literature data[32] into a formal spectrum.

**Table 5.10.** Comparison of the $^{13}C$ NMR data ($CDCl_3$) of natural and synthetic horiolide.

| **Position** | **Reported** [32] δ (ppm) [125 MHz] | **This work** δ (ppm) [150 MHz] | **Δδ** (ppm) |
|---|---|---|---|
| **1** | 40.2 | 40.4 | 0.2 |
| **2** | 43.6 | 43.7 | 0.1 |
| **3** | 204.3 | 204.4 | 0.1 |
| **4** | 49.8 | 50.0 | 0.2 |
| **5** | 43.5 | 43.7 | 0.2 |
| **6** | 206.7 | 206.8 | 0.1 |
| **7** | 35.9 | 36.1 | 0.2 |
| **8** | 201.8 | 201.9 | 0.1 |
| **9** | 51.5 | 51.7 | 0.2 |
| **10** | 76.3 | 76.4 | 0.1 |
| **11** | 35.2 | 36.1 | 0.9 |
| **12** | 46.9 | 47.0 | 0.1 |
| **13** | 35.9 | 35.4 | 0.5 |
| **14** | 31.5 | 31.7 | 0.2 |
| **15** | 145.6 | 145.8 | 0.2 |
| **16** | 113.8 | 114.0 | 0.2 |
| **17** | 22.7 | 22.6 | 0.1 |
| **18** | 28.8 | 29.0 | 0.2 |
| **19** | 175.2 | 175.3 | 0.1 |

### 5.3.6 (+)-Kavaranolide

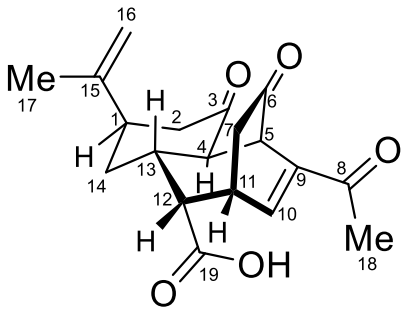


**Table 5.11.** Comparison of the $^{13}C$ NMR data ([$D_6$]-DMSO)) of natural and synthetic kavaranolide; numbering scheme as shown in the insert**.**

| **Position** | **Reported**[33] δ (ppm) [*J* (Hz), 700 MHz] | **This work** δ (ppm) [*J* (Hz), 600 MHz] | **Δδ** (ppm) |
|---|---|---|---|
| **1** | 2.62 (m) | 2.64 (td, 6.2, 3.4) | 0.02 |
| **2a** | 2.50 | 2.45 (m) | 0.05 |
| **2b** | 2.36 (m) | 2.36 (dt, 14.8, 2.6) | 0 |
| **3** | | | |
| **4** | 3.12 (d, 12.6) | 3.15 (d, 12.8) | 0.03 |
| **5** | 4.30 (br s) | 4.31 (m) | 0.01 |
| **6** | | | |
| **7a** | 2.19 | 2.20 (m) | 0.01 |
| **7b** | 2.24 (m) | 2.20 (m) | 0.04 |
| **8** | | | |
| **9** | | | |
| **10** | 7.36 (br d, 7.5) | 7.36 (dd, 7.6, 1.6) | 0 |
| **11** | 3.17 (m) | 3.15 (m) | 0.02 |
| **12** | 2.29 (dd, 7.5, 5.2) | 2.25 (m) | 0.04 |
| **13** | 1.84 (m) | 1.86 (tt, 11.7, 4.1) | 0.02 |
| **14a** | 1.55 (m) | 1.54 (dq, 14.0, 2.9) | 0.01 |
| **14b** | 2.44 (m) | 2.45 (m) | 0.01 |
| **15** | | | |
| **16a** | 4.75 (br s) | 4.75 (q, 1.4) | 0 |
| **16b** | 4.43 (br s) | 4.44 (td, 1.6, 0.8) | 0.01 |
| **17** | 1.63 | 1.64 (dd, 1.4, 0.7) | 0.01 |
| **18** | 2.21 | 2.20 (s) | 0.01 |
| **19** | | | |

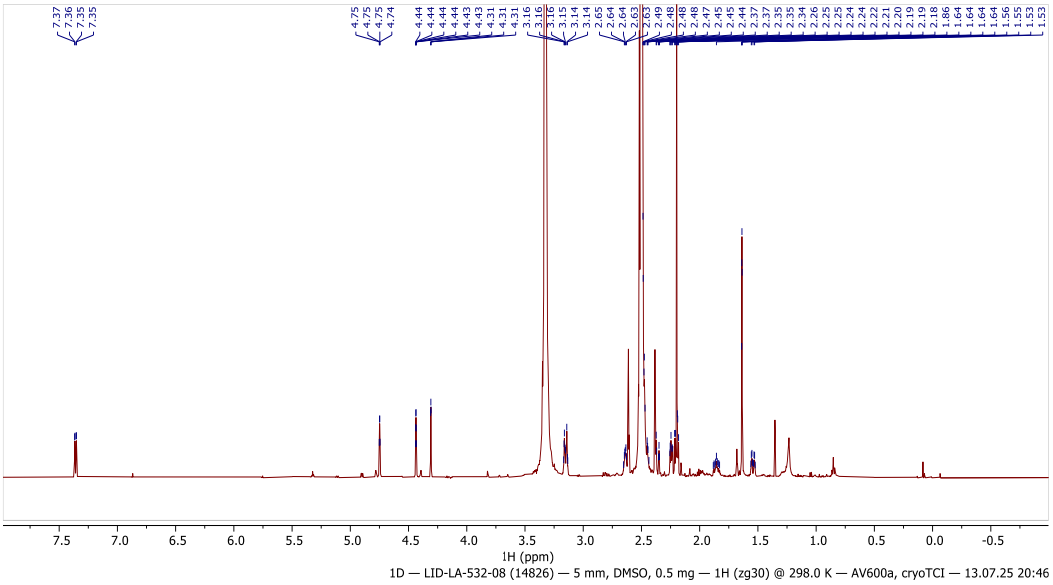


**Figure 5.11.** Copy of the $^{1}H$ NMR spectra of synthetic kavaranolide in [$D_6$]-DMSO.

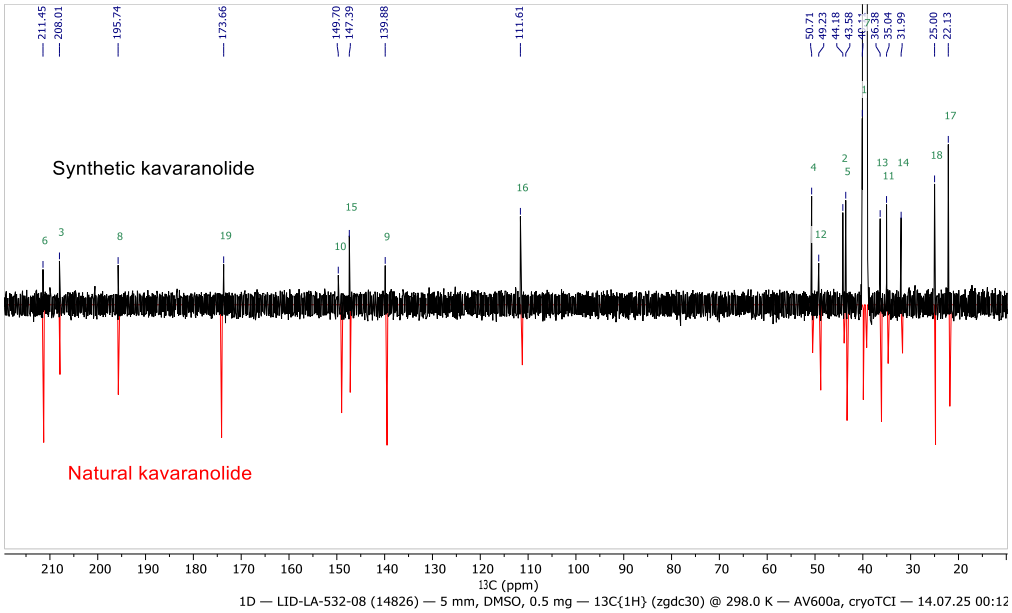


**Figure 5.12.** Visual comparison of the $^{13}C$ NMR spectra of natural and synthetic kavaranolide. Top: synthetic kavaranolide; bottom: spectrum generated (MestReNova) by converting the literature data[33] into a formal spectrum.

**Table 5.12.** Comparison of the $^{13}C$ NMR data ([$D_6$]-DMSO) of natural and synthetic kavaranolide.

| **Position** | **Reported**[33] δ (ppm) [175 MHz] | **This work** δ (ppm) [151 MHz] | **Δδ** (ppm) |
|---|---|---|---|
| **1** | 39.9 | 40.1 | 0.2 |
| **2** | 43.9 | 44.2 | 0.3 |
| **3** | 207.9 | 208.0 | 0.1 |
| **4** | 50.5 | 50.7 | 0.2 |
| **5** | 43.3 | 43.6 | 0.3 |
| **6** | 211.3 | 211.5 | 0.2 |
| **7** | 39.2 | 39.4 | 0.2 |
| **8** | 195.7 | 195.7 | 0 |
| **9** | 139.5 | 139.9 | 0.4 |
| **10** | 149.0 | 149.7 | 0.7 |
| **11** | 34.7 | 35.0 | 0.3 |
| **12** | 48.8 | 49.2 | 0.4 |
| **13** | 36.1 | 36.4 | 0.3 |
| **14** | 31.7 | 32.0 | 0.3 |
| **15** | 147.2 | 147.4 | 0.2 |
| **16** | 111.2 | 111.6 | 0.4 |
| **17** | 21.8 | 22.1 | 0.3 |
| **18** | 24.8 | 25.0 | 0.2 |
| **19** | 174.1 | 173.7 | 0.4 |

## 5.4 Supporting crystallographic data

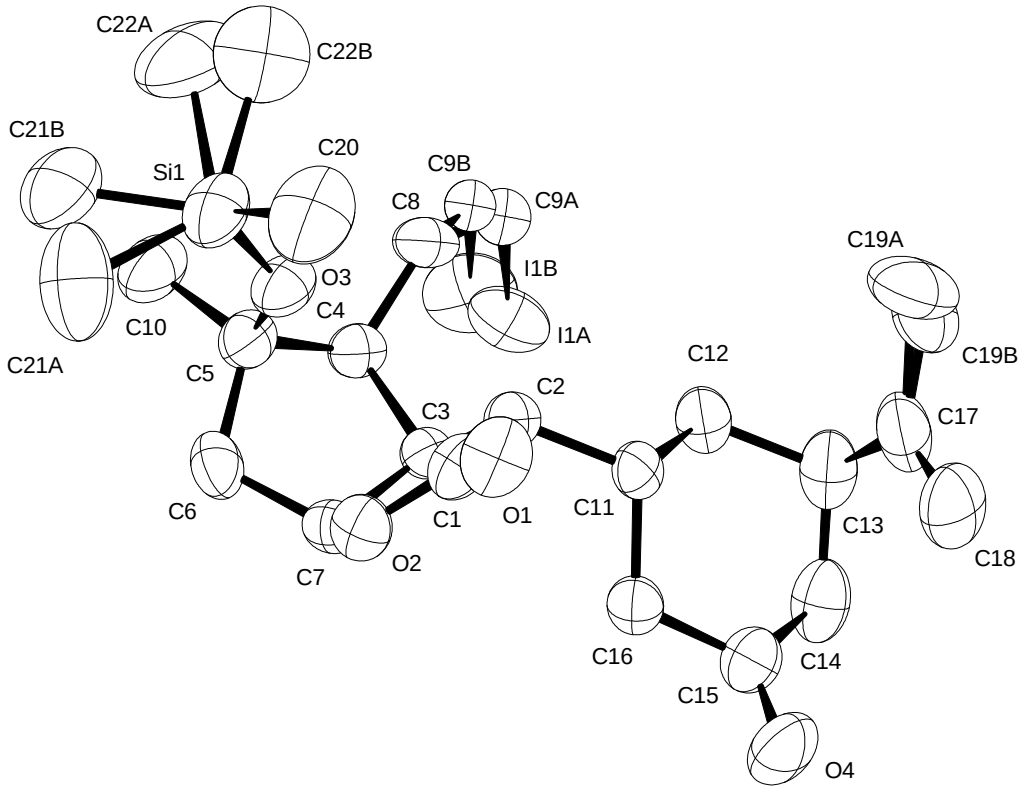


**Figure 5.13.** Structure of compound **151** in the solid state (crystallographic numbering scheme).

**X-ray crystal structure analysis of compound 151**: $C_{22}$ $H_{34}$ I $O_4$ Si, $M_r$ = 517.48 g · mol$^{-1}$, colourless plate, crystal size 0.110 x 0.104 x 0.021 mm$^3$, orthorhombic, space group $P2_12_12_1$ [19], $a$ = 9.7885(13) Å, $b$ = 10.6475(14) Å, $c$ = 23.806(3) Å, $V$ = 2481.2(6) Å$^3$, $T$ = 150(2) K, $Z$ = 4, $D_{calc}$ = 1.385 g · cm$^3$, $\lambda$ = 0.71073 Å, $\mu$(*Mo-K*$_\alpha$) = 1.361 mm$^{-1}$, analytical absorption correction ($T_{min}$ = 0.87, $T_{max}$ = 1.00), Bruker-AXS D8 Venture diffractometer with Photon-II detector and IμS micro focus X-ray source, 2.095 < $\theta$ < 28.699°, 74135 measured reflections, 6415 independent reflections, 4127 reflections with $I > 2\sigma(I)$, $R_{int}$ = 0.1007, 299 parameters, $S$ = 1.016, absolute structure parameter = 0.010(13), residual electron density +0.4 (1.18 Å from I1A) / –0.4 (1.09 Å from C9A) e · Å$^{-3}$. The structure was solved by *SHELXT* and refined by full-matrix least-squares (*SHELXL*) against $F^2$ to $R_1$ = 0.047 [$I > 2\sigma(I)$], $wR_2$ = 0.118. **CCDC-2366849**

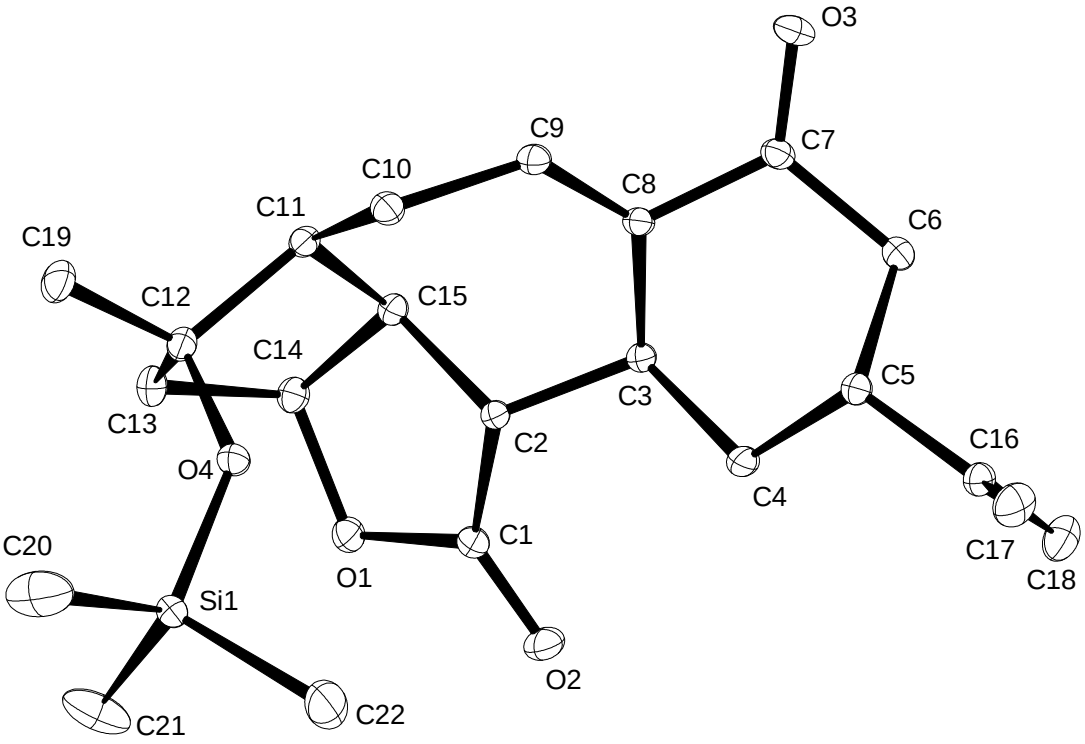


**Figure 5.14.** Structure of compound **162** in the solid state (crystallographic numbering scheme).

**X-ray crystal structure analysis of compound 162**: $C_{22}$ $H_{32}$ $O_4$ Si, $M_r$ = 388.56 g · mol$^{-1}$, colourless plate, crystal size 0.110 x 0.104 x 0.021 mm$^3$, orthorhombic, space group $P2_12_12_1$ [19], $a$ = 8.0376(4) Å, $b$ = 11.9017(7) Å, $c$ = 21.6885(12) Å, $V$ = 2074.7(2) Å$^3$, $T$ = 100(2) K, $Z$ = 4, $D_{calc}$ = 1.244 g · cm$^3$, $\lambda$ = 0.71073 Å, $\mu$(*Mo*-$K_\alpha$) = 0.137 mm$^{-1}$, analytical absorption correction ($T_{min}$ = 0.96, $T_{max}$ = 0.97), Bruker-AXS D8 Venture diffractometer with Photon-II detector and IμS micro focus X-ray source, 1.878 < $\theta$ < 36.899°, 134574 measured reflections, 10431 independent reflections, 10149 reflections with $I > 2\sigma(I)$, $R_{int}$ = 0.0251, 269 parameters, $S$ = 1.097, absolute structure parameter = -0.005(9), residual electron density 0.5 and -0.2 e · Å$^{-3}$. The structure was solved by *SHELXT* and refined by full-matrix least-squares (*SHELXL*) against $F^2$ to $R_1$ = 0.0243 [$I > 2\sigma(I)$], $wR_2$ = 0.068.

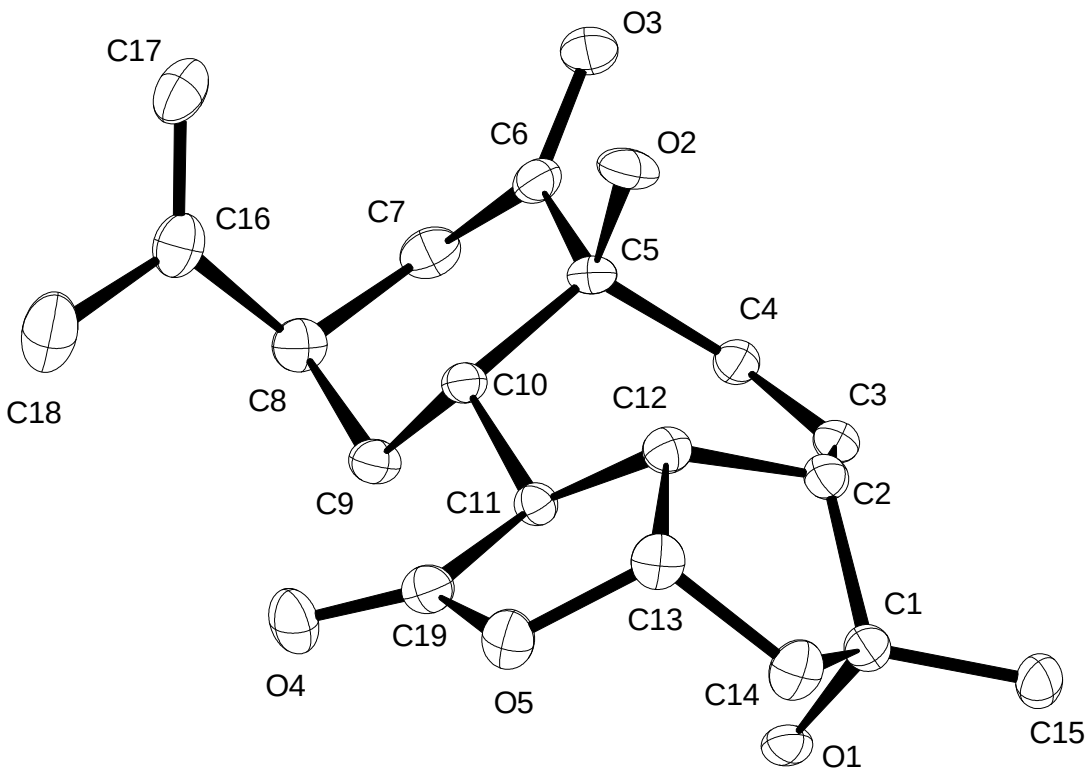


**Figure 5.15.** Structure of compound **171** in the solid state (crystallographic numbering scheme).

**X-ray crystal structure analysis of compound 171**: $C_{19}H_{23}O_5$, $M_r$ = 331.37 g · mol$^{-1}$, colourless plate, crystal size 0.190 x 0.152 x 0.108 mm$^3$, orthorhombic, space group $P2_12_12_1$ [19], $a$ = 8.7046(16) Å, $b$ = 9.5722(18) Å, $c$ = 19.628(3) Å, $V$ = 1635.5(5) Å$^3$, $T$ = 100(2) K, $Z$ = 4, $D_{calc}$ = 1.346 g · cm$^3$, $\lambda$ = 0.71073 Å, $\mu$(*Mo-K*$_\alpha$) = 0.097 mm$^{-1}$, analytical absorption correction ($T_{min}$ = 0.99, $T_{max}$ = 0.99), Bruker-AXS D8 Venture diffractometer with Photon-II detector and IμS micro focus X-ray source, 2.075 < $\theta$ < 31.562°, 108889 measured reflections, 5453 independent reflections, 4717 reflections with $I > 2\sigma(I)$, $R_{int}$ = 0.1241, 255 parameters, $S$ = 1.079, absolute structure parameter = 0.2(4), residual electron density 0.6 and -0.2 e · Å$^{-3}$. The structure was solved by *SHELXT* and refined by full-matrix least-squares (*SHELXL*) against $F^2$ to $R_1$ = 0.038 [$I > 2\sigma(I)$], $wR_2$ = 0.104.

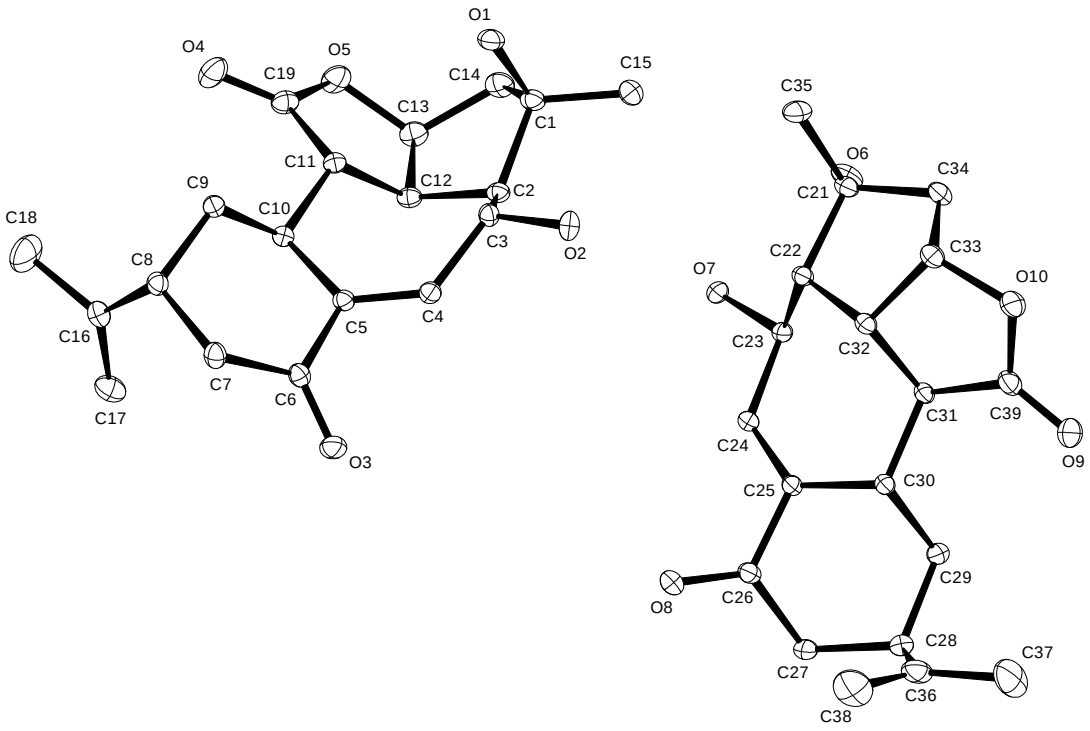


**Figure 5.16.** Structure of compound **175** in the solid state (crystallographic numbering scheme).

**X-ray crystal structure analysis of compound 175**: $C_{19}H_{24}O_5$, $M_r$ = 332.38 g · mol$^{-1}$, colourless plate, crystal size 0.124 x 0.111 x 0.102 mm$^3$, orthorhombic, space group $P2_12_12_1$ [19], $a$ = 5.5552(4) Å, $b$ = 19.7891(11) Å, $c$ = 24.7009(17) Å, $V$ = 3204.2(2) Å$^3$, $T$ = 100(2) K, $Z$ = 8, $D_{calc}$ = 1.378 g · cm$^3$, $\lambda$ = 0.71073 Å, $\mu$(*Mo-K*$\alpha$) = 0.099 mm$^{-1}$, analytical absorption correction ($T_{min}$ = 0.99, $T_{max}$ = 0.99), Bruker-AXS D8 Venture diffractometer with Photon-II detector and IμS micro focus X-ray source, 1.944 < $\theta$ < 31.555°, 212566 measured reflections, 10717 independent reflections, 10346 reflections with $I > 2\sigma(I)$, $R_{int}$ = 0.0567, 625 parameters, $S$ = 1.097, absolute structure parameter = -0.05(11), residual electron density 0.3 and -0.2 e · Å$^{-3}$. The structure was solved by *SHELXT* and refined by full-matrix least-squares (*SHELXL*) against $F^2$ to $R_1$ = 0.029 [$I > 2\sigma(I)$], $wR_2$ = 0.078.

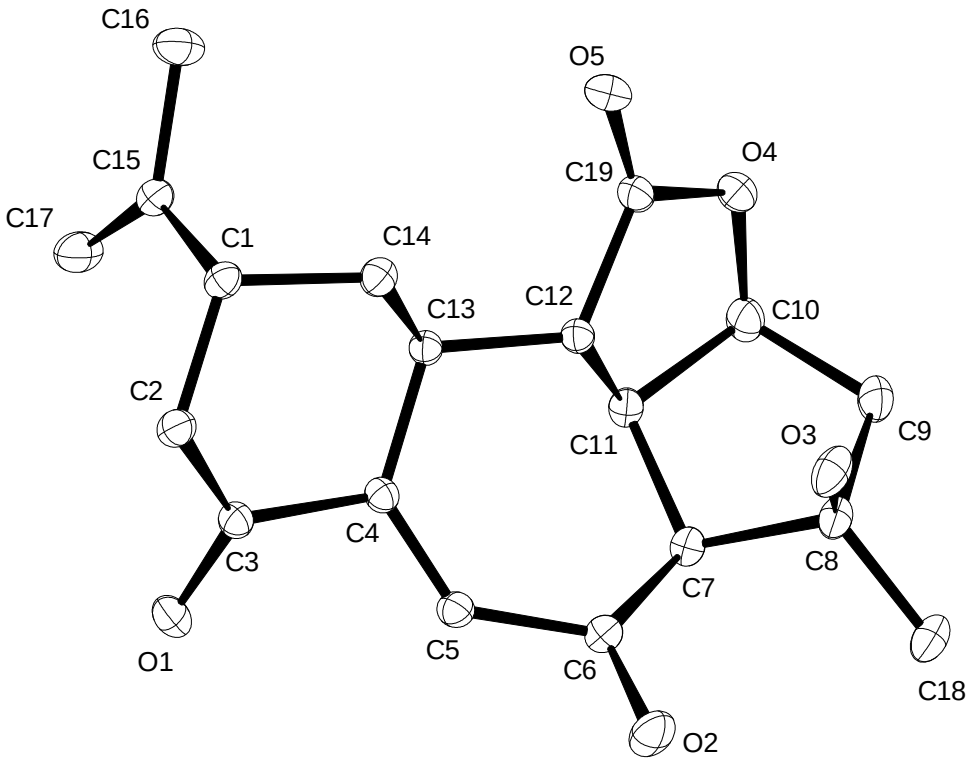


**Figure 5.17.** Structure of **34** in the solid state (crystallographic numbering scheme).

**X-ray crystal structure analysis of compound 34**: $C_{19}H_{22}O_5$, $M_r$ = 330.36 g · mol$^{-1}$, translucent colourless prism, crystal size 0.381 x 0.213 x 0.120 mm$^3$, tetragonal, space group $P4_12_12$ [92], $a$ = 11.6959(4) Å, $b$ = 11.6959(4) Å, $c$ = 23.5582(10) Å, $V$ = 3222.6(2) Å$^3$, $T$ = 100(2) K, $Z$ = 8, $D_{calc}$ = 1.362 g · cm$^3$, $\lambda$ = 0.71073 Å, $\mu$(*Mo-K*$_\alpha$) = 0.098 mm$^{-1}$, analytical absorption correction ($T_{min}$ = 0.94, $T_{max}$ = 0.99), Bruker-AXS D8 Venture diffractometer with Photon-II detector and IμS micro focus X-ray source, 1.944 <$\theta$ < 45.363°, 689801 measured reflections, 13541 independent reflections, 12402 reflections with $I > 2\sigma(I)$, $R_{int}$ = 0.0988, 255 parameters, $S$ = 1.074, absolute structure parameter = 0.04(10), residual electron density +0.4 (0.68 Å from C6) / –0.2 (0.21 Å from H5) e · Å$^{-3}$. The structure was solved by *SHELXT* and refined by full-matrix least-squares (*SHELXL*) against $F^2$ to $R_1$ = 0.032 [$I > 2\sigma(I)$], $wR_2$ = 0.090. **CCDC-2366850**.

## 5.5 DP4+ Probability analyses of Scabrolide B

The work presented in this section was written by Dr. Lianne H. Wieske and Dr. Christophe Farès.

**Overview and Context.** The first characterization in 2002 of the marine natural product scabrolide B proposed the structure **20** based on NMR data.[26] It was however established by total synthesis in 2022 that its correct structure differed from the one proposed.[14] It is well known that NMR-based elucidations of novel structures suffer from sparse and semi-quantitative data and it is not uncommon that erroneously reported natural product structures are later revised to a constitutional isomer or diastereoisomer.[6, 96] For scabrolide B, it was even postulated that the inverted chirality at position $C_{12}$ was a likely solution, but the synthetic 12-*epi*-**2** did not produce a matching NMR spectrum either.[14]

In the last 20 years, there has been some important progress in the ability to evaluate structure candidates against a set of experimental NMR data. The popular parameter DP4 scores the probability of structure candidates by correlating experimental and calculated NMR shifts (and couplings) using Bayesian statistics.[27] With the advent of efficient DFT prediction of NMR parameters, the accuracy of this approach has made it a convenient tool in structure elucidation.

In the absence of access to a sample of authentic scabrolide B or to the original NMR spectra from 2002,[26] we reasoned that a statistical evaluation of the data available in the original article might give us a new lead to consider for a second attempt at its total synthesis. With the nominal scabrolide B having potentially one or more wrongly assigned stereocentres out of seven, we decided to evaluate systematically all possible diastereoisomers. Furthermore, a close look at the original assignment revealed nearly overlapping $^{13}C$ shifts for the two ketones at positions C3 and C6 (202.6 vs 202.3 ppm). This situation could lead to the misinterpretation of a decisive long-range C-H correlation; indeed, the correlation from H13 to one of the ketones is crucial to identifying the olefinic end (C4 or C5) at which the ring-closing bond from C13 is formed. We therefore rationalized that

our statistical evaluation should also consider the constitutional isomer (and its diastereoisomers) for which a bond exists between C13 and C4 (rather than C5) leading to a 6-7-5 fused ring system rather than the proposed 7-6-5 (Figure 5.18).

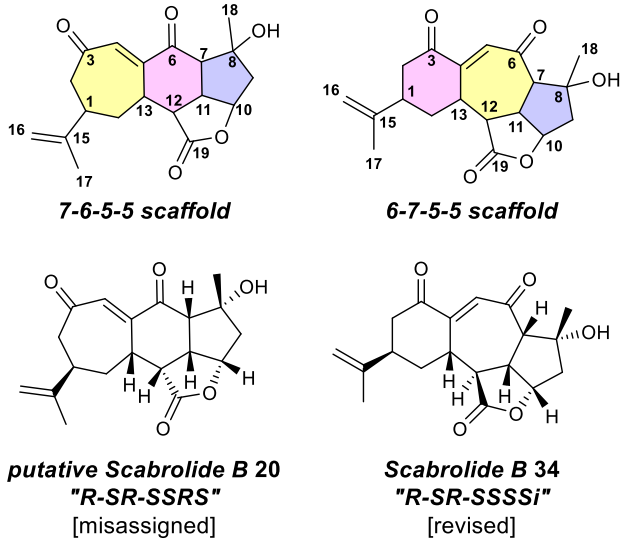


**Figure 5.18.** Basic ring scaffolds 7-6-5 and 6-7-5 with carbon numbering considered in the probabilistic analysis and the two reported constitutional isomers of scabrolide B: the original structure proposal **20** (2002)[26] (and the revised structure **34** (2023)).[29] The configuration nomenclature ***R*-*SR*-*SSSS*** refers to [1***R***, 7***S***, 8***R***, 10***S***, 11***S***, 12***S***, 13***S***]; the suffix ***i*** refers to the alternate scaffold 6-7-5.

Here we report the application of a thorough DFT-based probabilistic study to identify the correct constitutional isomer of scabrolide B in the correct stereochemical format based on the available NMR $^{1}$H, $^{13}$C chemical shifts combined with $J_{HH}$ coupling constants. The plausible scabrolide B constitutional isomers (7-6-5 and 6-7-5) comprise seven stereocentres, each resulting in 128 alternative diastereoisomers, which are grouped into 64 pairs of NMR-equivalent enantiomers. Therefore, the DFT calculations aiming to determine Boltzmann-averaged $^{1}$H and $^{13}$C chemical shieldings and coupling constants over an ensemble of interchanging conformers were applied to a total of 128 configurations (64 for each of the two constitutional isomers). The results were compared to the values of natural scabrolide B reported by Sheu *et al.*[26] and evaluated with a Bayesian analysis, the J-DP4+ tool as proposed by the group of Sarotti.[27]

The results of this approach, which we benchmarked on the known rigid terpenoid fragilolide A (see below), points to a single compound with very high confidence. It features a 6-7-5 scaffold and is characterized by the stereochemistry ***R-SR-SSSSi*** as shown in Figure 5.18. This result supports our intuition that scabrolide B is a constitutional isomer of the nominal structure rather than a diastereoisomer. This convincing result launched us onto a new total synthesis towards this target.
The revision of the structure of scabrolide B reported in 2023 by X-ray crystallography[29] preceded the completion of our total synthesis reported herein but confirmed that the correct target was predicted and pursued.

**Methods.** The strategy for the probabilistic study comprised the following steps

1. Initial conformation ensemble generation (MCMM or CREST)
2. DFT-based energetic sorting (CENSO/ORCA + GFN-xTB)
    a. Cheap pre-screening
    b. Pre-screening
    c. DFT-Optimization
    d. Higher DFT Refinement
    e. NMR parameter calculation
3. Bayesian probabilistic evaluation (J-DP4+)

and was implemented on fragilolide A – a known terpenoid for benchmarking – and on scabrolide B to determine it structure.

**1. Initial conformation ensemble generation (MCMM or CREST).**

All configurations for conformational sampling were generated using Maestro 13.7 by Schrödinger.[97] Monte Carlo Multiple Minimum (MCMM) conformational searches were performed using MacroModel[98] as implemented in the Schrödinger package.[99] The conformational searches were performed using the OPLS4 force field with $CHCl_3$ as solvation model, 5.000 iterations for the minimization, 10.000 search steps, an RMSD cutoff of 0.4 Å and an energy window for saving structures

of 25.1 kJ/mol (6.00 kcal/mol). Typically, this procedure produced between 6 and 125 conformers for the numerous diastereoisomers with differing flexibilities.
For the benchmarking (fragilolide A) of the J-DP4+ method, CREST-GFN1[100] and CREST-GFN2[101] conformational searches were also performed as an alternative using an energy window of 6 kcal/mol (25.1 kJ/mol), an RMSD cutoff of 0.4 Å, and chloroform as a solvation model.

**2. DFT-based Energetic Sorting (CENSO/ORCA + GFN-xTB)**

The various conformer ensembles were then submitted to two pre-screening steps. The first cheap pre-screening was used to discard high-lying conformers and rotamers based on single-point energies (>4.0 kcal/mol) calculated with B3LYP-D3/def2-SV(P). The resulting conformers were further pre-screened by single-point calculations including accurate electronic and solvation energies at the r2SCAN-3c level keeping only conformers below a threshold of 3.5 kcal/mol. These were then optimized at the r2SCAN-3c level and their Boltzmann weights were calculated; those contained within a 2.5 kcal/mol window and contributing to a total Boltzmann population of 99% were further considered. Then, the Boltzmann weights were refined at a higher (hybrid) DFT level (pw6b95/def2-TZVPD) and again Boltzmann populations up to 99% were preserved. Finally, the ensemble-averaged NMR properties ($^{1}$H and $^{13}$C shieldings and coupling constants) were calculated (pbe0/def2-TZVP) for the populated conformers based on their Boltzmann weights. For all computations except the initial B3LYP-D3/def2-SV(P) single-point calculations and the NMR shift calculations, thermostatic contributions were calculated within the rigid rotor harmonic oscillator approximation at the GFN2-xTB level, while the solvent was implicitly considered using the CPCM model[102] for chloroform. Conformer sorting, optimization, and NMR calculations were performed using the CENSO v1.1.2 code[103] linked to the ORCA 5.0.1[104] and xTB 6.5.0[100] codes.

### 3. Bayesian probabilistic evaluation (J-DP4+)

All shielding values were extracted from the CENSO results and converted directly to unscaled chemical shifts by subtracting the reference shielding values of TMS ($^{1}$H = 31.545 ppm and $^{13}$C = 188.653 ppm), calculated with the same energetic sorting procedure. The relevant $^{2}J_{HH}$ and $^{3}J_{HH}$ coupling constants were also directly extracted. For the J-DP4+ analysis the assigned $^{1}$H and $^{13}$C chemical shifts and $^{1}$H-$^{1}$H couplings available from the literature were introduced in the Excel spreadsheets freely available at https://sarotti-nmr.weebly.com. Custom J-DP4+ settings are shown in Table 5.13 and are based on custom probability distribution parameters, evaluated with the custom-DP4+ Excel sheet.[105]

**Table 5.13.** J-DP4+ custom settings used.

| | TMS | ⚜ | ⚜ |
|---|---|---|---|
| **H** | 31.545 | 0.185 | 14.18 |
| **C** | 188.653 | 2.306 | 11.38 |
| **J** | - | 0.992 | 3.06 |
| | **Slope scaling J** | 0.9509 | |
| | **Intercept scaling J** | -0.1405 | |

**Results.** As far as we know, the use of the ensemble-averaged NMR parameters calculated with the open-access package CENSO/ORCA (rather than the commonly used Gauge-including-atomic-orbital (GIAO) NMR shielding calculations (e.g. Gaussian)) in the J-DP4+ evaluation tool was not reported previously. This combination was therefore benchmarked using NMR data of the known terpenoid fragilolide A (8 stereocenters).[28] The alternative 7-6-5 scaffold (Figure S4), similar to the one reported for scabrolide B[26] was created in addition to the reported structure, to generate a representative structure pool for the problem at hand. The conformational searches for all diastereoisomeric configurations of the 6-7-5 and 7-6-5 scaffolds were performed, the results were optimized and the NMR data were extracted as described.

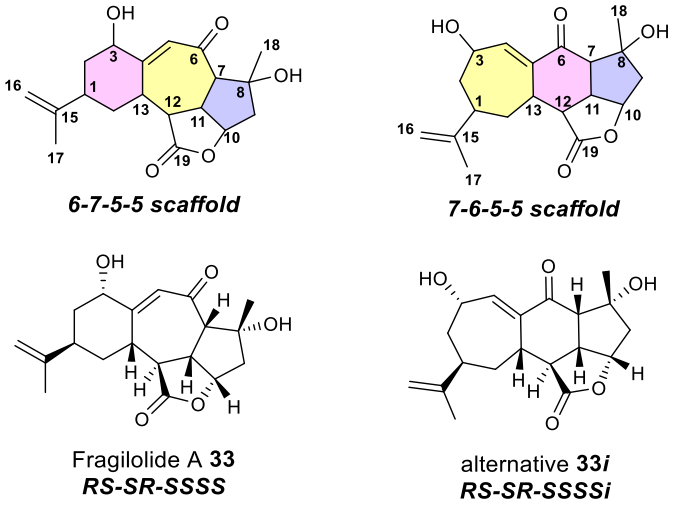


**Figure 5.19.** Basic ring scaffolds 6-7-5 and 7-6-5 with carbon numbering used in the test run. The target known structure of fragilolide A **33**[28] and a generated alternative constitutional isomer **33*i***. The configuration nomenclature **RS-SR-SSSS** refers to [1**R**, 3**S**,7**S**, 8**R**, 10**S**, 11**S**, 12**S**, 13**S**]; the suffix ***i*** refers to the alternate scaffold 7-6-5.

The two scaffolds in Figure 5.19 result in 256 diastereoisomers each, or 128 pairs of enantiomers, which were submitted to conformational sampling. Given the low degree of flexibility of these fused ring-systems, we anticipated that low-level Monte Carlo Multiple Minima (MCMM) conformational searches using MacroModel as implemented in the Schrödinger package[97] would be able to give a suitable ensemble for this purpose. Besides MCMM, we used Conformer-Rotamer Ensemble Sampling Tool (CREST) using two different semi-empirical quantum mechanical methods to compute Geometries, Frequencies and Non-covalent (GFN) interactions. We generated CREST ensembles using both GFN1[100] and GFN2[101] for the 6-7-5 isomers in addition to the MCMM searches. For the 7-6-5 isomer, only MCMM searches were performed.

As shown in Figure 5.20, the J-DP4+ probability scores of more than 99+% clearly identifies the correct isomer of fragilolide A **33** out of all 256 possibilities. The method used to generate the conformational ensemble (CREST-GFN1, CREST-GFN2 or MCMM) did not influence the probabilities significantly for the top five selected conformations. Only conformations from the 6-7-5 scaffold were selected from the 256 MCMM generated ensemble (Figure 5.20c). In all cases, the

correct diastereoisomer ***RS-SR-SSSS*** was given a probability score over 99.99%, independent of the conformational search method employed. When comparing the calculated NMR parameters from all three conformational search methods on the diastereoisomer ***RS-SR-SSSS*** with J-DP4+, all ensembles were selected with significant probabilities (Figure 5.20d). This indicates that the three conformational search methods all give reliable results and so only MCMM was used for the configurational question at hand regarding scabrolide B. Table 5.14 summarizes the experimental and back-calculated $^{1}H$ and $^{13}C$ chemical shifts for the three different methods for the best fitting configuration, with a probability of 99%+ according the J-DP4+ analysis.

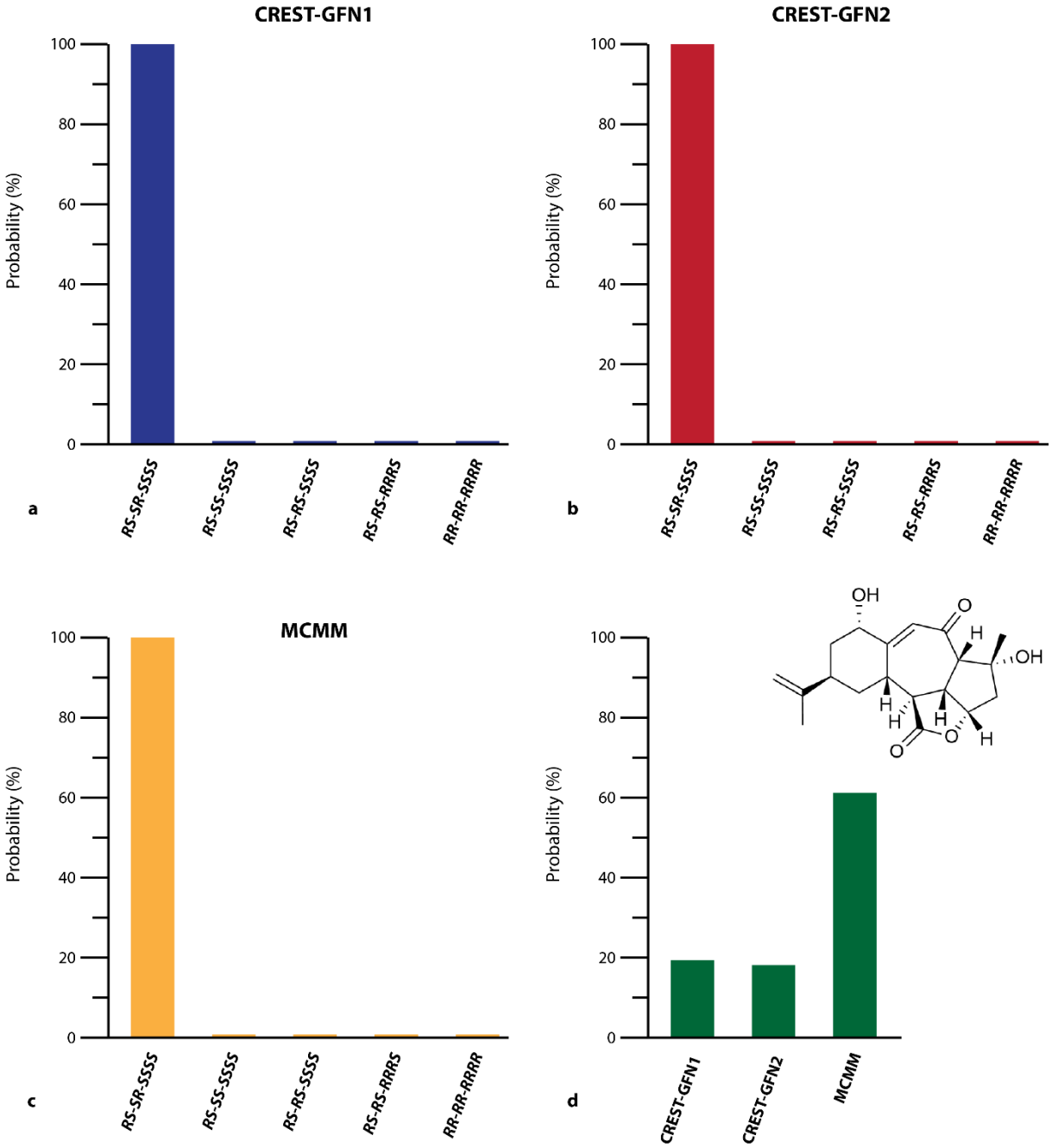


**Figure 5.20.** The five best J-DP4+ probability scores for the structure candidates based on the NMR data of fragilolide A using three different conformation sampling methods: a) CREST-GFN1 in blue, b) CREST-GFN2 in red and c) MCMM in yellow. Only the latter considered both constitutional isomers. The same five diastereoisomers were selected by all three methods, and ***RS-SR-SSSS*** was selected with a probability over 99.99% in each case. Interestingly, only constitutional isomers corresponding to the 6-7-5 scaffold were selected among the five best (c). The graph in green (d) shows the J-DP4+ probability scores of ***RS-SR-SSSS*** from the different conformational search methods.

**Table 5.14.** Assignment of fragilolide A ***RS-SR-SSSS*** (**33**)[28] and back-calculated shifts according the J-DP4+ analysis for the three different conformational sampling methods (CREST-GFN1, CREST-GFN2 and MCMM).

| | Experimental | | CREST-GFN1[7] | | CREST-GFN2[7] | | MCMM | |
|---|---|---|---|---|---|---|---|---|
| **Atom** | **$^{13}$C (ppm)** | **$^{1}$H (ppm)** | **Calc. $^{13}$C (ppm)** | **Calc. $^{1}$H (ppm)** | **Calc. $^{13}$C (ppm)** | **Calc. $^{1}$H (ppm)** | **Calc. $^{13}$C (ppm)** | **Calc. $^{1}$H (ppm)** |
| **1** | 38.3 | 2.59 | 40.18 | 2.60 | 40.26 | 2.58 | 40.07 | 2.60 |
| **2a** | 40.0 | 2.58 | 39.45 | 2.63 | 40.20 | 2.64 | 41.14 | 2.58 |
| **2b** | | 1.64 | | 1.59 | | 1.54 | | 1.62 |
| **3** | 69.1 | 4.35 | 69.32 | 4.36 | 69.36 | 4.28 | 68.90 | 4.31 |
| **4** | 160.2 | - | 165.92 | - | 165.99 | - | 163.41 | - |
| **5** | 122.0 | 6.27 | 117.84 | 6.15 | 117.96 | 6.14 | 118.76 | 6.18 |
| **6** | 203.6 | - | 202.05 | - | 201.90 | - | 203.03 | - |
| **7** | 62.6 | 2.94 | 62.91 | 3.07 | 62.35 | 3.06 | 63.08 | 3.08 |
| **8** | 81.0 | - | 80.88 | - | 80.94 | - | 80.66 | - |
| **9a** | 47.4 | 2.38 | 46.19 | 2.20 | 46.28 | 2.28 | 45.80 | 2.13 |
| **9b** | | 2.22 | | 2.16 | | 2.13 | | 2.17 |
| **10** | 79.5 | 4.98 | 80.39 | 4.79 | 80.10 | 4.80 | 80.62 | 4.79 |
| **11** | 45.2 | 3.12 | 46.00 | 3.10 | 46.09 | 3.09 | 45.44 | 3.15 |
| **12** | 45.0 | 3.38 | 45.52 | 3.46 | 44.81 | 3.53 | 46.24 | 3.46 |
| **13** | 41.5 | 2.48 | 43.24 | 2.56 | 42.71 | 2.60 | 43.02 | 2.62 |
| **14a** | 34.5 | 3.35 | 35.15 | 3.50 | 35.40 | 3.47 | 35.06 | 3.55 |
| **14b** | | 1.34 | | 1.28 | | 1.29 | | 1.27 |
| **15** | 145.3 | - | 148.77 | - | 148.67 | - | 148.96 | - |
| **16a** | 111.5 | 5.02 | 107.10 | 5.11 | 107.20 | 5.12 | 107.23 | 5.10 |
| **16b** | | 5.02 | | 5.10 | | 5.14 | | 5.09 |
| **17** | 22.5 | 1.87 | 22.25 | 1.94 | 22.11 | 1.94 | 22.16 | 1.93 |
| **18** | 30.5 | 1.63 | 28.06 | 1.52 | 28.63 | 1.52 | 27.35 | 1.53 |
| **19** | 176.6 | - | 175.08 | - | 175.35 | - | 175.35 | - |

Since this method precisely selected the correct structure of fragilolide A with unanimous J-DP4+ scores of nearly 100%, we employed the same conformation sampling, DFT-based energetic sorting, NMR parameters calculation and J-DP4+ analysis on all the constitutional and stereoisomers of scabrolide B (Figure 5.18, 128 configurations) with the hope of clearly identifying a dominant candidate. Based on the comparison of the calculated and experimental NMR parameters (Table 5.14), the configuration ***R-SR-SSSSi*** (or its enantiomeric partner)

[7] For CREST-GFN1 and CREST-GFN2 only the 128 diastereoisomers corresponding to the 6-7-5 scaffold were included, whereas for the MCMM analysis 256 configurations were included coming from both the 6-7-5 and the 7-6-5 scaffold.

corresponding to structure **3** was determined to be the best fit. As for fragilolide A, the J-DP4+ analysis resulted in a clear-cut conclusion in favour of this structure with a probability close to 100% (Figure 5.21). This structure corresponds to a 6-7-5 isomer of nominal scabrolide B, where a covalent bond exists between C13 and C4; the stereocenter C12 is inverted compared to that in nominal scabrolide B. Table 5.15 summarizes the experimental data and the back-calculated NMR data for the best fitting diastereoisomer.

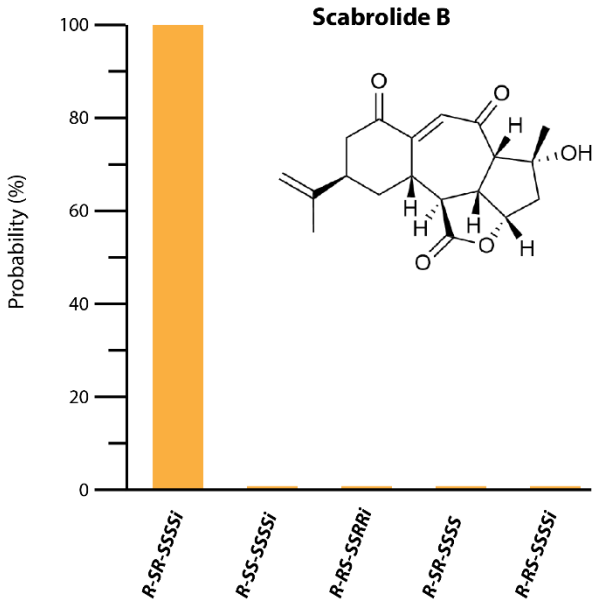


**Figure 5.21.** The five best J-DP4+ probability scores for the structure candidates of scabrolide B, based on the originally published NMR parameters ($^{1}$H and $^{13}$C chemical shifts and $^{1}$H homonuclear coupling constants).[26] The candidate pool includes all possible alternate diastereoisomers of 2 (7-6-5 scaffold) as well as of the constitutional isomer **34** (6-7-5 scaffold). The selected structure (**R**-**SR**-**SSSS*i***) (99%+)) corresponds to the scabrolide B structure with 6-7-5 scaffold recently obtained by X-ray crystallography.[29]

**Table 5.15.** Assignment of scabrolide B ***R*-*SR*-*SSSSi*** (**34**) and back-calculated shifts according the J-DP4+ analysis, with the data as reported by Sheu *et al.*

| Atom | Exp. $^{13}C$ (ppm) | Exp. $^{1}H$ (ppm) | Multiplet | Exp. $J_{HH}$ in Hz (identified coupling partner) | Calc. $^{13}C$ (ppm) | Calc. $^{1}H$ (ppm) | Calc. $J_{HH}$ in Hz (identified coupling partner) |
|---|---|---|---|---|---|---|---|
| **1** | 38.9 | 2.81 | m | | 41.12 | 2.89 | |
| **2a** | 45.0 | 2.90 | ddd | 16.0 (2b)<br>4.0<br>2.5 (5) | 45.24 | 3.05 | 16.95 (2b)<br><br>0.29 (5) |
| **2b** | | 2.60 | dd | 16.0 (2a)<br>6.0 | | 2.70 | 16.95 (2a) |
| **3** | 202.2 | - | - | - | 201.91 | - | - |
| **4**[8] | 150.8 | - | - | - | 152.64 | - | - |
| **5**[8] | 130.5 | 6.34 | d | 3.0 (2a) | 127.73 | 6.37 | 0.29 (2a) |
| **6** | 202.5 | - | - | - | 203.17 | - | - |
| **7** | 62.4 | 2.93 | d | 7.2 | 63.25 | 3.18 | 7.05 (11) |
| **8** | 81.3 | - | - | - | 80.51 | - | - |
| **9a** | 47.4 | 3.36 | d | 16.0 (9b)<br>2.5 (10) | 46.01 | 2.25 | 16.26 (9b)<br>0.97 (10) |
| **9b** | | 2.21 | ddd | 16.0 (9a)<br>9.0 (10)<br>1.6 | | 2.14 | 16.26 (9a)<br>7.91 (10) |
| **10** | 79.5 | 4.98 | td | 2.5 (9a)<br>9.0 (9b) | 80.41 | 4.88 | 0.97 (9a)<br>7.91 (9b) |
| **11**[9] | 45.3 | 3.45 | t | 10.5 (12) | 45.56 | 3.19 | 8.70 (12) |
| **12**[9] | 45.3 | 3.14 | dt | 10.5 (11)<br>7.8 | 47.10 | 3.40 | 8.70 (11) |
| **13** | 41.6 | 2.75 | m | | 43.67 | 2.83 | - |
| **14** | 30.5 | 3.30 | dtd | 10.0 (14b)<br>4.0<br>2.5 | 30.25 | 3.45 | 14.12 (14b) |
| **14** | | 1.71 | tdd | 10.0 (14a)<br>5.0<br>2.5 | | 1.74 | 14.12 (14a) |
| **15** | 146.4 | - | - | - | 150.51 | - | - |
| **16a** | 112.7 | 4.95 | s | - | 108.82 | 4.92 | - |
| **16b** | | 4.72 | s | - | | 5.14 | - |
| **17** | 21.8 | 1.83 | s | | 21.38 | 1.93 | - |
| **18** | 30.0 | 1.63 | s | | 26.59 | 1.56 | - |
| **19** | 175.9 | - | - | - | 174.22 | - | - |

[8] The atom numbers of 4 and 5 are switched for the correct constitutional isomer (**20**) as compared to Sheu *et al.* [26] because of the difference in atom-labeling between the two isomers.

[9] Chemical shift for 11 and 12 were used as reported by Sheu *et al.* for the J-DP4+ analysis.[26] Once the total synthesis of the scabrolide B was successful, it turned out the chemical shifts of 11 and 12 were assigned incorrectly in the original publication.

# 6. Abbreviations

| | |
|---|---|
| 2-MeTHF | 2-methyltetrahydrofuran |
| 3,5-DMP | 3-5-dimethylpyrazole |
| ABSA | 4-acetamidobenzenesulfonyl azide |
| Ac | acetyl |
| acac | acetylacetonate |
| AIBN | azobisisobutyronitrile |
| aq. | aqueous |
| BBN | borabicyclo[3.3.1]nonane |
| BINAP | 2,2′-bis(diphenylphosphino)-1,1′-binaphthyl |
| br s | broad singlet |
| brsm | based on recovered starting material |
| Bu | butyl |
| cat. | catalytic |
| CSA | camphorsulfonic acid |
| d | doublet |
| DABCO | 1,4-diazabicyclo[2.2.2]octane |
| dba | dibenzylideneacetone |
| DBN | 1,5-diazabicyclo[4.3.0]non-5-ene |
| DBU | 1,8-diazabicyclo[5.4.0]undec-7-ene |
| DCM | dichloromethane |
| DIPEA | dimethylethylamine |
| DMAc | *N*,*N*-dimethyl acetamide |
| DMAP | 4-dimethylaminopyridine |
| DMF | *N*,*N*-dimethyl formamide |
| DMP | Dess-Martin periodinane |
| DMS | dimethyl sulfite |
| DMSO | dimethyl sulfoxide |
| EDC | 1-ethyl-3-(3-dimethylaminopropyl)carbodiimide |
| ee | enantiometic excess |
| ent | enantiomeric |
| epi | epimeric |
| eq | equivalent |
| Et | ethyl |
| EtOAc | Ethyl acetate |
| hept | heptet |
| HG-II | Hoveyda-Grubbs second generation catalyst |
| HMDS | bis(trimethylsilyl)amine |

| | |
|---|---|
| HMPA | hexamethylphosphoramide |
| HPLC | high performance liquid chromatography |
| HRMS | high resolution mass spectrometry |
| IBX | 2-iodoxybenzoic acid |
| *i*Pr | isopropyl (branched) |
| iso | isomer |
| LDA | lithium diisopropylamine |
| lit. | literature |
| m | multiplet |
| M | molar |
| Me | methyl |
| MeCN | acetonitrile |
| MeOH | methanol |
| Ms | mesyl |
| NBS | *N*-bromosuccinimide |
| NHC | *N*-heterocyclic carbene |
| NMO | *N*-methylmorpholine N-oxide |
| NMR | nuclear Magnetic Resonance |
| NOE | nuclear Overhauser effect |
| *o* | ortho |
| *p* | para |
| PCC | pyridinium chlorochromate |
| PDC | pyridinium dichromate |
| Ph | phenyl |
| PMP | 1,2,2,6,6-pentamethylpiperidine |
| *Pr* | propyl (branched) |
| PSP | (phenylseleno)phthalimide |
| pyr | pyridine |
| q | quartet |
| RCM | ring closing metathesis |
| RT | room temperature |
| s | singlet |
| sat. | saturated |
| SCX | strong cation exchange |
| *t* | tert (branched) |
| t | triplet |
| TASF | tris(dimethylamino)sulfonium difluorotrimethylsilicate |
| TBAB | tetra-n-butylammonium bromide |

| | |
|---|---|
| TBAF | tetra-n-butylammonium fluoride |
| TBS | *tert*-butyldimethylsilane |
| Tf | trifluoromethanesulfonate |
| THF | tetrahydrofuran |
| TIPS | triisopropylsilane |
| TMG | *N*,*N*,*N*,*N*-tetramethylguanidine |
| TMP | 2,2,6,6-tetramethylpiperidine |
| TMS | trimethylsilane |
| TPAP | tetra-n-propylammonium perruthenate |
| Ts | tosyl |

# 7. Bibliography


[1] F. Wöhler, *Annalen der Physik* **1828**, *88*, 253-256.

[2] H. Kolbe, *Justus Liebigs Ann. Chem.* **1845**, *54*, 145-188.

[3] P. Rabe, *Berichte der deutschen chemischen Gesellschaft* **1907**, *40*, 3655-3658.

[4] H. Fischer, K. Zeile, *Justus Liebigs Ann. Chem.* **1929**, *468*, 98-116.

[5] L. H. Briggs, H. T. Openshaw, R. Robinson, *J. Chem. Soc.* **1946**, 903-908.

[6] a) K. C. Nicolaou, S. A. Snyder, *Angew. Chem. Int. Ed.* **2005**, *44*, 1012-1044; b) M. E. Maier, *Nat. Prod. Rep.* **2009**, *26*, 1105-1124.

[7] M. Heinrich, J. J. Murphy, M. K. Ilg, A. Letort, J. T. Flasz, P. Philipps, A. Fürstner, *J. Am. Chem. Soc.* **2020**, *142*, 6409-6422.

[8] a) S. Omura, A. Nakagawa, H. Yamada, T. Hata, A. Furusaki, T. Watanabe, *Chem. Pharm. Bull.* **1973**, *21*, 931-940; b) S. J. Gould, N. Tamayo, C. R. Melville, M. C. Cone, *J. Am. Chem. Soc.* **1994**, *116*, 2207-2208; c) S. Mithani, G. Weeratunga, N. J. Taylor, G. I. Dmitrienko, *J. Am. Chem. Soc.* **1994**, *116*, 2209-2210.

[9] a) L. Laraia, H. Waldmann, *Drug Discov. Today: Technol.* **2017**, *23*, 75-82; b) D. J. Newman, G. M. Cragg, *J. Nat. Prod.* **2020**, *83*, 770-803; c) M. Grigalunas, S. Brakmann, H. Waldmann, *J. Am. Chem. Soc.* **2022**, *144*, 3314-3329; d) S. B. Bharate, C. W. Lindsley, *J. Med. Chem.* **2024**, *67*, 20723-20730.

[10] M. Kobayashi, K. M. C. A. Rao, M. M. Krishna, V. Anjaneyulu, *ChemInform* **1995**, *26*.

[11] C.-Y. Duh, S.-K. Wang, M.-C. Chia, M. Y. Chiang, *Tetrahedron Lett.* **1999**, *40*, 6033-6035.

[12] R. A. Craig, II, B. M. Stoltz, *Chem. Rev.* **2017**, *117*, 7878-7909.

[13] N. J. Hafeman, S. A. Loskot, C. E. Reimann, B. P. Pritchett, S. C. Virgil, B. M. Stoltz, *J. Am. Chem. Soc.* **2020**, *142*, 8585-8590.

[14] Z. Meng, A. Fürstner, *J. Am. Chem. Soc.* **2022**, *144*, 1528-1533.

[15] J. P. Tuccinardi, J. L. Wood, *J. Am. Chem. Soc.* **2022**, *144*, 20539-20547.

[16] B. M. Gross, S. J. Han, S. C. Virgil, B. M. Stoltz, *J. Am. Chem. Soc.* **2023**, *145*, 7763-7767.

[17] N. J. Hafeman, M. Chan, T. J. Fulton, E. J. Alexy, S. A. Loskot, S. C. Virgil, B. M. Stoltz, *J. Am. Chem. Soc.* **2022**, *144*, 20232-20236.

[18] N. J. Truax, S. Ayinde, J. O. Liu, D. Romo, *J. Am. Chem. Soc.* **2022**, *144*, 18575-18585.

[19] N. P. Thao, B. T. Luyen, R. Brun, M. Kaiser, P. Van Kiem, C. Van Minh, T. J. Schmidt, J. S. Kang, Y. H. Kim, *Molecules, 20*, **2015**, 12459-12468.

[20] S.-Y. Cheng, C.-T. Chuang, Z.-H. Wen, S.-K. Wang, S.-F. Chiou, C.-H. Hsu, C.-F. Dai, C.-Y. Duh, *Bioorg. Med. Chem.* **2010**, *18*, 3379-3386.

[21] a) A. F. Ahmed, R.-T. Shiue, G.-H. Wang, C.-F. Dai, Y.-H. Kuo, J.-H. Sheu, *Tetrahedron* **2003**, *59*, 7337-7344; b) C.-Y. Huang, Y.-J. Tseng, U. Chokkalingam, T.-L. Hwang, C.-H. Hsu, C.-F. Dai, P.-J. Sung, J.-H. Sheu, *J. Nat. Prod.* **2016**, *79*, 1339-1346; c) S. A. L. Thomas, J. L. von Salm, S. Clark, S.

Ferlita, P. Nemani, A. Azhari, C. A. Rice, N. G. Wilson, D. E. Kyle, B. J. Baker, *J. Nat. Prod.* **2018**, *81*, 117-123; d) W.-X. Cui, M. Yang, H. Li, S.-W. Li, L.-G. Yao, G. Li, W. Tang, C.-H. Wang, L.-F. Liang, Y.-W. Guo, *Bioorg. Chem.* **2020**, *94*, 103350.

[22] N. J. Truax, S. Ayinde, K. Van, J. O. Liu, D. Romo, *Org. Lett.* **2019**, *21*, 7394-7399.

[23] I. I. R. A. Craig, J. L. Roizen, R. C. Smith, A. C. Jones, S. C. Virgil, B. M. Stoltz, *Chem. Sci.* **2017**, *8*, 507-514.

[24] Y. Li, G. Pattenden, *Nat. Prod. Rep.* **2011**, *28*, 429-440.

[25] Y. Li, G. Pattenden, *Tetrahedron* **2011**, *67*, 10045-10052.

[26] J.-H. Sheu, A. F. Ahmed, R.-T. Shiue, C.-F. Dai, Y.-H. Kuo, *J. Nat. Prod.* **2002**, *65*, 1904-1908.

[27] a) N. Grimblat, M. M. Zanardi, A. M. Sarotti, *J. Org. Chem.* **2015**, *80*, 12526-12534; b) S. G. Smith, J. M. Goodman, *J. Am. Chem. Soc.* **2010**, *132*, 12946-12959.

[28] W. Cheng, M. Ji, X. Li, J. Ren, F. Yin, L. van Ofwegen, S. Yu, X. Chen, W. Lin, *Tetrahedron* **2017**, *73*, 2518-2528.

[29] Y. Du, L. Yao, X. Li, Y. Guo, *Chin. Chem. Lett.* **2023**, *34*, 107512.

[30] J. Liu, Q. Tang, J. Huang, T. Li, H. Ouyang, W. H. Lin, X. J. Yan, X. Yan, S. He, *J. Org. Chem.* **2022**, *87*, 9806-9814.

[31] B. R. Chitturi, V. B. Tatipamula, C. B. Dokuburra, U. K. Mangamuri, V. R. Tuniki, S. V. Kalivendi, R. A. Bunce, V. Yenamandra, *Tetrahedron* **2016**, *72*, 1933-1940.

[32] P. Radhika, P. V. Subba Rao, V. Anjaneyulu, R. N. Asolkar, H. Laatsch, *J. Nat. Prod.* **2002**, *65*, 737-739.

[33] K. E. Lillsunde, C. Festa, H. Adel, S. De Marino, V. Lombardi, S. Tilvi, D. A. Nawrot, A. Zampella, L. D'Souza, M. V. D'Auria, P. Tammela, *Mar. Drugs* **2014**, *12*, 4045-4068.

[34] B. A. Pratt, PhD thesis, The Scripps Research Institute **2008**.

[35] G. Liu, PhD thesis, Texas A&M University **2012**.

[36] M. Breunig, PhD thesis, University of Konstanz **2019**.

[37] P. A. Roethle, P. T. Hernandez, D. Trauner, *Org. Lett.* **2006**, *8*, 5901-5904.

[38] K. Moeller, *Synlett* **2009**, *2009*, 1208-1218.

[39] a) E. J. Horn, J. S. Silverston, C. D. Vanderwal, *J. Org. Chem.* **2016**, *81*, 1819-1838; b) E. J. Horn, PhD thesis, UC Irvine **2014**.

[40] a) J. L. Roizen, A. C. Jones, R. C. Smith, S. C. Virgil, B. M. Stoltz, *J. Org. Chem.* **2017**, *82*, 13051-13067; b) R. A. Craig, II, R. C. Smith, J. L. Roizen, A. C. Jones, S. C. Virgil, B. M. Stoltz, *J. Org. Chem.* **2018**, *83*, 3467-3485; c) R. A. Craig, II, R. C. Smith, J. L. Roizen, A. C. Jones, S. C. Virgil, B. M. Stoltz, *J. Org. Chem.* **2019**, *84*, 7722-7746; d) J. L. Roizen, PhD thesis, CalTech **2010**; e) R. A. Craig II, PhD thesis, CalTech **2015**.

[41] E. J. Simmons, D. B. Ryffel, D. A. Lopez, Y. D. Boyko, D. Sarlah, *J. Am. Chem. Soc.* **2025**, *147*, 130-135.

[42] Y. Boyko, PhD thesis, University of Illinois Urbana-Champaign **2021**.
[43] R. Serrano, Y. D. Boyko, L. W. Hernandez, A. Lotuzas, D. Sarlah, *J. Am. Chem. Soc.* **2023**, *145*, 8805-8809.
[44] K. Yu, A. Gorou, D. Huang, T. J. Maimone, *J. Am. Chem. Soc.* **2025**, *147*, 44727-44732.
[45] S. Y. Yun, J.-C. Zheng, D. Lee, *J. Am. Chem. Soc.* **2009**, *131*, 8413-8415.
[46] L. O. Jeroncic, M. P. Cabal, S. J. Danishefsky, G. M. Shulte, *J. Org. Chem.* **1991**, *56*, 387-395.
[47] Z. G. Brill, H. K. Grover, T. J. Maimone, *Science* **2016**, *352*, 1078-1082.
[48] J. Chen, J. N. Marx, *Tetrahedron Lett.* **1997**, *38*, 1889-1892.
[49] E. M. Simmons, B. Mudryk, A. G. Lee, Y. Qiu, T. M. Razler, Y. Hsiao, *Org. Process Res. Dev.* **2017**, *21*, 1659-1667.
[50] J. Tsuji, I. Minami, I. Shimizu, H. Kataoka, *Chem. Lett.* **1984**, *13*, 1133-1136.
[51] A. M. D'Souza, S. K. Paknikar, V. Dev, P. S. Beauchamp, S. P. Kamat, *J. Nat. Prod.* **2004**, *67*, 700-702.
[52] A. B. Charette, H. Lebel, *J. Org. Chem.* **1995**, *60*, 2966-2967.
[53] B. Movassagh, M. Nazari, *Synlett* **2009**, *2009*, 1803-1805.
[54] a) J. Liu, M. A. Marsini, T. A. Bedell, P. J. Reider, E. J. Sorensen, *Tetrahedron* **2016**, *72*, 3713-3717; b) T. Ohkubo, H. Akino, M. Asaoka, H. Takei, *Tetrahedron Lett.* **1995**, *36*, 3365-3368; c) T. Gatzenmeier, P. S. J. Kaib, J. B. Lingnau, R. Goddard, B. List, *Angew. Chem. Int. Ed.* **2018**, *57*, 2464-2468.
[55] T. Mukaiyama, *Angew. Chem. Int. Ed. Engl.* **1977**, *16*, 817-826.
[56] W. Su, S. Raders, J. G. Verkade, X. Liao, J. F. Hartwig, *Angew. Chem. Int. Ed.* **2006**, *45*, 5852-5855.
[57] N. Ozasa, M. Wadamoto, K. Ishihara, H. Yamamoto, *Synlett* **2003**, *2003*, 2219-2221.
[58] A. Fürstner, K. Langemann, *Synthesis* **1997**, *1997*, 792-803.
[59] A. K. Chatterjee, T.-L. Choi, D. P. Sanders, R. H. Grubbs, *J. Am. Chem. Soc.* **2003**, *125*, 11360-11370.
[60] a) A. Deiters, S. F. Martin, *Chem. Rev.* **2004**, *104*, 2199-2238; b) M. Yu, S. Lou, F. Gonzalez-Bobes, *Org. Process Res. Dev.* **2018**, *22*, 918-946.
[61] R. H. Grubbs, *J. Macromol. Sci., Part A* **1994**, *31*, 1829-1933.
[62] I. C. Stewart, T. Ung, A. A. Pletnev, J. M. Berlin, R. H. Grubbs, Y. Schrodi, *Org. Lett.* **2007**, *9*, 1589-1592.
[63] a) W. Schmidt, T. M. Schulze, G. Brasse, E. Nagrodzka, M. Maczka, J. Zettel, P. G. Jones, J. Grunenberg, M. Hilker, U. Trauer-Kizilelma, U. Braun, S. Schulz, *Angew. Chem. Int. Ed.* **2015**, *54*, 7698-7702; b) K. A. Ahrendt, R. M. Williams, *Org. Lett.* **2004**, *6*, 4539-4541.
[64] a) Y. Schrodi, R. Pederson, *Aldrichimica Acta* **2007**, *40*, 45-52; b) M. Bieniek, A. Michrowska, D. L. Usanov, K. Grela, *Chem. Eur. J.* **2008**, *14*, 806-818.
[65] a) V. Gracias, A. F. Gasiecki, J. D. Moore, I. Akritopoulou-Zanze, S. W. Djuric, *Tetrahedron Lett.* **2006**, *47*, 8977-8980; b) J. R. Corte, D. J. P. Pinto, T. Fang, H. Osuna, W. Yang, Y. Wang, A. Lai, C. G. Clark, J. H. Sun, R.

Rampulla, A. Mathur, M. Kaspady, P. R. Neithnadka, Y. C. Li, K. A. Rossi, J. E. Myers, Jr., S. Sheriff, Z. Lou, T. W. Harper, C. Huang, J. J. Zheng, J. M. Bozarth, Y. Wu, P. C. Wong, E. J. Crain, D. A. Seiffert, J. M. Luettgen, P. Y. S. Lam, R. R. Wexler, W. R. Ewing, *J. Med. Chem.* **2020**, *63*, 784-803; c) T. H. West, S. S. M. Spoehrle, A. D. Smith, *Tetrahedron* **2017**, *73*, 4138-4149; d) K. S. Feldman, J. F. Antoline, *Tetrahedron* **2013**, *69*, 1434-1445.

[66] S. H. Hong, D. P. Sanders, C. W. Lee, R. H. Grubbs, *J. Am. Chem. Soc.* **2005**, *127*, 17160-17161.

[67] A. Fürstner, K. Langemann, *J. Am. Chem. Soc.* **1997**, *119*, 9130-9136.

[68] a) E. L. Dias, S. T. Nguyen, R. H. Grubbs, *J. Am. Chem. Soc.* **1997**, *119*, 3887-3897; b) M. S. Sanford, J. A. Love, R. H. Grubbs, *J. Am. Chem. Soc.* **2001**, *123*, 6543-6554.

[69] E. Kerste, M. P. Beller, U. Koert, *Eur. J. Org. Chem.* **2020**, *2020*, 3699-3711.

[70] a) K. Inanaga, Y. Ogawa, Y. Nagamoto, A. Daigaku, H. Tokuyama, Y. Takemoto, K. Takasu, *Beilstein J. Org. Chem.* **2012**, *8*, 658-661; b) K. Ishihara, H. Nakamura, S. Nakamura, H. Yamamoto, *J. Org. Chem.* **1998**, *63*, 6444-6445.

[71] K. C. Nicolaou, B. S. Safina, M. Zak, S. H. Lee, M. Nevalainen, M. Bella, A. A. Estrada, C. Funke, F. J. Zécri, S. Bulat, *J. Am. Chem. Soc.* **2005**, *127*, 11159-11175.

[72] a) T. Ankner, C. C. Cosner, P. Helquist, *Chem. Eur. J.* **2013**, *19*, 1858-1871; b) E. Piers, P. C. Marais, *J. Org. Chem.* **1990**, *55*, 3454-3455; c) E. Piers, J. Renaud, *J. Org. Chem.* **1993**, *58*, 11-13; d) A. B. Dounay, P. G. Humphreys, L. E. Overman, A. D. Wrobleski, *J. Am. Chem. Soc.* **2008**, *130*, 5368-5377; e) H. Cao, J. Yu, X. Z. Wearing, C. Zhang, X. Liu, J. Deschamps, J. M. Cook, *Tetrahedron Lett.* **2003**, *44*, 8013-8017; f) M. R. Stephen, M. T. Rahman, V. Tiruveedhula, G. O. Fonseca, J. R. Deschamps, J. M. Cook, *Chem. Eur. J.* **2017**, *23*, 15805-15819; g) J. Yu, X. Z. Wearing, J. M. Cook, *J. Org. Chem.* **2005**, *70*, 3963-3979; h) S. Zhao, X. Liao, J. M. Cook, *Org. Lett.* **2002**, *4*, 687-690; i) T. Wang, J. M. Cook, *Org. Lett.* **2000**, *2*, 2057-2059; j) D. Solé, X. Urbaneja, J. Bonjoch, *Org. Lett.* **2005**, *7*, 5461-5464.

[73] a) M. Utsugi, Y. Kamada, M. Nakada, *Tetrahedron Lett.* **2008**, *49*, 4754-4757; b) S. Hirai, M. Utsugi, M. Iwamoto, M. Nakada, *Chem. Eur. J.* **2015**, *21*, 355-359; c) T. Watanabe, K. Oga, H. Matoba, M. Nagatomo, M. Inoue, *J. Am. Chem. Soc.* **2023**, *145*, 25894-25902.

[74] M. A. Morin, *Org. Synth.* **2020**, *97*, 217-231.

[75] a) H. Shigehisa, T. Jikihara, O. Takizawa, H. Nagase, T. Honda, *Tetrahedron Lett.* **2008**, *49*, 3983-3986; b) D. Solé, E. Peidró, J. Bonjoch, *Org. Lett.* **2000**, *2*, 2225-2228.

[76] R. Bloch, P. Le Perchec, F. Rouessac, J. M. Conia, *Tetrahedron* **1968**, *24*, 5971-5989.

[77] a) F. W. Hartrampf, T. Furukawa, D. Trauner, *Angew. Chem. Int. Ed.* **2017**, *56*, 893-896; b) S. T. Staben, J. J. Kennedy-Smith, D. Huang, B. K. Corkey, R. L. LaLonde, F. D. Toste, *Angew. Chem. Int. Ed.* **2006**, *45*, 5991-5994.

[78] a) P. W. Davies, C. Detty-Mambo, *Org. Biomol. Chem.* **2010**, *8*, 2918-2922; b) N. Chernyak, S. I. Gorelsky, V. Gevorgyan, *Angew. Chem. Int. Ed.* **2011**, *50*, 2342-2345; c) S. V. O'Neil, C. A. Quickley, B. B. Snider, *J. Org. Chem.* **1997**, *62*, 1970-1975; d) M. Cao, A. Yesilcimen, M. Wasa, *J. Am. Chem. Soc.* **2019**, *141*, 4199-4203.

[79] a) J.-Q. Yu, E. J. Corey, *J. Am. Chem. Soc.* **2003**, *125*, 3232-3233; b) A. J. Catino, R. E. Forslund, M. P. Doyle, *J. Am. Chem. Soc.* **2004**, *126*, 13622-13623; c) Z. Yuan, X. Hu, H. Zhang, L. Liu, P. Chen, M. He, X. Xie, X. Wang, X. She, *Chem. Commun.* **2018**, *54*, 912-915; d) H. W. Mbatia, S. Ramalingam, V. P. Ramamurthy, M. S. Martin, A. K. Kwegyir-Afful, V. C. Njar, *J. Med. Chem.* **2015**, *58*, 1900-1914; e) L. Kaisalo, J. Koskimies, T. Hase, *Synthesis* **1996**, *1996*, 1122-1126; f) J. Frincke, Reading, C., HOLLIS-EDEN PHARMACEUTICALS, WO2008/039566, **2008**; g) A. R. Lippert, J. Kaeobamrung, J. W. Bode, *J. Am. Chem. Soc.* **2006**, *128*, 14738-14739; h) J. Li, W. Zhang, F. Zhang, Y. Chen, A. Li, *J. Am. Chem. Soc.* **2017**, *139*, 14893-14896; i) E. A. Djurendic, J. J. Ajdukovic, M. N. Sakac, J. J. Csanadi, V. V. Kojic, G. M. Bogdanovic, K. M. Penov Gasi, *Eur. J. Med. Chem.* **2012**, *54*, 784-792; j) H. Shi, I. N. Michaelides, B. Darses, P. Jakubec, Q. N. N. Nguyen, R. S. Paton, D. J. Dixon, *J. Am. Chem. Soc.* **2017**, *139*, 17755-17758; k) C. Y. Zheng, J. M. Yue, *Nat. Commun.* **2023**, *14*, 2399; l) A. B. Smith, III, B. D. Dorsey, M. Ohba, A. T. Lupo, Jr., M. S. Malamas, *J. Org. Chem.* **1988**, *53*, 4314-4325.

[80] I. Volchkov, D. Lee, *Chem. Soc. Rev.* **2014**, *43*, 4381-4394.

[81] a) B. M. Trost, W. Tang, F. D. Toste, *J. Am. Chem. Soc.* **2005**, *127*, 14785-14803; b) A. K. Mandal, J. S. Schneekloth, K. Kuramochi, C. M. Crews, *Org. Lett.* **2006**, *8*, 427-430; c) B. M. Trost, D. Amans, W. M. Seganish, C. K. Chung, *Chem. Eur. J.* **2012**, *18*, 2961-2971; d) S. Y. Yun, E. C. Hansen, I. Volchkov, E. J. Cho, W. Y. Lo, D. Lee, *Angew. Chem. Int. Ed.* **2010**, *49*, 4261-4263; e) Y. Numajiri, T. Takahashi, T. Doi, *Chem. Asian J.* **2009**, *4*, 111-125; f) H. H. Jung, J. R. Seiders, P. E. Floreancig, *Angew. Chem. Int. Ed.* **2007**, *46*, 8464-8467; g) I. Volchkov, D. Lee, *J. Am. Chem. Soc.* **2013**, *135*, 5324-5327.

[82] a) P. F. Li, H. L. Wang, J. Qu, *J. Org. Chem.* **2014**, *79*, 3955-3962; b) J. A. McCubbin, S. Voth, O. V. Krokhin, *J. Org. Chem.* **2011**, *76*, 8537-8542; c) F. Li, Y. Luo, X. Zhu, Y. Ye, Q. Yuan, W. Zhang, *Chem. Eur. J.* **2023**, *29*, e202300027.

[83] a) C. Morrill, R. H. Grubbs, *J. Am. Chem. Soc.* **2005**, *127*, 2842-2843; b) C. Morrill, G. L. Beutner, R. H. Grubbs, *J. Org. Chem.* **2006**, *71*, 7813-7825.

[84] J. Jacob, J. H. Espenson, J. H. Jensen, M. S. Gordon, *Organometallics* **1998**, *17*, 1835-1840.

[85] S. Raju, M.-E. Moret, R. J. M. Klein Gebbink, *ACS Catalysis* **2014**, *5*, 281-300.

[86] G. M. Atkins, Jr., E. M. Burgess, *J. Am. Chem. Soc.* **1968**, *90*, 4744-4745.

[87] C. F. Nising, S. Brase, *Chem. Soc. Rev.* **2012**, *41*, 988-999.

[88] S. Tshepelevitsh, A. Kütt, M. Lõkov, I. Kaljurand, J. Saame, A. Heering, P. G. Plieger, R. Vianello, I. Leito, *Eur. J. Org. Chem.* **2019**, *2019*, 6735-6748.
[89] C. F. Nising, S. Bräse, *Chem. Soc. Rev.* **2008**, *37*, 1218-1228.
[90] Y. Sato, S. Watanabe, M. Shibasaki, *Tetrahedron Lett.* **1992**, *33*, 2589-2592.
[91] J.-F. Lavallée, C. Spino, R. Ruel, K. T. Hogan, P. Deslongchamps, *Can. J. Chem.* **1992**, *70*, 1406-1426.
[92] T. Robert, J. Velder, H.-G. Schmalz, *Angew. Chem. Int. Ed.* **2008**, *47*, 7718-7721.
[93] D. S. P. Douglas Gamba, Jessie S. da Costa, Cesar L. Petzhold, Antonio C. A. Borges, Marco A. Ceschi, *J. Braz. Chem. Soc.* **2008**, *19*, 1270-1278.
[94] Y. Egoshi, R. Kondo, Y. Yoshimoto, T. Sugiyama, T. Usuki, *Tetrahedron Lett.* **2013**, *54*, 7029-7030.
[95] D. S. Lin, G. Späth, Z. Meng, L. H. E. Wieske, C. Farès, A. Fürstner, *J. Am. Chem. Soc.* **2024**, *146*, 24250-24256.
[96] B. K. Chhetri, S. Lavoie, A. M. Sweeney-Jones, J. Kubanek, *Nat. Prod. Rep.* **2018**, *35*, 514-531.
[97] Schrödinger Release 2023-3: Maestro, Schrödinger, LLC, New York, NY, **2023**.
[98] a) F. Mohamadi, N. G. J. Richards, W. C. Guida, R. Liskamp, M. Lipton, C. Caufield, G. Chang, T. Hendrickson, W. C. Still, *J. Comput. Chem.* **1990**, *11*, 440-467; b) K. S. Watts, P. Dalal, A. J. Tebben, D. L. Cheney, J. C. Shelley, *J. Chem. Inf. Model.* **2014**, *54*, 2680-2696.
[99] MacroModel, Schrödinger, LLC, New York, NY, **2023**.
[100] S. Grimme, C. Bannwarth, P. Shushkov, *J. Chem. Theory Comput.* **2017**, *13*, 1989-2009.
[101] C. Bannwarth, S. Ehlert, S. Grimme, *J. Chem. Theory Comput.* **2019**, *15*, 1652-1671.
[102] V. Barone, M. Cossi, *J. Phys. Chem. A* **1998**, *102*, 1995-2001.
[103] S. Grimme, F. Bohle, A. Hansen, P. Pracht, S. Spicher, M. Stahn, *J. Phys. Chem. A* **2021**, *125*, 4039-4054.
[104] a) F. Neese, *WIREs Comput. Mol. Sci.* **2022**, *12*, e1606; b) F. Neese, F. Wennmohs, U. Becker, C. Riplinger, *J. Chem. Phys.* **2020**, *152*, 224108.
[105] M. M. Zanardi, A. M. Sarotti, *J. Org. Chem.* **2021**, *86*, 8544-8548.